Capillary LC columns : packing techniques and applications

Please check the document version of this publication:

• A submitted manuscript is the version of the article upon submission and before peer-review. There can be important differences between the submitted version and the official published version of record. People interested in the research are advised to contact the author for the final version of the publication, or visit the DOI to the publisher's website.
• The final author version and the galley proof are versions of the publication after peer review.
• The final published version features the final layout of the paper including the volume, issue and page numbers.
[Link to publication](#)

CAPILLARY LC COLUMNS
Packing Techniques and Applications

J.P.C. Vissers
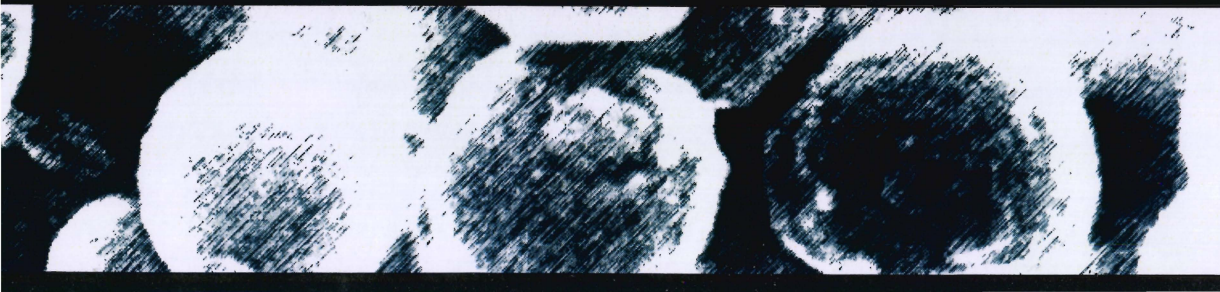
CAPILLARY LC COLUMNS
Packing Techniques and Applications

Proefschrift

ter verkrijging van de graad van doctor aan de
Technische Universiteit Eindhoven, op gezag van
de rector Magnificus, prof.dr. M. Rem, voor
een commissie aangewezen door het College
voor Promoties in het openbaar te verdedigen op
vrijdag 18 december 1998, om 16.00 uur

door

JOHANNES PETRUS CORNELIS VISSERS

geboren te Zevenbergen

Dit proefschrift is goedgekeurd door de promotoren:

prof.dr.ir. C.A.M.G. Cramers
en
prof.dr. P.J.F. Sandra

copromotor:

dr. J. Lavèn

if you compare yourself with others, you may become vain and bitter;
for always there will be greater and lesser persons than yourself

be yourself

Max Ehrmann "Desiderata" (1927)

in herrinering aan mijn grootmoeder Janssen-Akkermans

aan mijn ouders

CONTENTS

i

CHAPTER 1

GENERAL INTRODUCTION AND SCOPE

1.1 INTRODUCTORY REMARKS

Analytical chemistry is involved with the separation, identification and quantitation of target compounds in complex matrices. With today's analysis techniques, the identification and quantitation of reasonably pure compounds does not pose serious problems. There is however an increasing demand for the analysis of small sample quantities in which the compounds of interest are present as minor constituents. Hence, there is a growing need for sensitive, reliable analytical procedures that provide qualitative and quantitative information. In practice this involves the development of both sample preparation and separation methods – as well as suitable detection techniques.

Gas chromatography (GC) and column liquid chromatography (LC) have found wide spread acceptance as the separation technique in numerous application areas. Environmental chemistry, food and polymer chemistry and the bioanalysis field are just a few areas to which they have been applied. GC remains the method of choice for volatile and thermally-stable compounds because of its high separation power and favorable limits of detection for many classes of compounds. Moreover, the on-line coupling with mass spectrometry (MS) is well established allowing separation and subsequent identification on a routine bases. Ionic, polar, non-volatile, thermally-label and high-molecular weight compounds are typically separated by LC since they are not directly amenable to GC. Despite the reduced separation efficiency and detectability obtainable with LC compared to GC, the range of compounds that can be directly analyzed is much greater and as a matter of fact still expanding. In virtue of this widespread applicability of LC, much effort has been put into the development of sensitive identification techniques for LC. Especially LC-MS has gained in popularity after the recent introduction of atmospheric pressure ionization based interfaces and has found its way into routine applications in the biochemical and environmental field. Although other "liquid-based" separation techniques have become available – among them electrophoresis, supercritical fluid chromatography and electrochromatography – they have not found a broad acceptance yet, which is mainly due the versatility, robustness and ease of use of LC.

Despite that sensitive detection and identification techniques have become available for LC, there is a continuous need for detecting lower concentrations and analyzing increasingly smaller sample quantities. Although miniaturized LC has the potential to fulfill these requirements, these techniques are not yet generally accepted and still in development.

Miniaturization in separation sciences has been evident for some time [4-7]. The introduction of open tubular capillary columns for gas chromatography by Golay in the late 50's is generally regarded as one of the first steps towards miniaturization in chromatography. Decreasing the particle size has been the main stimulus towards miniaturization in column liquid chromatography, and still is nowadays [8]. Consistent efforts towards decreasing the column diameter of packed columns were not started before the early 80's. The groups of Kucera, Ishii and Novotny [9-11] were among the first who recognized the advantages of reducing the column size in LC. Their work attracted the attention of a significant number of groups, each pursuing significantly different aims, e.g. increased detection sensitivity due to the reduced chromatographic dilution, the ability to work with small quantities of sample in case of limited availability, easier interfacing to flame based detectors and mass spectrometry, hyphenation to other separation techniques, and other inherent advantages of reducing the column i.d.

Other directions towards miniaturization in LC are the use of coated open tubular columns with an i.d. of 5–50 μm and etched channels on a micro-chip as separation columns. In potential, open tubular LC is a very promising technique since it can produce large theoretical plate numbers in short analysis times [12]. However, the technique has been applied with limited success so far, which is mainly due to the demanding instrumental requirements. Micro-chip LC is still in its development stage and seems to move towards "sensor-type" of applications. Generally this type of separation devices lack the resolving power of more conventional LC techniques due to the limited column length. Furthermore, the difficulty with techniques such as open tubular LC and micro-chip LC remains sample preparation and introduction.

Packed LC columns with an i.d. of 50–300 μm haven proven to provide the best analytical results so far. Although such columns may not be the ultimate goal in miniaturization in column liquid chromatography, they already provide the possibility to separate complex mixtures. More importantly, the advantages of miniaturization with such columns can be achieved relatively easy, allowing them ultimately to be used in routine analysis.

1.2 THEORETICAL ASPECTS OF COLUMN LIQUID CHROMATOGRAPHY

Key parameters

The retention time of an unretained compound and the pressure drop are normally the limiting parameters for any system in practice. These key parameters determine the efficiency of a packed column and how this can be optimized. Following the same approach as Knox [13], the pressure drop Δp across a packed bed is given by:

$$\Delta p = \frac{\phi' \eta L u}{d_p^2} = \frac{\eta L u}{K^0} \qquad (1.1)$$

where ϕ' is the column resistance factor – a dimensionless constant in the range 500–1000. η is the viscosity of the mobile phase, L is the column length, u is the linear velocity of the mobile phase, d_p is the particle diameter and K^0 is the specific column permeability. Substitution of u = L/t_0 in equation (1.1) gives:

$$\Delta p = \frac{\phi' \eta L^2}{t_0 d_p^2} = \frac{\phi' \eta}{t_0} \lambda^2 \qquad (1.2)$$

where t_0 is the residence time of an unretained solute and λ is the reduced column length (λ is in fact directly proportional to the plate number N – as will be shown below – and can therefore be regarded as a dimensionless column efficiency parameter too).

Equation (1.2) shows that columns with the same reduced length λ require the same pressure drop to give – with the same mobile phase – the same elution time t_0. The optimum column will be the column that provides the highest number of plates N. The plate number N is defined as:

$$N = \frac{L}{H} = \frac{\lambda d_p}{H} \qquad (1.3)$$

where H is the absolute plate height. For a fixed value of λ, the highest number of plates N is equivalent to the lowest ratio of H/d_p. This ratio is the number of particles to the plate height and is called the reduced plate height h, which concept was introduced by Giddings [14]. Substitution of equation (1.3) into equation (1.2) provides a more general way of relating the pressure drop, elution time and plate height:

$$t_0 = \frac{N^2 h^2 \phi' \eta}{\Delta p} \qquad (1.4)$$

or for the retention time t_r in general:

$$t_r = \frac{N^2 h^2 \phi' \eta}{\Delta p} \cdot (1+k) \qquad (1.5)$$

3

where k is the retention factor, i.e. dimensionless retention time. The given equations show that for the fastest elution – given a required number of plates N and stated η and Δp – it is necessary to choose the parameters in such a manner that the column is operated at the

lowest possible value of the reduced plate height h. This implies that the optimum particle size has to be calculated to work at the minimum of h when the number of plates, the column resistance factor ϕ', the mobile phase viscosity η and the pressure drop Δp are specified.

Peak dispersion

The reduced plate height h depends on the physical properties of the packed column and the mobile phase, as well as the velocity of the mobile phase. The reduced plate height h is – analogous to the absolute plate height – defined as:

$$h = \left(\frac{\sigma}{d_p}\right)^2 \cdot \frac{d_p}{L} = \left(\frac{\sigma}{d_p}\right)^2 \cdot \frac{1}{\lambda} \tag{1.6}$$

where σ is the variance of the chromatographic band. The increase in variance during migration of a compound through a packed column – as first shown by Van Deemter *et al.* [15] – arises from three kinetic or dynamic processes, i.e. longitudinal molecular diffusion, dispersion due to inhomogeneities in mobile phase flow and resistance to mass transfer in the mobile and the stationary phase within the column. These three dispersive processes are believed to be random and independent of each other, and their sum to give the total variance. Accordingly, the total reduced plate height equals [13,16]:

$$h = h_{diff} + h_{flow} + h_{mass\ transfer} \tag{1.7}$$

Dispersion from longitudinal diffusion. The diffusion of a static solute band in a packed column can be described according to the Einstein equation:

$$\sigma_z^2 = 2Dt \tag{1.8}$$

where σ_z^2 is the variance, D is the diffusion coefficient and t is the time. The extend of the diffusion is equal in flowing and static systems. Hence, for solutes that do not reside in the stationairy phase, equation (1.8) can be rearranged to:

$$h_{diff} = \frac{2D(1+k)}{ud_p} \tag{1.9}$$

4

In fact, he molecules diffuse within the mobile phase for a fraction $1/(1 + k)$ of the total time and within the stationary phase for a fraction $k/(1 + k)$ of the total time. This finally leads to the following expression for the longitudinal dispersion:
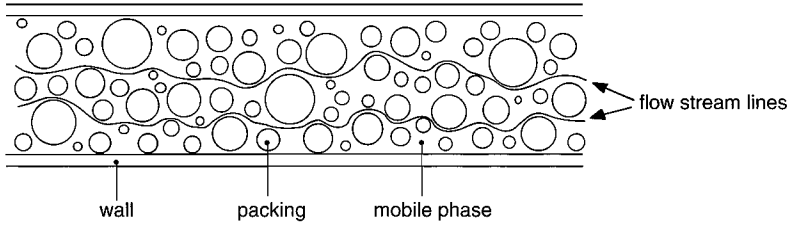
Fig. 1.1. Flow pattern in a packed chromatographic bed showing stream lines.

$$h_{diff} = \frac{2\gamma D_m + 2\gamma' D_s k}{ud_p} = \left(2\gamma + 2\gamma' k \frac{D_s}{D_m}\right)\left(\frac{D_m}{ud_p}\right) \tag{1.10}$$

where γ and γ' are tortuosity factors – normally ~ 0.6 – which allow for the restriction to diffusion by the skeleton of the particles. D_m and D_s are the diffusion coefficients of the solute in the mobile and stationary phase respectively. The factor ud_p/D_m is a dimensionless velocity – often referred to as the reduced velocity v, accordingly to Giddings' concept [14]. Equation (1.10) is often simplified to $h_{diff} = B/v$.

Dispersion from flow inhomogeneity. In a packed bed the solute molecules will describe a tortuous path through the interstices between the particles. Hence, some of the solute molecules will travel shorter paths than the average and some longer paths. Consequently, some molecules will move ahead of the average and some will lag behind, thus causing dispersion. The dispersion from flow inhomogeneity is schematically depicted in Fig. 1.1. In reality, molecules will also diffuse across the streamlines and sample randomly-varying velocities more frequently than if they remain fixed to streamlines. Dispersion arising from this kind of diffusion is therefore dependent on the mobile phase velocity. Although no theory accurately describes this dispersion mechanism, experiments show that it can be approximated by:

$$h_{flow} = Av^{1/3} \tag{1.11}$$

where A is a constant which is believed to increase slightly with k. In practice, A reflects how well a column is packed. Well packed columns have A values between 0.5 and 1, while poorly packed columns have larger values of A, for example, 2 to 5.

Dispersion from resistance to mass transfer in the stationary phase. A retained solute spends a fraction $k/(1 + k)$ of its time in the stationary phase. Since the mobile phase in the pores of the particles is stagnant, molecules within the particles will only migrate by diffusion. The average residence time within a particle is proportional to d_p^2. The remainder of the time – i.e. for the fraction $1/(1 + k)$ – the solute molecules are in the moving mobile phase and travel with the average velocity of the mobile phase.

5

If a solute molecule is in the stationary phase it will evidently lag behind the main solute band, and when it is in the moving mobile phase it will run ahead. The migration of a solute molecule through a packed column is regarded as a series of random steps alternately behind and ahead of the main solute band. The dispersion – measured on a particle scale – depends upon the equilibrium between the flow rate over a particle and the rate of diffusion over a particle. Theoretical treatment of the dispersion due to slow mass transfer in the stationary phase shows that the contribution to the reduced plate height equals [14]:

$$h_{m_t} = q\frac{k}{(1+k)^2}\frac{D_m}{D_s}v \qquad (1.12)$$

where q is a configurational factor that reflects the particle shape and its internal pore structure, For spherical, porous particles, q equals 1/30. Equation (1.12) is often summarized to: $h_{m_t} = Cv$. In practice C is often to be found in the range 0.05–0.2.

The complete plate height equation. The total reduced plate height is obtained by adding together the contributions of the three dispersion processes, giving:

$$h = \frac{B}{v} + Av^{1/3} + Cv \qquad (1.13)$$

Other plate height equations have been suggested [15,17-19] and appear to be more or less similar. Equation (1.13) has limited use in column design since it was derived by means of a curve fitting procedure. However, it is extremely valuable in accessing the quality of the packed bed.

Comparison of Column Types in Liquid Chromatography
Rearrangement of equation (1.4) gives:

$$h^2\phi' = \frac{t_0\Delta p}{N^2\eta} = E \qquad (1.14)$$

Both sides of equation (1.14) are dimensionless. The right hand side represents the elution time per plate for an unretained solute multiplied by the pressure drop per plate and is corrected for by the viscosity of the mobile phase and is called the separation impedance E. This parameter was introduced by Bristow and Knox [20] and indicates the "difficulty" of achieving a given number of plates N. The left hand side of equation (1.14) gives the separation impedance in terms of chromatographic and hydrodynamic parameters. The highest performance is achieved using a column that combines low resistance to flow and minimum chromatographic dispersion.

The minimum value of E for a packed column is about 2000, assuming values of 2 and 500 for h and φ' respectively. In practice, h values of 3 are not uncommon and φ' is more usually around 1000, giving an E value equal to 9000. E is in fact the only satisfactory parameter that can be used to compare different column types, e.g. columns packed with spherically or irregularly shaped particles, conventional LC columns, small i.d. LC columns, drawn packed columns and open tubular columns.

The separation impedance E can be obtained by measurement of external properties only for any column type. Because E depends on the elution time, it is recommended to rank columns either on their minimum E value or the E value at a predefined set of conditions – which may be well determined by practical considerations. However, it is necessary to define suitable reduced parameters based on the structure of the column. Four different column types will be considered: conventional and small i.d. packed columns, drawn packed columns and open tubular LC columns. Drawn-packed columns are made on a glass drawing machine from glass tubes already filled with particles of appropriate diameter. For conventional and small i.d. columns and drawn-packed columns the characteristic dimension is the particle diameter – i.e. $h = H/d_p$. For open tubular LC columns this would be the inside column diameter d_c. Hence, analog to capillary GC columns, $h = H/d_c$ for open tubular LC.

Column resistance factor φ' and h_v curves. Conventional and small i.d. packed columns have similar φ' values in the 500–1000 range. Drawn-packed columns have a more open structure and appear to have φ' values of around 120–250. For open tubes φ' can be obtained from the Poiseuille equation and equals 32. The h_v curves for packed and drawn-packed columns can be adequately described by equation (1.13). Minimum h values of h = 2 can be achieved at reduced velocities between 1–10. For open tubular columns the Golay equation applies:

$$h = \frac{2}{v} + \frac{1+6k+11k^2}{96(1+k)}v + \frac{2}{3}\frac{k}{(1+k)^2}\left(\frac{d_f}{d_c}\right)^2\left(\frac{D_m}{D_s}\right)v \tag{1.15}$$

where d_f is the thickness of the stationary phase layer. The second term arises from slow mass transfer across the flowing fluid and the third term from slow mass transfer within the stationary phase. The minimum h value is a function of the retention factor k. At the optimum reduced velocity of a slightly retained compound – i.e. a retention factor k = 3 – the reduced plate height equals 0.8 for open tubular LC columns.

Comparison of different column types under optimum conditions. The elution parameters for optimal columns of different types are given in Table 1.1 using the equations described above. Three types of "packed" columns and an open tubular LC column are considered. First of all it can be noted for packed columns that the elution time and column length are not a function of the column i.d., which is in agreement with current plate height–velocity theories. Thus, the i.d. of the column in itself has no effect of the column efficiency. Deviations from

Table 1.1 Ultimate optimum operating conditions for different columns types

number of plates	t_0 (s)	d_p or d_c (μm)	L (mm)	σ_{t_0} (s)	F (mm³ s⁻¹)	σ_{V_0} (mm³)
packed conventional column ($d_c = 5$ mm)[a]						
10000	10	1.6	30	0.10	50	5
30000	90	2.7	170	0.5	30	15
100000	1000	5	1000	3	15	50
packed small i.d. column ($d_c = 1$ mm)[a]						
10000	10	1.6	30	0.10	1.9	0.2
30000	90	2.7	170	0.5	1.1	0.6
100000	1000	5	1000	3	0.6	2
drawn packed column[b]						
10000	3	0.9	17	0.03	$1.7 \cdot 10^{-5}$	$5 \cdot 10^{-7}$
30000	27	1.5	90	0.16	$3.0 \cdot 10^{-5}$	$3 \cdot 10^{-6}$
100000	300	2.7	550	1.0	$5.5 \cdot 10^{-5}$	$5 \cdot 10^{-5}$
open tubular LC column[c]						
10000	0.1	0.25	2	0.001	$1.0 \cdot 10^{-6}$	$1 \cdot 10^{-9}$
30000	0.9	0.45	10	0.005	$1.6 \cdot 10^{-6}$	$1 \cdot 10^{-8}$
100000	10	0.8	60	0.030	$3.0 \cdot 10^{-6}$	$1 \cdot 10^{-7}$

assumed values: $\eta = 10^{-3}$ Pa s; $D_m = 10^{-9}$ m² s⁻¹; $\Delta p = 200$ bar

[a] $\phi' = 500$; $h_{min} = 2$; $v_{opt} = 5$; $E_{min} = 2000$; $\varepsilon_t = 0.75$

[b] $\phi' = 150$; $h_{min} = 2$; $v_{opt} = 5$; $E_{min} = 600$; $\varepsilon_t = 0.80$; $d_c/d_p = 2.5$

[c] $\phi' = 32$; $h_{min} = 0.8$; $v_{opt} = 5$; $E_{min} = 20$

this rule will be treated in chapter 2. However, the reduction of the column i.d. has a major impact on the volumetric flow rate and the peak volume, which is very advantageous with gas and flame-based detection techniques and for the coupling with mass spectrometry.

Drawn-packed and open tubular LC columns at first appear very attractive with respect to column efficiency and analysis time. A closer look at Table 1.1 shows however that extreme experimental requirements have to be met – as indicated by the extremely small calculated variance for an unretained compound σ_{t_0} – to operate these type of columns at optimum conditions. In fact, these type of columns have almost always been operated fairly far from the optimum conditions and under the actual experimental conditions they are not much better in terms of E values than packed column of the same plate number.

Extracolumn bandbroadening.

Besides the column, also the various parts of the LC system contribute to broadening of the peaks. Especially the dispersion produced by the injection device and detection system are critical in case of small i.d. packed LC columns – as shown by the small peak volumes given in Table 1.1. In general, the dispersion produced by the injector and detector are allowed to give a 5% loss in chromatographic resolution. From this condition, the maximum allowable extracolumn bandbroadening can be calculated for retained components. An extensive description of extracolumn bandbroadening is given in chapter 2 of this thesis. Here only the effect and its importance are mentioned.

1.3 STATIONARY PHASES AND FILLING TECHNIQUES

Silica

During the past three decades, macroporous silica-based materials have been the dominating stationary phase in liquid chromatography [21-24]. Silica is usually produced by precipitating sodium silicate with acid, followed by washing and drying of the gel. Milling, sieving, agglomeration, condensation, etc. give various forms. The combination of certain properties of silica make it an extremely useful support for liquid chromatography. Silica is mainly characterized by its surface chemistry, specific surface area and pore diameter. However, for chromatographic applications the pore volume, the apparent density, the particle shape, a narrow particle size distribution, a high purity and the surface pH are important characteristics too.

Silica can be applied for the separation of polar compounds, aromatic hydrocarbons, olefins and saturated hydrocarbons, to which it is – to some extent – fairly selective. For most applications however the adsorption on bare silica is too strong. Silica can be deactivated – i.e. made more specific – by means of derivatization of its surface. This can be achieved by bonding chemicals to the silanol groups of the silica. The most chemically stable bonds are obtained with n-alkylated silanes, and are almost exclusively used for the production of derivatized

9

silicas for chromatography. The polarity of silanes can be adapted by altering the alkyl length, or by replacing the alkyl chain by an amino, cyano or alcohol function bonded on a short alkyl chain. The number of ligands connected to the silicon atom can be changed to allow multiple condensation reactions with the silanol groups on the silica surface. In addition, the bonded silica can be partially hydrolyzed and react with other silanes or with the silanol functions again. This chemistry is rather complex, but generally, monofunctional silanes lead to a mono-meric phase – i.e. single bonded to the silica surface – and polyfunctional silanes to polymeric phases. Both monomeric and polymeric phases will have a number of free silanol functions after the binding reaction, which can be the source of unwanted active "sites" in certain type of separations. Removing as many of the active "sites" – as possible by trimethyl silanization – is called "end-capping" or "deactivation". Alternatively, the residual silanol functions can be "masked" by the bonding of polyfunctional silanes that contain "bulky" side groups such as di-isobutyl-n-octadecylsilane, resulting in so-called base-deactivated or stable-bond silicas. Research on this is still on-going, indicated by the frequent appearance of papers on this topic in the literature.

Alumina/zirconium based supports

Alumina can be employed as a stationary phase in LC too, but the performance of alumina packed columns have been proved to be inferior to silica based packings. It is prepared by dehydration and thermal treatment of crystalline bayerite [25,26]. After conditioning with an acid or a base, its apparent surface pH can be adjusted between pH 3–9. The solubility of alumina at high pH values is much less than that of silica and can be applied over the pH range 2–12. A major drawback of alumina – however – isthat stable bonded phases cannot be formed by direct reaction with alumina. Hence, only normal phase separations are feasible.

Zirconia is a mechanically and thermally stable material that also has been applied as a support in column liquid chromatography. It is pH stable and shows little or no changes in pore volume or surface area at elevated temperatures [27,28]. It is however difficult to pro-duce robust reversed phase and ion exchange phases from zirconia. Zr–O–Si bonds are much less stable than Si–O–Si bonds. Hence, silanization cannot be used to covalently bond station-ary phase to the surface. However, the surface of zirconia can be modified with strong Lewis bases such as phosphate and fluoride allowing the separation of proteins [27]. The modifica-tion of the zirconia surfaces is not permanent and is sensitive to changes in the chromato-graphic conditions. Alternatively a polymer layer can be deposited on the surface and into the pores of the zirconia particles, allowing cross-linking and functionalizing the support. The latter method has been originally developed for silica particulates. Hu and Carr [28] have applied this technique for the cation exchange separation of proteins on zirconia particles too.

Macroporous polymer/graphite carbon packings

Macroporous polymer packings are typically used in applications for which silica based packings are not suitable due to their hydrolythic instability or surface heterogeneity [26]. Macroporous polymers are generally prepared by a two-phase suspension polymerization in a mixture of water, an organic solvent, a cross-linking reagent, an initiator and a stabilization reagent. The suspension is rapidly stirred forming droplets in which the growing polymer chains form and eventually precipitate when reaching their critical size. The formed beads are approximately spherical in shape and consist of many hard microspheres with both pores and channels. The particle size ranges from 5-20 µm and the pore diameters are around 2-600 nm [29,30]. The chromatographic properties of porous polymers can be modified by selecting different starting materials of by functionalizing – i.e. chemical reaction – the polymeric particles [29]. Polystyrene and polyvinylbenzene packings can be chemically modified with C_{18} and C_8 into the polymer structure to give packings that are chromatographically more comparable to silica based reversed phase packings. A more common chemical modification is the introduction of ionic functional groups into the polymeric structure to give packings for ion exchange and ion chromatography [26,31]. The main application area of macroporous polymers remains size exclusion chromatography.

Graphite carbon packings are basically polymers too [26,32]. However, they are prepared quite differently compared to macroporous polymer packings. A wide pore silica-based packing is impregnated with a phenolformaldehyde or a phenolhexamine solution and polymerized. Next, the packing is carbonized in an inert atmosphere at around 1000°C and the silica template dissolved by treating the carbon-silica composite with a hot potassiumhydroxide solution. The remaining carbon skeleton is heated to above 2000°C to induce graphitization. Graphite carbon packings are very hydrophobic and are typically used for the separation of basic compounds. Their application can however also be found in the analysis of peptides.

Monolithic supports

The introduction of capillary electrochromatography (CEC) has stimulated the development of monolithic column packings. The purpose is to have a chromatographic bed that is pH-stable over a very broad range – preferably up to pH values of 8 or higher – and to reduce negative side-effects that arise from sintered frits, i.e. bubble formation, adsorption-induced tailing and extracolumn bandbroadening. Monolithic column packings are not used exclusively for CEC. Hjertén *et al.* [33] demonstrated that a monolithic LC column could be constructed by compressing a solvent-swollen copolymer. Despite the lack of a continuous pore size distribution, its was shown that this material could be used for the ion exchange separation of proteins. Somewhat later, Svec and Fréchet [34] reported on the preparation of a continuous rod of porous polymer. After molding the polymeric rod by an in situ polymerization in the tube of a chromatographic column, the polymer was functionalized with either a diol or an amino group. Also in this case the performance of the monolithic bed was demonstrated by the ionic exchange separation of proteins. Another approach towards the produc-

tion of a monolithic chromatographic bed is the construction of a functionalized silica skel-eton. The construction of such a column was demonstrated by Minikucho et al. [35]. The chromatographic performance in terms of plate height was found to be comparable with 5 µm stationary phase particles. Fields [36] demonstrated a similar approach for the develop-ment of a continuous column support for capillary LC columns. Minimum plate heights were found to be around 75 µm, which is considerably higher than plate heights that are achievable with silica particles.

These LC column approaches towards the development of a monolithic bed have been extended and optimized for CEC columns. Palm and Novotny [37] and Ericson et al. [38] reported on gel-matrixes as the monolithic support. Both groups conducted the polymeriza-tion of the gel in situ in the chromatographic tube. As a first step, the capillary wall was pretreated with a reagent that allows a covalent bond of the resulting gel inside the fused silica capillary. After in-situ polymerization of the gel, the matrix was functionalized with ei-ther a C_4, C_6 or C_{12} ligand [37] or with a C_{18} ligand [38]. The plate numbers for the C_4, C_6 and C_{12} functionalized matrixes were about 360000 plates m^{-1}, 300000 plates m^{-1} and 240000 plates m^{-1} respectively under CEC conditions [37]. The plate number for the C_{18} functionalized columns was about 120000 plates m^{-1} [38]. No explanations for these apparent ligand-depen-dant plate counts were given. Peters et al. [39-41] have published a series of papers on a one-step in-situ copolymerization in 100 and 150 µm i.d. fused silica capillaries. The obtained monolithic columns have efficiencies higher than 120000 plates m^{-1} under CEC conditions. This number of plates can also be achieved in capillary LC. However, these type of monolithic columns – as well as the gel-matrix monolithic columns – do not suffer from limited bed stability and the formation of bubbles within the column during analysis. Furthermore, no supporting frits are required. Hence, no unwanted interactions arising due to interaction with the frit material are to be expected. The group of Horváth produced a monolithic silica column by sintering bare 6 µm silica particles along the complete column length [42]. After sintering, the fused particles were functionalized with a C_{18} ligand. The plate height of such a monolithic was 16 µm in the pressure driven LC mode and 8 µm in the electrokinetic CEC mode.

Slurry packing vs. gas, supercritical fluid and electrokinetic packing

The selection of the method for filling – i.e. packing – a column depends mainly of the mechanical strength of the packing material, the particle size, particle type and column di-mensions. Particles larger than 20 µm in diameter can be dry packed without too much diffi-culty. For particles smaller than 20 µm in diameter, slurry packing techniques are usually ap-plied since the surface energy to mass ratio of such particles is relatively high, resulting in unstable bed structures with dry packing. Knox [43] has summarized the criteria for slurry packings as follows:

-    the particles must not settle too quickly during the filling procedure
-    the particles must not agglomerate
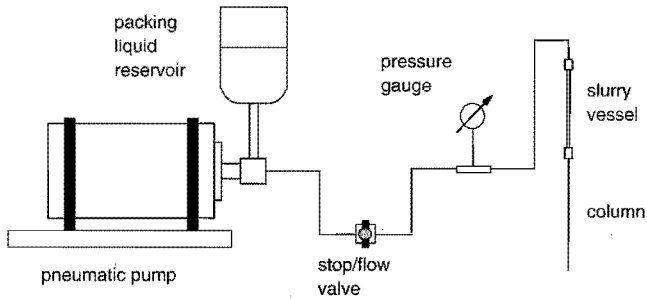
Fig. 1.2. Down-fill slurry packing equipment.

- the particles must hit the accumulating bed with a high impact velocity
- each particle should have sufficient time to settle in before it is buried by other particles
- the liquid used to support the slurry must be easily washed out of the packing and should not react with it.

These criteria were suggested for conventional sized, large i.d. LC columns and are believed to be applicable for small i.d. LC columns too. In-line with these criteria, many different slurry packing techniques have been developed and suggested for the packing of miniaturized LC columns.

Fig. 1.2 depicts a typical column packing equipment setup and will be used as a guide to describe the packing procedure. A slurry containing the stationary phase particles is displaced from the slurry vessel into the column at constant pressure or velocity using a pneumatically amplified liquid pump. A porous frit, filter or screen is attached to the lower end of the column blank to retain the packing during filling. The top end of the column is directly connected to the base of a slurry reservoir, which size should be scaled in proportion to the dimension of the column. The top end of the slurry reservoir is – via a pressure gauge and a stop/flow valve – connected to the head of the pneumatic pump. Prior to packing of the column, all transfer lines are purged with either the packing or slurry liquid and the pump pressurized to its initial value. Next, the stop/flow valve is opened and the pressure or velocity maintained for a certain period of time. Fig. 1.2 depicts a downward-filling packing setup. The equipment used for upward-filling techniques is basically the same as in Fig. 1.2. The only difference is the construction of the slurry reservoir. Upward packing is applied for very low viscous slurry liquids such as pentane and hexane, and in case of very dilute slurries [44,45]. Slurry packing techniques are often subdivided in packing methods that refer to the stabilization of the stationary phase slurry: balanced and non-balanced density methods, chemical and mechanical stabilization methods, and high and low-viscosity slurry methods [46].

13

Physical stabilization. Physical stabilization of the slurry can be achieved by the balanced and non-balanced density method, and by the viscosity slurry method. The balanced density method uses mixtures of solvents, of which the composition is adjusted to have the same density as the stationary phase particles [47-50]. Suitable solvents are tetrabromomethane, tetrachloroethylene, carbon tetrachloride and diiodoethane with modifiers. The major drawback is the toxicity of the halogenated compounds. In the non-balanced method, slurry liquids usually consist of solvents like acetone, methanol, tetrahydrofurane, etc. [51-59]. To prevent particle settling, the packing of the column has to be carried out quickly. The viscosity slurry method uses viscous solvents as glycol and glycerine to prevent particle settling [51,60]. As of the high viscosity of the slurry liquid, column packing by this method is very time consuming.

Chemical and mechanical stabilization. Packing materials can also be stabilized by chemical stabilization. The slurry liquid is made up of a polar solvent and an ionizing component – i.e. surfactants – to electrostatically stabilize the slurry [61-65]. With mechanical stabilization, the slurry is stirred continuously during the packing process in a specially constructed slurry vessel [44].

Low-viscosity method. The goal of using a low density-viscosity suspension is to prevent selective sedimentation of the particles and to increase the homogeneity of the packed bed. Suitable slurry liquids are pentane, hexane and diethylether [45,66]

Dry-packing and supercritical fluid packing. Although more commonly applied for conventional LC columns, dry packing methods are sometimes also used to pack capillary LC columns [67-69]. Dry packing is also referred to as tap filling and can be performed with relatively simple equipment. It is recommended for particles with a diameter > 20 μm. In the dry packing of columns, the stationary phase is conditioned first with methanol or ethanol to "discharge" the particles. Next, the conditioned phase is put into a stainless steel reservoir, which is connected to a regulated high pressure nitrogen cylinder on one end, and to the microcolumn on the other end. Like the stationary phase, the retaining frit has to be wetted first with methanol or ethanol prior to use. The column is then placed into an ultra sonic bath and the gas pressure is applied to the slurry reservoir. The gas pressure is increased slowly in time. Before use, the columns have to be conditioned first for at least 2 hours. Critical parameters in this type of microcolumn packing are the applied gas pressure, the pressure gradient and the sonication time. The selection of the particle aggregation reducer is less critical and based on factors like polarity, vapor pressure and toxicity. The long conditioning times seem to suggest that rearrangement of the particles occurs during the initial transport of mobile phase through the column. Hence, the structure of the chromatographic bed is primarily determined by the selection and flow rate of the conditioning liquid. The advantage of the use of gases over liquids in column packing is however that relatively long columns can be packed without too much difficulty.

The use of supercritical carbon dioxide as the packing medium has been introduced recently for the preparation of capillary LC columns [70-75]. As supercritical fluids have intermediate properties between liquids and gases – as far as the density and viscosity are concerned

– it is expected that this method combines the advantages of slurry and dry packing. As with gases – owing to the low viscosity of supercritical carbon dioxide – longer columns can be packed compared to the slurry packing techniques. Columns lengths up to 10 m have been reported with this packing method [70]. Furthermore, the density of supercritical carbon dioxide can easily be varied by varying the pressure and temperature, and the polarity affected by adding a modifier. Carbon dioxide is non-toxic and thus quite harmless to work with compared to the toxic solvents that are sometimes used in slurry packing.

The packing equipment is very similar to the apparatus used in slurry packing. The main differences are a constant pressure pump – i.e. in most cases a supercritical fluid pump is used – that allows to displace supercritical carbon dioxide, a restriction that is placed at the end of the column to maintain supercritical pressures within the slurry reservoir and column, and an ultrasonic water bath to keep the temperature within the column above the critical point. In some cases also the slurry vessel is placed into the water bath [75].

Most papers about the packing of capillary LC columns with supercritical fluids deal with the practical aspects and the instrumental requirements of the technique. An exception is the work of Tong *et al.* [73], who attempted to clarify the effect of sonication of the column during the packing process on the column performance and porosity by means of a mathematical model. The lowest reported plate numbers were achieved with constant pressure packing [72], which appears to be in contrast with other studies where it was claimed that pressure gradients provide more efficient columns [75]. The reported plate numbers are comparable with those obtained with slurry packing techniques – i.e. reduced plate height of about 2–3. The main advantage of supercritical fluid packings is the extremely long columns can be packed. Although these kind of long columns have no practical use in capillary LC due to their large back pressure, they have a big potential in packed supercritical fluid chromatography (SFC). The loadability of such columns is much higher than that of open tubular columns and due to its length sufficient plates can be generated.

Electrokinetic packing. All previously discussed packing techniques are based on the displacement of stationary phase particles by means of pressure. However, several groups have demonstrated that it is also possible to migrate particulate materials using an electric field. For example, Hjertén *et al.* [76] have characterized and separated viral particles, and McCormick [77] colloidal silica sols with diameters in the 5 to 500 nm range applying capillary zone electrophoresis – an electrokinetic based separation technique. Pretorius and coworkers [78] showed already in 1974 that columns could be filled – with packing densities that are comparable to those obtained by centrifugation – by using an electro-osmotic flow. More recently, Yan [79] has presented an electrokinetic packing method for the packing of charged and neutral particles of stationary phase material in capillary sized columns for capillary electrochromatography and microcolumn LC. Their experimental setup is shown in Fig. 1.3. Electrokinetic packing has a number of distinct advantages compared to slurry packing:

15
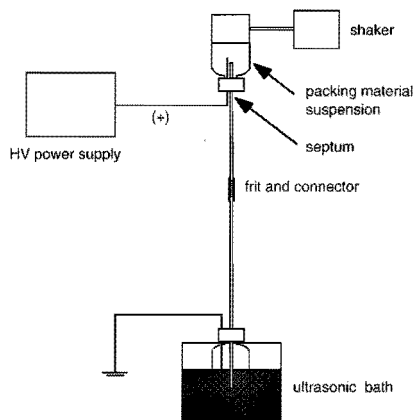
Fig. 1.3. Packing apparatus for the electrokinetic packing of microcolumns [79].

- there is no high back pressure as is generated in slurry packing because particles under a strong electric field are moved by electro-osmotic flow in the column and move with their own electrophoretic mobility – if charged – allowing to pack longer column and smaller particles, i.e. 1 µm
- to some extent, the electrokinetically packed column is more homogeneous in the radial direction of the column because of the more uniform solvent profile, i.e. all particles are packed at more or less the same packing velocity since no velocity distribution exist over the cross section of the column.

There are – however – some shortcomings: (i) the particle velocity will depend on the charge-to-size ratio, resulting in a size distribution of the particles along the longitudinal direction of the column and (ii) the electrokinetic packing process is rather slow. The latter argument may in fact be an advantage – as will be explained in chapter 5 of this thesis.

The method proposed by Yan [79] produced packed 75 µm i.d. fused silica columns that have reduced plate heights of 3.5, 3.7 and 5.4 for thiourea, benzylalcohol and benzaldehyde respectively. This relative low efficiency can be explained for by the fact that the column was packed with a 3 µm aluminum oxide-based C_{18} reversed phase, which is known to produce lower efficiencies than silica-based packings. Remarkable is the fact that this specific material generated lower efficiencies in CEC, which was accounted for by the fact that the internal surface of the column is different from the surface of the stationary phase particles which may result in an electro-osmotic profile that is not plug-like. However, other factors such as frit quality and column connection may contribute to peak broadening too. The same setup has been applied for the packing of silica-based C18 reversed phase materials but no results have yet been published in recent literature.

1.4 SCOPE

This thesis describes colloidal and hydrodynamic parameters involved in the slurry packing process of silica based reversed phase stationary phases into columns with capillary dimensions for liquid chromatography. The goal of the studies is to obtain a better understanding of the effects of these parameters on the chromatographic performance of packed microcolumns.

Chapter 2 reviews some of the theoretical aspects, detection techniques, hyphenation and the current application areas of microcolumn LC. The theoretical section of this chapter deals in particular with extracolumn bandbroadening effects. The sections on detection techniques, hyphenation and applications are mainly practically oriented.

The colloidal properties and sedimentation behaviour of spherically shaped reversed phase silicas in non-aqueous solvents are discussed in chapter 3. It is shown how the coagulation of chemically-modified silicas can be described numerically by expressing the experimentally observed rates of sedimentation of stationary phase particles as a function of the theoretically calculated sedimentation rates. Furthermore, it is demonstrated that the processing of silica-suspensions affects the colloidal stability.

The colloidal stability experiments described in chapter 3 form the basis of the column packing experiments in chapter 4. In the first section of this chapter different spherically shaped octadecyl-modified porous silicas are packed using various organic solvents as the slurry and packing liquid to study the effect of particle coagulation on the performance of the column. The outcome of these experiments is used to develop criteria for the selection of proper slurry and packings liquids. In the second section of chapter 4 the developed selection criteria are applied to pack capillary LC columns with spherically and irregularly shaped stationary phase particles. The packed columns will be compared with respect to chromatographic performance and speed of analysis.

A theoretical and experimental study on the effect of the packing pressure and filtration speed on the porosity and chromatographic performance of packed capillary LC columns is described in chapter 5. The filling process is simulated using a model that is based on Stokesian-dynamics. The applied model accounts for aspects such as filtration velocity, particle attraction and film drainage. The results from the modeling experiments are compared with experimentally obtained results from different packing experiments. The porosity of the packed columns is determined chromatographically. The possibilities of magnetic resonance imaging to study the porosity of a packed bed are evaluated in this chapter as well.

A number of applications using packed capillary columns will be shown in chapter 6. The first example involves the calculation of the retention factors of uncharged species in capillary electrochromatography (CEC) based on chromatographic and electrophoretic data. Expressions are given for the calculation of retention in CEC and their validity compared with experimentally obtained results. The removal of ionic detergents prior to capillary LC/Electrospray Ionization Mass Spectrometry (ESI-MS) is the second application that will be presented in chapter 6. Using a micro-column switching set-up it will be demonstrated that ionic deter-

gents can be removed from peptide samples to allow for the unambiguous identification of the peptides by ESI-MS after separation on a capillary LC column. The third application involves the description of a capillary LC system for fractionation based two-dimensional separations. Different types of two-dimensional capillary LC – involving reversed phase/ reversed phase and anion exchange/reversed phase separations – are shown for the separation of complex peptide mixtures originating from different origin. On-line capillary LC/ESI-MS is performed to identify the peptides in the different dimensions to confirm the orthogonality of the applied two-dimensional techniques.

In appendix A a method is described for estimating the Hamaker attraction constant of composite, spherical particles, that is stationary phase packing materials. The calculated attraction constants are compared with results obtained with other methods described in literature and will be used in chapter 3 of this thesis

1.5 REFERENCES

[1]   E. Heftmann (ed.), *Chromatography; part B: applications*, Elsevier, Amstedam, 1992

[2]   L.R. Snyder and J.J. Kirkland, *Introduction to Modern Liquid Chromatography*, Wiley & Sons, New York, 1974

[3]   D. Barceló (ed.), *Applcations of LC-MS in Environmental Chemistry*, Elsevier, Amsterdam, 1996

[4]   P. Kucera (ed.), *Microcolumn High-Performance Liquid Chromatography*, Elsevier, Amsterdam, 1984

[5]   M.V. Novotny and D. Ishii (ed.), *Microcolumn Separations; columns instrumentation and anchillary techniques*, Elsevier, Amsterdam, 1985

[6]   F.J. Yang (ed.), *Microbore Column Chromatography; a unified approach to chromatography*, Marcel Dekker, Inc., New York, 1989

[7]   B.G. Belin'kii, E.S. Gankina and V.G. Mal'tsev, *Capillary Liquid Chromatography*, Plenum Publishing, New York, 1987

[8]   H. Gieshe, K.K. Unger, U. Esser, B. Eray, U. Trüdinger, J.N. Kinkel, *J. Chromatogr. A* 465 (1989) 39

[9]   R.P.W. Scott and P. Kucera, *J. Chromatogr.* 125 (1976) 251

[10]   T. Tsuda and M. Novotynu, *Anal. Chem.* 50 (1978) 271

[11]   D. Ishii, K.Asia, K. Hibi, T. Jonokuchi and M. Nagaya, *J. Chromatogr.* 144 (1977) 157

[12]   R. Swart, J.C. Kraak and H. Poppe, *J. Chromatogr. A* 732 (1996) 201

[13]   J.H. Knox, in C.F. Simpson (ed.), *Pritical High Performance Liquid Chromatography*, Heyden and son Ltd., 1972, pp. 19

[14]   J.C. Giddings, *Dynamics of Chromatography*, Marcel Dekker, New York, 1965

[15]   J.J. Van Deemter, F.J. Zuiderweg and A. Klinkenberg, *Chem. Eng. Sci.* 5 (1956) 271

[16]   R.P.W. Scott, *Liquid Chromatography Column Theory*, John Wiley & Sons, Chichester, 1992

[17]   J.C. Giddings, *J. Chromatogr.* 5 (1961) 46

[18]   J.F.K. Huber and J.A.R.J. Hulsman, *Anal. Chim. Acta* 38 (1967) 305

[19]   C. Horváth and H.-J Lin, *J. Chromatogr.* 149 (1978) 43

[20]   P.A. Bristow and J.H. Knox, *Chromatographia* 10 (1977) 279

[21]   K.K. Unger, *Porous Silica*, Elesvier, Amsterdam, 1979

[22]   K.K. Unger (ed.), *Packings and Stationary Phases in Chromatographic Techniques*, Marcel Dekker, Inc. New York, 1990

[23]   R.K. Iler, *The Chemistry of Silica*, Wiley & Sons, New York, 1979

[24]   J. Nawrocki, *J. Chromatogr. A* 779 (1997) 29

[25]   T. Cserháti, *Chromatographia* 29 (1990) 593

[26]   C.F. Poole and S.K. Poole, *Chromatography Today*, Elsevier, Amsterdam, 1991, pp. 312

[27]   W.A. Schafer and P.W. Carr, *J. Chromatogr.* 587 (1991) 149

[28]   Y. Hu and P.W. Carr, *Anal. Chem.* 70 (1998) 1934

[29]   F. Nevejans and M. Verzele, *J. Chromatogr.* 406 (1987) 325

[30]   D.P. Lee, *J. Chromatogr.* 443 (1988) 143

[31]   R.E. Barron and J.S. Fritz, *J. Chromatogr.* 284 (1984) 13

[32]   B.J. Bassler and R.A. Hartwick, *J. Chromatogr. Sci.* 27 (1989) 162

[33]   S. Hjertén, J.-L. Liao and R. Zhang, *J. Chromatogr.* 473 (1989) 273

[34]   F. Svec and J.M.J. Fréchet, *Anal. Chem.* 64 (1992) 820

[35]   H. Minakuchi, K. Nakanishi, N. Soga, N. Ishizuka and N. Tanaka, *Anal. Chem.* 68 (1996) 3498

[36]   S.M. Fields, *Anal. Chem.* 68 (1996) 2709

[37]   A. Palm and M.V. Novotny, *Anal. Chem.* 69 (1997) 4499

[38]   C. Ericson, J.-L. Liao, K. Nakazato and S. Hjertén, *J. Chromatogr. A* 767 (1997) 33

[39]   E.C. Peters, M. Petro, F. Svec and J.M.J. Fréchet, *Anal. Chem.* 69 (1997) 3646

[40]   E.C. Peters, M. Petro, F. Svec and J.M.J. Fréchet, *Anal. Chem.* 70 (1998) 2288

[41]   E.C. Peters, M. Petro, F. Svec and J.M.J. Fréchet, *Anal. Chem.* 70 (1998) 2296

[42]   R. Asiaie, X. Huang, D. Farnan and C. Horváth, *J. Chromatogr. A* 806 (1998) 251

[43]   J.H. Knox, *J. Chromatogr. Sci.* 15 (1977) 353

[44]   K.B. Tomer, M.A. Mosely, L.J. Deterding and C.E. Parker, *Mass Spectrom. Rev.* 13 (1994) 431

[45]   M. Verzele, *J. Chromatogr.* 295 (1984) 81

[46]   M. Verzele and C. Dewaele, *LC•GC* 4 (1986) 614

[47]   F. Androlini, C. Borra and M. Novotny, *Anal. Chem.* 59 (1987) 2428

[48]   R.F. Meyer and R.A. Hartwick, *Anal. Chem.* 56 (1984) 2211

[49]   M. Stastná, M. Krejcí and V. Kahle, *LC•GC* 10 (1992) 878

[50]   S. Hoffman and L. Blomberg, *Chromatographia* 24 (1987) 416

[51]   D.C. Shelly and T.J. Edkins, *J. Chromatogr.* 411 (1987) 185

[52]   D.C. Shelly, V.L. Antonucci, T.J. Edkins and T.J. Dalton, *J. Chromatogr.* 458 (1989) 267

[53]   J.P.C. Vissers, H.A. Claessens, J. Laven, C.A. Cramers, *Anal. Chem.* 67 (1995) 2103

[54]   J.P.C. Vissers, E.C.J. van den Hoef, H.A. Claessens, J. Laven and C.A. Cramers, *J. Microcol. Sep.* 7 (1995) 239

[55]   J.C. Gluckman, A. Hirose, V.L. McGuffin and M. Novotny, *Chromatographia* 17 (1983) 303

[56] K.E. Karlson and M. Novotny, *Anal. Chem.* 60 (1988) 1662

[57] D. Ishii and T. Takeuchi, *J. Chromatogr.* 225 (1983) 349

[58] T. Takeuchi and D. Ishii, *J. Chromatogr.* 213 (1981) 23

[59] K. Bächmann, I. Haag and T. Prokop, *Frenzenius' J. Anal. Chem.* 345 (1993) 545

[60] Y. Hirata and K. Jinno, *J. High Resolut. Chromatogr.* 6 (1983) 197

[61] C. Borra, S.M. Han and M. Novotny, *J. Chromatogr.* 385 (1987) 75

[62] R.T. Kennedy and J.W. Jorgenson, *Anal. Chem.* 61 (1989) 1128

[63] A. Capiello, P. Palma and F. Mangani, *Chromatographia* 32 (1991) 389

[64] T. Zimina, R.M. Smith, P. Meyers and B.W. King, *Chromatographia* (1995) 662

[65] T. Zimina. R.M. Smith, J.C. Highfield, P. Meyers and B.W. King, *J. Chromatogr. A* 728 (1996) 33

[66] S. Hsieh and J.W. Jorgenson, *Anal. Chem.* 68 (1996) 1212

[67] Y. Guan, L. Zhou and Z. Shang, *J. High Resolut. Chromatogr.* 15 (1992) 434

[68] G. Crescentini and A.R. Mastrogiacomo, *J. Microcol. Sep.* 3 (1991) 539

[69] G. Crescentini, F. Bruner, F. Mangani and Y. Guan, *Anal. Chem.* 60 (1988) 1659

[70] A. Malik, W. Li and M.L. Lee, *J. Microcol. Sep.* 5 (1993) 361

[71] W. Li, A. Malik and M.L. Lee, *J. Microcol. Sep.* 6 (1994) 557

[72] D. Tong, K.D. Bartle and A.A. Clifford, *J. Microcol. Sep.* 6 (1994) 249

[73] D. Tong, K.D. Bartle, A.A. Clifford and A. M. Edge, *J. Microcol. Sep.* 7 (1995) 265

[74] R. Trones, A. Iveland and T. Greibrokk, *J. Microcol. Sep.* 7 (1995) 505

[75] P. Koivisto, R. Danielsson and K.E. Markides, *J. Microcol. Sep.* 9 (1997) 87

[76] S. Hjertén, K. Elenbring, F. Kilar, J.L. Liao, A.J.C. Chen, C.J. Siebert and M.D. Zhu, *J. Chromatogr.* 403 (1987) 47

[77] R.M. McCormick, *J. Liquid Chromatogr.* 14 (1991) 939

[78] V. Pretorius, B.J. Hopkins and J.D. Schieke, *J. Chromatogr.* 99 (1974) 23

[79] C. Yan, *Electrokinetic Packing of Capillary Columns*, US Patent 5453163, 1995

CHAPTER 2

MICROCOLUMN LIQUID CHROMATOGRAPHY: AN OVERVIEW OF INSTRUMENTATION, DETECTION AND APPLICATIONS

ABSTRACT

This chapter discusses different aspects of microcolumn liquid chromatography (LC) and reflects the areas of microcolumn LC research interest over the past decades. A brief theoretical discussion on a number of major issues, like column characterisation, chromatographic dilution effects and extracolumn bandbroadening in microcolumn LC is given. Recent progress in column technology and the demands and developments of instrumentation and accessoires for microcolumn LC are also reviewed. Besides that, the developments in a large number of established and also more recent detection techniques for microcolumn LC are discussed.

The potential of hyphenation of microcolumn LC with other techniques, more particularly of multidimensional chromatography and microcolumn LC coupled to mass spectrometry are reviewed. Finally, the perspectives of microcolumn LC separation methods are stressed by a number of relevant applications.

21

INTRODUCTION

The continuing interest in microcolumn liquid chromatography (LC) is indicated by the large number of review articles that appeared in literature, covering the general aspects of microcolumn LC [1-10], column technology [11-15], detection in microcolumn LC [16-25], instrumentation [26,27] and multidimensional chromatography [28]. The introduction of microcolumn LC is attributed to Horváth et al. in 1967 [29,30], who used 0.5–1.0 mm inner diameter (i.d.) stainless steel columns packed with pellicular particles for the separation of ribonucleotides. The following decades high performance liquid chromatography research was mainly focussed on packed columns with an i.d. of 4.6 mm. Therefore, it was not until the mid 1970's before Ishii et al. demonstrated the use of slurry packed teflon microcolumns in a series of publications [31-36], which initiated a breakthrough in the development of microcolumn LC. Other type of microcolumns with capillary dimensions – i.e. smaller than 1.0 mm in i.d. – were introduced shortly thereafter [37-43]. In about the same time frame the group of Scott [44-48] reported on their work with packed 1.0 mm i.d. columns to achieve efficient, high speed separations. The work of Novotny and coworkers [40-42], Yang [37] and Scott et al. [44-48] are regarded as key publications in the field of microcolumn LC. The initial developments towards miniaturization in high performance liquid chromatography were quickly followed by a number of laboratories worldwide [49-51].

Microcolumn LC has established itself as a complementary technique to conventional sized LC columns – which are more commonly used in high-performance liquid-chromatography. There are an increasing number of applications where conventional high-performance liquid-chromatography does not satisfy, or can not compete with microcolumn LC. The most important advantages of microcolumn LC are the benefits that arise from the ability to work with minute sample sizes and small volumetric flow rates, and the improvement in detection performance with the use of concentration sensitive detection devices as a result of the strongly reduced chromatographic dilution [2-5]. Nowadays microcolumn LC is almost exclusively performed – as a research tool and in routine analysis – with slurry packed columns of various dimensions. This chapter will therefore focus on recent technological advances with this type of microcolumns. Special attention will be given to the many detection techniques applied in microcolumn separations. In addition, the general advantages, and some applications are discussed.

NOMENCLATURE

22

The use of the abbreviations microbore LC, micro LC and capillary LC are used interchangeable for packed microcolumns of different i.d. Definitions have been suggested in the literature [52-53], but have not found a general acceptance. Microcolumn liquid chromatography is used frequently as the overall term to describe small i.d. packed LC columns at different leading conferences and in most scientific journals, and will therefore be followed in this chapter.

Table 2.1. Suggested nomenclature for microcolumns for LC having different inner diameters

column i.d.	abbreviation
0.5–1.0 mm	micro LC
100–500 µm	capillary LC
10–100 µm	nanoscale LC

Furthermore, there seems to be a tendency to describe 0.50–1.0 mm i.d. columns as micro LC, 100–500-µm i.d. columns as capillary LC, and 10–100-µm i.d. columns as nanoscale LC [54]. A summary of the suggested nomenclature is given in Table 2.1. As mentioned in the section introduction of this chapter, open tubular LC and drawn-packed type of columns will not be considered in this chapter, nor the nomenclature for conventional sized LC columns – i.e. LC columns with an i.d. of 2.0–4.6 mm – will not be addressed here.

THEORETICAL CONSIDERATIONS

Column characterization

Column characterization in liquid chromatography is a very arbitrary matter, since it depends on the users point of view. For instance, can acceptable column life times be expected under certain separation conditions, or can stationary phase and column manufacturers supply columns of constant and reproducible quality are practical but certainly valid aspects. These points will however not be addressed in this chapter. Here, only column performance – e.g. separation potential – and which column performance criteria should be used will be discussed.

A number of column performance evaluation methods have been suggested [55-59]. Till now however little consensus exists between the different methods with respect to test compounds, eluent, and other conditions to evaluate LC columns and none of these methods has found general acceptance in chromatographic practice. Apart from that also the many available separation modes and columns in LC and the different principles behind the suggested test methods have contributed to the present unsatisfactory and confusing situation for column test protocols. Generally, the retention factor k, selectivity α and the peak asymmetry A_s are believed to be representative parameters for the thermodynamic properties of a column.

The kinetic characteristics are often expressed in the dimensionless magnitudes reduced plate height h, separation impedance E and flow resistance factor ϕ'. The question whether small i.d. LC columns show better kinetic properties compared to their conventional counterparts has been subject of much discussion in literature [60-65]. The results of these investigations covering different column i.d.s and performed under not always similar test conditions can be summarized as follows. h-values are typically in the same range as conventional LC

23

columns. However, at very small column i.d.s (< 50-μm) a clear but steady decrease in the h-values can be observed, indicating the improved kinetics in microcolumn LC, which will be discussed in more detail in the section column developments. At the same time, it was also observed that E and φ' values tend to be somewhat higher at decreasing i.d.s, which is most likely caused by the less dense structure of the packed chromatographic bed.

Chromatographic dilution

A sample compound will be subjected to dilution during the chromatographic separation process. The chromatographic dilution D at the end of the column equals:

$$D = \frac{c_0}{c_{max}} = \frac{\varepsilon \pi r^2 (1+k)\sqrt{2\pi LH}}{V_{inj}} \tag{2.1}$$

where c_0 is the original compound concentration in a sample, c_{max} is the final compound concentration at the peak maximum, r is the column radius, L is the column length, H is the column plate height, ε is the column porosity and V_{inj} is the injected sample volume. D will increase proportionally to the square of the column radius and to the square root of the length and plate height of the column. Under further identical chromatographic and injection conditions and assuming Gaussian peak shapes c_{max} increases with inverse proportion to r^2. For example, from equation (2.1) it can be calculated that this will result in a 235-fold increase in peak height and mass sensitivity for a reduction in the diameter of a column from 4.6 mm to 300-μm i.d. It must be stressed however that this advantage of small i.d. columns can only be fully exploited, when the same sample size can be loaded and the operating characteristics of such columns are identical compared to their conventional counterparts. In fact since the sample size that can be loaded on a column is proportional to the amount of stationary phase in the column, this advantage is only valid in cases where the amounts of sample mass are restricted.

Extracolumn bandbroadening

Miniaturizing essentially falls down to the reduction of the i.d. of a column. At the same time the outer or extracolumn bandbroadening effects must be reduced accordingly, to achieve maximal performance of a miniaturized column. More specifically this is of major importance to prevent considerable loss of efficiency, resulting in decreased resolution of the column.

Usually the plate number of a column is calculated from the standard deviation of a peak, resulting in the statement of column efficiency. From a principal point of view such a statement is doubtful, since virtually both the column and the instrumental bandbroadening contribute to the standard deviation of a chromatographic peak. Therefore, together with the presentation of column efficiencies the applied equipment should be discussed unless the extracolumn bandbroadening contribution is negligible compared to the peak broadening of
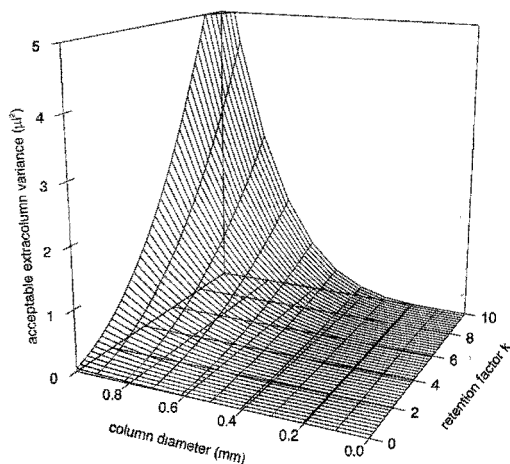
Fig. 2.1. Acceptable extracolumn variance $\sigma^2_{e(acc)}$ as a function of the column diameter and the retention factor k. See text for details.

a specific column. Since – for obvious reasons – extracolumn effects will always be manifest, this matter comes down to the question which extracolumn bandbroadening can be maximally accepted for an LC column under specific experimental conditions.

Starting from the generally accepted criterion that extracolumn bandbroadening may reduce the resolution R of a chromatographic separation maximally by 5%, it can be derived that:

$$R = \frac{\Delta t}{\sigma_t} = \frac{\Delta t}{1.05\sigma_c} \tag{2.2}$$

where Δt is the time difference between two closely migrating peaks, σ_c is the peak standard deviation caused by the chromatographic process, and σ_t is the peak standard deviation originating from column plus extracolumn effects.

Keeping in mind that $\sigma_t^2 = \sigma_c^2 + \sigma_e^2$ (volume or time units) this condition is satisfied when the extracolumn variance $\sigma_e^2 \leq 0.1025\sigma_c^2$ and consequently the loss in column plate number should not exceed 10% by extracolumn effects [23,25,27]. For a specific LC system the maximally acceptable variance $\sigma^2_{e(acc)}$ equals:

$$\sigma^2_{e(acc)} \leq 0.10\sigma_c^2 \leq 0.10\frac{\pi^2 L^2 r^4 \varepsilon^2 (1+k)^2}{N} \tag{2.3}$$

where N is the plate number of the column [23-25]. Taking practical numerical values of e.g.

25
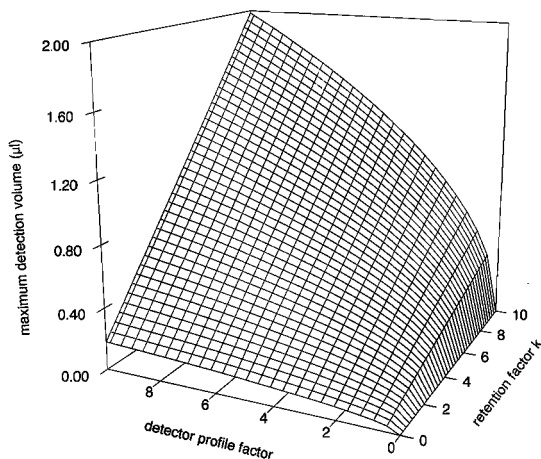
Fig. 2.2. Maximum allowed detection volume V_D as a function of the detector profile factor K_D^2 and the retention factor k. See text for details.

L = 0.15 m, e = 0.75 and N = 15 000 the corresponding $\sigma_{e(acc)}^2$ values can easily be calculated as a function of column diameter and retention factor, as depicted in Fig. 2.1. From the results in Fig. 2.1 it is obvious that for smaller i.d. columns the corresponding acceptable extracolumn contributions are rapidly decreasing. Hence, the use of small i.d. columns must be accompanied by a strong reduction of extracolumn effects. The approximation of the maximally allowed equipment bandbroadening outlined above can also be used to estimate the maximally acceptable contributions of the separate contributions of injector, detector, tubing and electronic time constants. E.g., assuming arbitrarily that these latter four main effects contribute in equal ratio to $\sigma_{e(acc)}^2$ it follows that $\sigma_D^2 = 1/4\sigma_{e(acc)}^2$, where σ_D^2 is the contribution of the variance of the detector to $\sigma_{e(acc)}^2$.

From $\sigma_D^2 = V_D^2 / K_D^2$, where V_D is the detector volume and K_D^2 is the detector profile factor [23], and taking the same numerical data of L = 0.15 m, ε = 0.75 and N = 15 000 at constant linear eluent velocity, the resulting plot of the maximally allowed detection volume versus k and K_D^2 is for a column of 500-μm i.d. given in Fig. 2.2. K_D^2 – equalling 12 under ideal on-column detection conditions – accounts for dispersion, mixing and diffusion effects in the detection system. From the graph in Fig. 2.2 it can be seen that at low values of k a detector volume of 200 nl is maximally allowed. From this example it is obvious that severe reduction of extracolumn effects is mandatory in microcolumn LC. Such an approximation as outlined above also allows a reasonable estimation of the other contributions to $\sigma_{e(acc)}^2$, viz. injector, tubing and electronic time constant. This can be helpful in design and assembling equipment for microcolumn LC.

COLUMN DEVELOPMENTS

Different filling techniques have been reported for the preparation of packed capillary LC columns, applying gases [66-68], supercritical fluids [67-71] or liquids [72,73] to transport the stationary phase particles into the column. For micro LC columns liquids are used exclusively to pack columns [74,75]. The basic concept of these packing techniques remains however the same: a frit – composed of a metal screen, glass wool, polymeric membranes or condensed silica particles – is mounted at one of the end of the column blank, and the particles are pushed into the columns from the other side. Basically, the packing process can be regarded as filtration.

The separation efficiency of microcolumns is influenced by a large number of parameters – not only so-called packing parameters like solvent selection, packing pressure, slurry concentration, the use of surfactants to stabilize the particle suspension, slurry vessel dimensions, etc. [76-82] – but also by column parameters like column blank material, frit selection, etc. [76,83-86]. The majority of these suggested packing techniques are empirically developed and mainly based on assumptions and trial and error methods. Nevertheless, good, efficient microcolumns can be produced by the packing methods described above, and their performance regarded as optimal – i.e. reduced plate heights near 2 – according to classical chromatographic theory.

Some research groups have tried to develop a better understanding of the packing processes – incorporating colloid chemical studies, filtration theories and stress behaviour during bed compression [69,87-90]. Although certain trends could be assigned with these studies, a sound theoretical description and understanding of packing methods for microcolumns is not available yet. For example, Vissers et al. [87,88] related the coagulating properties of a number of octadecyl reversed phases in different slurry and packing liquids with the final chromatographic performance of microcolumns. They found that coagulation of stationary phase particles is of less importance than normally is assumed. Tong et al. [69] developed a shear stress model to describe particle movement during column packing with supercritical fluids. It was found that relatively low packing pressures yielded more dense packing structures. However, no quantitative relationships were given. Furthermore, novel packing techniques – applying continuous vibration of the stationary phase slurry suspension with the aid of an ultra sonification probe – do not seem to produce significant better columns in terms of efficiency and column lifetime [91].

At present, columns with an i.d. of ~ 200–300-µm are the subject of many papers. There is however a tendency to use columns with an even smaller i.d. Driving forces towards this even further miniaturization are the use of such columns in capillary electrochromatography (CEC) [91-93] and electrospray ionization mass spectrometry (ESI-MS). In CEC columns with an i.d. of 50–100-µm are required to prevent Joule heating of the mobile phase, whereas in LC-ESI-MS the use of 50–100-µm i.d. LC columns leads to a tremendous increase in sensitivity of the electrospray interface. A detailed description of both techniques is beyond the scope of this chapter though.

There is however also a scientific interest in the use of very narrow fused silica capillaries. Several research groups [63,65,94,95] reported that the plate height of packed columns reduces by a factor of approximately 2 when the column to particle diameter ratio – also known as the Knox-Parcher ratio – is smaller than 6. Classical plate height equations suggest however that the column diameter does not influence the plate height of packed columns – as indicated by the following simplified Horvath-Lin equation:

$$H = \frac{1.4 D_m}{u} + 1.5 d_p + \frac{2}{5} \frac{\left(k_0 + k + k_0 k\right)^2}{\left(1 + k_0\right)^2 \left(1 + k\right)^2} \frac{d_p^2}{D_m} u \tag{2.4}$$

where D_m the diffusion coefficient of the analyte in the mobile phase, u is the linear mobile phase velocity, k_0 is the ratio of the interparticle void volume to the interstitial void volume in the column, and d_p is the particle diameter.

This contradiction between theory and experimental observations was explained by Kennedy and Jorgenson [63] by the fact that inhomogeneities in mobile phase flow paths are strongly reduced due to the more uniform cross-sectional packing structures of such small i.d. packed columns, resulting in flow paths of almost identical permeability. Peak dispersion is reduced since only wall-ordered packing structures are possible. The decrease in the packing structure variation gives also rise to more uniform retention factors, reducing column bandbroadening. Both effects contribute to the decrease to bandbroadening. Finally, small column i.d.s allow for more rapid transcolumn diffusion between all possible flow paths and retention regions, enabling the analyte to diffuse across the entire column cross section. The smallest published reduced plate heights equal 1.0 for almost unretained compounds and 1.2–1.3 for slightly retained compounds using 5-μm reversed octadecyl modified particles [95].

INSTRUMENTATION

Solvent delivery and gradient systems

The flow spectrum for miniaturized high performance liquid chromatography systems discussed in this paper runs from the nl to μl per minute scale for 50-μm i.d. up to 1.0 mm i.d. columns, respectively. At the present time and state of the technique reciprocating and syringe pumps are favourite solvent delivery systems for conventional and for microcolumn LC as well. The reciprocating pumping systems are however favorable over syringe pumps for their large column back pressure compensation abilities, rapid flow equilibrium and stability and good possibilities for micro-gradient delivery [96-102]. Especially the rather time-consuming flow equilibrium due to eluent compressibility and viscosity, and difficulties in the mixing of micro-flows for gradient analysis are inherent to syringe pumps. Moreover, column pressurization is a very time consuming task at low flow rates and can increase gradient delays significantly when syringe pumps are applied. For flows in the order of 50–150 μl min⁻¹ reciprocating

and syringe pump systems are commercially available, including in most cases devices for binary, ternary or quaternary gradient formation. These delivery and gradient systems have proven to be useful down to column i.d.s of approximately 1.0 mm.

The delivery of flows in the nl and the low µl-range for columns of i.d.s of approximately < 500-µm cannot be readily performed by direct pumping. For such flows the use of split-flow techniques can be an attractive alternative. These systems are based on the application of packed restrictor columns [96,103,104] or flow splitting devices based on a microflow processor concept [105]. Since this latter system compensates for viscosity changes of the eluent, e.g. during gradient analysis, it can be used in isocratic and gradient modes as well. For gradient analysis the microflow processor can be connected to a conventional gradient device, by which part of the flow is split in a constant adjustable ratio to the microcolumn.

Injection devices

Using Eqn. (2.3) the maximally allowed injection volume for different i.d. and length of columns can be estimated. For 50–100-µm i.d. columns injection volumes are in the order of a few nl up to approximately 1 µl for 1.0 mm i.d. columns. For manual and automated injection the majority of the present injection systems in high performance liquid chromatography consists of injection valves. Manual injections from the µl range down to approximately 20 nl can be routinely performed with (micro-) injection valves equipped with a replaceable internal loop. Below 20 nl manual valve injections can be performed by positioning a split vent between the injector and the column [54]. Alternatively, for these very small volumes the moving injection technique [106,107], the static split [108] or the pressure-pulse-driven stopped-flow injection technique [109] can be used too. These techniques have in common that by controlling the injection time and flow through the injector only a small part of the injection plug is injected on the top of the column. Automated injection in the µl range can easily be performed by many of the available autosamplers available on the market. Injection automation in the nl range usually requires a thorough adjustment of a conventional autosampler. Such modifications of conventional autosamplers for use in capillary LC have been described in literature [110]. Furthermore, the use of an automated micro-injector has been described [111]. With this latter system however, only one sample at the time can be injected. Recently an autosampler for the injection of very small samples has been described [112]. This commercially available injection devices claims the reproducible injection of 50 nl to 5 µl sample volumes from minute samples with nearly no loss of sample.

A general problem in microcolumn LC techniques is the loss of detection sensitivity due to the small injection volumes or masses. In a number of cases this problem can be overcome by the use of so-called on-column focusing techniques [113-116]. These techniques have in common that the sample solvent has a significantly lower eluent strength compared to the actual eluent. After arriving of the sample plug on the column top the compounds will be focussed in a small plug. Focusing enrichment factors of several hundreds have been reported, so significantly increasing detectability in microcolumn LC techniques. For example, for the separa-

29

tion of a test mixture consisting of resorcinol, benzaldehyde, phenol, nitrobenzene and toluene under reversed phase conditions a focusing enrichment factor of 200 in micro LC could be achieved resulting in similar chromatograms compared to a standard injections [114].

Since the loading time of a certain sample volume under focusing conditions increases at decreasing column i.d., this technique becomes impractical for capillary and nanoscale LC. This problem can be overcome by the use of packed precolumns, which must be properly connected to the analytical column and are essentially a part of the separation systems. The advantages of this approach are in the much larger sample flow rate, which can be obtained during the sample focusing step. In addition also the selectivity of the isolation of the sample compounds of interest can be controlled by the selection of a specific stationary phase in the precolumn [117-125].

Tubing and connections

Since the tubing, which is used to connect the different parts of the equipment, contributes linearly to its length and to the power four of its radius to the extracolumn band broadening variance, the selection of the connecting tube dimensions is extremely important. For columns of 500-µm–1.0 mm i.d. specially designed stainless steel tubing of 0.25 or 0.125 mm i.d. is usually applied. Alternatively, polyetheretherketone or fused silica tubing can be used for this purpose. For smaller i.d. columns the use of tubing is as much as possible avoided. Direct connections of the column to injector and detector are preferred or connecting tubing i.d.s of   50-µm are applied. Apart from the proper selection of the connecting tube i.d., the length of these tubes should be taken as short as possible to prevent loss in resolution. In addition, the different parts connecting the column to the injector and detector must be properly designed to avoid dead volumes and should be compatible with the applied devices in the microcolumn LC equipment.

Detectors

Refractive index detection. Refractive index (RI) detection has received only little attention in microcolumn LC and capillary separation techniques in general, although it is a widely applied detection technique in conventional high performance liquid chromatography due to its universal character. Modifications to existing commercially available RI detectors have been reported for the use of RI detection with micro LC columns [126-129]. These studies mostly involved the reduction of extracolumn bandbroadening effects and the demonstration of the separation of test-mixtures. For instance, Fujimote *et al.* [127] reported a limit of detection of 2-3 ng for dipentylphtalate separated isocratically on a reversed phase column. Synovec [129] studied the theoretical aspects of RI detection in more detail. Tracing diagrams for cylindrical detector flow cell designs were studied. Furthermore, RI detection was optimized for different eluent and flow cell conditions.

With capillary LC, RI detection is even more difficult due to the fact that RI differences have to be measured in extremely small volumes [130]. With the highly collimating nature of lasers, nanoliter to picoliter volumes can easily be probed. Laser based RI detection has among others been applied by Bornhop and coworkers [130-132] and Bruno et al. [133,134]. The capillary flow cell developed by Bruno et al. [134] is based on the so-called forward scatter, off-axis technique. With the use of an RI-matching fluid surrounding the capillary flow cell and active temperature control of the flow cell assembly improved performance is feasible. The limitations of this method are the off-axis alignment and the need to remove the polyimide coating of the fused silica capillary to math the refractive index.

A novel approach for measuring RI changes in capillary separation techniques is reported by Tarigan et al. [130]. With this technique the interference produced fringes are detected below the plane of excitation in a direct backscatter configuration. The spatial shift in the fringes is a measure of the refractive index for the fluid streaming through the capillary flow cell. Flow cells with i.d. of 75–775-µm were probed with no modification to the polyimide coated capillary flow cell, no changes in the optical set-up, and no reduction in the signal-to-noise ratio. The optical configuration of such a system is very straightforward. It consists of a He-Ne laser, a thermal controlled flow cell assembly, and a silica photodetector to collect the reflected light. The flow cell assembly is tilted slightly to allow detection by the photodetector. With flow injection analysis 3.2 pg of glycerol could be detected in a probed volume of approximately 2.6 nl. The change in RI at three times the standard deviation of the noise was for this flow cell volume equal to $1.9 \cdot 10^{-7}$ RI units. The detector response was found to be linear over a dynamic range of three decades.

UV absorbance detection. The most universally applied detector – in conventional and microcolumn LC – is the UV absorbance detector because of its ease of use and broad application area. To prevent extracolumn bandbroadening – i.e. keeping detection volumes at the submicroliter or nanoliter level – on-column detection is often a first approach. A packing-free part of the column is used as the optical window – i.e. detector cell – and is brought into the light path of an UV absorbance detector. The construction of such a cell has been discussed [135,136]. Vindevogel et al. [137] developed design guidelines for tubular UV absorbance detection flow cells. Their study involved the investigation of parameters like reflection of the incident light on the capillary wall, the distance between the photodetector and the flow cell, changes in the refractive index of the mobile phase, different cell designs, wavelength, and the linearity and noise. Due to the large variety of configurations no general recommendations were given. Further it was suggested that not only the i.d. of the flow cell in this type of studies should be mentioned, but also parameters relating to light beam width and photocell distance should be used in the description of a flow cell.

The main disadvantage of on-column detection is the limited concentration sensitivity because of the limited path lengths. Limits of detection reported for on-column detection are typically around $1–5 \cdot 10^{-6}$ mol l⁻¹ for compounds like uracil, cytosine and thymine with a 100-µm i.d. flow cell [138]. Despite the extremely small path lengths, detection is feasible at the

subnanogram level. Fiber optics have been suggested to collimate the excitation light onto the flow cell and for the collection of the UV light that has passed through the flow cell [139,140]. The limits of detection that were obtained with this system are however not favorable compared to on-column detection. A more successful approach towards improvement of the detection sensitivity with UV absorbance detection in microcolumn LC was the introduction of longitudinal flow cells with an optical path length up to 3–8 mm [141]. This type of flow cell and on-column flow cells have been studied extensively with respect to sensitivity, linear dynamic range, and its contribution to extracolumn bandbroadening and noise [138,142]. The sensitivity of longitudinal type of cells is normally 50–100 higher compared to on-column detection. However, the noise of longitudinal cells is generally somewhat higher than those with on-column UV detection. Consequently, limits of detection are about 25–50 times lower compared to on-column detection. For instance, the limit of detection for uracil with on-column detection was $3.1 \cdot 10^{-6}$ mol l^{-1} and with the longitudinal flow cell equal to $9.8 \cdot 10^{-8}$ mol l^{-1} [138]. The contribution of longitudinal flow cells to extracolumn bandbroadening, i.e. chromatographic resolution, is generally negligible.

Laser based UV absorption detection has been applied in capillary separation techniques too [131]. This system consisted of a dual laser set-up, optical devices like polarizers, a quarter wave plate, lenses and objectives, and a photodiode. Simultaneous RI and UV absorbance detection was feasible. Limits of detection were $6 \cdot 10^{-6}$ M for a strongly absorbing compound. Considering the complexity, costs and sensitivity of such a set-up the use or on-column detection of longitudinal shaped flow cells seems to be favourable.

Photodiode array (PDA) detection has been studied extensively in microcolumn LC research [143-147]. In practice it is however hardly applied for structural conformation detection. For example, Verzele et al. [144] adapted two commercially available PDA detectors for capillary LC by replacing the detector cell by a miniaturized detector cell. Cell designs – with respect to loss in spectral resolution due to extracolumn bandbroadening – were discussed and the sensitivity of conventional versus capillary LC compared. 10 times better limits of detection were found with capillary LC – despite the small optical path length of the PDA flow cell. Another example is the work of Sandra et al. [143], who applied PDA detection in capillary LC for the detection and identification of hop bitter acids from CO_2 extracted hop samples. The recorded PDA UV spectra showed that two groups could be differentiated: α-acids (humulones) and β-acids (lupulones). This capillary LC separation showed to be favourable compared to conventional high performance liquid chromatography and micellar elektrokinetic chromatography because of the insufficient resolution obtained on conventional columns and solubility problems in micellar elektrokinetic chromatography respectively.

32

Fluorescence detection. Among the various miniaturized detection techniques, fluorescence detection seems to be particularly attractive. Fluorescence emission provides more selectivity and increased sensitivity compared to UV absorption and RI detection. Further, emission spectra can be utilized to reveal structural information of unknown compounds [148,149], and the ability to measure in the packing of the column [150,151].

Straight-forward on-column fluorescence detection is hardly applied in microcolumn LC. Most applications deal with laser-induced fluorescence detection or – as mentioned earlier – detection of fluorescence emission in the packing. Exceptions are the work of Gluckman et al. [148,149] who used a miniaturized fluorimetric array detector for the detection and identification of large polyaromatic compounds. The utility of fluorescence emission data was represented by comparing mass spectral data and the emission spectra from well resolved peaks from a separation of neutral polycyclic aromatic compounds extracted from fuel oil. Based on the mass spectra alone the compounds could not be identified. Spectral subtraction was used to resolve coeluting compounds, which can be an important tool in the identification of compounds contained in complex sample mixtures or the determination of peak impurity. Takeuchi et al. [154] studied the mass detection limits achievable with a commercially available fluorescence detector in capillary LC. By tiling the photomultiplier, using cut-off filters and a packed flow cell, mass detection limits of 0.25–2.4 pg were obtained for aromatic hydrocarbons. In a separate paper the design of this packed flow cell was described [155]. Fluorescence detection has also been applied in environmental studies for the analysis of organotin species complexed with fluorescent tags [156], and for the analysis of water tracers to study distribution phenomena on the North Sea [122]. Another field where fluorescence detection is applied is in bioanalysis, in particular for the analysis of glutathion in human blood samples [157]. Especially the latter application is of great interest. Due the reduced chromatographic dilution on small i.d. columns, less sample is required to achieve the same limits of detection as in conventional high performance liquid chromatography. Hence, a patient can be sampled more often without putting too much burden on the patient.

In the section on UV absorbance detection of this chapter, the term on-column detection was introduced to describe the measurement of electromagnetic radiation in a detection window after the end-frit of the column. The same name has been used by others for the measurement of fluorescence emission in the packing [151-153]. Interchangeable use of this term should be circumvented. Verzele and Dewaele [150] therefore suggested to use the term in-column detection for the measurement of emission light in the packed part of the column, which will be followed in this paper. With in-column detection the analyte is in a partitioning region. It can be deduced that the sensitivity of in-column detection will be $(1 + k)$ times better than with on-column detection [153]. This effect was demonstrated by Verzele and Dewaele [150], who found limits of detection of 3 pg with on-column fluorescence detection and about 100–200 fg with in-column detection for the analysis of drugs. According to the authors this improvement in sensitivity was in agreement with what theoretically had to be expected. However, the environment in which the analytes reside – e.g. in solution or in an absorbed state – are usually different, which results in different fluorescence characteristics. For instance, improvements in limits of detection of a factor of 100 were reported when the in-column detection principle was applied for the detection of pyrene [151], which was attributed to the higher fluorescence quantum yield in the absorbed state. Takeuchi et al. [158,159] reported similar effects in signal enhancement for in-column detection in capillary columns packed with cyclodextrin-bond stationary phases.

33
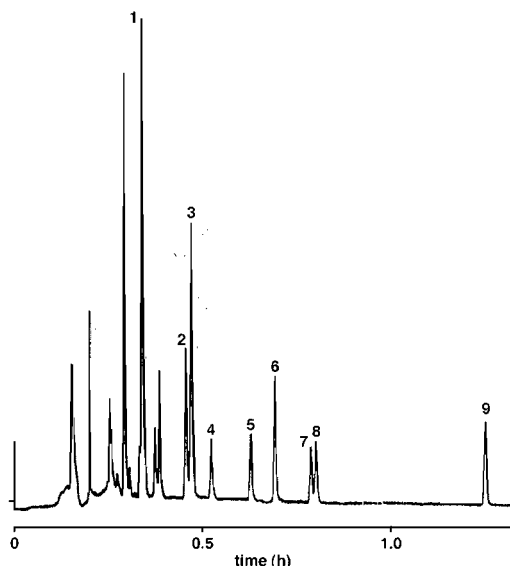
Fig. 2.3. Chromatogram of a standard mixture of bile acids derivatized with bromomethylcoumarin. Column: 0.66 m x 250-μm i.d. packed with 5 μm C_{18}; continuous gradient from 75–100% aqueous acetonitrile at 1.5 μl min^{-1}. Peak identification: (1) glycocholic acid; (2) glycocheno-deoxycholic acid; (3) glycodeoxycholic acid; (4) cholic acid; (5) urodeoxycholic acid; (6) glycolitocholic acid; (7) deoxycholic acid; (8) chenodeoxycholic acid; (9) lithocholic acid (reprinted from *J. Chromatogr.*, 317, Gluckman *et al.*, Laser fluorimetry for capillary column liquid chromatography: high sensitivity detection of derivatized biological amines, 443, ref. [165], Copyright (1984) with kind permission from Elsevier Science).

The major draw-back of in- and on-column fluorescence detection is the rather poor sensitivity compared to longitudinal UV-absorption flow cells and to conventional high performance liquid chromatography with fluorescence detection. The reason for this limited detection performance is the short optical path length and small excitation area of on-column flow cells. It is obvious that for a higher excitation energy, a larger fluorescence intensity will be observed. This will however not immediately lead to better limits of detection, unless the noise – e.g. stray light, fluorescence from the cell wall or window and fluorescence or Raman scattering from the mobile phase – is independent on the intensity of the excitation source [160]. Due to the highly collimating nature of lasers, most of these noise sources – especially the fluorescence and Raman scattering of the solvent – can be strongly reduced. Furthermore, nanoliter to picoliter volumes can be probed at the outlet of the column. Various flow cell designs and instrumental set-up's for laser-induced fluorescence detection have been described in literature. More detailed discussions about flow cells and illumination options can be found elsewhere [160,161]. More recent designs, properties and descriptions of laser-induced fluo-

rescence detection for microcolumn LC can be found in literature too [162,163]. Mass limits of detection – routinely obtained – are typically in the amol range.

Some interesting work – applying laser-induced fluorescence detection in microcolumn LC – has been published by Novotny and coworkers [164,165] and by McGuffin and Zare [166]. McGuffin and Zare [166] detected and analyzed carboxylic acids – after derivatization with 4-bromomethyl-7-methoxycoumarin to match the emission wavelength of an He-Cd laser (325 nm) – in saponified peanut and sesame oils. The compounds were identified on retention time. An almost similar tag was used by Gluckman *et al.* [165] for the analysis of bile acids and solvolyzed plasma steroids. A steroid standard – containing nine standard bile acids of approximately 50 pg of each acid – was separated on a capillary LC column, of which a chromatograms is shown in Fig. 2.3. The experimental conditions are summarized in the caption of Fig. 2.3.

Electrochemical detection. The three basic detection modes of electrochemical detection are amperometric and potentiometric detection, and conductivity. The principle of these different detection modes can be found in many text books [23,167] and literature [16]. Amperometry is the most commonly used because of its ease of implementation. However, the design and application of conductivity and potentiometric detectors for microcolumn LC have been described too [168-172].The initial developments in miniaturized electrochemical detection – or the use of micro-electrodes – were reported for open tubular liquid chromatography by the groups of Manz [173,174] and Jorgenson [175,176], which were later also applied in microcolumn LC [63,95,177]. Such detectors typically consist of a small wire that is placed into the outlet of an open tubular column. For instance, Manz and Simon [173,174] used an 1-μm diameter ion-selective electrode for the potentiometric detection of K$^+$ ions. Jorgenson *et al.* constructed a 9-μm diameter carbon electrode for the amperometric detection of catechols and ascorbic acid [175], and for the voltametric analysis of hydroquinone and catechol. Detection limits achievable with these detection schemes are in the fmol–pmol range.

Many different cell designs for electrochemical detection can be found in literature. Very simple, cost-effective flow-through cell designs for amperometric detection in capillary LC were demonstrated by Ruban [178,179]. The cell construction of one of these detectors is depicted in Fig. 2.4. The proposed design permitted the use in capillary LC, e.g. no significant bandbroadening was observed. Mass limits of detection of 0.14 pg for adrenaline were reported. Other designs, like wall-jet cells have been described too [180,181].

As stated before, amperometric response is the most commonly used detection mode in microcolumn LC. However, since the potential of the electrode is hold at one value, only compounds that are easily oxidized and reduced at the set potential are detected. By scanning the potential – or by applying triangular potential waveform to the electrode – the number of detectable components that are electroactive in the applied potential range may increase [16,182]. The latter technique is called voltametric analysis and can provide – if the waveform is applied quickly enough – real-time voltametric scans from components eluting from a micro or capillary LC column. Thus, analytes can be identified and co-eluting peaks resolved if there
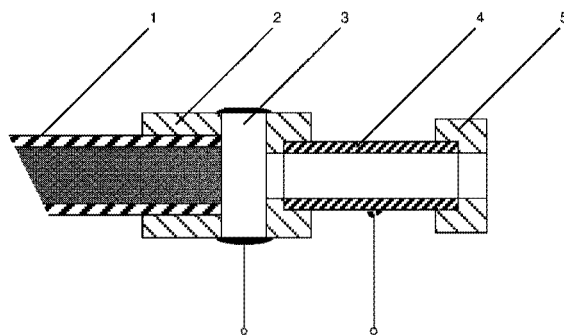
Fig. 2.4. Cell construction of an amperometric detector. 1. capillary LC column; 2. fluoroplastic body; 3. working electrode; 4. reference electrode (reprinted with permission from V.F. Ruban, *J. High Resol. Chromatogr. Chromatogr.* 13 (1990) 112, ref. [178]).

voltagrams are significantly different. The major limitation of voltametry is the approximately 100 times worse mass sensitivity compared to amperometric detection [16].

Voltammetric detection has been applied in open tubular chromatography [175,176] and conventional liquid chromatography [183-185], but has found only little acceptance in microcolumn LC so far. An exception is the work of Goto and Shimada [182] who presented a rapid-scanning electrochemical voltametric detector for capillary LC. Square-wave voltametries were applied because of their suitability for rapid-potential scanning.

The main application area of electrochemical detection in microcolumn LC is bioanalysis. The detection of serotonin and its metabolites in rat brain dialysate [186], the analysis of terbutaline in human plasma [187] and the detection of biogenic amines in brain tissue [188] are just a few examples. A more detailed description about the use of electrochemical detection in bioanalysis will be given in the section applications of this chapter.

Gas Chromatographic detectors. Microcolumns are typically operated – as shown earlier – at volumetric flow rates of a few microliters per minute for capillary LC columns and 30–50 microliters per minute for micro LC columns and are therefore more suited to work with detector systems currently used in gas chromatography (GC) than conventional sized high performance liquid chromatography columns. Obviously, the introduction of analytes dissolved into a detection zone at elevated temperatures – or a flame – is a fundamental problem. Although successfully applied in certain fields, compromises have to made with respect to linearity, sensitivity and capability to accept the complete effluent and all of the compounds, with GC detectors in microcolumn LC.

The LC eluent can either be transported into the GC detector, or be directly introduced [18]. The first approach has the main disadvantage of the very likely risk of sample loss and is therefore hardly applied as an interface. Tsuda *et al.* [186] and Veening *et al.* [190] have reported on the use of a moving-wire flame ionization detector for capillary and micro LC

respectively. Typical mass limits of detection were 10–20 ng for triolin with the capillary LC system, and 160 and 400 ng for xylose and lactose with the micro LC system.

Shortly after the introduction of microcolumn LC, various types of direct introduction based GC detectors – flame-based and flameless thermionic detection, flame photometric detection, and electron capture detection – were evaluated by different research groups.

Thermionic detection. Novotny and coworkers [191-193] introduced a flame-based thermionic detector (TID) as a detection technique in capillary LC. The microcolumn LC mobile phase is nebulized with a hydrogen/nitrogen mixture into a primary flame. The combustion products are combined with additional fuel gas and are transported into the secondary, analytical flame. This dual-flame thermionic detector was optimized for organophosphorus compounds, i.e. organophosphorus pesticides. The mass sensitivity of detection for phosphorus compounds was equal to 20 pg s^{-1} and the response was found to be linear over at least three orders. The same thermionic detector has been used for selective nitrogen detection [194]. Mass detection limits were of the same order of magnitude as with selective phosphorus detection, i.e. 14 pg N s^{-1}, and a linear response of three orders as well. The use of nitrogen selective detection was demonstrated for the analysis of barbiturates.

Kientz *et al.* [195,196] demonstrated the use of thermionic detection for non-volatile polar compounds. The system performance was found to be dependent on the mobile phase modifier concentration. Further it was found that relatively high buffer salt concentration could be tolerated. The introduction of non-volatile samples into the flame was achieved by plug-type solvent introduction. Detection limits were comparable to that published by Novotny and coworkers. Flameless thermionic detection was studied by Brinkman and coworkers [197-199] for trace-level detection of organopesticides in environmental samples and different vegetables.

Flame photometric detection. Detector designs for flame photometric detection are very similar to those of thermionic detectors [191,200]. The main disadvantage of flame photometric detectors is the sensitivity dependence of modifier concentrations. Further, acetonitrile significantly increases the background noise and quenches the detector signal at even low percentages. Various interface designs have been proposed to overcome these problems [201-205]. Kientz and Brinkman [18] recently summarized and discussed the advantages and limitations of the use of flame photometric detection in microcolumn LC.

A very interesting application using flame-based photometric type of detection has been published by Chang and Taylor [203]. Detection was based on the chemiluminescence reaction of ozone with sulfurmonoxide – a combustion product when sulfur containing compounds are introduced into a reducing hydrogen/air flame. The compounds were reduced in the flame of a commercially available flame ionization detector. Operated at optimized conditions, mass detection limits are feasible of 3 pg S s^{-1} at a mobile phase composition of methanol/water (50:50, v/v). The performance of the detector was demonstrated by the analysis of PTH-amino acids and thiocarbamates, which are normally detected with UV absorption or PDA detection. The separation and detection of several PTH amino acids is shown in Fig. 2.5.
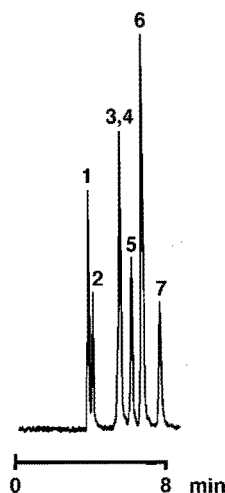
Fig. 2.5. Capillary LC–sulfur selective chemiluminescence detection analysis of PTH amino acids. Mobile phase: methanol/water (50:50, v/v); column: 0.15 m x 320-μm i.d.; 3-μm C_{18}; detector temperature: 375°C; sample 3–6 ng of each compound. (1) PTH-alanine; (2) PTH-proline; (3) PTH-methionine; (4) PTH-phenylalanine; (5) PTH-leucine; (6) PTH-norleucine (reprinted with permission from ref. [203]. Copyright (1991) American Chemical Society).

Electron capture detection. There are only a few publications that deal with electron capture detection in microcolumn LC. Brazhinov *et al.* [206] used an electron capture detector to determine extracolumn bandbroadening. This to examine its usability for 1.0 mm i.d. micro LC column testing under normal phase conditions. The application of electroncapture detection with reversed phase analysis at flow rates up to 50 μl min⁻¹ was demonstrated by Brinkman *et al.* [207]. The column effluent was evaporated with the aid of a miniaturized interface. However, clogging of the interface occurred occasionally when non-volatile acidic modifiers were applied. Furthermore, the interface clogged more rapidly at lower mobile flow rates. Hence, reversed phase capillary LC with this type of interface is not feasible.

Zegers *et al.* [208] described recently an interface for the direct coupling of reversed phase capillary LC with electron capture detection. The interface consists of a piece of fused silica capillary that is positioned in a stainless steel capillary that connects the capillary LC column with the detector. A make-up gas had to be used to cool the fused silica capillary. The interface allows for the detection of relatively non-volatile and polar compounds. Results were demonstrated for the analysis of chlorophenols, pesticides and benzodiazepines. The response of the system for all classes of compounds was linear over two to three orders and the limits of detection ranged from 10–440 pg. With large volume injections the concentration sensitivity could be increased by two to three orders of magnitude allowing for the detection of approximately 150 ng l⁻¹ of chlorophenols in river Meuse water.
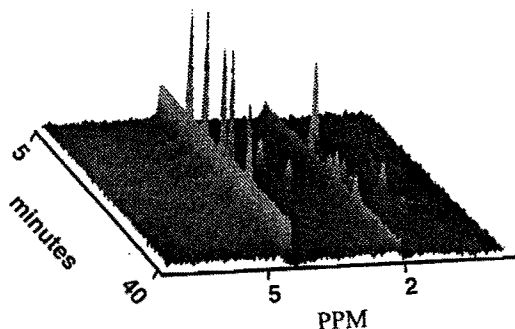
Fig. 2.6.. Two-dimensional chromatogram of a mixture of 67 mM alanine, 33 mM arginine, 35 mM lysine, 14 mM leucine-arginine and 11 mM oxytocin-glycine (order of elution). A complete NMR spectrum was acquired every 9 s which was constructed from 64 consecutive scans with a 0.06 s pulse delay (512 point free induction decays over a ± 4000 Hz spectral window). The micro LC system comprised a 0.15 m x 1.0 mm i.d. column packed with 5 μm C_{18} that was operated at a flow rate between 10 and 50 μl min^{-1}. The mobile phase consisted of 2% TFA in D_2O (pD 2.4)/CD$_3$CN (74:26, v/v) (reprinted with permission from ref. [218]. Copyright (1994) American Chemical Society).

Other detection principles. Besides the detection techniques discussed, other principles of detection have been studied for microcolumn LC too, including (Fourier transform) infrared spectrometry – either measured online [209] or via deposition on thin layer plates [210], chemiluminescence [211], indirect detection schemes [212-214], inductively coupled plasma atomic emission spectrometry [215], or evaporative light scattering [216]. These detection techniques have been applied with only limited success and have not found – mainly due to the fact that the detection technique is too selective or not robust enough – their way into the routine use of microcolumn LC.

A very interesting and promising novel approach towards detection miniaturization is the coupling between continuous-flow techniques – such as microcolumn LC and capillary electrophoresis – and nuclear magnetic resonance spectrometry (NMR) [217-219]. The hyphenation of microcolumn LC with NMR has a number of advantages compared to the coupling of conventional high performance liquid chromatography with NMR spectroscopy. Fully deuterated solvents can be used due to the low solvent consumption. Suppression of the solvent signal is therefore not necessary allowing the use of the complete chemical shift range for structural elucidation of the analytes. Furthermore, theoretical and feasibility studies have shown that a 400-fold reduction in cell volume only results in a 2-fold reduction in signal-to-noise ratio, allowing the use of 50 nl volume continuous-flow NMR detection cells. Shortcomings of continuous-flow NMR are the poor sensitivity due to limited time to measure each individual analyte and the flow rate dependency of the NMR line with. Typical analyte concen-

trations are at the high mM level. Further, substantial bandbroadening – e.g. loss in chromato-graphic resolution – is observed in NMR flow-trough cells. However, this is often compensated by the profits of structural information detection of NMR.

Continuous-flow detection allows for the use of proton-NMR chemical shift values as the second dimension, which was demonstrated for the separation of amino acids and peptides [218], and vitamine A derivatives [219]. Two-dimensional NMR spectra can be recorded with stop-flow techniques. An example of a two dimensional chromatogram of a amino acid/pep-tide mixture is given in Fig. 2.6. The number of theoretical plates that was observed for ala-nine at a flow rate of 50 µl min^{-1} equalled 20000 plates m^{-1}, indicating very poor separation efficiency or excessive extracolumn bandbroadening.

HYPHENATION

Multidimensional chromatography

As with flame-based detectors, microcolumns are well suited for the coupling with sec-ondary separation techniques, i.e. multidimensional chromatography. Microcolumn LC has been interfaced with thin layer chromatography applying infrared detection [220], conven-tional high performance liquid chromatography [221], microcolumn LC [222-224], gas chro-matography [225-231], supercritical chromatography [232] and capillary electrophoresis [233]. The coupling of individual separation techniques increases the total peak capacity of the chro-matographic system, which is equal to the product of the peak capacities of the individual dimensions. The improved peak capacity allows for the separation of very complex samples.

The coupling of microcolumn LC with gas chromatographic (GC) techniques seems to be the most challenging since a liquid mobile phase has to be converted into a GC compatible – i.e. gaseous – sample. Different type of interfaces have been developed. Among them are retention gap based interfaces like on-column injectors [225] and loop-type interfaces [226], pyrolysis interfaces and (multi-capillary) stream splitters. The retention gap based interfaces have been applied most extensively because of its ease of use. Retention gaps were originally developed for the introduction of large sample volumes onto GC columns. An uncoated inlet capillary – having negligible retention for the compounds of interest – is placed in front of the GC column. The large solvent volume is vaporized and the solute bands – that were spread out along the retention gap – are concentrated at the beginning of the separation column. An example of the successful application of an on-column injector as an on-line interface for microcolumn LC-GC is given in Fig. 2.7, illustrating the two-dimensional separation of a fuel oil sample. Heart-cutting was applied to introduce a part of the first dimension onto the secondary separation system. With heart-cutting techniques only a fraction of the original sample is separated, with a peak capacity that is typical for a single dimension.

The full power of a two-dimensional separation system was used by Holland and Jorgenson [222] to separate biological amines with anion exchange chromatography coupled to reversed phase chromatography. Via a loop type interface, samples from the first dimension were tem-
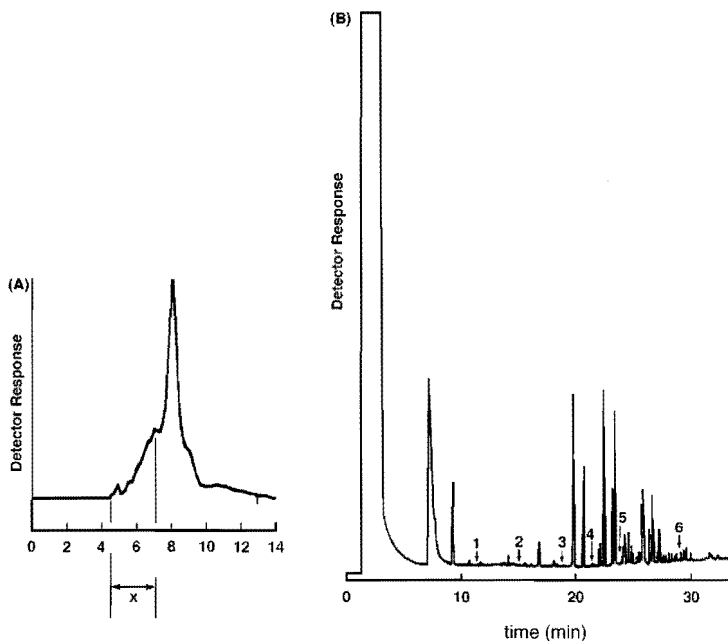
Fig. 2.7. Two-dimensional separation of a fuel oil sample by microcolumn LC-GC. (A) capillary LC chromatogram; (B) gas chromatogram; x = fraction introduced into the GC. Conditions capillary LC separation: column: 105 cm x 250 µm i.d. packed with 7 µm silica; mobile phase: heptane; flow rate: 10.6 µl min^{-1}; UV absorption at 214 nm. GC conditions: column: 30 m x 0.25 mm i.d.; retention gap 15 m x 250-µm fused silica; helium at 70 cm s^{-1}; flame ionization detection at 275°C (make up gas: nitrogen at 30 ml min^{-1}); oven at 105°C for 9 min and programmed to 245°C at 5°C min^{-1}. Peak identification: (1) chlorobenzene; (2) 1,2-dichlorobenzene; (3) 1,2,4,5-tetrachlorobenzenen; (4) 1,2,3,4-tetrachlorobenzene; (5) pentachlorobenzene; (6) hexachlorobenzene (reprinted from J. Chromatogr., 296, Cortes et al., Determination of trace chlorinated on-line multidimensional chromatography using packed-capillary liquid chromatography and capillary gas chromatography, 55, ref. [225], Copyright (1985) with kind permission from Elsevier Science).

porarily stored, before the were transferred to the second dimension. To obtain a high sampling frequency, the 90 cm x 100-µm i.d. anion exchange column was operated at a flow rate of 33 nl min^{-1}, while the flow through the secondary 3 cm x 100-µm i.d. reversed phase column was maintained at 6 µl min^{-1}. The peak capacity of the two-dimensional system was estimated to be 1400 peaks.

Another attractive way to achieve high sampling frequencies is to use capillary electrophoresis (CE) as the second dimension, which allows to obtain high efficiencies in short periods of time. Lemmo et al. [233] applied a two-dimensional separation system for the study of protein standards based on microcolumn size exclusion chromatography (SEC) and CE. Two
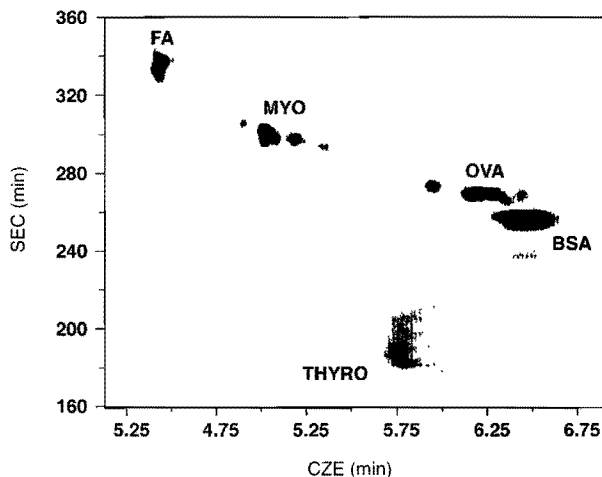
Fig. 2.8. Separation of protein standard by two-dimensional SEC-CZE with a flow gating interface. Each protein was present at 0.5% (w/v) with 2.5% (w/v) formamide. THYRO = thyroglobulin; BSA = bovine serum albumin; OVA = chicken egg albumin; MYO = horse hartmyoglobulin; FA = formamide. The 110 cm x 110 µm i.d. SEC column was operated at a flow rate of 20 nl min^{-1}. Injection was 8 min at 7 bar. The electrophoresis capillary had a length of 53 cm (33 cm to the detection window). CZE conditions: 30 s electromigration injection at 0 kV and 4 min overlapped runs at -11 kV. The actual CZE run time was 8 min. The buffer used for both separations was 10 mM tricine, 25 mM Na$_2$SO$_4$, 0.005% sodium azide (w/v), pH 8.23 (reprinted with permission from reference [233]. Copyright (1993) American Chemical Society).

approaches were presented – a loop/valve interface and a so-called flow gating interface. The chromatographic SEC dimension consisted of a 105 cm x 250-µm i.d. or a 110 cm x 100-µm i.d. column packed with a size exclusion stationary phase. The flow through these columns was 235–360 nl min^{-1} or 23 nl min^{-1} respectively. CE was performed in untreated 50-µm i.d. fused silica capillaries of different lengths. The applied voltage was ± 30 kV. Because of the relatively large dead-volume of the bores of the loop/valve interface it was only applicable for the coupling with the 250-µm i.d. SEC column, i.e. too much extracolumn bandbroadening. Furthermore, the loop/valve interface hampered continuous sample collection. With the flow gating interface – which basically consists of a teflon gasket having a 1 mm channel that is sandwiched in between two stainless steel plates – these problems were overcome. Injection into the CE capillary was achieved by selectively sending a transfer liquid flow through the teflon channel or to waste. When an injection was made, the SEC effluent was sent to waste. An example of the results obtained with the new type of interface is given in Fig. 2.8, which depicts the two dimensional separation of protein standards by SEC-CZE.

Microcolumn LC-Mass Spectrometry

The introduction of continuous flow fast atom bombardment and atmospheric pressure ionization techniques (electrospray and atmospheric pressure chemical ionization) have contributed to a very large extend of the current success of microcolumn LC and have been one of the major driving forces behind the development of microcolumn LC. However, other type of interfaces have been used for the coupling with mass spectrometry (MS) too. Among them are electron impact and chemical ionization and the particle beam interface. Interfaces like the moving belt interface [234] and thermospray-type of interfaces [235] are rarely applied in microcolumn LC. Microcolumns can either be directly coupled to the ion source or via transfer lines. The latter will obviously increase bandbroadening, i.e. decreasing the chromatographic obtained resolution. On the other hand, also the mass spectrometer will add to the overall bandbroadening.

Electron impact/chemical ionization (direct liquid introduction). Direct introduction of the microcolumn LC effluent into the source of the MS is sometimes applied. A recent study by Ranalder *et al.* [236] involved the separation and quantification of metabolites of retionic acid in human plasma. The column was directly coupled to the source of the MS and negative ionization conditions were obtained by coaxial introduction of reagent gas. Alborn and Stenhagen [237] reported on the connection of a 220-μm i.d. packed capillary LC column with an electron impact source for the analysis of plant extracts, phenolic acids and other polar compounds. Another interesting application of direct liquid introduction was published by Esmans *et al.* [238] who evaluated the system for the identification and detection of nucleosides in human urine after separation on a micro LC column. These are just a couple of examples of the use of direct liquid introduction interfaces for microcolumn LC-MS. Many others have been published. The advantages and limitations of microcolumn LC-MS with direct liquid introduction have been discussed by Lee and Henion [239].

Particle beam. The group of Capiello has published a number of papers on the design and performance of a modified particle beam interface in conjunction with capillary LC [240-242]. By increasing the orifice diameter of the aerosol generator, i.e. the coaxial helium tubing – droplet formation of the mobile phase on the end of the capillary transfer tubing was circumvented and aerosol formation promoted. Further a restriction was made in the capillary transfer tubing, which also aids the formation of an aerosol. Improved sensitivity was found of one order of magnitude compared to a standard particle beam interface with conventional liquid chromatography. The interface was applied for basic, neutral and acidic low volatile and thermally instable pesticides [242] and coumarins in plant extracts [240].

Continuous flow fast atom bombardment. The first successfully applied microcolumn LC-MS interface was continuous flow fast atom bombardment (CF-FAB), which has been applied mainly for the analysis and identification of biochemical compounds. This interface has been applied for the coupling with microcolumn LC since the mid 1980s, but its breakthrough came some years later when a 220 cm x 50-μm i.d. packed capillary LC column was coaxially interfaced with CF-FAB [243]. The dead-time of such a system – operated at a flow rate of ~

43
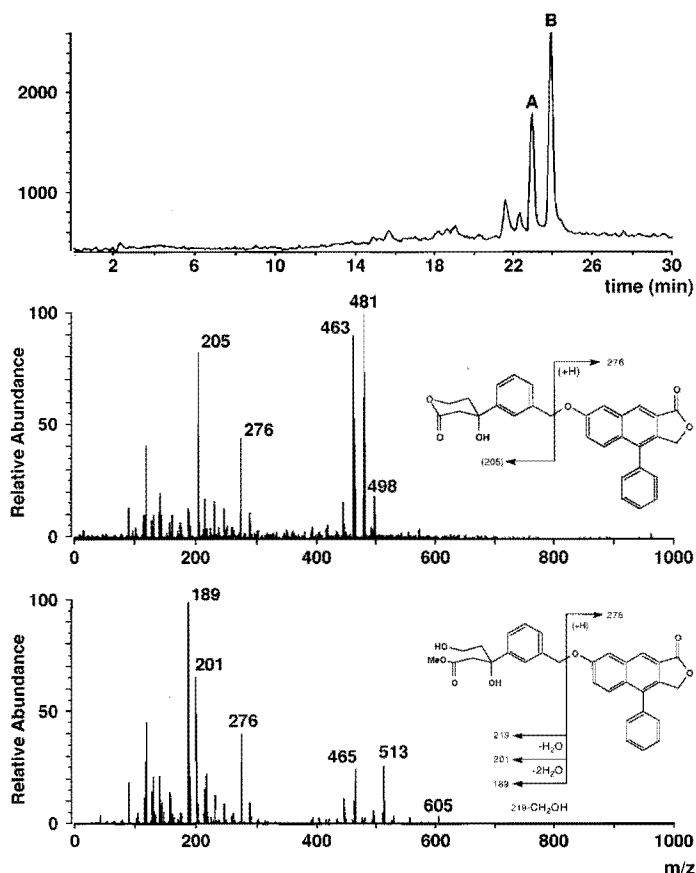
Fig. 2.9. Capillary LC-CF-LSIMS analysis (reconstructed ion chromatogram; m/z ~ 400–550 g mol⁻¹) of an isolated metabolite after treatment with CH_2N_2 (top) and positive ion LSIMS spectra of product A (middle) and its methylester product B (bottom). See text for details (reprinted with permission from ref. [250]. Copyright (1995) American Chemical Society).

30 nl min⁻¹ – is 79 min and found to be impractical. However, since then, the CF-FAB interface has undergone many modifications, making it a very attractive desorption ionization technique for polar and ionic compounds. CF-FAB is based on secondary ionization sputtering processes and requires a viscous matrix to produce ions. This matrix generally consists of aaqueous glycerol solution. The matrix solution can either be coaxially added to the column effluent [243,244] of post-column via an addition tee [245,246]. Alternatively, the glycerol matrix can be added to the mobile phase [247,248]. The latter will obviously affect chromatographic separation. Each interface design has its own advantages and limitations. The coaxial addition of matrix solution does not require any transfer tubing – therefore reducing extracolumn

bandbroadening. The transfer line interface – where the glycerol is added via a tee – permits for simultaneous on-line UV absorption and MS detection. Optimization of the separation and ionization conditions can be with both interfaces optimized independently.

The number of applications dealing with microcolumn LC-CF-FAB is extensive. In a recent review paper, Tomer *et al.* [249] summarized a large number of publications dealing with capillary LC-MS. In this paper two recent published examples will be discussed. Li *et al.* [250] applied capillary LC continuous flow liquid secondary ion MS (CF-LSIMS) – a technique very closely related to CF-FAB – for the rapid screening and identification of metabolites. Capillary LC-CF-LSIMS was used as a part of an integrated approach for discovery stage *in-vitro* metabolites. Excellent sensitivity was obtained in detecting model compounds in both the positive and the negative ion mode. Full scan mass spectra could be obtained when 5 pmol of compounds was injected onto a 10 cm x 300-µm i.d. capillary LC column. Fig 2.9 shows a typical example obtained with this system. Fig. 2.9 (top) corresponds to a reconstructed ion chromatogram of an oxidative metabolite that was – after treatment with CH_2N_2 – slowly converted into components A and B. In the bottom and middle trace of Fig. 2.9 the positive ion LSIMS mass spectra of product A and B are given respectively.

Li and coworkers [251] used cation-exchange capillary LC-FAB-MS in order to characterize reaction products after proteolytic cleavage of neuropeptides. A continuous bed, i.e. a gel that is covalently bond to the capillary wall, was used as the stationary phase material. The 15% glycerol make-up solution was added to the post-column flow via a zero-dead-volume tee. The potential of such columns for on-line mass spectrometry and peptide analysis was investigated. The system allowed limits of detection at the pmol level.

Electrospray ionization. Electrospray ionization (ESI) was almost simultaneously introduced with CF-FAB and has become a very popular techniques for the analysis of biochemical macromolecules. The coupling of an ESI-interface to microcolumn LC is relatively easy. A schematic representation of one of the earliest developed ESI-interfaces is given in Fig. 2.10 [252]. The liquid stream is introduced into the electrospray chamber at a flow rate of typically 5–20 µl min^{-1} through a stainless steel needle. This needle is grounded and the cylindrically shaped electrode is kept at -3.5 kV for positive ion detection. The metalized inlet and outlet of the glass capillary that passes ion-bearing gas into the first stage of the vacuum system are maintained at -4.5 kV and +40 V respectively. The skimmer is set at -20 V and the ion lens in front of the quadrupole at -100 V. To produce negative ions, voltage of the same magnitude but of opposite sign have to be applied.

As a result of the applied electric field, a part of the positive ions in the column effluent will drift towards the liquid surface and a part of the negative ions will be pushed away from it until near complete charge relaxation is achieved. The accumulating positive charge at the surface of the liquid leads to destabilization of the liquid surface, which is drawn out of the capillary downfield, forming a stable, conically shaped fluid yet. At higher voltages the tip of the the fluid cone starts to emit very small positively charged droplets; the so-called stable jet mode. The next step in the ionization process is the evaporation of solvent molecules from the

45
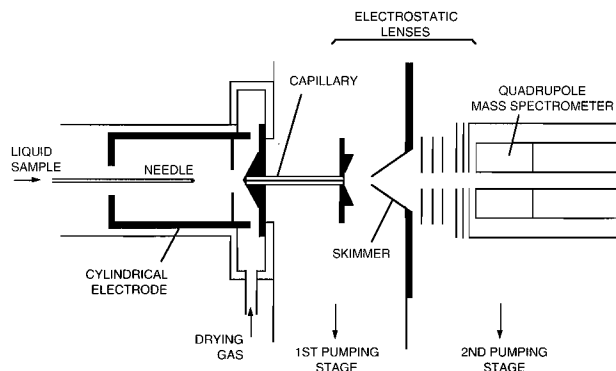
Fig. 2.10. Schematic representation of an electrospray interface (reprinted with permission from ref. [252]. Copyright (1985) American Chemical Society).

charged droplets, resulting in an increment in the charge to volume ratio, and to repeated disintegrations at the Rayleigh instability limit. Ultimately, positive gas-phase ions are produced. A detailed description of the mechanism of ESI is given in literature [253]. However, theory is not yet completely understood.

LC-ESI-MS interfaces have a near-linear relationship upon the concentration of the analyte making it an important tool in quantitative analysis. For instance, Whitehouse *et al.* [252] reported a linear behaviour of 4 orders of magnitude for their ESI interface. Furthermore, the mass spectrometer signal intensity was found to be almost independent of the liquid flow rate. Hence, ESI interface can be operated at extremely low mobile flow rates that are typically used with nanoscale LC columns, resulting in extremely low mass sensitivity limits of detection.

As with CF-FAB interfaces, ESI interfaces are coupled with capillary LC either directly or via a transfer line. The advantages and limitations of transfer lines have been discussed earlier. Primarily, applications of capillary and nanoscale LC-ESI-MS have been in protein and peptide analysis. An extensive overview of ESI-MS in conjunction with capillary and and nanoscale LC has been given in literature [249]. In the section applications some selected examples will be discussed, demonstrating the successful use of microcolumn LC-ESI-MS.

Microcolumn LC-MS is still in development. Current research is focussed on achieving even lower limits of detection. Just some examples are the coupling of microcolumn LC with matrix assisted laser desorption ionization (MALDI) techniques, the coupling of nanoscale columns with an ESI interface to an orthogonal time-of-flight mass spectrometer, and the use of micro LC columns with an ESI source interfaced to an ion trap storage/reflectron time-of-flight mass spectrometer [254].

Figure. 2.11. Total ion current chromatogram obtained from an on-line capillary LC-ESI-MS analysis of an *in-situ* digestion of a protein spot from a two-dimensional gel. The amount of protein was ~ 2 pmol. Peptide separation was conducted on a 180 μm-i.d. capillary LC column (reprinted with permission from ref. [257]).

APPLICATIONS

Microcolumn LC can be applied in many different fields. However, at present its main application areas are bioanalysis, neuroscience and protein/peptide research. In these cases, sample availability or mass spectrometric compatibility are often the driving force towards miniaturization. Other application areas are chiral separations and the analysis of industrial samples, e.g. polymers and additives. Some selected examples will be briefly discussed.

Protein/peptide research

The amount of applications that can be found in literature that deal with the analysis of biological compounds are numerous. Among the best examples of the use of microcolumn LC can be found in the protein/peptide research. For example, Henzel *et al.* [255-257] reported on the identification of proteins from two-dimensional gels by means of capillary LC and mass spectrometry. Typically, a protein is characterized by means of an *in-situ* digestion. The generated peptides are analyzed by means of MALDI-MS and with capillary LC followed by ESI-MS or by protein-sequencing. The combination of the analysis results of these three techniques finally leads to the complete amino acid sequence of the protein. A typical example of a

47

capillary LC separation of an *in-situ* digested protein spot is given in Fig. 2.11. The most demanding and laborious steps in these type of protein characterization techniques are still the manual sample preparation steps required to recover the protein from the gel. However, this example shows that capillary LC has produced significant advances in the development of capillary LC-MS in protein/peptide research.

Other, similar examples have been published by Yates *et al.* [258,259]. The tandem mass spectra of modified and unmodified phosphorylated peptides, and high molecular weight proteins isolated with two-dimensional gel-electrophoresis were used to determine the amino acid sequence of the peptide and proteins respectively. This method employs a reverse pseudo-mass spectral library search. For each amino acid sequence – that has some similarity to the sequence represented in the observed tandem mass spectrum – a library spectrum is predicted for the sequence and compared to the tandem mass spectrum.

Tempst *et al.* have published on the micro LC purification of peptides for combined chemical sequencing and MALDI-MS [260], and described in detail on the microcolumn LC assembly and fraction collection, sample handling and peak selection for sequencing [261]. A very experimentally orientated paper, i.e. description of the capillary LC system and sample preparation, has been published by Moritz *et al.* [262] on protein isolation and peptide mapping with capillary LC. Tryptic peptide maps derived from *in-situ* digested murine plasmacytoma were developed on an 0.2 mm i.d. capillary columns. Limits of detection were not given. Kassel *et al.* [263] evaluated packed capillary perfusion columns for the rapid sequencing of enzymatic digest with ESI-MS-MS. 180, 320 and 1000-μm i.d. LC columns – either packed with small pore materials or perfusion particles – were directly coupled to the ESI source of the mass spectrometer. Retention times were reduced by a factor of 3–5 with the capillary perfusion columns. Some loss in chromatographic resolution was found with the use of perfusion columns. However, capillary perfusion LC-MS permitted for the identification of the same peptide fragments at the 25–50 pmol level.

All previously discussed examples deal with MS as the identification method for the peptide fragments. Battersby *et al.* [264] demonstrated the characterization of recombinant DNA-derived human growth hormone (rhGH) isolated from an *in-vivo* rat model using capillary LC. The chemical changes that occur in rhGH following intravenous administration were identified on retention time. Prior to characterization, the protein of interest was isolated with an affinity column. The recovered protein was then digested and analyzed on a capillary LC column. Deamination and oxidation of rhGH were found to occur *in-vivo* and were identified on the sub pmol level (< 10 pmol).

48 *Chiral separations*

The chromatographic analysis of enantiomers is a rapidly growing research area, which also has been the subject of some microcolumn LC studies. Microcolumn LC is a very attractive technique for enatiomeric separations since it is possible to apply new types of stationary phases that are normally too expensive, e.g. monoclonal antibodies or receptor proteins [265].

Furthermore, the consumption of expensive stereoselective mobile phase additives is lower, and the chromatographic efficiency and selectivity higher. The latter is not yet understood, but experimental data show improved plate numbers and chromatographic separation factors on capillary LC columns.

Chiral separations can be achieved by the use of chiral stationary phases [265-270], a chiral selector that is adsorbed on the packing material [265,271,272] or by using chiral mobile phase additives [265,273-275]. For instance, Wännman et al. [265] reported on the separation of chiral ethanol and propanol derivatives on a Pirkle phase. The authors concluded that every originally developed method for chiral separations on conventional high performance liquid chromatography columns can be transferred to capillary LC systems with little effort. Kientz et al. [266] showed the analysis of chiral organophosphoros pesticides and found that capillary LC has a five-fold improved separation impedance, an approximately two-fold increase in column permeability and better inertness compared to conventional LC. Cortes and Nicholson [267] showed in a feasibility study the potential of chiral separations on capillary sized LC columns. Comparable results were found on conventional sized columns at almost identical linear mobile phase velocities.

Takeuchi and coworkers [273-275] demonstrated the use of β- and γ-cyclodextrin as mobile phase additive for the separation of analogs of dansyl phenylalanine [273] and phosphate enantiomers [274,275]. The stationary phase was ordinary octadecylsilica. The use of small i.d. microcolumns allowed for the use of these very expensive mobile phase additives. As an example, the work of Vindevogel et al. [271] will be used as an example of the adsorption of a chiral selector on a stationary phase surface. The elution order of N-nitroarylaminoacid on bovine serum albumin coated silica gel was determined and it was concluded that column overloading effects on protein-based stationary phases occur at lower concentration than on other stationary phases. Furthermore, as a result of this effect, the retention times of the chiral analytes shift non-predictably, especially for the last eluting compound. This effect was explained by blocking of the adsorption sides by the first eluting compounds, or that enantioselectivity was obtained through adsorption sides that interact uniquely with one enantiomer. A quantitative description was not given.

Bioanalysis and Neuroscience

On-line capillary LC – interfaced with either continuous-flow FAB-MS-MS or ESI-MS-MS – was applied by Vouros et al. [276,277] for the detection of *in-vivo* formed DNA adducts. This technique was used for rapid screening of the reaction between carcinogenic adducts and calf thymus DNA in order to elucidate the biochemistry of the interaction [276]. Multiple reaction monitoring provided limits of detection below 50 fmol. Further, the technique was able to detect structural data of the adducts that were formed. In a successive paper a similar application was demonstrated [277]. In this case the study involved the detection of heterocyclic aromatic amine DNA adducts of food derived carcinogenic compounds. The limit of detection
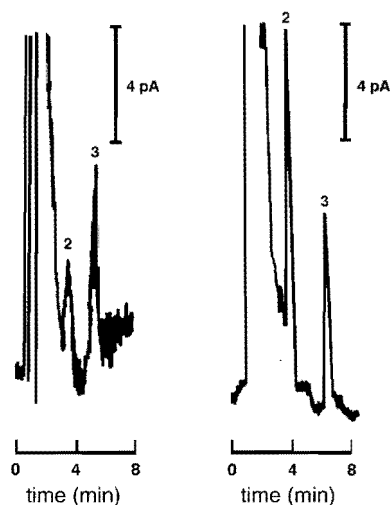
Fig. 2.12. Micro LC separation of an indole amine standard at the limit of detection level (left) and indoleamines in rat hypothalmus extract 0.94 µg tissue (right). Column: 0.25 m x 1.0 mm i.d. packed with 5-µm C$_{18}$; mobile phase: 0.1 M sodium acetate, 0.02 M acetate, 0.02 M citric acid, 50 mg l^{-1} EDTA, 100 mg l^{-1} sodium octyl sulphate and 4.5% acetonitrile (v/v); flow rate: 40–50 µl min^{-1}; detection: +0.6 V vs Ag/AgCl. Compound identification: (2) 5-hydroxy-tryptamine-HCl; (3) 5-hydroxyindoleacetic acid (reprinted from Brain. Res., 296, Caliguri and Mefford, Femtogram detection limits for biogenic amines using microbore HPLC with electrochemical detection, 156, ref. [188], Copyright (1984) with kind permission from Elsevier Science).

of the target adduct was approximately 80 fmol, which was achieved monitoring characteristic fragmentation patterns.

The group of Vouros also reported on the analysis of vitamin D metabolites [278]. Vitamine D metabolites may have a therapeutic effect in the treatment of leukemia. However, overdosage of this steroidal hormone can cause severe side effects. Capillary LC-tandem MS was employed to provide a high degree in sensitivity and selectivity at low levels. A derivatization step was introduced by reacting the vitamine D metabolites with 4-phenyl-1,2,4-triazoline-3,5-dione. The derivatives were characterized by continuous-flow FAB.

Femtogram detection limits for biogenic amines in rat brain tissues using micro LC with electrochemical detection was reported by Caliguri and Mefford [188]. The chromatographic separation of some indoleamine standards on a 25 cm x 1.0 mm i.d. micro LC column is given in Fig. 2.12. The chromatogram represents the quantity of two compounds present in 0.84 µg of tissue. Under the presented conditions it would be feasible to quantitate the indoles present in in 90 ng of tissue. The obtained concentration values agreed with literature. Besides the separation of indoleamines, the authors also reported on the analysis of cathecholamines.

Straub *et al.* [279] determined β-lactam residues in milk using perfusion capillary LC combined with ESI-MS. β-lactam antibiotics are a widely used drug in veterinary medicine for the treatment of bacterial infections and are assigned as target drugs with high priority. The separation detection of six key components was presented. The ability to confirm these β-lactam residues at the 10 ppb level was regarded as a significant breakthrough. Further, the ability to concentrate and analyze the components in less than 13 min was also found to be of importance for repetitive screening.

The presented applications in this paper cover only a small part of microcclumn LC applications that can be found in literature. However, this section gives a flavor and a first impression of the application area of microcolumn LC and demonstrates the versatility of the technique.

REFERENCES

[1]   D. Ishii and T. Takeuchi, *TrAC Trends Anal. Chem.* 9 (1990) 152

[2]   K. Jinno and C. Fujinoto, *LC•GC* 7 (1989) 328

[3]   M. Novotny, *Anal. Chem.* 60 (1988) 502A

[4]   M. Verzele, C. Dewaele and M. De Weerdt, *LC•GC* 6 (1988) 966

[5]   K. Jinno, *Chromatographia* 25 (1988) 1004

[6]   M. Novotny, *J. High Resolut. Chromatogr. Chromatogr. Commun.* 10 (1987) 248

[7]   M. Verzele and C. Dewaele, in F. Bruner (ed.), *The Science of Chromatography* (Journal of Chromatography Library, No. 32), Elsevier, Amsterdam, 1985, pp. 435

[8]   F.J. Yang, *J. High Resolut. Chromatogr. Chromatogr. Commun.* 6 (1983) 348

[9]   D. Ishii and T. Takeuchi, *Rev. Anal. Chem.* 6 (1982) 87

[10]   M. Novotny, *Anal. Chem.* 53 (1981) 1294A

[11]   T. Takeuchi, *Fresenius' J. Anal. Chem.* 337 (1990) 631

[12]   M. Verzele and C. Dewaele, *Chromatogr. Sci.* 45 (1989) 37

[13]   M. Verzele and C. Dewaele, *J. High Resolut. Chromatogr. Chromatogr. Comm.* 10 (1987) 280

[14]   D. Ishii and T. Takeuchi, *Adv. Chromatogr.* 21 (1983) 131

[15]   M. Novotny, *J. Chromtogr. Sci.* 18 (1980) 473

[16]   A.G. Ewing, J.M. Mesaros and P.G. Galvin, *Anal. Chem.* 66 (1994) 527A

[17]   J.W. Jorgenson and J. De Wit, *Chem. Anal.* 121 (1992) 395

[18]   Ch.E. Kientz and U.A.Th. Brinkman, *TrAC Trends Anal. Chem.* 12 (1993) 363

[19]   E.S. Yeung and W.G. Kuhr, *Anal. Chem.* 63 (1991) 275A

[20]   J.C Gluckman and M.V. Novotny, *Chromatogr. Sci.* 45 (1989) 145

[21]   B.G. Belenkii, *J. Chromatogr.* 434 (1988) 337

[22]   N. Sagliano and R.A. Hartwick, *J. Chromatogr. Sci.* 24 (1986) 506

[23]   M. Goto, in M.V. Novotny and D. Ishii (ed.), *Microcolumn Separations* (Journal of Chromatography Library, No. 30), Elsevier, Amsterdam, 1985, pp. 309

[24]   K. Jinno, C. Fujimoto, Y. Hirata and D. Ishii, in M.V. Novotny and D. Ishii (ed.), *Microcolumn*

Separations (Journal of Chromatography Library, No. 30), Elsevier, Amsterdam, 1985, pp. 177

[25] E.S. Yeung, in M.V. Novotny and D. Ishii (ed.), *Microcolumn Separations* (Journal of Chromatography Library, No. 30), Elsevier, Amsterdam, 1985, pp. 117

[26] V.V. Berry and H.E. Schwartz, *Chromatogr. Sci.* 45 (1989) 67

[27] J.C. Gluckman and M.V. Novotny, in M.V. Novotny and D. Ishii (ed.), *Microcolumn Separations* (Journal of Chromatography Library, No. 30), Elsevier, Amsterdam, 1985, pp. 57

[28] H.J. Cortes, *Chromatogr. Sci.* 45 (1989) 211

[29] C.G. Horváth, B.A. Preiss and S.R. Lipsky, *Anal. Chem.* 39 (1967) 1422

[30] C.G. Horváth and S.R. Lipsky, *Anal. Chem.* 41 (1969) 1227

[31] D. Ishii, K. Asai, K. Hibi, T. Jonokuchi and M. Nagaya, *J. Chromatogr.* 144 (1977) 157

[32] D. Ishii, K. Hibi, K. Asai and T. Jonokuchi, *J. Chromatogr.* 151 (1978) 147

[33] D. Ishii, K. Hibi, K. Asai and M. Nagaya, *J. Chromatogr.* 152 (1978) 341

[34] D. Ishii, K. Hibi, K. Asai, M. Nagaya, K. Mochizuki and Y, Mochida *J. Chromatogr.* 156 (1978) 173

[35] D. Ishii, A. Hirose, K. Hibi and Y. Iwasaki, *J. Chromatogr.* 157 (1978) 43

[36] D. Ishii, A. Hirose and I. Horiuchi, *J. Radioanal. Chem.* 45 (1978) 7

[37] F.J. Yang, *J. Chromatogr.* 236 (1982) 265

[38] T. Takeuchi and D. Ishii, *J. Chromatogr.* 213 (1981) 25

[39] T. Takeuchi and D. Ishii, *J. High Resolut. Chromatogr. Chromatogr. Commun.* 49 (1981) 469

[40] Y. Hirata and M. Novotny, *J. Chromatogr.* 186 (1979) 521

[41] T. Tsuda and M. Novotny, *Anal. Chem.* 50 (1978) 632

[42] T. Tsuda and M. Novotny, *Anal. Chem.* 50 (1978) 271

[43] C. Dewaele and M. Verzele, *J. High Resolut. Chromatogr. Chromatogr. Commun.* 1 (1978) 174

[44] C.E. Reese and R.P.W. Scott, *J. Chromatogr. Sci.* 18 (1980) 479

[45] R.P.W. Scott, *J. Chromatogr. Sci.* 18 (1980) 49

[46] P. Kuchera, *J. Chromatogr.* 198 (1980) 93

[47] R.P.W. Scott and P. Kuchera, *J. Chromatogr.* 169 (1979) 51

[48] R.P.W. Scott, P. Kuchera and M. Munroe, *J. Chromatogr.* 186 (1979) 475

[49] C. Eckers, K.K. Cuddy and J.D. Henion, *J. Liq. Chromatogr.* 6 (1983) 2383

[50] Y. Hirata and K. Jinno, *J. High Resolut. Chromatogr. Chromatogr. Commun.* 6 (1983) 96

[51] W.T. Kok, U.A.Th. Brinkman, R.W. Frei, H.B. Hanekamp, F. Nooitgedacht and H. Poppe *J. Chromatogr.* 237 (1982) 357

[52] H.G. Barth, W.E. Barber, C.H. Lochmüller, R.E. Majors and F.E. Reguier, *Anal. Chem.* 60 (1988) 387R

[53] M. Verzele and D. Dewaele, *J. High Resolut.Chromatogr. Chromatogr. Commun.* 10 (1987) 280

[54] J.P. Chervet, M. Ursem and J.P. Salzmann, *Anal. Chem.* 68 (1996) 1507

[55] P. Jandera and J. Roskosná, *J. Chromatogr.* 556 (1991) 145

[56] C. Horváth, W. Melander and J. Molnár, *Anal. Chem.* 49 (1977) 142

[57] S.V. Galushko, *Chromatographia* 36 (1993) 39

[58]   M.J. Walters, *J. Assoc. Off. Anal. Chem.* 70 (1987) 465

[59]   H. Engelhardt, H. Löw and W. Götzinger, *J. Chromatogr.* 544 (1991) 371

[60]   M. Ghijs and P. Sandra, *J. Microcol. Sep.* 3 (1991) 443

[61]   C. Borra, S.M. Han and M. Novotny, *J. Chromatogr.* 385 (1987) 75

[62]   V.L. McGuffin and M. Novotny, *J. Chromatogr.* 255 (1983) 381

[63]   R.T. Kennedy and J.W. Jorgenson, *Anal. Chem.* 61 (1989) 1128

[64]   P.A. Bristow and J.H. Knox, *Chromatographia* 10 (1977) 279

[65]   K.E. Karlsson and M. Novotny, *Anal. Chem.* 60 (1988) 1662

[66]   Y. Guan, L. Zhou and Z. Shang, *J. High Resolut. Chromatogr.* 15 (1992) 434

[67]   G. Crescentini and A.R. Mastrogiacomo, *J. Microcol. Sep.* 3 (1991) 539

[68]   G. Crescentini, F. Bruner, F. Mangani and Y. Guan, *Anal. Chem.* 60 (1988) 1659

[69]   D. Tong, K.D. Bartle, A.A. Clifford and A. M. Edge, *J. Microcol. Sep.* 7 (1995) 265

[70]   D. Tong, K.D. Bartle and A.A. Clifford, *J. Microcol. Sep.* 6 (1994) 249

[71]   A. Malik, W. Li and M.L. Lee, *J. Microcol. Sep.* 5 (1993) 361

[72]   S. Hoffmann and L. Blomberg, *Chromatographia* 24 (1987) 416

[73]   J.C. Gluckman, A. Hirose, V.L. McGuffin and M. Novotny, *Chromatographia* 17 (1983) 303

[74]   R.F. Meyer and R.A. Hartwick, *Anal. Chem.* 56 (1984) 2211

[75]   P. Roumeliotism N. Chatziathanassiou and K.K. Unger, *Chromatographia* 19 (1984) 145

[76]   T.M. Zimina, R.M. Smith, P. Meyers and B.W. King, *Chromatographia* 40 (1995) 662

[77]   K. Baechmann, I. Haag and T. Prokop, *Fresenius' J. Anal. Chem.* 345 (1993) 545

[78]   F. Francolini, C. Borra and M. Novotny, *Anal. Chem.* 59 (1987) 2428

[79]   P. Welling, H. Poppe and J.C. Kraak, *J. Chromatogr.* 321 (1985) 450

[80]   J.C. Kraak, *LC Mag.* 3 (1985) 88

[81]   H. Menet, P. Gareil, M. Caude and R. Rosset, *Chromatographia* 18 (1984) 73

[82]   J.C. Gluckman, J.C. Hirose, V.L. McGuffin and M. Novotny, *Chromatographia* 17 (1983) 303

[83]   A. Capiello, P. Palma and F. Mangani, *Chromatographia* 32 (1991) 389

[84]   M. Verzele, C. Dewaele, M. De Weerdt and S. Abbott, *J. High Resolut. Chromatogr.* 12 (1989) 164

[85]   S.M. Han and D.W. Armstrong, *Anal. Chem.* 59 (1987) 1583

[86]   K. Masaharu, Y. Mori and T. Amano, *Anal. Chem.* 57 (1985) 2235

[87]   J.P.C. Vissers, H.A. Claessens, J. Laven and C.A. Cramers, *Anal. Chem.* 67 (1995) 2103

[88]   J.P.C. Vissers, E.C.J. van den Hoef, H.A. Claessens, J. Laven and C.A. Cramers, *J. Microcol. Sep.* 7 (1995) 239

[89]   D.C. Shelly and T.J. Edkins, *J. Chromatogr.* 411 (1987) 185

[90]   D.C. Shelly, V.L. Antonucci, T.J. Edkins and T.J. Dalton, *J. Chromatogr.* 458 (1989) 267

[91]   R.J. Boughtflouwer, T. Underwood and J. Maddin, *Chromatographia* 41 (1995) 398

[92]   M.M. Ditmann, K. Wienand, F. Bek and G.P. Rozing, *LC•GC Int.* 13 (1995) 800

[93]   J.H. Knox and I.H. Grant, *Chromatographia* 32 (1991) 317

[94]   W.H. Wilson, H.M. McNair, Y.F. Man and K.F. Hyver, *J. High Resolut. Chromatogr.* 13 (1990) 18

[95]   S. Hsieh and J.W. Jorgenson, *Anal. Chem.* 68 (1996) 1212

[96]   V. Berry and H. Schwartz, in F.J. Yang (ed.), *Microbore Column Chromatography: A unified approach to Chromatography,* Marcel Dekker, New York, 1989, pp. 67

[97]   M. Saito, K. Hibi, D. Ishii and T.Takeuchi, in D. Ishii (ed), *Introduction to Microscale High Performance Liquid Chromatography,* VCH, Weinheim, Germany, 1988, pp. 7

[98]   E.C. Huang T. Wachs, J. Conboy and J.D. Henion, *Anal. Chem.* 62 (1990) 713A

[99]   P.R. Brown, *Anal. Chem.* 62 (1990) 995A

[100]   D. Ishii, in K. Jinno and P. Sandra (ed.), *12th International Symposium on Capillary Chromatography,* Industrial Publishing & Consulting, Tokyo, Japan, 1990, pp. 14

[101]   C.L. Flurer, C. Borra, F. Andreolini and M.V. Novotny, *J. Chromatogr.* 448 (1988) 73

[102]   J.F. Banks Jr. and M.V. Novotny, *J. Microcol. Sep.* 2 (1990) 84

[103]   Sj. Van der Wal and F.J. Yang, *J. High Resolut. Chromatogr. Chromatogr. Commun.* 6 (1983) 216

[104]   N. Nagae, H. Itoh, N. Nimura, T. Kinoshita and T. Takeuchi, *J. Microcol. Sep.* 3 (1991) 5

[105]   J.P. Chervet, C.J. Meijvogel, M. Ursem, and J.P. Salzmann, *LC•GC Int.* 10 (1992) 140

[106]   H.A. Claessens, A. Burcinova, C.A. Cramers, Ph. Mussche and C.E. van Tilburg, *J. Microcol. Sep.* 2 (1990) 132

[107]   M.C. Harvey, S.D. Stearns and J.P. Averette, *LC Liq. Chromatogr. HPLC Mag.* 3 (1985) 5

[108]   J.W. Jorgenson and E.J. Guthrie, *J. Chromatogr.* 255 (1983) 335

[109]   A. Manz and W. Simon, *J. Chromatogr.* 387 (1987) 187

[110]   R.C. Simpson, *J. Chromatogr.* A 691 (1995) 163

[111]   H.J. Cortes, J.R. Larson and G.M. McGowan, *J. Chromatogr.* 607 (1992) 131

[112]   J.P.C. Vissers, J.P. Chervet and J.P. Salzmann, *Int. Lab.* January 1996 12

[113]   G. Kamperman and J.C. Kraak, *J. Chromatogr.* 337 (1985) 384

[114]   H.A. Claessens and M.A.J. Kuyken, *Chromatographia* 23 (1987) 331

[115]   Takeuchi and D. Ishii, in T. Hanai and H. Hatano (ed.), *Advances in Liquid Chromatography, Methods in Chromatography,* Vol. 1, World Scientific, Singapore, 1996, pp. 169

[116]   M.J. Mills, J. Maltas and W.J. Lough, *J. Chromatogr. A* 759 (1997) 1

[117]   T. Takeuchi, Y. Jin, Y.Y.Y. Yuye and D. Ishii, *J. Chromatogr.* 321 (1985) 159

[118]   M.W.F. Nielen, R.C.A. Koordes, R.W. Frei and U.A.Th. Brinkman, *J. Chromatogr.* 330 (1985) 113

[119]   E. Noroozian, F.A. Maris, M.W.F. Nielen, R.W. Frei, G.J. de Jong and U.A.Th. Brinkman, *J. High Resolut. Chromatogr. Chromatogr. Commun.* 10 (1987) 17

[120]   Ch.E. Kientz, A. Verweij, G.J. de Jong and U.A.Th. Brinkman, *J. High Resolut. Chromatogr.* 12 (1989) 793

[121]   C. Moore, K. Sato and Y. Katsumata, *J. Chromatogr.* 539 (1991) 215

[122]   R.E.J. van Soest, J.P. Chervet, M. Ursem and J.M. Suijlen, *LC•GC Int.* 9 (1996) 586

[123]   J. Cai and J. Henion, *Anal. Chem.* 56 (1996) 72

[124]   J.P.C. Vissers, W.P. Hulst, J.P. Chervet, H.M.J. Snijders and C.A. Cramers *J. Chromatogr. B* 686 (1996) 119

[125]   H. Shen, C.A. Aspinwall and R.T. Kennedy, *J. Chromatogr. B* 689 (1997) 295

[126]   C. Fujimoto, T. Morita and K. Jinno, *Chromatographia* 22 (1986) 91

[127]   C. Fujimoto, T. Morita and K. Jinno, *J. High Resolut. Chromatogr. Chromatogr. Commun.* 9

(1986) 623

[128] G.D. Reed, *J. High Resolut. Chromatogr. Chromatogr. Commun.* 9 (1986) 250

[129] R.E. Synovec, *Anal. Chem.* 59 (1987) 2877

[130] H.J. Tarigan, P. Neill, C.K. Kenmore and D.J. Bornhop, *Anal. Chem.* 68 (1996) 1762

[131] D.J. Bornhop and N.J. Dovichi, *Anal. Chem.* 59 (1987) 1632

[132] D.J. Bornhop, T.G. Nolan and N.J. Dovichi, *J. Chromatogr.* 384 (1987) 181

[133] A.E. Bruno, K. Kuhn and H.M. Widmer, *Anal. Chim. Acta* 234 (1990) 259

[134] A.E. Bruno, B. Krattinger, F. Maystre and H.M. Widmer, *Anal. Chem.* 63 (1991) 2689

[135] M. Kamahori, Y. Watanabe, J. Muri, M. Taki and H. Miyagi, *J. Chromatogr.* 465 (1989) 227

[136] C. Kientz and A. Verweij, *J. High Resolut. Chromatogr. Chromatogr. Commun.* 11 (1988) 294

[137] J. Vindevogel, G. Schuddinck, C. Dewaele and M. Verzele, *J. High Resolut. Chromatogr. Chromatogr. Commun.* 11 (1988) 317

[138] G.J.M. Bruin, G. Stegeman, A.C. van Asten, X. Xu, J.C. Kraak and H. Poppe, *J. Chromatogr.* 559 (1991) 163

[139] M. Janecek, V. Kahle and M. Krejci, *J. Chromatogr.* 438 (1988) 409

[140] M. Janecek, F. Foret, K. Slais and P. Bocek, *Chromatographia* 25 (1988) 815

[141] J.P. Chervet, M. Ursem, J.P. Salzmann and R.W. Vannoort, *J. High Resolut. Chromatogr.* 12 (1989) 278

[142] J.P. Chervet, M. Ursem, J.P. Salzmann and R.W. Vannoort, *LC•GC* 7 (1989) 514

[143] P. Sandra, G. Steenbeke, M. Ghys and G. Schomburg, *J. High Resolut. Chromatogr.* 13 (1990) 527

[144] M. Verzele, G. Steenbeke and J. Vindevogel, *J. Chromatogr.* 477 (1989) 87

[145] T. Takeuchi and D. Ishii, *J. Chromatogr.* 288 (1984) 451

[146] D. Ishii, M. Goto and T. Takeuchi, *J. Chromatogr.* 316 (1984) 441

[147] T. Takeuchi and D. Ishii, *J. High Resolut. Chromatogr. Chromatogr. Commun.* 7 (1984) 151

[148] J.C. Gluckman and M. Novotny, *J. High Resolut. Chromatogr. Chromatogr. Commun.* 8 (1985) 672

[149] J.C. Gluckman, D.C. Shelly and M. Novotny, *Anal. Chem.* 57 (1985) 1546

[150] M. Verzele and C. Dewaele, *J. Chromatogr.* 395 (1987) 85

[151] T. Takeuchi and D. Ishii, *Chromatographia* 25 (1988) 697

[152] D. Shelly, J. Gluckman and M. Novotny *Anal. Chem.* 56 (1984) 483

[153] E.J. Guthrie and J.W. Jorgenson, *Anal. Chem.* 56 (1984) 483

[154] T. Takeuchi, T. Asano and D. Ishii, *J. Chromatogr.* 471 (1989) 297

[155] T. Takeuchi and D. Ishii, *Chromatographia.* 25 (1988) 697

[156] W.R. Blair, E.J. Parks, G.J. Olsen, F.E. Brinckman, M.C. Valeiras-Price and J.M. Bellama, *J. Chromatogr.* 410 (1987) 383

[157] B. Lin Ling, W.R.G. Baeyens, C. Dewaele and B. Del Castillo, *J. Pharm. Biomed. Anal.* 10 (1992) 985

[158] T. Takeuchi and D. Ishii, *J. High Resolut. Chromatogr. Chromatogr. Commun.* 11 (1988) 841

[159] T. Takeuchi and T. Miwa, *Chromatographia* 38 (1994) 555

[160] E.S. Yeung, in M.V. Novotny and D. Ishii (ed.), *Microcolumn Separations* (Journal of Chro-

matography Library, No. 30), Elsevier, Amsterdam, 1985, pp. 135

[161] T.J. Edkins and D.C. Shelly, in G. Patonay (ed.), *HPLC Detector: newer methods*, VCH, New York, 1992, pp. 1

[162] Z. Rosenzweig and E.S. Yeung, *Appl. Spectrosc.* 47 (1993) 1175

[163] A.A. Abbas and D.C. Shelly, *J. Chromatogr. A* 691 (1995) 37

[164] F. Adreolini, S.C. Beale and M. Novotny, *J. High Resolut. Chromatogr. Chromatogr. Commun.* 11 (1988) 20

[165] J. Gluckman, D. Shelly and M. Novotny, *J. Chromatogr.* 317 (1984) 443

[166] V.L. McGuffin and R.N. Zare, *Appl. Spectrosc.* 39 (1985) 847

[167] A. Manz, Z. Fröbe and W. Simon, in M.V. Novotny and D. Ishii (ed.), *Microcolumn Separations* (Journal of Chromatography Library, No. 30), Elsevier, Amsterdam, 1985, pp. 297

[168] J.E. Baur, E.W. Kristensen and R.W. Wightman, *Anal. Chem.* 60 (1988) 2334

[169] K. Slais and B. Oscik-Mendyk, *J. Chromatogr.* 456 (1988) 370

[170] K. Slais, *J. Chromatogr.* 436 (1988) 413

[171] M. Janecek and K. Slais, *J. Chromatogr.* 471 (1989) 303

[172] T. Takeuchi, T. Miwa, A. Hemmi and T. Maeda, *Chromatographia* 37 (1993) 173

[173] A. Manz and W. Simon, *J. Chromatogr. Sci.* 21 (1983) 326

[174] A. Manz and W. Simon, *Anal. Chem.* 59 (1987) 74

[175] L.A. Knecht, E.J. Guthrie and J.W. Jorgenson, *Anal. Chem.* 56 (1984) 479

[176] J.C. White, R.L. St. Claire III and J.W. Jorgenson, *Anal. Chem.* 58 (1986) 293

[177] M. Goto, K. Shimada, T. Takeuchi and D. Ishii, *Anal. Sci.* 4 (1988) 17

[178] V.F. Ruban, *J. High Resolut. Chromatogr.* 13 (1990) 112

[179] V.F. Ruban, *J. High Resolut. Chromatogr.* 16 (1993) 663

[180] K. Slais and D. Kourilova, *Chromatographia*, 16 (1982) 265

[181] L.J. Nagels, J.M. Kaufman, G. Schuddink, C. Dewaele, G.J. Patriarche and M. Verzele, *J. Chromatogr.* 459 (1988) 163

[182] M. Goto and K. Shimada, *Chromatographia* 21 (1986) 631

[183] C.N. Svendsen, *Analyst* 18 (1993) 123

[184] A. Aoki, T. Matsue and I. Uchia, *Anal. Chem.* 64 (1992) 44

[185] M. Takahashi, M. Morita, O. Niwa and H. Tabei, *J. Electroanal. Chem.* 335 (1992) 253

[186] S. Sarre, Y. Michotte, C.A. Marvin and G. Ebiger, *J. Chromatogr.* 582 (1992) 29

[187] K.A. Sager, M.T. Kelly, T. Mary and M.R. Smith, *J. Chromatogr.* 577 (1992) 109

[188] E.J. Caliguri and I.N. Mefford, *Brain Res.* 296 (1984) 156

[189] T. Tsuda, A. Nago, G.Nakagawe and M. Maseki, *J. High Resolut. Chromatogr. Chromatogr. Commun.* 6 (1983) 694

[190] H. Veening, P.P. Tock, J.H. Kraak and H. Poppe, J. Chromatogr. 352 (1986) 345

[191] V.L. McGuffin and M. Novotny, *J. Chromatogr.* 218 (1981) 179

[192] V.L. McGuffin and M. Novotny, *Anal. Chem.* 55 (1983) 2296

[193] J.C Gluckman and M. Novotny, *J. Chromatogr.* 314 (1984) 103

[194] J.C. Gluckman and M. Novotny, *J. Chromatogr.* 333 (1985) 291

[195] Ch.E. Kientz, A. Verweij, G.J. de Jong and U.A.Th. Brinkman, *J. Chromatogr.* 626 (1992) 59

[196] Ch.E. Kientz, A. Verweij, G.J. de Jong and U.A.Th. Brinkman, *J. Chromatogr.* 626 (1992) 71

[197] U.A.Th. Brinkman and F.A. Maris, *LC•GC Int.* 1 (1987) 45

[198] F.A. Maris, R.J. van Delft, R.W.Frei, R.B. Geerdink and U.A.Th. Brinkman, *Anal. Chem.* 58 (1996) 1634

[199] J.C. Gluckman, D. Barcelo, G.J. de Jong, R.W. Frei, F.A. Maris and U.A.Th. Brinkman, *J. Chromatogr.* 367 (1986) 35

[200] V.L. McGuffin and M. Novotny, *Anal. Chem.* 53 (1981) 946

[201] S. Folestad, B. Josefsson and P. Marstop, *Anal. Chem.* 59 (1987) 334

[202] Ch.E. Ki̇entz, A. Verweij, H.L. Boter, A. Poppema, R.W. Frei, G.J. de Jong and U.A.Th. Brinkman, *J. Chromatogr.* 467 (1989) 385

[203] H.-C.K. Chang and L.T. Taylor, *Anal. Chem.* 63 (1991) 486

[204] A.L. Howard, C.L.B. Thomas and L.T. Taylor, *Anal. Chem.* 66 (1994) 1432

[205] J.F. Karnicky, L.T. Zitelli and Sj. van der Wal, *Anal. Chem.* 59 (1987) 327

[206] V.V. Brazhnikov, L.M. Yakashina, E.M. Syanava and Sh.A. Karaptyan, *J. High Resolut. Chromatogr. Chromatogr. Commun.* 6 (1983) 451

[207] F.A. Maris, J.A. Stäb, G.J. de Jong and U.A.Th. Brinkman, *J. Chromatogr.* 445 (1988) 129

[208] B.N. Zegers, J.F.C. de Brouwer, A. Poopema, H. Lingeman and U.A.Th. Brinkman, *Anal. Chim. Acta* 304 (1995) 47

[209] A.J. Lange, P.R. Griffits and D.J.J. Fraser, *Anal. Chem.* 63 (1991) 782

[210] C. Fujimoto, T. Morita, K. Jinno and K.H. Shafer, *J. High Resolut. Chromatogr. Chromatogr. Commun.* 11 (1988) 810

[211] G.J. De Jong, N. Lammers, F.J. Spruit, C. Dewaele and M. Verzele *Anal. Chem.* 59 (1987) 1458

[212] T. Takeuchi and T. Miwa *Chromatographia* 37 (1993) 281

[213] S.H. Chen, C.E. Evans and V.L. McGuffin, *Anal. Chim. Acta* 246 (1991) 65

[214] J. Chu, R. Hu, T. Miwa and T. Takeuchi, *Chromatographia* 40 (1995) 379

[215] R. Gotz, J.W. Elgersma, J.C Kraak and H. Poppe, *Spectrochim. Acta B* 49B (1994) 761

[216] S. Hoffmann, H.R. Norli and T. Greibrokk, *J. High Resolut. Chromatogr.* 12 (1989) 260

[217] H. Wu, T.L. Peck, A.G Webb, R.L. Magin and J.V. Sweedler, *Anal. Chem.* 66 (1994) 3849

[218] H. Wu, A. Webb, T.L. Peck and J.V. Sweedler, *Anal. Chem.* 67 (1995) 3101

[219] K. Albert, G. Schlotterback, L.-H. Tseng and U. Braumann, *J. Chromatogr. A* 750 (1996) 303

[220] C. Fujimoto, T. Morita and K. Jinno, *J. Chromatogr.* 438 (188) 329

[221] T. Takeuchi, M. Asai, H. Haraguchi and D. Ishii, *J. Chromatogr.* 599 (1990) 549

[222] LA. Holland and J.W. Jorgenson, *Anal. Chem.* 67 (1995) 3275

[223] D.B. Kassel, T.G. Cousler, M. Shalaby, P. Selchri, N. Gorden and T. Nadler, in R.J.W. Crabb (ed.), *Tech. Protein. Chem. VI*, Academic Press, San Diego, 1995, pp. 39

[224] T.E. Mulligan, R.W. Blain, N.F. Oldfied and B.A. Mico, *J. Liq. Chromatogr.* 17 (1994) 133

[225] H.J. Cortes, B.E. Richter, C.D. Pfeiffer and D.E. Jenssen, *J. Chromatogr.* 349 (1985) 55

[226] K. Grob and J.-M. Stoll, *J. High Resolut. Chromatogr. Chromatogr. Commun.* 9 (1986) 518

[227] H.J. Cortes, L. Green. C. Shayne and M. Robert, *Anal. Chem.* 62 (1991) 2719

[228] F. Munari, A. Frisciani, G. Mapelli, S. Tristianu, K. Grob and J.M. Colin, *J. High Resolut. Chromatogr. Chromatogr. Commun.* 8 (1985) 601

[229] I.L. Davis, K.D. Bartle, G.E. Andrews and P.T. Williams, *J. Chromatogr. Sci.* 26 (1988) 125

[230] D. Duquet, C. Dewaele, M. Verzele and S. McKinley, *J. High Resolut. Chromatogr. Chromatogr. Commun.* 11 (1988) 824

[231] K. Welch and N.E. Hoffman, *J. High Resolut. Chromatogr.* 15 (1992) 171

[232] R. Moulder, K.D. Barttle and A.A. Clifford, *Analyst* 116 (1991) 1293

[233] A.V. Lemmo and J.W. Jorgenson, *Anal. Chem.* 65 (1993) 1576

[234] A.C. Barefoot and R.W. Reiser, *Biomed. Environ. Mass Spectrom.* 19 (1989) 77

[235] A. Carrier, L.Varfalvy and M.J. Bethrand, *J. Chromatogr. A.* 705 (1995) 205

[236] U.B. Ranalder, B.B. Lausecker and C. Huselton, *J. Chromatogr.* 617 (1993) 129

[237] H. Albron and G. Stenhagen, *J. Chromatogr.* 394 (1987) 35

[238] E.L. Esmans. P. Geboes, Y. Luyten and F.C. Alderweirelt, *Biomed. Mass Spectrom.* 12 (1985) 241

[239] E.D. Lee and J.D. Henion, *J. Chromatogr. Sci.* 23 (1985) 253

[240] A. Capiello, G. Famiglini, F. Mangani and B. Tirillini, *J. Am. Soc. Mass Spectrom.* 6 (1995) 132

[241] A. Capiello and G. Famiglini, *Anal. Chem.* 66 (1994) 3970

[242] A. Capiello, G. Famiglini and F. Bruner, *Anal. Chem.* 66 (1994) 1416

[243] M.A. Moseley, L.J. Deterding, J.S.M. de Wit, K.B. Tomer, R.T. Kennedy, N. Brag and J.W. Jorgenson, *Anal. Chem.* 61 (1989) 1577

[244] M.A. Mosely, L.J. Deterding, K.B. Tomer and J.W. Jorgenson, *Anal. Chem.* 61 (1991) 1467

[245] J.E. Coutant, T.M. Chen and B.L. Ackermann, *J. Chromatogr.* 529 (1990) 265

[246] S. Pleasence, P. Thibault, M.A. Moseley, L.J. Deterding, K.B. Tomer and J.W. Jorgenson, *J. Am. Soc. Mass Spectrom.* 1 (1990) 312

[247] J.P. Gagné, A. Carrier, L. Varfalvy and M.J. Berthrand, *J. Chromatogr.* 647 (1993) 13

[248] J.P. Gagné, A. Carrier, L. Varfalvy and M.J. Berthrand, *J. Chromatogr.* 647 (1993) 21

[249] K.B. Tomer, M.A. Moseley, L.J. Deterding and C.E. Parker, *Mass Spectrom. Rev.* 13 (1994) 431

[250] C. Li, N. Chaurut, Y. Ducharme, L.A. Trimble, D.A. Nicoll-Griffith and J.A. Yergey, *Anal. Chem.* 67 (1995) 2931

[251] Y.-M. Li, P. Hjerten, N. Stellen, F. Nyberg and J. Silberring, *J. Chromatogr. B.* 664 (1995) 426

[252] C.M. Whitehouse, R.N. Dreyer, M. Yamashita and J.B. Fenn, *Anal. Chem.* 57 (1985) 675

[253] M.G. Ikonomou, A.T. Blades and P. Kebarle, *Anal. Chem.* 63 (1991) 1989

[254] M.G. Qian and D.M. Lubman, *Anal. Chem.* 67 (1995) 2870

[255] S.C. Wong, C. Grimley, A. Oadau, J.H. Bourell and W.J. Henzel, in R.H. Angeletti (ed.), *Tech. Protein. Chem. IV*, Academic Press, San Diego, 1993, pp. 371

[256] W.J. Henzel, T.M. Billeci, J.T. Stults, S.C. Wong, C. Grimley and C. Watanabe, *Proc. Natl. Acad. Sci.* 90 (1993) 5011

[257] W.J. Henzel, C. Grimely, J.H. Bourell, T.M. Billeci, S.C. Wong and J.T. Stults, *Methods: Comparison Methods Enzymol.* 6 (1994) 239

[258] A.J. Link, J. Eng and J.R. Yates III, *Am. Lab.* 8 (1996) 27

[259] J.R. Yates III, J.K. Eng and A.L. McCormack, *Anal. Chem.* 67 (1995) 3203

[260] P. Tempst, S. Geromanos, C. Elicone and H. Erdjument-Bromage, *Methods: Comparison Methods Enzymology* 6 (1994) 252

[261]   C. Elicone, M. Lui, S. Geromanos, H. Erdjument-Bromage and P. Tempst. *J. Chromatogr. A* 676 (1994) 121

[262]   R.L. Moritz, G.E. Reid, L.D. Ward and R.J. Simpson, *Methods: Comparison Methods Enzymology* 6 (1994) 213

[263]   D.B. Kassel, B. Sushan, T. Sakuma and J.P. Salzmann, *Anal. Chem.* 66 (1994) 236

[264]   J.E. Battersby, V.R. Mukku, R.S. Clark and W.S. Hancock, *Anal. Chem.* 57 (1995) 447

[265]   H. Wännman, A. Walhagen and P. Erlandson, *J. Chromatogr.* 603 (1992) 121

[266]   Ch.E. Kientz, J.Langenberg, G.J. De Jong and U.A.Th. Brinkman, *J. High Resolut. Chromatogr.* 14 (1991) 460

[267]   H.J. Cortes and L.W. Nicholson, *J. Microcol. Sep.* 6 (1994) 257

[268]   V. Schurig, M. Jung, S. Mayer, M. Fluck, S. Negura and H. Jacubetz, *J. Chromatogr. A* 694 (1995) 119

[269]   J. Hermansson, I. Hermansson and J. Nordin, *J. Chromatogr.* 631 (1993) 79

[270]   T. Takagi, Y. Itabashi and T. Tsuda, *J. Chromatogr. Sci.* 27 (1989) 574

[271]   J. Vindevogel, J. van Dijck and M. Verzele, *J. Chromatogr.* 447 (1988) 297

[272]   S.M. Han and D.W. Armstrong, *J. Chromatogr.* 389 (1987) 256

[273]   T. Takeuchi and N. Nagae, *J. High Resolut. Chromatogr.* 15 (1992) 121

[274]   T. Takeuchi, *J. High Resolut. Chromatogr.* 14 (1991) 560

[275]   R. Hu, T. Takeuchi, J.-Y Jin and T. Miwa, *Anal. Chim. Acta* 295 (1994) 173

[276]   D. Rindgen, R.J. Turesky and P. Vouros, *Chem. Res. Toxicol.* 8 (1995) 1005

[277]   S.M. Wolf and P. Vouros, *Chem. Res. Toxicol.* 7 (1994) 82

[278]   B. Yeung, P. Vouros and G. Reddy, *Am. Lab.* 7 (1994) 12

[279]   R. Straub, M. Linder and R.D. Voyksner, *Anal. Chem.* 66 (1994) 3651

CHAPTER 3

SEDIMENTATION BEHAVIOUR AND COLLOIDAL PROPERTIES OF POROUS, CHEMICALLY-MODIFIED SILICAS IN NON-AQUEOUS SOLVENTS

ABSTRACT

The sedimentation behaviour and colloidal properties of porous, chemically-modified silicas dispersed in non-aqueous solvents have been studied. The free settling behaviour of non-aggregated silica suspensions could effectively be described with a modified Stokes' equation that takes into account the possible inclusion of gas in the pores of the particles. The effects of hindered settling and of the dimensions of the sedimentation vessel on the rate of sedimentation were investigated too. The colloidal properties of the silica particles were compared with predictions by the DLVO theory. The Hamaker and Lifshitz theories were utilized to describe the attraction forces between the chemically-modified silica particles. The electrophoretic mobilities of the particles in the non-aqueous liquids were determined in order to quantify the electrostatic repulsion forces. The electrostatic repulsion appears to generate a large barrier against coagulation with all investigated porous silicas. However, the way in which the particle suspensions are prepared determines whether the particles remain in the primary minimum or are colloidally stable. The level of gas entrainment provides information on the homogeneity of the particle coating.

61

INTRODUCTION

Hydrophobic silicas are widely used in different fields of chemical technology. Examples of application are as fillers in polymer materials and pharmaceutical products, as thickeners in varnishes and paints, and as stabilizers or additives in detergents [1,2]. Future applications may be the use of silica sols – which can be applied in non-aqueous systems – in making magnetic colloids and recording media, high technology ceramic composites and catalytic supports [3]. Silica organosols may also be used as low temperature binder, as adhesion promoter or as silica source for magnesia refractories [3]. Thus, silica containing suspensions are studied in detail with regard to their rheological behaviour and adsorption, immersion and optical properties [1,4-8]. A very important scientific application of chemically-modified silicas is as stationary phases in high performance liquid chromatography and supercritical fluid chromatography [9-10]. The performance of a packed chromatographic column may vary considerably when comparing similar silicas from different manufacturers. The colloidal stability of the slurries employed in the column preparation is of critical importance in achieving stable chromatographic column beds using slurry packing techniques [11]. Colloidal stability may also play a role in the often not adequate mechanical stability of the column (shrinkage of the packed bed) over its life time: bed shrinkage can lead to a reduced resolution.

In the present study we examine the colloidal characteristics of porous silicas with chemically-modified surfaces in non-aqueous solvents, that are applied as stationary phases. The colloidal stabilities of the suspensions were studied by sedimentation experiments. The experimentally determined settling rates are compared with theoretical predictions for single particles in a suspension, as based on a modified Stokes' relation. To this end, the particles had also to be characterized by size, porosity and amount of air entrapped in the pores.

THEORETICAL

Sedimentation

The colloidal stability of porous silicas can be studied by sedimentation experiments, because aggregated silica particles will show increased rate of sedimentation and volume of the final sediment. Taking into account the full two-body hydrodynamic interactions it has been derived that the sedimentation velocity u of a colloidally stable suspension can be written as [12]:

$$u = u_{Stokes} + u_{back} + u_{extra} + u_{hydro} \tag{3.1}$$

62

where u_{Stokes} is the normal Stokes' velocity and u_{back} is a velocity-decreasing term. The latter term accounts for the fact that – at finite volume fractions ϕ of settling particles – the liquid phase velocity in an overall quiescent suspension is non-negligible and directed upwards. The term u_{extra} reflects the velocity-increasing extra hydrodynamic pressure gradient and u_{hydro} stands

for the velocity decreasing effect of the "near field" hydrodynamic interactions between the particles. For monodisperse hard spheres the contributions of the last three terms to the sedimentation velocity ratio u/u_{Stokes} are -5.5ϕ, +0.5ϕ and -1.55ϕ respectively, giving:

$$\frac{u}{u_{Stokes}} = 1-6.55\phi + O\left(\phi^2\right) = 1+K_2\phi + O\left(\phi^2\right)$$ (3.2)

where ϕ is the volume fraction of particles. Inter-particle attractions reduce the linear coefficient K_2 in the equation, long-range repulsions tend to increase it. In practice this coefficient is often found to be at its hard sphere value or at a somewhat lower value. Polydispersity leads to differences in settling velocities, i.e. a particle velocity gradient. However, these differences in particle velocity are smaller than those between monodisperse dispersions consisting of large and small particles. One of the experimental methods for determining u in a suspension is by monitoring the boundary between the free settling suspension and the upper, clear fluid region. The theoretical prediction of the sedimentation velocities at higher ϕ (outside the "Einstein" and the "Batchelor" regimes, for which linear and quadratic dependencies do not hold) is less straightforward. It has been found that a fairly good fit to experimental data both at low and large ϕ can be obtained – in case of low Reynolds numbers – using the equation originally proposed by Richardson and Zaki [13]:

$$\frac{u}{u_{Stokes}} = \left(1-\phi\right)^{-K_2}$$ (3.3)

A complication with porous particles is that they have pores which are only partially filled with liquid. This can be taken into account by calculating the effective mass of the particles. Thus, the sedimentation velocity of the particles applied in this study can be written as:

$$u = \frac{\left(1-\phi\right)^{-K_2} d_p^2 \left\{\rho_{skel}\left(1-\varepsilon_i\right) + \rho\left(\varepsilon_f - 1\right)\right\} g}{18\eta}$$ (3.4)

where d_p is the hydrodynamic diameter of the particles, ρ_{skel} is the skeleton density of the particles, ρ and η are the density and viscosity of the suspension liquid, g the gravitational constant, and ε_i is the particle porosity [8]. ε_f is the fraction of a total particle volume, i.e. particle + pores, that is filled with suspension liquid. In other words, the fraction of the pores that is filled with liquid equals $\varepsilon_f/\varepsilon_i$. Implicitly it was assumed that the permeability through the particles during sedimentation is low.

For the sedimentation of doublets of particles analytical solutions are available for low ϕ. A doublet of equal spheres has a settling velocity of $1.381 u_{Stokes}$ if the line connecting the centres of the spheres is horizontal [12]. If this line is oriented vertically the velocity becomes $1.550 u_{Stokes}$ Suspensions in which the settling velocity significantly exceeds the theoretical one are inter-

63

preted as aggregated. With larger aggregates analytical solutions for the settling velocity appear to be too complicated. Numerical approaches taking into account multi body interactions are more successful [14,15]. With colloidally instable suspensions, one can qualitatively say that larger aggregates settle faster. For a given aggregate this speed is slightly faster if the aggregate is more compact.

Colloidal stability and inter-particle interaction

Thermodynamically two charge-stabilized particles in a quiescent liquid mutually exert a Van der Waals attractive and an electrostatic repulsive force. The sum of these effects is called 'total interaction' [16]. Aggregation may proceed if the secondary minimum ('flocculation') is sufficiently pronounced or if the repulsive barrier to the primary minimum is sufficiently shallow ('coagulation'). In order to assess the secondary minimum and the barrier, the equations used in this paper for assessing the Van der Waals and electrostatic forces are briefly discussed.

Van der Waals attraction

The principles of Van der Waals forces has been treated elsewhere [16]. However, the problem of heterogeneous particles – as stationary phase particles are – has not been dealt with yet. In a separate paper the Van der Waals interaction between composite particles in a medium will be discussed, both along the lines of the classical Hamaker theory and of the Lifshitz approach [17]. Here we only refer to the main results.

In the Hamaker approach the basic assumption is that the long-range, attractive forces between molecules are additive. Based on this an expression for the Hamaker constant A_t of composite particles in a medium was derived [17]:

$$A_t = A_{oo} - 2\sum_{i=1}^{n} \phi_i A_{oi} - \sum_{i=1}^{n}\sum_{j=1}^{n} \phi_i \phi_j A_{ij} \tag{3.5}$$

where A_{ij} is the Hamaker constant of interaction between two particles, of medium i and j respectively. The index o refers to the medium and the indices 1..n refer to the components in the composed particle. These components with volume fractions ϕ_i are supposed to be distributed over the whole particles uniformly in such a way that the granularity of the mixing is not noticeable in the inter-particle interaction. Within the framework of the Lifshitz theory the composite character of the particles can be taken into account by calculating the absorption spectrum of a composite from adding their respective spectra with the volume fraction as the weighing factor. This again requires the granularity of the particle to be small enough to not giving rise to light scattering. The Lifshitz theory has two major advantages. First of all, the retardation is dealt with automatically. Secondly, the evaluation of A_{ij} is better than when using the Hamaker theory.

Electrostatic interactions

For assessing the electrostatic repulsion V_r the following equation was used:

$$V_r = 2\pi\varepsilon_0\varepsilon_r a\Psi_0^2 \ln\left(1+e^{-kh}\right)$$
(3.6)

where Ψ_0 is the surface potential, h is the interparticle distance, ε_0 is the permittivity of vacuum and ε_r is the relative dielectric constant of the liquid medium [12,16]. Here it is assumed that the constant-potential approach holds for the moderate-polarity slurry liquids investigated: complete dissociation of the ionic groups on the surface of the particles is umlikely. Additionally, the surface potential will be opproximated by ζ-potentials

EXPERIMENTAL

Chemicals

Acetone, carbontetrachloride (CCl_4), methanol and isopropanol were purchased from Merck (Darmstadt, Germany). Acetonitrile (CH_3CN) was from Janssen Chemica (Beerse, Belgium) and tetrahydrofurane from Biosolve LTD (Barneveld, The Netherlands). All chemicals were of p.a. grade. Water was purified and demineralized with a Milli-Q water purification system (Waters-Millipore, Milford,MA, USA) prior to use.

The Zorbax ODS and Zorbax SB-C18 ODS modified silicas were obtained from Rockland Technologies Inc. (New Port, DE, USA). Nucleosil 100-5 C18 was from Machery-Nagel GmbH & Co KG (Düren, Germany), Bio-Sil C18 HL 90-5 S from Bio-Rad (Nazareth, Belgium) and Spherisorb ODS-1 from Phase Separations (Deerfield, UK). All used silicas were spherically shaped and were used as received, having been chemically modified by using octadecylsilanes. The functionality of the silane varies from 1 to 3. In case of monofunctionality the silicon atom had been eitherdimethyl- or diisobutyl-substituted. The available information for the different types of silica particles is given in Table 3.1.

Particle characterization

The particle sizes and the particle size distributions of the silicas were measured with a Malvern 2600 particle sizer (Malvern Instruments, Worcestershire, UK). The light-scattering pattern of a He-Ne, 5 mW laser was converted into a particle size distribution by means of home made software, dedicated for porous materials. The median d_{50} was taken as the average particle diameter d_p. Particle porosities were determined using the relationship [18]:

$$\varepsilon_i = \frac{V_{pore}}{V_{particles}} = \frac{V_{pore}}{V_{pore}+1/\rho_{skel}}$$
(3.7)

65

Table 3.1. Characteristics of chemically modified silicas studied

hydrophobic silica	d_p (µm)	span[a]	V_{pore} (10^{-6} m³/kg)	ρ_{skel} (kg/m³)[#]	ρ_{app} (kg/m³)[b]	specific surface (10^3 m² kg⁻¹)	carbon content (%)	functionality silane	end capped	ε_i
Bio-Sil C18 HL 90-5	5.70	0.67	357	2104	560	200	16	di or tri	yes	0.429
Nucleosil 100-5 C18	5.10	0.54	809	2106	360	340	15	—	yes	0.630
Spherisorb ODS-1	4.84	0.60	430	2166	620	220	7	tri	yes	0.482
Zorbax ODS	4.40	0.74	358	1987	700	300	17	mono[d]	—	0.413
Zorbax SB-C18	5.24	0.60	318	2194	810	180	10	mono[e]	no	0.411

[a] span = $(d_{90}-d_{10})/d_{50}$; [b] after chemical modifcation; [c] ρ_{app} = apparent density (packed dry density); [d] two methyl side-groups; [e] two isobutyl side-groups

where V_{pore} is the pore volume per mass of the particles, $V_{particle}$ is the total hydrodynamic volume per mass of the particle, and ρ_{skel} is the skeleton density. This indirect method for assessing ε_i was used since direct methods are destructive and require large amounts of material. Skeleton densities of the materials were determined with a gas pycnometer (Stereopycnometer, Quanta-Chrome Corp., Greenvale, NY, USA). Pore volumes were assessed with a BET apparatus (Sorptomatic 1900, Carlo Erba Instruments, Milan, Italy). All particle characteristics are summarized in Table 3.1.

The ratio of mass and volume of the particles (solid + entrapped gas) as dispersed in a liquid medium were determined with a 10 ml capped liquid pycnometer, after sonication for 10 minutes and thermostating at 20°C in a water bath for 15 minutes. The fraction of the pores that is filled with liquid equals $\varepsilon_f/\varepsilon_i$. For the different combinations of particles and liquids these data are summarized in Table 3.2. From Table 3.2 it can be seen that Zorbax ODS and Zorbax SB-C18 particles enclose large amounts of gas in acetone and CH_3CN. Generally, it can be concluded that the amount of gas entrapped in the pores of the hydrophobic silicas is larger for the Zorbax materials. This is most likely caused by the wettability of the different materials in the non-aqueous solvents [5,6]. Tetrahydrofurane, isopropanol, methanol and CCl_4 seem to have the best wetting properties for these kind of hydrophobic silicas.

Particle settling device

A particle settling device was constructed from a 7 mm inner diameter glass tube, with a length of 130 mm. The silica slurries were transferred into the tube by means of a pipette. The tube was shut by means of a rubber stopper to prevent solvent evaporation and held in a vertical position. The distance travelled by the upper boundary of the slurry was measured with 5 minutes intervals until the final height of the sediment was reached. All experiments were conducted twice. It was found that with 7 mm tubes the effect of the wall on the sedimentation rate was negligible.

Zeta-potential measurements

The ζ-potentials of the hydrophobic silicas in the different liquids were measured with a Malvern Zeta-sizer 3 (Malvern Instruments) equipped with a AZ4 cell and using the Helmholtz-Scholuchowski equation [16]. Low-conductivity ζ-potential experiments were conducted with an AZ26 cell. Electrophoretic mobility measurements on the hydrophobic silica particles in liquids with a relatively high dielectric constant ($\varepsilon_r > 10$) were conducted at a voltage drop over the measuring cell of approximately 100 V. In case of liquids with $\varepsilon_r < 10$ this voltage drop was kept at 50 V.

67

Conductivity measurements

Conductivity measurements were conducted with a CDM 83 conductivity meter (Radiometer, Copenhagen, Denmark), equipped with a CDC 134 conductivity cell. All measurements were performed at ambient temperature.

Table 3.2. Density of hydrophobic silica particles as measured by immersion (the ratio of mass and volume of solids and entrapped gas) and, in parentheses, fraction $\varepsilon_f/\varepsilon_i$ of the pores that is filled with liquid

hydrophobic silica	$\rho_{particle}$ (kg m^{-3}) ($\varepsilon_f/\varepsilon_i$)											
	acetone		CH$_3$CN		CCl$_4$		isopropanol		methanol		THF	
Bio-Sil C18 HL 90-5	1607	(0.594)	1463	(0.420)	1622	(0.646)	1466	(0.632)	1726	(0.700)	1674	(0.660)
Nucleosil 100-5 C18	1605	(0.817)	1504	(0.765)	1645	(0.837)	1648	(0.837)	1526	(0.778)	1635	(0.832)
Spherisorb ODS-1	1802	(0.782)	1730	(0.730)	1817	(0.795)	1935	(0.871)	1924	(0.865)	1876	(0.836)
Zorbax ODS	1494	(0.528)	1494	(0.530)	1719	(0.777)	1609	(0.666)	1660	(0.721)	1731	(0.789)
Zorbax SB-C18	1706	(0.591)	1683	(0.564)	1821	(0.708)	1870	(0.752)	1857	(0.740)	1834	(0.718)

RESULTS AND DISCUSSION

Sedimentation

Sedimentation of slurries of all combinations of particles and solvents was investigated at levels of ϕ of approximately 0.05, 0.10 and 0.15. As a typical example of a stable hydrophobic silica suspension, the result with Spherisorb in CH_3CN is depicted in Fig. 3.1(a), where the experimentally determined height S_e of the clear, particle-free, top layer is plotted as function of the settling time. The distance travelled by the interface between suspension and top layer increases linearly for times up to approximately 2500 s for all the concentrations investigated. After 2500 s the whole slurry becomes influenced by the presence of the sediment and settling starts to become retarded. Thus for the first 2500 s the settling velocities are time independent, which indicates that the particles do not aggregate during sedimentation. The solid lines in Fig. 3.1(a) represent the theoretical progress of sedimentation S_t for hard non-aggregated spheres according to equation (3.3) when using a value of K_2 equal to -5.4. Theoretical and empirical settling rates show good agreement confirming the assumption that the silica suspensions are stable. The results in Fig. 3.1(a) also show that the settling rate is strongly dependent on the hydrophobic silica particle concentration.

The distance travelled by the suspension as a function of time for the colloidally unstable suspension Spherisorb in CCl_4 is presented in Fig. 3.1(b). The experimentally determined sedimentation curves S_e indicate much faster settling of the particles than the theoretical curves of S_t with $K_2 = -5.4$, indicating that the particles are aggregated. Remarkable is the fact that with these aggregated suspensions the higher volume fraction suspensions settle slower than those with lower volume fractions. This indicates that the more concentrated suspensions are either aggregated less compactly [19], form smaller aggregates [20], or that the effective volume fraction becomes that high that excessive hindering of the sedimentation occurs.

The optimal coefficient K_2 for colloidally stable suspensions in most cases is -5.4. The optimal value of K_2 only deviated significantly for two suspensions that are definitely stable: for Spherisorb in isopropanol ($K_2 \sim -4.0$) and for Nucleosil in CH_3CN ($K_2 \sim -4.6$). However, their sedimentation speeds – to be discussed later on – are slightly higher than the theoretical value indicating that some agglomeration had occurred in these cases. How K_2 was evaluated can be seen in Fig. 3.2 for the colloidally stable suspensions of Nucleosil in acetone at $\phi = 0.05$, 0.10 and 0.15. In this figure the experimentally sedimentation distances S_e of the sediment during settling are given as a function of the theoretical values of S_t for three different values of K_2. Both axes have been non dimensionalized by the filling height of the tube h_0. Note that the variations in S_t at fixed S_e – being due to variations in K_2 – are larger for higher ϕ as can be understood from inspection of Eq. (3.2).

Aggregated suspensions can be characterized also by the height of the sediment after complete sedimentation. Fig. 3.3 shows the normalized final height h_{final}/h_0 of the sediment of Zorbax SB-C18 as a function of the initial volume fraction of the particles in the suspension. All liquids, except for CCl_4, show a linear relationship between the normalized height of the
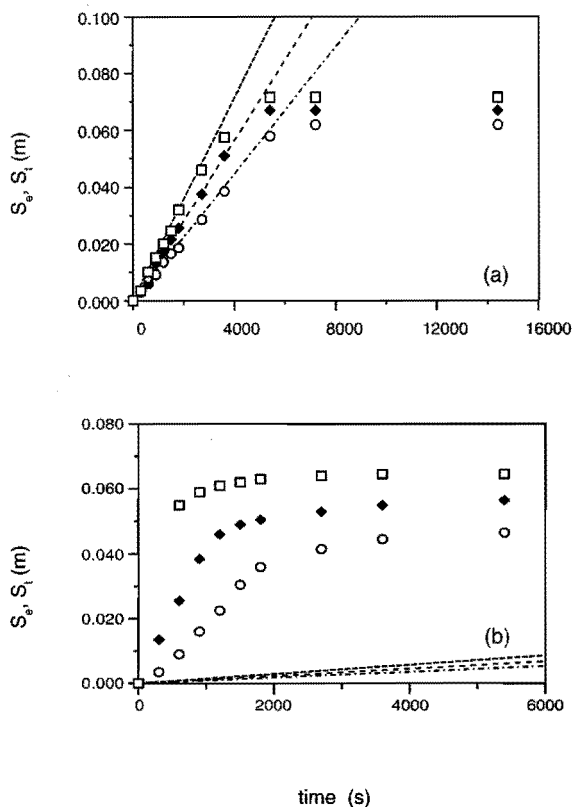
69

Fig. 3.1 (a) and (b). The height S_e of the clear liquid layer on top of a settling suspension of Spherisorb ODS-1 in acetonitrile (a) and CCl_4 (b) as a function of time. Slurry concentrations: (□) 50 kg m^{-3}, (◆) 100 kg m^{-3} and (O) 150 kg m^{-3}. The solid and dashed lines represent S_t.

settled slurry and the volume fraction. Based on these results only CCl_4, and to a lesser extent methanol, are definitely aggregating liquids for Zorbax SB-C18. The theoretical rate of sedimentation yields absolute information on the extent to which the particles are aggregated, whereas the height of the sediment provides only relative information. To describe to what extent the particles are aggregated the "instability ratio" is introduced, which is defined as the ratio of the experimental sedimentation rate of a suspension and the theoretical sedimentation rate for that suspension in the absence of any colloidal interaction between the particles. A summary of the instability ratios of all the systems investigated is given in Table 3.3.

70

Zeta-potential measurements

The Helmholtz-Schmoluchowski equation was employed to convert mobilities into ζ-potentials. Strictly speaking this equation is only applicable at low potentials and with values of
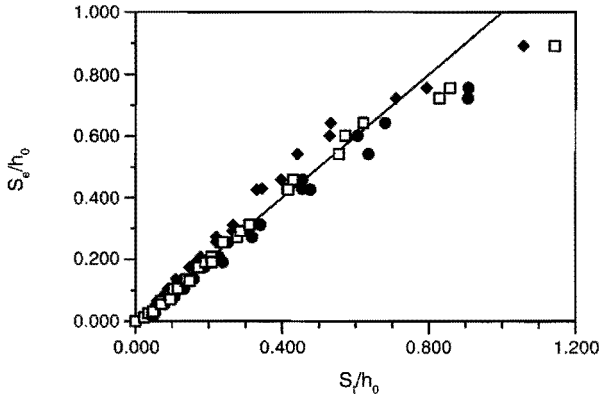
Fig. 3.2. Experimental versus theoretical values of the normalized sedimentation distance for Nucleosil 100-5 C18 in acetone with K_2 equal to ($\blacklozenge$) -4.7, ($\square$) -5.4 and ($\bullet$) -6.6.
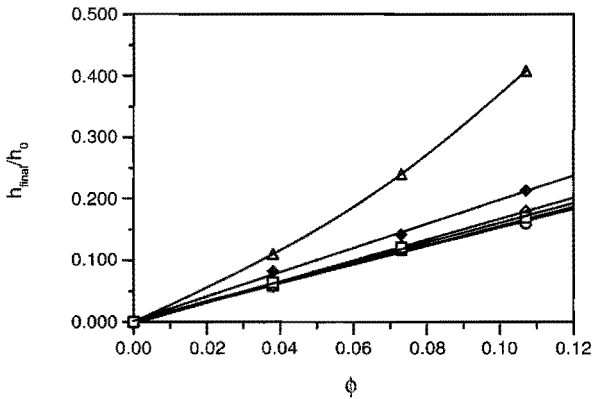
Fig. 3.3. Normalized final height h_{final}/h_0 of the sediment versus the volume fraction ϕ for Zorbax SB C-18 in ($\bullet$) acetone, (O) acetontrile, ($\triangle$) CCl$_4$, ($\square$) isopropanol, ($\blacklozenge$) methanol and ($\blacksquare$) tetrahydrofuran.

$\kappa a > 100$. With low potentials and $\kappa a < 1$ this equation would underestimate the ζ-potential by a factor 2/3 [16]. It is evident that from the values of κ and the ζ-potentials, the Helmholtz-Schmoluchowski equation is not exactly applicable. However, it will be used in view of the fact that (i) the nature and amount of the dissolved electrolyte are not accurately known thus leading to uncertainties in applying more sophisticated theories, and that (ii) the exact values of the high ζ-potentials found seem not to be critical for the conclusions (coagulation should not occur anyhow). κ was derived from conductivity measurements of the pure liquids in order to assess κa, assuming an 1:1 electrolyte with an ionic radius of 10^{-10} m [21]. The conductivity of the pure liquids and the calculated value κ of are given in Table 3.4.

71

Table 3.3 Instability ratio of chemically-modified silicas in non-aqueous solvents

hydrophobic silica	instability ratio					
	acetone	CH_3CN	CCl_4	isopropanol	methanol	THF
Bio-Sil HL 90-5 S	1.02	∞	∞	1.07	∞	0.99
Nucleosil 100-5	1.05	1.19	12.7	5.70	1.80	1.01
Spherisorb ODS-1	0.96	0.98	34.1	1.21	1.08	0.95
Zorbax ODS	1.14	1.33	4.30	1.07	∞	1.01
Zorbax SB-C18	0.96	1.02	45.0	0.99	1.22	0.99

The calculated ζ-potentials for the different systems are summarized in Table 3.5. In all cases the ζ-potential of the chemically modified particles is negative, in line with what would be expected for native silica particles. In a number of cases the particles were severely aggregated and settled quicker than they could be measured. In addition, no ζ-potentials of particles in CCl_4 could be recorded. This is due to the fact that these suspensions are almost transparent. Whereas their sedimentation behaviour could be recorded, the laser-Doppler detector in the z-potential equipment used could not detect the electrophoretic movements.

Colloidal stability and the DLVO theory

In Fig. 3.4 the electrostatic repulsion, the Van der Waals attraction and the total interaction energy of two Zorbax ODS particles in methanol are shown. This result is typical for all suspensions investigated. The Van der Waals attraction – and especially the electrostatic repulsive energy – are large at small distances due to the fact that both are proportional to the radius of the particles – which is very large: ~ 2.5 μm. The Van der Waals interaction at small distances drops with the inverse of the interparticle distance. At larger distances this drop

Table 3.4. Conductivity of the neat liquids and the calculated double-layer thickness

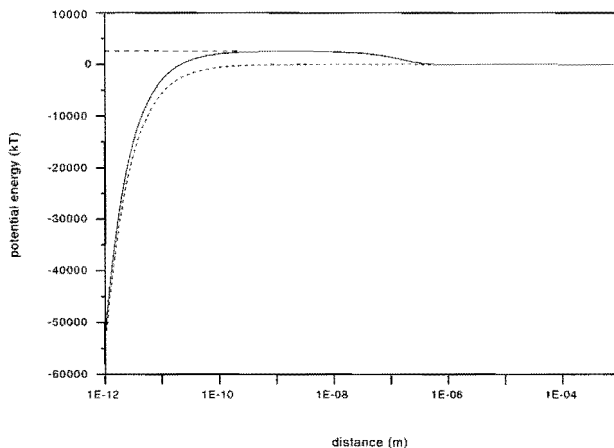| liquid	conductivity $(10^{-5} \, W^{-1}m^{-1})$	$\kappa \, (10^6 \, m^{-1})$
acetone	1.27	3.19
CH_3CN	0.04	0.43
isopropanol	0.27	4.31
methanol	7.09	8.26
tetrahydrofurane	0.08	7.75

Fig. 3.4. Potential energy as a function of the interparticle distance for Zorbax ODS in methanol using Lifshitz theory.

is even more severe due to the retardation effect. However, the electrostatic interaction is large and almost constant until the distance rises beyond the double layer thickness κ^{-1} which typically is 0.1–1 µm. The result is that a large barrier exists that should be adequate in avoiding coagulation in the "primary minimum". The curve also indicates that the "secondary minimum" is negligible. On increasing the distance to the point that the repulsion has dropped to 1 kT the attraction always has been reduced to less than 10^{-2} kT. This excludes flocculation in the secondary minimum as the mechanism for aggregation: aggregation should be inter-

Table 3.5. Zeta-potential of the investigated chemically-modified silicas in various liquids

hydrophobic silica	ζ-potential (mV)				
	acetone	CH_3CN	isopropanol	methanol	THF
Bio-Sil HL 90-5 S	-84.5	-[a]	-102.7	-[a]	-56.9
Nucleosil 100-5	-48.6	-40.9	-[a]	-[a]	-[b]
Spherisorb ODS-1	-64.8	-60.8	-94.4	-71.4	-83.7
Zorbax ODS	-76.6	-62.5	-88.1	-[a]	-80.8
Zorbax SB-C18	-57.5	-61.4	-94.4	-56.4	-65.6

[a] too quickly settling suspension; [b] not measured

preted as being coagulation in the primary minimum. Note that calculations indicate that with these systems for ζ-potentials larger than a few mV an effective barrier against coagulation exists.

In order to gain insight into the role of attractive and repulsive forces on the stability, the instability ratios as summarized in Table 3.3 are plotted in Fig. 3.5 as a function of the attraction and repulsive potentials at a fixed very short interparticle distance, at 10^{-10} m. For completeness also the suspensions for which no ζ-potential were available have been plotted, at $V_{rep} = 0$. The results in Fig. 3.5. indicate that it should be possible to obtain stable suspensions over the whole range of repulsive and attractive potentials investigated. No criterion for instability as found in practice can be deduced from these data. However, in case of severe coagulation (most of the data plotted at $V_{rep} = 0$), larger attraction seems to promote practical instability. Note that the effect of entrapped gas on the Hamaker constant of composite particles in a medium largely depends on the medium employed. Using Lifshitz theory, as an example, values of $1.0 \cdot 10^{-21}$ and $0.91 \cdot 10^{-21}$ J were found for Zorbax ODS particles in methanol and CCl_4 respectively. The same calculations with the assumption of no entrapped gas would have led to $1.60 \cdot 10^{-21}$ and $0.07 \cdot 10^{-21}$ J respectively.

Colloidal stability and processing

The question remains why some slurries are colloidally stable and others are not, while on the other hand they should all be stable for theoretical reasons. A possible answer may be that particles in the systems that contain aggregates, in reality have been in contact with each other from the start of the preparation of the suspension and have never been separated from each other while being stirred or vibrated ultrasonically. Two types of experiments were conducted to check whether it is possible to change the degree of aggregation by changing the method of preparation of the suspension. In the first type of experiments a slurry of 100 mg Bio-Sil in 1 ml acetone was prepared. As expected, it was colloidally stable. The liquid was gradually replaced by CH_3CN. The final slurry and all the intermediates were completely stable, while according to Table 3.3 the final slurry should be instable. Apparently the processing dominates over the thermodynamic arguments. Once two particles have been separated, on gradually replacing the liquid, the ζ-potential presumably remains large enough to keep a sufficient barrier against coagulation. Note that this explains why replacement of liquid does not induce coagulation. However, it does not explain why acetone disperses dry Bio-Sil particles better than CH_3CN does.

In the second type of experiments, the influence of the way of mixing the dry particles with the liquid was investigated. Two experiments were performed (in all cases 500 mg particles in 5 ml liquid):

(i) Instead of adding the liquid to the dry silica particles, the particles were slowly strewn on top of the liquid until the top of the liquid was covered with a very thin layer of these poorly-wetting particles, whereafter the mixture was shaken in order to disperse the added particles. This procedure was repeated until all particles had been added. In that way the final height of the sediment of Spherisorb particles in CCl_4 reduced significantly with respect to the
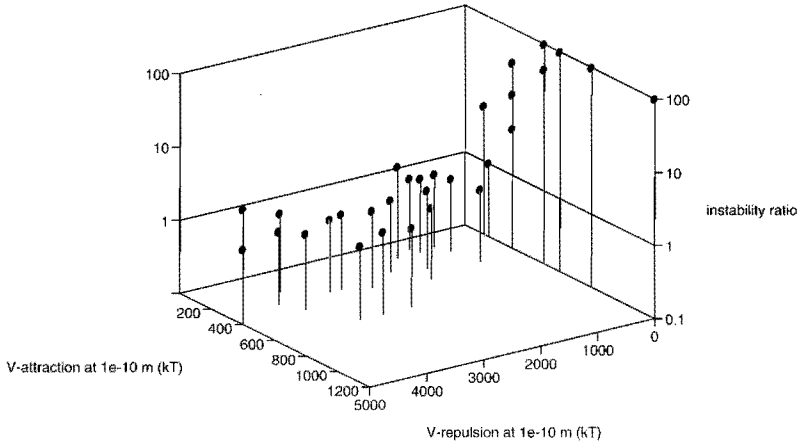
Fig. 3.5. Instability ratios of the slurries as function of their repulsive and attractive potentials at 10^{-10} m. Note that data located at $V_{rep} = 0$ represent suspensions for which no ζ-potential had been measured.

adding-liquid-to-particles process, suggesting a reduction of the degree of aggregation. The final height of the sediment was, however, higher than that of stable suspensions, indicating that the particles are still aggregated to some extent.

(ii) Suspensions of Spherisorb in CCl_4 were prepared in a number of ways, as described in Table 3.6. In all cases after the addition step the suspension was vibrated in an ultrasonic bath for 10 minutes. The sedimentation patterns for the first 90 minutes are shown in Fig. 3.6. From these curves the initial sedimentation rates were evaluated. The corresponding colloidal instability ratios – to be compared with data in Table 3.3 – were calculated and shown in Table 3.6 together with the final heights of the settled suspensions. Note that the individual data points in Fig. 3.6 scatter slightly around the smoothed curve because it is difficult to observe the slurry boundaries in the almost transparent suspensions in CCl_4. It is clear that samples A and C settle down faster indicating larger aggregates. The fact that sample A has a relatively low final sediment volume suggests that its aggregates are more compact. Samples B and D are definitely less agglomerated although they are colloidally still quite instable.

The fact that typically 25% of the pores of these particles was filled with gas after prolonged immersion in any of the liquids used indicates that the coverage by the octadecyl coating is rather inhomogeneous. The reason is that if the coverage would have been homogeneous, either a 0% or a 100% entrapment of gas could be expected, given the small sizes of the pores. In this respect Nucleosil and Spherisorb can be considered as having the best homogeneity in coverage by the octadecyl chains. As the better wetting areas in a particle do presumably not form a continuous, totally interconnected area, wetting will at least partly proceed by gas diffusion. This is a much slower process then when liquid is simply sucked in by
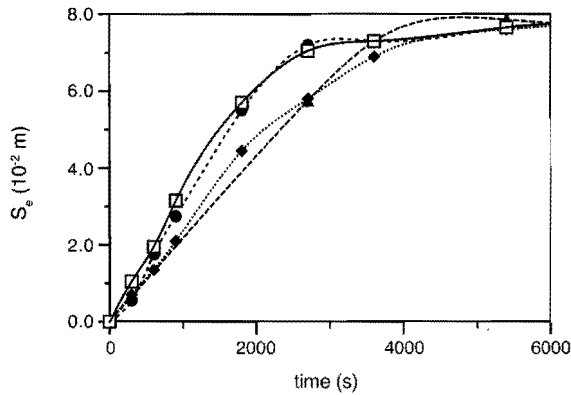
Fig. 3.6 Heights of sediments for the conditions mentioned in Table 3.6: (□) A, (◆) B, (●) C, (▲) D.

capillary forces. Because wettability of particles will be related to the liquid content of a particle, the wettability itself during mixing can be expected to rise slowly up to its equilibriumlevel. This is confirmed by the observation of initially very poor and the finally adequate wet-tability (after prolonged immersion the particles did not stick to the surface any more). It is reasonable to expect that poor initial wettability may keep together any particlesthat initially touch each other. Initially a gas bridge between the particles may assist in keeping

Table 3.6. Influence of processing conditions on colloidal stability

test	addition method	time	instability ratio (from settling rate)	h_{final}/h_0
A	liquid poured on top of particles	1 s	31	0.166
B	particles slowly strewn by hand on top of the liquid (liquid shaken a number of times)	5 min	23	0.179
C	particles slowly strewn by hand on top of liquid (ultra sonic vibration of the liquid)	5 min	31	0.177
D	particles slowly strewn on top of liquid by vibration chute (ultra sonic vibration of the liquid)	5 min	21	0.145

the particles together [22]. However, the fact that the severely agglomerated dispersions in CCl_4 were almost perfectly transparent suggests that gas bubbles as bridges between the particles are absent in the final suspensions. Once the particles are kept together they will have a larger chance to be kept together in the primary minimum. Thus adding single particles sequentially onto a liquid will avoid this sticking mechanism and improve their colloidal stability. This is confirmed by the results with process D in Table 3.6.

CONCLUSIONS

The degree of aggregation of chemically-modified silica particles in non-aqueous liquids can be determined by means of sedimentation experiments. The ratio of the experimentally observed rate of sedimentation of a suspension and the theoretically calculated rate of sedimentation of a non-aggregated silica particle suspension proved to be a very accurate and sensitive method for the determination of the colloidal stability of chemically-modified silica suspensions. The colloidal stability of the suspension is controlled by processing rather than thermodynamical arguments. An important aspect in the application of this method is that the amount of entrapped gas in the particles pores and the effect of hindered settling have to be taken into account. The surfaces of the particles are not chemically modified homogeneously. The ζ-potential was found to be negative in all cases and was relatively large, i.e. $-\zeta > 40$ mV. All investigated chemically modified silica suspensions should be colloidally stable according to the Van der Waals interaction theories. However, slurry processing is found to be very important in achieving colloidal stability in practice.

REFERENCES

[1]   W.M. Jiao, A. Vidal, E. Papirer and J.B. Donnet, *Colloids Surfaces* 40 (1989) 279

[2]   Schriftenreihe Pigmente, Vol. 13, 18, 31, 49, 54, 63, 68 and 73, Degussa, Frankfurt (Germany)

[3]   C.C. Payne, Applications of Colloidal Silica: Past, Present and Future, in H.E. Bergma (ed.), *The Colloidal Chemistry of Silica, American Chemical Society*, Washington, 1994, pp. 581

[4]   G. Lee and H. Rupprecht, *J. Colloid Interface Sci.* 105 (1985) 257

[5]   G. Lee, S. Murray and H. Rupprecht, *Colloid Polym. Sci.* 265 (1987) 535

[6]   G. Machula and I. Dékány, *Colloids Surfaces* 61 (1991) 331

[7]   G. Machula, I. Dékány and L.G. Nagy, *Colloids Surfaces* 71 (1993) 241

[8]   D. Heath and Th.F. Tadros, *J. Colloid Interface Sci.* 49 (1983) 320

[9]   K.K. Unger, in K.K. Unger (ed.), *Packings and Stationay Phases in Chromatographic Techniques*, Marcel Decker Inc., New York, 1990, pp. 43

[10]   M. Peterson, *J. Chromatogr.* 505 (1990) 3.

[11]   J.P.C. Vissers, H.A. Claessens, J. Laven and C.A. Cramers, *Anal. Chem.* 67 (1995) 2103

[12]   W.B. Russel, D.A. Saville and W.R. Schowalter, in W.B. Russel, D.A. Saville and W.R. Schowalter (ed.), *Colloidal Suspensions*, Cambridge University Press, 1989, pp. 395

[13]   J.F. Richardson and W.N. Zaki, *Trans. Inst. Chem. Eng.* 32 (1954) 38

[14]   J.F. Brady and G. Bossis, *Ann. Rev. Fluid Mech.* 20 (1988) 111

[15]   B. Cichocki, B.U. Felderhof, K. Hinsen, E. Wajnryb and J. Blawzdziewicz, *J. Chem Phys.* 100 (1994) 3780

[16]   R.J. Hunter, *Introduction to Modern Colloid Science*, Oxford University Press,Oxford, 1993

[17]   J. Laven and J.P.C. Vissers, submitted for publication

[18]   K.K. Unger, *Porous Silica: its properties and use as support in colomn liquid chromatography*, Elsevier Scientific Publishing Company, Amsterdam, 1979, pp. 147

[19]   N.P. Brown, in N.P. Brown and N.I. Heywood (ed.), *Slurry handling: design of solid-liquid systems*, Elsevier Applied Science, London, 1991, pp. 17

[20]   M. Zrinyi, M. Kabai-Faix and F. Horkay, *Prog. Colloid Polymer Sci.* 77 (1988) 165

[21]   T.J.C. Arts, J. Laven, F. van Voorst Vader and Th. Kwaaital, *Colloids Surfaces A* 85 (1994) 149

[22]   H. Schubert, *Kapillarität in porösen Feststoffsystemen*, Springer, Berlin, 1982

CHAPTER 4.1

COLLOID CHEMICAL ASPECTS OF SLURRY PACKING TECHNIQUES IN MICROCOLUMN LIQUID CHROMATOGRAPHY

ABSTRACT

The relationship between the coagulating properties of slurry suspensions, type of packing liquids, and final performance of slurry-packed microcolumns for liquid chromatography (LC) was investigated. The colloidal stability of stationary phase suspensions was examined by means of sedimentation and zeta-potential experiments. Expressions for the theoretical sedimentation rate of non-coagulated particle suspensions were derived for spherical particles with completely and incompletely filled pores, and irregularly shaped particles with incompletely filled pores. The performance of the slurry-packed microcolumns was predominantly determined by the selection of the packing liquid. It is shown that the packing liquid preferably has to be coagulating to obtain efficient and stable packed capillary LC columns. The selection of the slurry liquid on the column performance was of minor importance.

79

INTRODUCTION

The relatively poor column efficiency and long-term stability of packed capillary columns have delayed the introduction and application of microcolumn liquid chromatography as an analytical technique. Possible reasons for this are the coagulating properties of slurry suspensions, containing alkyl modified silica or polystyrene-divinylbenzene packing materials particles, and the physical/chemical properties of the applied packing liquids. Different packing techniques are proposed to overcome these problems.

Most of the packing procedures of columns in liquid chromatography (LC) are performed by using slurry packing techniques [1]. As a result of the dispersion of the stationary phase particles in a solvent, the attraction between the particles is drastically reduced, resulting in favourable packing conditions compared with dry packing methods [2,3]. However, the type of slurry solvent strongly determines the stability of the slurry suspension. Bristow [4], and more recently Shelly et al. [5,6] and Wang et al. [7], pointed out that the colloidal stability of packing material suspensions, that is the coagulating behaviour of stationary phase particles in a solvent, can be critically important in slurry packing methods. These effects become even more critical in packed fused silica capillary columns of 100–350-μm-internal diameter (i.d.) because of the large value for the column length to column i.d. ratio of such columns [5]. In slurry packing methods efforts are made to avoid coagulation of the stationary phase particles. Currently applied slurry packing techniques are balanced and non-balanced density methods, chemical and mechanical stabilization methods, and high and low slurry-viscosity methods [8].

This chapter reports a quantitative method describing the colloidal stability of porous, reversed phase particles in apolar liquids, as based on the sedimentation rate of the particles. In addition, zeta-potential measurements were performed to study slurry stabilities in more detail. The effect of the type of slurry and packing liquids on the resulting chromatographic performance (plate height, separation impedance, flow resistance parameter) is investigated extensively for nominally identical stationary phases. The results of this study were used to develop selection criteria for slurry packing techniques in microcolumn LC.

THEORY

Spherically shaped particles

Bristow [5] pointed out that the theoretical sedimentation rate can be used to determine the colloidal stability of slurry suspensions. Suspensions in which the particle settling rate exceeded the calculated one, were regarded as coagulated. The theoretical sedimentation rate of spherical stationary phase particle suspensions can be determined with Stokes' equation, but is only valid for solid particles at infinite dilution. At present, most stationary phase particles are porous and infinite dilutions are impractical in column packing techniques. Both

effects can be corrected for by taking the particle porosity ε_i, and a hindered settling function [9-11] into account, which is represented by the term $(1-\phi)^{-K_2}$, resulting in a modified Stokes' expression for the theoretical sedimentation rate of non-coagulated stationary phase particles:

$$u = \frac{(1-\phi)^{-K_2} d_p^2 (\rho_{skel} - 1)(1-\varepsilon_i)g}{18\eta} \tag{4.1}$$

where ϕ is the volume fraction of the particles, K_2 a particle/solvent dependent constant, ρ_{skel} and ρ_l the density of the packing material and the liquid respectively, η the viscosity of the liquid and g the gravitational constant. ε_i can be expressed as [12,13]:

$$\varepsilon_i = \frac{V_{pore}}{V_{hydro}} = \frac{V_{pore}}{V_{pore} + \frac{1}{\rho_{skel}}} \tag{4.2}$$

where V_{pore} is the total pore volume per unit of mass and V_{hydro} the hydrodynamic particle volume per unit of mass. The application of ε_i to calculate the effective density of a particle is only valid for immiscible substances – as is the case for packing material suspensions. ε_i equals zero if the particle is completely solid and theoretically equals one if it is completely porous, meaning no silica backbone is present anymore. As is shown later, equation (4.1) can only be applied for particles with completely filled with slurry liquid: polystyrene-divinylbenzene (PS-DVB) particles. As a result of the possible inclusion of gas into the particle pores, equation (4.3) must be applied for alkyl-modified silicas to calculate the settling rate of non-coagulated porous particles:

$$u = \frac{(1-\phi)^{-K_2} d_p^2 \{\rho_{skel}(1-\varepsilon_i) + \rho_l(\varepsilon_f - 1)\}g}{18\eta} \tag{4.3}$$

where $\varepsilon_f / \varepsilon_i$ is the fraction of filled particle pores. In this equation it was assumed that the density of the gas phase was negligible for the calculation the effective mass of the particles.

Irregularly shaped particles

Predicting the theoretical sedimentation rate is more complicated for irregularly shaped porous packing materials than for spherically shaped particles. The description of the shape of such particles and its influence on the free-falling behaviour are complicating factors [14]. The final settling velocity for irregularly shaped particles is usually determined by means of iterative calculating schemes [14]. However, the theoretical sedimentation rate of non-coagulated particles can be calculated analytically by the combination of the equations that are applied in

iterative calculation schemes, resulting in:

$$u = \frac{(1-\phi)^{-K_2}\psi d_A^2 \left\{\rho_{skel}(1-\varepsilon_i) + \rho_l(\varepsilon_f - 1)\right\}g}{3\pi\eta}$$

(4.4)

where ψ is an empirical shape factor, which is defined as the volume of the particle divided by the volume term obtained from the mean projected area diameter of the particle [14-17]. d_A is the projected area diameter.

EXPERIMENTAL SECTION

Particle characterization

The particle size distribution of the different stationary phases was measured with a Malvern 2600 particle sizer (Malvern Instruments, Worcestershire, UK). The skeleton density of the materials was determined with a gas (He) volume densitometer (Stereopycnometer, Quanta-chrome Corp., Greenvale, NY, USA). Pore volumes were assessed with an automatic multipoint B.E.T. apparatus (Sorptomatic 1900, Carlo Erba Instruments, Milan, Italy). The projected area diameter of irregularly shaped particles was determined as described by Clift *et al.* [16]. Slurry densities were measured with a 10 ml capped liquid pycnometer, after sonication for 10 minutes and thermostating at 20°C for 15 minutes in a water bath.

Particle settling device

A particle settling device was constructed from 130 x 7 mm i.d. glass tubes. The stationary phase slurries were transferred into the tubes by means of a pipette. The tubes were closed by a rubber stopper to prevent solvent evaporation and placed in a home-made tube holder to ensure they were held in a vertical position. The height of the slurry was measured between 5 minutes to 48 hours after filling of the tubes. All sedimentation experiments were carried out twice.

Zeta-potential measurements

The electrophoretic mobility of the packing material particles in the selected slurry liquids was measured by means of a Malvern Zetasizer 3 (Malvern Instruments, Worcestershire, UK) equipped with an AZ-4 cell for moderate conductivity measurements, i.e. electrophoretic experiments in solvents with a relatively high di-electric constant, or an AZ-26 cell for low-conductivity measurements. The principles of detection and measurement, with the AZ-26 cell, are discussed by Arts *et al.* [16].

Column preparation and packing equipment

Columns were constructed from 0.40 m x 320-µm i.d. uncoated fused silica tubing (Chrompack, Middelburg, the Netherlands). An EPM2000 glass filter frit (Whatman, Maidstone, UK) was cut out by the column. To hold the frit in position a 0.080 m x 75-µm i.d./280 -µm outer diameter (o.d.) fused silica capillary (Polymicron Technologies, Phoenix, AZ, USA) was fixed into the larger capillary using epoxy resin.

The packing equipment consisted of a DSTV-122 air driven fluid pump (Haskel Eng., Burbank, CA, USA) for constant pressure packing and a 0.19 x 0.0020 m i.d. stainless-steel slurry reservoir. The column was connected to the slurry vessel with a 0.2 mm i.d./0.5 mm o.d. PVDF double cone (Merck, Darmstadt, Germany).

In this study only reversed phase particles were used. The packing material particles were suspended at a concentration of 100 kg m^{-3} in a slurry liquid by sonication for 10 minutes. Afterwards, the slurry was transferred to the slurry reservoir with a syringe. The columns were unless otherwise stated packed at a pressure of 500 bar during an one hour period.

Chromatographic instrumentation

The HPLC system consisted of a model 100 DM syringe pump (ISCO Inc., Lincoln, NE, USA), a microUVIS20 absorbance detector (Carlo Erba Instruments, Milan, Italy) and a 60 nl CI4W injection valve (VICI-AG Valco Europe, Schenkon, Switzerland). To ensure that no stationary phase could enter the injection valve, a 0.2-µm nylon membrane (Alltech Associates Inc., Deerfield, IL, USA) was positioned into the valve outlet to the column. UV detection was performed at 255 nm. A 900 Series Interface and Nelson 5.0 software (Perkin Elmer Nelson, Cupertine, CA, USA) were employed for data acquisition.

Column evaluation

The reversed phase columns were evaluated with a test-mixture containing four components: uracil (dead volume marker), naphthalene, phenanthrene and anthracene. The concentration of all components was approximately 0.1 mol m^{-3}. As the mobile phase acetonitrile/water (70:30, v/v) was used. The individual solvents of the mobile phase were filtered through a 0.45-µm filter. Prior to use, the mobile phase was degassed with helium. The peak of anthracene was used to calculate the column efficiencies. The reduced plate heights were calculated using an algorithm developed by Foley and Dorsey [19]. In the evaluation of the PS-DVB columns the mobile phase was acetonitrile/water (60:40, v/v) and the test-components were benzilidenacetone and 4-amino-acetophenone. Here the plate heights were calculated for the 4-amino-acetopheneone peak.

83

Chemicals

Acetone, carbontetrachloride, methanol, isopropanol and 4-amino-acetophenone were purchased from Merck (Darmstadt, Germany). Acetonitrile and benzylidenacetone were from

Janssen Chimica (Beerse, Belgium), uracil, anthracene, naphthalene and phenanthrene from Fluka AG (Buchs, Switzerland) and tetrahydrofurane (THF) from Biosolve LTD (Barneveld, The Netherlands). All chemicals were of p.a. grade. Water was purified and demineralized with a Milli-Q water purification system (Waters-Millipore Milford, MA, USA) prior to use.

The Zorbax ODS; 5-µm and Zorbax SB-C18; 5-µm modified silicas were obtained from Rockland Technologies Inc. (New Port, DE, USA). Nucleosil 100-5 C18 and Polygosil 60-5 C18 were from Machery-Nagel GmbH & Co KG (Düren, Germany) and Spherisorb ODS-1 from Phase Separations (Deerfield, UK). The PS-DVB polymer material, RoGel RP, and BioSil C18 HL 90-5 S were from BioRad RSL nv. (Nazareth, Belgium).

RESULTS AND DISCUSSION

Characterization of the particles

The particle diameter, skeleton density of the particles and the particle porosity must be known in order to determine the theoretical sedimentation rate of porous spherically shaped particles, according to equation (4.3). The results of the size distribution, nitrogen absorption and the stereopycnometric measurements on five different octadecyl bonded silicas (ODS) and a PS-DVB packing material are given in Table 4.1. As the average particle diameter d_p the median d_{50} was taken. The particle porosity is given in Table 4.1 too, which was calculated using equation (4.2).

Application of equation (4.1) to suspensions of non-coagulated silica-based packing materials resulted in an overestimation of the theoretical sedimentation rate compared to empirical determined settling rates. Assuming that the silica particles pores would be completely filled with liquid after 10 minutes of sonication, ρ_{skel} should compare well with values for the density obtained with a liquid pycnometer. However, average values as obtained by stereopycnometric experiments were $2.0 - 2.2 \cdot 10^3$ kg m^{-3}, whereas with a liquid pycnometer measurements values of $1.5 - 1.9 \cdot 10^3$ kg m^{-3} were found. These results indicate that the pores of the ODS-particles are only partly filled with liquid. During the sonication of the suspensions gas might remain entrapped in the pores of the silica particles. Additional evidence for this assumption was found with liquid pycnometer experiments carried out at elevated pressures. Compression and decompression was used to remove the gas out of the pores. As an example, with Nucleosil 100-5 C18 in acetone, skeleton densities were found of 1.6055, 1.6415 and 1.6878 10^3 kg m^{-3} at pressures of 1, 6 and 20 bar respectively. As shown by the latter results, the inclusion of air is the most likely reason for the entrapping of air in the particle pores during sonication.

84

The amount of entrapped air can be calculated by applying simple mass equations, knowing ρ_{skel} from a gas pycnometer, V_{pore} from B.E.T. analysis and the apparent skeleton density from a liquid pycnometer. Information about the filled pore fraction can be obtained by expressing the amount of entrapped air as a function of the particle porosity. All liquid pycnometer density measurements were duplicated. The repeatability of these experiments was found

Table 4.1. Median particle diameter d_p (µm), pore volume V_{pore} (10^{-3} m^3 kg^{-1}), skeleton density ρ_{skel} (10^3 kg m^{-3}) and particle porosity ε_i of reversed-phase packing materials

stationary phase	d_p	V_{pore}	ρ_{skel}	ε_i
silica-based (spherical)				
BioSil C18 HL 90-5 S	5.70	0.357	2.101	0.429
Nucleosil 100-5 C18	5.10	0.809	2.106	0.630
Spherisorb ODS-1	4.84	0.430	2.166	0.482
Zorbax ODS	4.40	0.358	1.987	0.413
Zorbax SB-C18	5.24	0.318	2.194	0.411
silica-based (irregular)[a]				
Polygosil 60-5 C18	6.39	0.658	2.077	0.577
polystyrene-based				
RoGel RP[b]	7.59	1.3	1.05	0.577

[a] averaged projected area diameter; [b] for RoGel RP the values for density and pore volume taken as specified by the manufacturer

to be better than 2%. In Table 4.2, $\varepsilon_f/\varepsilon_i$ is given for the different ODS particles in various liquids. Only 40–90% of the silica particle pores got filled with slurry liquid after sonication of the slurry during a ten minute period, as can been seen from the results of Table 4.2. With RoGel RP the pores were completely filled with liquid in all cases.

Sedimentation experiments

Two main types of particle suspensions can be distinguished: coagulated and non-coagulated. The former is characterized by the fact that the particles form clusters and will therefore settle faster than predicted by Stokes' equation for non-coagulated particles. In non-coagulated suspensions the particles are discrete and remain suspended for a relatively long period of time, depending on the particle size, the difference in density between particle and surrounding liquid, and liquid viscosity. Thus, coagulation of particles can be characterized by the sedimentation rate.

Experimental rates of sedimentation were measured with the ODS stationary phases and RoGel RP in a number of selected solvents. During the sedimentation experiments the position of the height of the settling slurry was recorded. To facilitate the comparison of the sedimentation rate for the different combinations of stationary phases and liquids of varying densities and viscosities, normalized parameters were introduced. Normalized height Λ:

Table 4.2. Fraction $\varepsilon_f/\varepsilon_i$ of the pores filled with slurry liquid after sonication for 10 minutes

stationary phase	$\varepsilon_f/\varepsilon_i$					
	acetone	CH$_3$CN	CCl$_4$*	isopropanol	methanol	THF
silica-based						
BioSil C18 HL 90-5 S	0.594	0.420	0.646	0.632	0.700	0.660
Nucleosil 100-5 C18	0.817	0.765	0.837	0.837	0.778	0.832
Spherisorb ODS-1	0.782	0.730	0.795	0.871	0.865	0.836
Zorbax ODS	0.528	0.530	0.777	0.666	0.721	0.789
Zorbax SB-C18	0.591	0.564	0.708	0.752	0.740	0.718
polystyrene-based						
RoGel RP	1.0	1.0	—	1.0	1.0	1.0

ª RoGel RP could not be suspended in CCl$_4$

$$\Lambda = \frac{h_{tot} - h_{clear}}{h_{tot}} \tag{4.5}$$

where h_{clear} and h_{tot} are the heights of the clear top layer and of the total slurry respectively. Normalized time τ:

$$\tau = \frac{tu}{h_{tot}} \tag{4.6}$$

where t is time elapsed since the start of the sedimentation experiments and u the theoretical sedimentation rate of non-coagulated particles according to equation (4.1), (4.3) or (4.4). For the hindered settling constant K$_2$ a value of -5.4 was used. A more detailed explanation about hindered settling is given elsewhere [20]. In that paper a detailed discussion is given on the coagulating behaviour of ODS particles, as based on Van der Waals interactions.

An example of a graph of normalized height of a sediment versus normalized time for two different slurry liquids at three different slurry concentrations is shown in Fig. 4.1(a) and 4.1(b). The solid lines in these figures represent the normalized theoretical sedimentation rate for non-coagulated suspensions. As can be seen from these figures, Nucleosil 100-5 C18 in acetone clearly shows non-coagulated behavior. The theoretical and experimental sedimentation curves are in good agreement. However, the same stationary phase, Fig. 4.1(b), coagulates in carbontetrachloride.
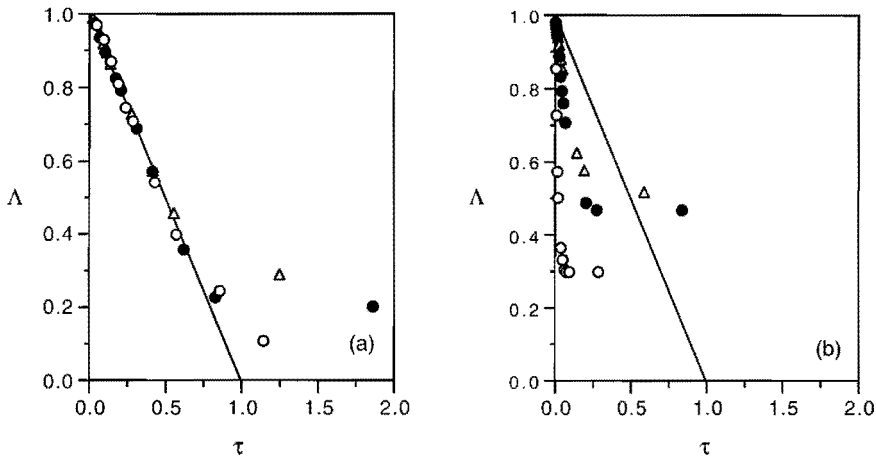
Fig. 4.1. Normalized height of the sediment Λ as a function of the normalized time τ for Nucleosil 100-5 C18 in acetone (a) and CCl_4 (b) as the dispersion liquid. Slurry concentrations: (O) 50 kg m^{-3}, ($\bullet$) 100 kg m^{-3} and ( ) 150 kg m^{-3}. The solid line represents the theoretical rate of sedimentation for non-coagulated stationary phase particles.

This approach for particle sedimentation provides information about the extent to which the particles are coagulated, whereas the sedimentation quotient as was introduced by Shelly et al. [5] provides only relative information. Furthermore, the sedimentation rate is more sensitive towards coagulation than the sedimentation quotient, especially for low suspension concentrations. All investigated silica-based stationary phase were not coagulated in acetone, acetonitrile, isopropanol and THF. Exceptions were BioSil C18 HL 90-5 S which was coagulated in acetonitrile, and Nucleosil 100-5 C18 which was coagulated in isopropanol. Coagulation of all silica materials took place in acetonitrile/H_2O (70:30, v/v), carbontetrachloride and methanol. Here, Spherisorb ODS-1 and Zorbax SB-C18 were exceptions because they did not coagulate in methanol and only moderately coagulated in acetonitrile/H_2O (70:30, v/v). RoGel RP coagulated in carbontetrachloride, isopropanol and methanol.

A comparison of the theoretical rates of sedimentation of irregularly shaped particles with the experimental settling rate can be performed in a similar way. To demonstrate this, Polygosil 60-5 C18 was employed for sedimentation experiments in acetone. The shape factor ψ was estimated to be 0.26. The slurry concentration was 100 kg m^{-3}. The results are shown in Fig. 4.2. The open spheres represent normalized times if a $\pm$ 5% deviation in ε_i – the most critical sedimentation parameter – was assumed. Again, the theoretical and experimental settling rate are in fairly good agreement for irregularly shaped particles.
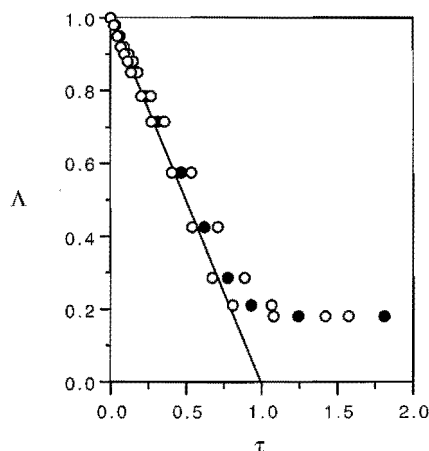
87

Fig. 4.2. Normalized height of the sediment Λ vs. the normalized time τ for Polygosil 60-5 C18 in acetone as the dispersion liquid. ($\bullet$) $\varepsilon_i = 0.577$ and ($\circ$) $\varepsilon_i \pm 5\%$. The solid line represents the theoretical rate of sedimentation for non-coagulated stationary phase particles, using $\varepsilon_i = 0.577$.

Zeta-potential measurements

ζ-potentials of the particles were measured to determine whether electrostatic or steric effects play a decisive role in slurry stabilization. A measure for the degree of coagulation is the ratio α of the initial slope of the experimentally determined and the theoretically calculated sedimentation rates, that is $\alpha = (\Delta\Lambda_{exp.}/\Delta\tau_{exp.})/(\Delta\Lambda_{theor.}/\Delta\tau_{theor.})$. $\alpha = 1$ for stable suspensions and $\alpha > 1$ for coagulated suspensions.

In Fig. 4.3, α is given of four types of packing material particles in methanol as a function of the ζ-potential. With all suspensions that are stable according to the sedimentation experiments, ζ-potentials in the order of -40 to -100 mV were found. Electrostatic repulsion forces are therefore believed to be predominant in the stabilizing effects of these kind of particles. Because of the geometry of the measuring cell and refractive index differences it was impossible to determine the ζ-potential of unstable and carbontetrachloride suspensions respectively.

Chromatographic results

88

A number of solvents was selected as slurry and packing liquids in the packing procedure for the microcolumns, based on the results of the sedimentation experiments. A representative example of the results obtained is given in Table 4.3, where the average chromatographic performances for capillary columns packed with Nucleosil 100-5 C18 as the stationary phase are summarized. Of each type of column at least three were prepared and tested. In all LC Fig.
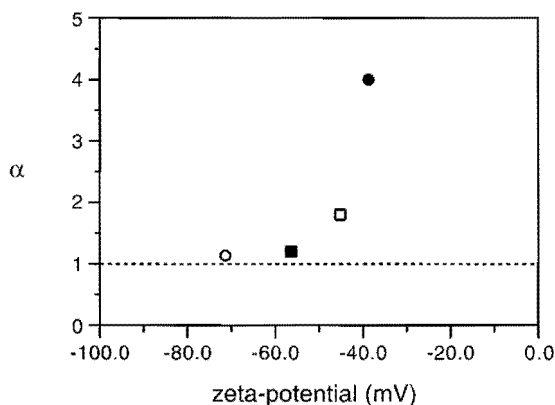
4.3. Degree of flocculation α *vs.* the ζ-potential for (○) Spherisorb ODS-1, (■) Zorbax SB-C18, (□) Nucleosil 100-5 C18 and (●) RoGel RP packing materials in methanol as the dispersion liquid. The concentration of the slurry from which α was derived was 100 kg m^{-3}.

experiments the mobile phase velocity was 4 µl min^{-1}, a value close to the optimum velocity of the mobile phase for each case. From the first three rows in this table it can be seen that if the same solvent was used as the slurry and the packing liquid, low efficient columns were obtained in terms of h, ϕ', and E irrespective the coagulating properties of the suspensions. However, acetone was a clear exception in this respect. Similar results were found for other stationary phases, as shown later. For all investigated stationary phases, the lowest efficiencies were obtained with THF as the slurry liquid and the packing liquid. Moreover, during the conditioning step of these columns, consolidation of the chromatographic bed was observed of about 20–30 mm over a total column length of 0.40 m. An explanation of this effect is discussed in the next section, where attention is paid to the contradiction between h and ϕ' for columns packed with THF as the slurry and packing liquid too.

Changing the packing procedure using the same slurry and packing liquid into a system consisting of non-coagulating or moderately coagulating slurry liquids and coagulating packing liquids resulted in good quality capillary columns, as can be seen from the second and third series of rows in Table 4.3. These results indicate that, to obtain well-packed capillary fused silica columns, the type of the slurry liquid is of minor importance compared with the type of the packing liquid. No consolidation was observed for columns packed with acetonitrile/H$_2$O (70:30, v/v). In all other cases, consolidation of the chromatographic bed was moderate.

Results similar to the Nucleosil 100-5 C18 microcolumns were obtained for columns packed with BioSil C18 HL 90-5 S as the stationary phase. In the latter experiments, the slurry liquid,

89

Table 4.3. Column performance of 320-μm i.d. capillary columns packed with Nucleosil 100-5 C18, using different slurry and packing liquids. Columns were tested with an eluent composition CH_3CN/H_2O (70:30, v/v). The eluent velocity was 4 μl min^{-1}. The test compound was anthracene (k ~ 4)

slurry liquid*	packing liquid*	h	φ'	E
acetone	acetone	2.08	587	2530
methanol	methanol	4.25	493	11100
THF	THF	7.48	1150	68000
acetone	methanol	2.35	639	3740
THF	methanol	2.68	701	5320
acetone	CH_3CN/H_2O	2.43	608	3630
CH_3CN/H_2O	CH_3CN/H_2O	2.42	571	3340
methanol	CH_3CN/H_2O	2.25	609	3100
THF	CH_3CN/H_2O	2.34	849	4600

* CH_3CN/H_2O: (70:30, v/v)

carbontetrachloride, was used constantly and the packing liquids were varied. In Fig. 4.4 the obtained Knox h-v curves are depicted for the applied slurry solvents for the BioSil C18 HL 90-5 S stationary phase. From the results in Fig. 4.4, it can be seen that good columns were obtained with the coagulating packing liquids, acetonitrile, acetonitrile/H_2O (70:30, v/v) andmethanol. The non-coagulating packing liquids, isopropanol and THF, yielded columns of lower separation efficiency. In these experiments acetone was an exception too. Although acetone showed non-coagulating properties, it yielded very good results when applied as the packing liquid. As yet, no reasonable explanation for this has been found.

Application of the results of the experiments described above to the other investigated reversed-phase packing materials showed similar results. In summary, going from a non-coagulating slurry/packing liquid system, isopropanol/isopropanol, to a non-coagulating/coagulating system, acetone/methanol, for Spherisorb ODS-1 h-values decreased from 8.3 to 3.9. For Zorbax SB-C18, h was 19.1 in a THF/THF system; this value decreased to 4.7 for a system using acetone as the slurry liquid and methanol as the packing liquid. For Zorbax ODS the h-value was 3.5 for a non-coagulating/coagulating system THF/(acetonitrile/H_2O (70:30, v/v)). These results of reduced plate heights are moderate compared to the results obtained for Nucleosil 100-5 C18 and BioSil C18 HL 90-5 S. However, in the latter experiments the particles coagulated moderately in the applied packing liquids. Application of more coagulating packing liquids might increase the performance of these columns. For RoGel RP a h-value of 6.4
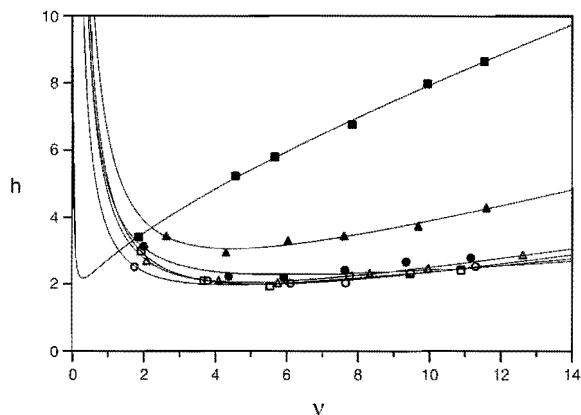
Fig. 4.4. Knox h-v plots for fused silica capillary columns packed with Bio-Sil C18 HL 90-5 S. CCl$_4$ was used as the slurry liquid. The packing liquids were: (O) acetone, (●) acetonitrile, ( ) acetonitrile/H$_2$O (70:30, v/v), (▲) isopropanol, (□) methanol and (■)THF. Test conditions as in Table 4.3.

was observed when acetonitrile was applied as the slurry and packing liquid. For a non-coagulating/ coagulating system, THF/ (acetonitrile/H$_2$O (70:30, v/v)), h was reduced to 4.4. Similar results were reported recently by Cortes and Pfeiffer [21] for another PS-DVB material tested in the size exclusion chromatography mode for incompletely permeating compounds.

Chromatographic bed structures

The most plausible explanation for the extreme consolidation phenomena, observed in the experiments for columns packed with THF as the slurry and the packing liquid, is that the electrostatic repulsion forces between the particles during the packing process could not be overcome by the applied packing pressure. Alternatively, the particles were pushed away from each other by the same kind of electrostatic forces, after disconnecting the column from the packing equipment, both resulting in a very loosely packed bed. During conditioning of the THF/THF packed capillary columns the loosely packed stationary phase particles coagulate and reorganization of the chromatographic bed takes place. This consolidation process is random and results in a very disordered bed, as indicated by the reduced plate height and flow resistance parameter of the Nucleosil 100-5 C18 THF/THF packed columns. These ideas are supported by scanning electron microscope pictures of cross-sections of packed capillary columns, of which examples are given in Fig. 4.5. To obtain correct information about the structure of the chromatographic bed, the particles were embedded in a low viscosity resin [22] prior to the cutting of the column. The main demands for such a resin are a low viscosity in its monomeric state and a negligible difference in density between the monomeric and polymeric state.
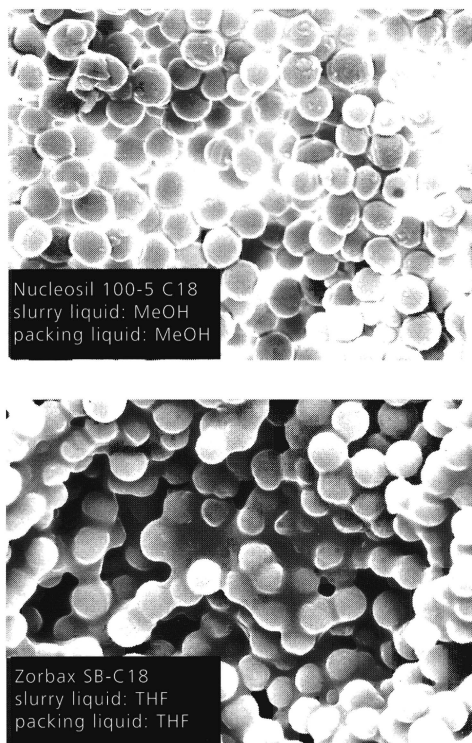
Fig. 4.5. Scanning electron microscope picture of the cross-section of a fused silica capillary column packed with Nucleosil 100-5 C18 (top); slurry liquid methanol; packing liquid methanol; h = 2.9 and Δp = 94.3 bar, or Zorbax SB C18 (bottom); slurry liquid THF; packing liquid THF; h = 21.9 and Δp = 165.8 bar.

Fig. 4.5 (top) shows the cross-section of a chromatographic bed of a Nucleosil 100-5 C18 packed column, using methanol as the slurry and packing liquid respectively. This column showed a relatively low h value of 2.7 and a moderate back pressure Δp of 94.3 bar over a column length of 0.412 m, which is in agreement with the observed bed structure, i.e. a homogeneous tightly-packed bed. In Fig. 4.5 (bottom) a packed bed cross-section is shown for a Zorbax SB-C18 packed columns, using THF as the slurry and the packing liquid respectively. This column showed a very high h of 21.9 and a Δp of 165.8 bar over a column length of 0.445 m. The reason for the low performance of the column is obvious. As can be seen from the bottom picture in Fig. 4.5, the bed structure is very disordered and even channels are present. However, examination of other slices of cross-sections of this column also showed tightly-packed particles, explaining the very high back pressure of the column.

Table 4.4. Average values (n = 5) of the reduced plate height h, separation impedance E and flow resistance factor φ' with relative standard deviation (%, in parentheses) for 320-µm i.d. capillary columns packed with with BioSil C18 HL 90-5 S applying six different packing liquids and CCl_4 as the slurry liquid; columns were tested with an eluent composition CH_3CN/H_2O (70:30, v/v). The test compound was anthracene (k ~ 4)

packing liquid	h		E		φ'	
acetone	2.37	(16.3)	3980	(32)	698	(12.7)
CH_3CN	2.41	(14.0)	3570	(31)	600	(5.8)
CH_3CN/H_2O (70:30, v/v)	2.11	(2.2)	2650	(10)	595	(10.7)
isopropanol	2.79	(24.2)	5180	(25)	629	(4.7)
methanol	2.32	(15.8)	3240	(31)	597	(9.3)
THF	4.05	(66.0)	19300	(12)	832	(20.6)

Reproducibility studies

BioSil C18 HL 90-5 S was also used to test the reproducibility of packing procedures using the same slurry and packing liquids as described in the section chromatographic results. Eachpacking procedure was repeated five times in order to gain statistical information about the repeatability in h, E and φ' at the optimum mobile phase velocity of these procedures. The results are given in Table 4.4.

The coagulating packing liquids acetonitrile, acetonitrile/H_2O (70:30, v/v) and methanol generally showed a better repeatability for h than the non-coagulating packing liquids acetone, isopropanol and THF. The repeatability obtained with acetone as the packing liquid was, however, only slightly higher. Far the best results were obtained with using acetonitrile/H_2O (70:30, v/v) as the packing liquid. h, E and φ' and the repeatability were significantly better compared to the other liquids. It is noteworthy that BioSil C18 HL 90-5 S particles in acetonitrile/H_2O (70:30, v/v) were more coagulated in acetonitrile/H_2O (70:30, v/v) compared to the other packing liquids.

CONCLUSIONS

The theoretical free settling rate of non-coagulated spherical and irregularly shaped reversed-phase packing materials in aqueous-organic solvents can be determined by means of a modified Stokes' equation that accounts for possible inclusion of air in the pores of the stationary phase particles. The degree of particle coagulation in slurry and packing liquids can be derived by comparison of the experimentally determined sedimentation rate of the particles with the theoretically calculated sedimentation rate of non-coagulated particles. No general rules for the coagulating behaviour of ODS particles can be derived. However, THF and acetone have

non-coagulating properties for all investigated ODS stationary phases. The results of the stability experiments of reversed phase particle suspensions, measured by sedimentation, were in good agreement with the ζ-potential measurements.

The chromatographic performance of a packed bed in a microcolumn is strongly influenced by the nature of the packing liquid, rather than by the slurry liquid. A packing liquid must preferably have coagulating properties to obtain good results in terms of reduced plate height and flow resistance parameter. From the results of this study, the slurry liquid obviously is of minor importance for the final performance of packed capillary columns. The applied pressures are most likely large enough to overcome the attraction forces between the particles during the packing process, even in the case of the use of coagulating slurry liquids. No general rules exist for the selection of a proper slurry liquid. Finally, it can be concluded that for each stationary phase the individual packing solvent and packing condition has to be optimized to achieve satisfactory chromatographic performance. However, the results from this research provide adequate tools for the proper selection packing liquid to be used in packing techniques for capillary LC columns.

REFERENCES

[1]   P.A. Bristow, P.N. Brittain, C.M. Riley and B.F. Williamson, *J. Chromatogr.* 131 (1977) 57

[2]   G. Crestinni and A.R. Mastrogiacomo, *J. Microcol. Sep.* 3 (1991) 539

[3]   Y. Guan, L. Zhou and Z. Shang, *J. High Resolut. Chromatogr.* 15 (1992) 434

[4]   P.A. Bristow, *Liquid Chromatography in Practice*; hetp: Handforth, 1977, pp. 34

[5]   D.C. Shelly and T.J. Edkins, *J. Chromatogr.* 411 (1987) 185

[6]   D.C. Shelly, L. Antonucci, T.J. Edkins, and T.J. Dalton, *J. Chromatogr.* 458 (1989) 267

[7]   H. Wang, R.A. Hartwick, N.T. Miller and D.C. Shelly, *J. Chromatogr.* 523 (1990) 23

[8]   M. Verzele and C. Dewaele, *LC•GC Int.* 4 (1986) 614

[9]   R.A. Khan and J.F. Richardson, *Chem. Eng. Comm.* 78 (1989)111

[10]   R.A. Davis and A. Acrivos, *Ann. Rev. Fluid Mech.* 17 (1985) 91

[11]   W.B. Russel, D.A. Saville and W.R. Schowalter, in W.B. Russel, D.A. Saville and W.R. Schowalter (ed.) *Colloidal Suspensions*, Cambridge University Press, Cambridge, 1989, pp. 395

[12]   K.K. Unger, in K.K. Unger (ed.), *Porous Silica: its properties and use as a support in column liquid chromatography*; Elsevier Scientific Publishing Company, Amsterdam, 1979, pp. 147

[13]   K.K. Unger, in K.K. Unger (ed.), *Packings and Stationary Phases in Chromatographic Techniques*; Marcel Dekker Inc., New York, 1990, pp. 43

[14]   N.P. Brown, in N.P. Brown and N.I. Heywood (ed.), *Slurry Handling: design of solid-liquid systems*, Elsevier Applied Science, London, 1990, pp. 17

[15]   R. Turton, and O. Levenspiel, *Powder Technol.* 47 (1986) 83

[16]   R. Clift, J.R. Grace and M.E. Weber, *Drops and Particles;* Academic Press, London, 1978, pp. 16

[17]   H. Heywood, in H. Heywood (ed.), *Interaction between Fluids and Particles,* Institution of

Chemical Engineers, London, 1962, pp. 1

[18]   T.J.C. Arts, J. Laven, F. van Voorst Vader and Th. Kwaaitaal, *Colloids Surfaces A* 85 (1994) 149

[19]   J.P. Foley and J.G. Dorsey, *Anal. Chem.* 55 (1983) 730

[20]   J.P.C. Vissers, J. Laven, H.A. Claessens, C.A. Cramers and W.G.M. Agterof, *Colloids Surfaces A* 126 (1997) 33

[21]   H.J. Cortes and C.D. Pfeiffer, *Anal. Chem.* 65 (1993) 1476

[22]   A.R. Spur, *J. Ultrastucture Research* 1969 (26) 31

CHAPTER 4.2

COMPARISON OF SPHERICALLY AND IRREGU-LARLY SHAPED STATIONARY PHASE PACKINGS IN MICROCOLUMN LIQUID CHROMATOGRAPHY

ABSTRACT

Spherically and irregularly shaped reversed phase packings were used to slurry pack capillary fused silica columns. The selection of the packing solvents was based on the colloidal properties of the stationary phase particles and investigated by sedimentation experiments. The chromatographic performance of the microcolumns was measured with conventional parameters from plate and rate theories, and the column resistance parameter and separation impedance. Also studied was the time of analysis. The performance of spherical and irregular packings was comparable with a light preference for spherically shaped materials when time of analysis is concerned.

97

INTRODUCTION

Spherically shaped stationary phase particles are generally believed to have better chromato-graphic properties, i.e. a higher number of plates and a better column life expectancy, than their irregularly shaped counter parts. This was especially the case after the introduction of spherical silica gels as support for stationary phases in liquid chromatographic (LC) columns [1,2]. Later studies showed, however, that no or limited advantages arise from the use of spherically shaped particles as compared to irregularly shaped particles [3-9]. In order to com-pare packing materials with different particle shaped, and their use in LC, the particle geom-etry has to be characterized and the packing method optimized for each type of stationary phase individually. Most comparative studies on the performance of spherical and irregular silicas lack of proper particle characterization, resulting in incorrect conclusions when reduced parameters, like reduced plate height h, separation impedance E and Knox-plots, are used.

In microcolumn LC, spherical stationary phases are almost exclusively used. Exceptions are the work of McGuffin and Novotny [9], who did pioneering work on the optimization and evaluation of packed capillary columns using spherically and irregularly shaped materials, and the work of Wilson et al. [10], who studied the effect of the column to particle diameter for both irregular and spherically packings. Both studies [9,10] involved normal phase chromatog-raphy. A detailed comparison on the use of spherically and irregularly shaped particles has, by the knowledge of the authors, not been done yet. Furthermore, slurry packing optimization in microcolumn LC has only been performed on spherical packing materials.

This chapter reports how the packing of fused silica capillaries can easily be optimized using proper packing solvents. Furthermore it is demonstrated whether the shape of the par-ticles influences the LC performance. This study employs reversed phase chromatography to determine microcolumn efficiencies. Columns are compared by the number of plates per unit of length N/L, the plate height H_{min} at optimum linear mobile phase velocity, the reduced plate height h_{min} at optimum reduced mobile phase velocity, the flow resistance parameter ϕ', the separation impedance E and the time of analysis.

EXPERIMENTAL

Chemicals

In this study only reversed phase particles were used. The packing material particles were suspended at a concentration of 100 kg m^{-3} in a range of slurry liquids by sonication for 10 minutes. Thereafter the slurry was transferred to the slurry reservoir with a syringe. Acetone and methanol were purchased from Merck (Darmstadt, Germany). Acetonitrile was from Janssen Chimica (Beerse, Belgium), uracil, anthracene, naphthalene and phenanthrene from Fluka AG (Buchs, Switzerland) and tetrahydrofurane (THF) from Biosolve LTD (Barneveld, The Nether-lands). All chemicals were of p.a. grade. Water was purified and demineralized with a Milli-Q water purification system (Waters-Millipore, Milford, MA, USA) prior to use.

Basically, the same silicas with the same bonding chemistry should be used when spherical particles are to be compared with irregulars. This is practically, however, not achievable since different kinds of chemistry are involved in the production of respectively spherically and irregularly shaped silica sols, resulting in chemically different species. Therefore, spherically and irregularly shaped reversed phase packing materials were purchased from two different manufacturers. The materials per manufacturer had the same bonding chemistry. Nucleosil 100-5 C18 and Polygosil 100-5 C18 were obtained from Machery-Nagel GmbH & Co KG (Düren, Germany). BioSil C18 HL 90-5 S and BioSil C18 HL 90-5 were obtained from BioRad RSL nv. (Nazareth, Belgium).

Stationary Phase Characterization

The particle settling device, the construction of the fused silica capillary columns and the packing equipment are described in a previous paper [11]. The mean particle diameters (median) of the spherically shaped stationary phases were determined by means of light scattering techniques [11]. The average particle size of Nucleosil 100-5 C18 and BioSil C18 HL 90-5 S, both spherically shaped, was 5.10 and 5.70 μm respectively. The irregularly shaped packings were characterized by their projected area diameter [11,12]. The mean projected area diameter of the particles of Polygosil 100-5 C18 and BioSil C18 HL 90-5, both irregularly shaped, were 6.33 and 6.57 μm respectively. Nucleosil 100-5 C18 and Polygosil 100-5 C18 were packed at a pressure of 500 bar, and BioSil C18 HL 90-5 S and BioSil C18 HL 90-5 were packed at a pressure of 300 bar.

Capillary LC Instrumentation

The HPLC system consisted of a Phoenix 20 CU syringe pump and a Phoenix 20 syringe slave pump (Carlo Erba Instruments, Milan, Italy), a 785A Programmable Absorbance detector (Applied Biosystems, San Jose, CA, USA) equipped with a z-shaped detection cell (LC Packings, Amsterdam, The Netherlands) and a 60 nl CI4W injection valve (VICI-AG Valco Europe, Schenkon, Switzerland). A 0.2-μm nylon membrane (Alltech Associates Inc., Deerfield, IL, USA) was positioned into the valve outlet to the column in order to prevent that stationary phase particles could enter the injection valve. UV detection was performed at 254 or 275 nm. The output of the detector and the pressure of the pump were monitored with a BD41 potentiometric recorder (Kipp & Zonen, Delft, The Netherlands). Data handling was performed with Nelson 5.2 software (Perkin Elmer Nelson, Cupertine, CA, USA).

The reversed phase columns were evaluated isocratically with a test-mixture containing four components: uracil (dead volume marker), naphthalene, phenanthrene and anthracene. The concentration of all components was approximately 0.1 mol m^{-3}. As the mobile phase acetonitrile/water (70:30, v/v) was used. The individual solvents of the mobile phase were filtered through a 0.45-μm filter. Prior to use, the mobile phase was degassed with helium. The peak of naphthalene or phenantrene was used to calculate column efficiencies. Plate heights were calculated using an algorithm developed by Foley and Dorsey [13]. The diffusion

coefficients D_m of the test compounds in the mobile phase were calculated as proposed by Wilke and Chang [16].

RESULTS AND DISCUSSION

Column packings conditions

In order to obtain efficient, reproducible packed fused silica capillary columns the stationary phase particles should preferably have coagulating properties in the packing liquid [11]. However, instead of kinetic settling experiments, involving very detailed particle characterization, the coagulating properties of packing liquids can also be determined by means of the final height of the sediment, i.e. the height of the sediment after the particles are completely settled [14,15]. A high sediment is found with coagulated particles, a low sediment in the case of non-coagulated particles.

In Fig. 4.6 the final height of the sediments of four reversed phase packing materials, two spherically and two irregularly shaped, is given in four different kind of liquids. A good example is Nucleosil 100-5 C18, which is coagulated much more severely in acetonitrile/H_2O (70:30, v/v) than in THF. These results give however only relative information. To what extent the particles are coagulated, or if the particles are not coagulated at all, can not be derived from these kind of experiments. Coagulation of the stationary phase particles in the slurry liquid is less critical [11]. For Nucleosil 100-5 C18, Polygosil 100-5 C18 and BioSil C18 HL 90-5, the mixture acetonitrile/H_2O (70:30, v/v) was used as the packing liquid. For BioSil C18 HL 90-5 S this was acetonitrile/H_2O (70:30, w/w). As slurry liquid acetone was used, because of its low viscosity (increased packing speed) and relatively low toxicity, for all stationary phases.

Chromatographic Results

Van Deemter (H vs. u) and Knox (h vs. v) curves for all stationary phase for a retained compound with a retention factor of ~ 3.5–4 were measured and are given in Fig. 4.7 (a) and Fig. 4.7 (b). All Van Deemter curves show – as expected – very small increments in plate height with increasing mobile phase velocity. Based on the H-u plots, the spherical-particle stationary phases would be interpreted as the 'best' column packing materials, i.e. lowest plate number at optimum mobile phase velocity. However, taking into account the repeatability of the packing process, which is ~ 5–6%, all the H–u curves should be the same. Efficiencies obtained on spherically and irregularly shaped materials, as measured by the plate height, are therefore the same too.

The differences in the minimal reduced plate height h between the spherical and irregular materials are somewhat larger than in the Van Deemter curves. As already mentioned in the experimental section, the irregular materials have a larger particle diameter, and are the reason why they do somewhat better in the h–v curves. These results are confirmed by the data given in Table 4.6, discussed in the next section.
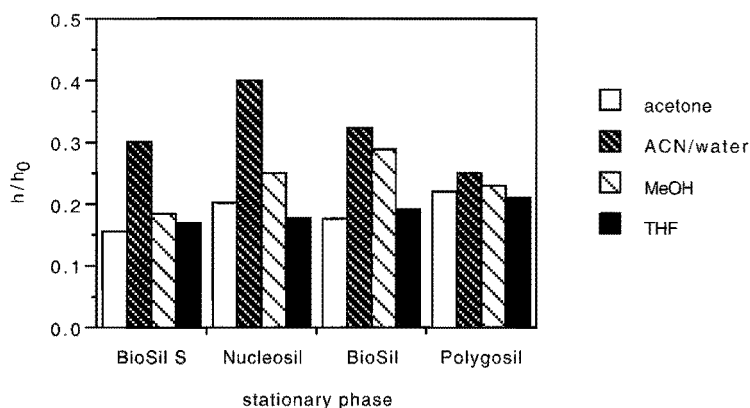
100

Fig. 4.6. Normalized height, i.e. height of sediment over height of slurry, for spherically and irregularly shaped particles in a number of selected liquids. The ratio acetonitrile/H_2O was (70:30, v/v) in all cases, BioSil C18 HL 90-5 S excepted (70:30, w/w).

Other useful column characteristics are the flow resistance factor ϕ' and the separation impedance E, both dimensionless parameters [17]. ϕ' reflects how much pressure is needed for an analysis, or which column length may be used at a given pressure and mobile phase velocity. For packed microcolumns ϕ' is between 500 and 1000. E includes the obtained number of plates and the time and pressure needed for a separation. Its lowest expected value is 2000. The flow resistance factor and the separation impedance for all investigated stationary phases are given in Table 4.5. With all packing materials and packing conditions, three columns were packed and tested. The number of plates per meter N/m, the minimal plate height H_{min}, the minimal reduced plate height h_{min}, the total column porosity ε_t and the column permeability K_0 are given in Table 4.5 too.

Table 4.5 indicates once more the minor differences in the number of plates and the plate height H_{min} that were obtained with spherical and irregular packing materials. The differences in h_{min} are however significant and show that the irregulars are packed more efficiently. Almost all ϕ'-values fall in the range 500–1000, but are all at the high end, Nucleosil 100-5 C18 excepted, compared to conventional 4.6 mm i.d. stainless-steel columns. However, neither the spherical nor the irregularly shaped particles showed a pronounced better flow resistance parameter. Thus their resulting separation impedance values are also all of the same magnitude. Table I also indicates the minor differences in number of plates that as obtained with spherically and irregularly shaped particles. The permeability of the columns was found to be somewhat higher than reported by others [18].

101
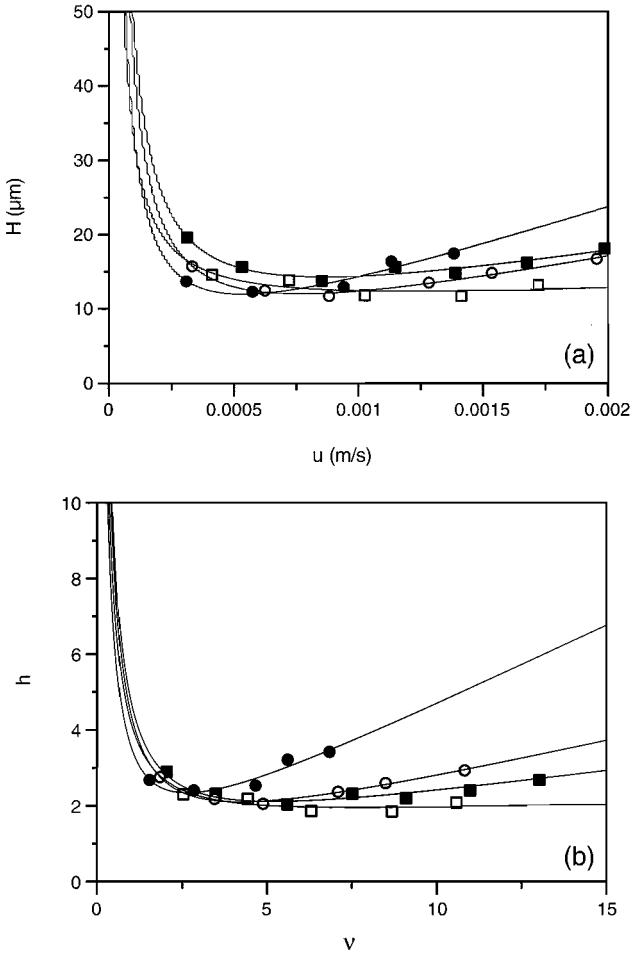
Fig. 4.7. *Van Deemter* curves for spherically and irregularly shaped particles (a) and *Knox* curves for spherically and irregularly shaped particles (b). (O) BioSil C18 HL 90-5 S, (●) Nucleosil 100-5 C18, (□) BioSil C18 HL 90-5 and (■) Polygosil 100-5 C18. See the text for conditions.

The performance of packed microcolumns can also be compared with respect to the speed of analysis. The time t_r required to generate a certain number of plates is given by:

$$t_r = N \frac{h}{v} \frac{d_p^2}{D_m} (1+k) \qquad (4.7)$$

where v is the reduced mobile phase velocity, d_p the particle diameter and k the retention

Table 4.5. Comparison of column efficiencies of different stationary phases (spherically and irregularly shaped particles; n = 3)

stationary phase	N m^{-1}	H$_{min}$ (μm)	h$_{min}$	ε_t	K$_0$ [10^{14} m^2]	ϕ'	E
Spherically shaped							
BioSil C18 HL 90-5 S	77800	13.0	2.54	0.68	3.21	830	5330
Nucleosil 100-5 C18	69500	14.8	2.59	0.56	5.20	630	4420
Irregularly shaped							
BioSil C18 HL 90-5	77100	13.1	2.00	0.57	4.01	1080	4330
Polygosil 100-5 C18	71800	13.3	1.94	0.76	4.67	860	3260

factor. Naphthalene was, as a retained solute, used as the test compound to compare the times required to generate – for example – 100000 plates on the different types of stationary phase packings. The results from the calculations are listed in Table 4.6. The h/v dependence of naphthalene was experimentally determined. Besides the retention time, also the column length, pressure drop and H/u are given in Table 4.6.

At first sight, the results seem to be very similar for both kind of packings. This is true as far as the column length and pressure drop are concerned. Nucleosil 100-5 C18 and Polygosil 60-5 C18 yield shorter analysis times compared to BioSil HL C18 90-5 S and BioSil C18 HL 90-5, which is caused by the higher carbon-loading of the BioSil materials. Comparing the spherical and irregular stationary phases per manufacturer, it can be concluded that faster analysis times can be achieved on spherical packings. Nucleosil 100-5 C18 provides 1.07 quicker analysis times as compared to Polygosil 100-5 C18 for naphthalene at optimum reduced mobile phase velocity. For BioSil C18 HL 90-5 S compared to BioSil C18 HL 90-5 this value is 1.57. Furthermore, the BioSil materials show less favourable H/u values than Nucleosil 100-5 C18 and Polygosil 100-5 C18 for naphthalene. The results in Table 4.6 show clearly why LC columns are operated near the optimum reduced mobile phase velocity. To achieve an acceptable number of plates at two or five times the optimum velocity of the mobile phase already results in undesired inlet pressures. At five times the optimum rate of the mobile phase the inlet pressure exceeds the pressure limit of all LC pumps applied at present.

Applications

To show the potential of capillary LC, a polycarbonate sample – after microwave assisted solvent extraction – was separated by gradient analysis on a 0.40 m x 320-μm i.d. fused silica capillary column packed with BioSil C18 HL 90-5 S. The chromatogram is given in Fig. 4.8. The mobile phase consisted of acetonitrile/H$_2$O (65:35, v/v) and was programmed to acetonitrile/H$_2$O (95:5, v/v) in 15 minutes. In an additional 15 minutes the mobile phase was program-

Table 4.6. Retention time t_r, column length L and pressure drop Δp required to generate 100000 plates for a retained compound for columns packed with spherically and irregularly shaped particles

v/v_{opt}	t_r (min)	L (m)	Δp (bar)	H/u (s)
BioSil C18 HL 90-5 S				
0.25	1171	2.93	69	0.229
0.5	531	1.76	83	0.069
1	215	1.42	135	0.028
2	132	1.76	332	0.017
5	106	3.52	1660	0.013
Nucleosil 100-5 C18				
0.25	562	1.69	62	0.080
0.5	185	1.11	81	0.026
1	79	0.95	139	0.011
2	46	1.10	322	0.007
5	30	1.83	1345	0.004
BioSil C18 HL 90-5				
0.25	2831	3.74	66	0.361
0.5	838	2.21	79	0.107
1	337	1.78	126	0.043
2	209	2.22	314	0.027
5	171	4.54	1609	0.022
Polygosil 100-5 C18				
0.25	661	2.26	60	0.131
0.5	204	1.39	75	0.040
1	84	1.15	123	0.017
2	51	1.39	297	0.010
5	38	2.63	1404	0.008

med to 100% acetonitrile and was kept constant for 30 minutes. The rate of the mobile phase was 5 µl min^{-1}. UV-absorbance detection was performed at 264 nm.

As another example, the efficient separation of a polymer-additives sample is demonstrated in Fig. 4.9. This chromatogram was obtained on a 0.40 m x 320-µm i.d. microcolumn packed with Polygosil 100-5 C18. The mobile phase consisted of acetonitrile/CHCl$_3$ (95:5, v/v)
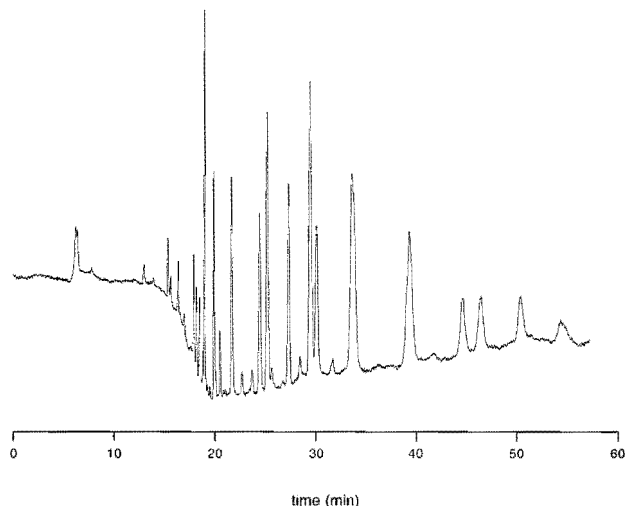
time (min)

Fig. 4.8. Capillary LC separation of a polycarbonate sample after microwave assisted solvent extraction on a BioSil C18 HL 90-5 S column. The mobile phase consisted initially of acetontrile/H_2O (65:35, v/v). The amount of acetontrile was increased up to 95% (v/v) in 15 min. In an additional 15 min the amount of acetontrile was programmed to 100% and was kept constant for 30 minutes. The length of the column was 0.40 m and the i.d. 320-μm. The flow rate was 5 μl min^{-1}. UV-absorption detection was performed at 264 nm.

and the rate of the mobile phase was 10 μl min^{-1}. Detection was carried out at 254 nm. Especially the second example shows a very good performance, as regarding the excellent resolution at short retention times.

CONCLUSIONS

Good, efficiently packed capillary LC columns can be obtained with spherically as well as irregularly shaped particles. The proper packing solvents can easily be selected by means of sedimentation experiments. Suspension liquids in which the particles are coagulated are to be preferred as the packing liquid. The selection of the slurry liquid is not determined by the coagulating properties of the stationary phase particles in the slurry liquid. Particles have to be characterized properly by size if reduced parameters are to be used as optimization criteria. Based on the obtained results, no distinction can be made on whether spherically or irregularly shaped packing material particles give the best chromatographic performance. Considering the time of analysis the spherical packings appear slightly to be preferred over the irregularly shaped packings. Maybe the main advantage of irregulars is their low cost compared to spherical particles. On the other hand, spherical particles are believed to be better pressure resistant than irregularly shaped particles.
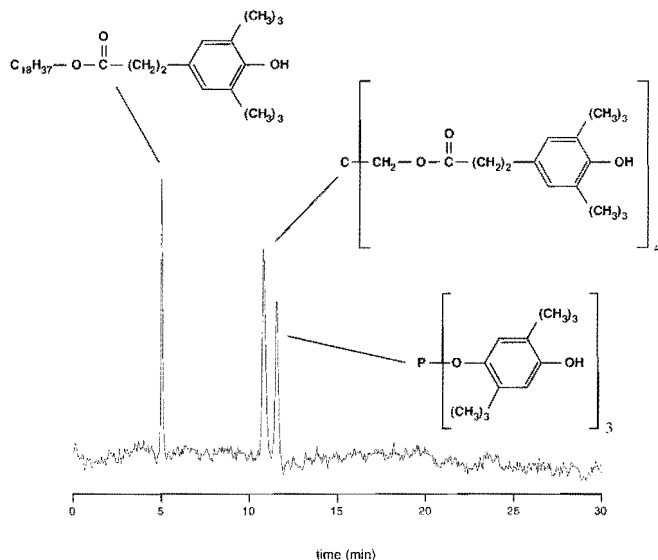
Fig. 4.9. Capillary LC analysis of polymer additives on a Polygosil 100-5 C18 column. The mobile phase consisted of acetontrile/CHCl$_3$ 95:5 (v/v) and the flow rate was 10 µl min^{-1}. The column length was 0.40 m and the i.d. 320-µm. UV-absorption detection was performed at 254 nm.

REFERENCES

[1]   J. Asshauer and I. Halász, *J. Chromatogr. Sci.* 12 (1974) 139

[2]   J.J. Kirkland, *J. Chromatogr. Sci.* 10 (1972) 593

[3]   G.R. Laird, J. Jurand and J.H. Knox, *Proc. Soc. Anal. Chem.* 11 (1974) 311

[4]   K.K. Unger, W. Messner and K.F. Krebs, *J. Chromatogr.* 149, (1978) 1

[5]   K.K. Unger, *Porous Silica*, Elsevier, Amsterdam, 1979, pp. 184

[6]   R. Ohmacht and I. Halász, *Chromatographia* 14 (1981) 216

[7]   M. Verzele, J. van Dijck, P. Mussche and C. Dewaele, *J. Liq. Chromatogr.* 5 (1982) 31

[8]   M. Verzele, C. Dewaele and D. Duquet, *J. Chromatogr.* 39 (1987) 111

[9]   V.L. McGuffin and M. Novotny, *J. Chromatogr.* 255 (1983) 381

[10]   W.H. Wilson, H.M. McNair, Y.F. Maa, and K.J. Hyver, *J. High Resol. Chromatogr.* 13 (1990) 18

[11].   J.P.C. Vissers, H.A. Claessens, J. Laven and C.A. Cramers, *Anal. Chem.* 67 (1995) 2103

[12]   R. Clift, J.R. Grace, M.E. Weber, *Bubbles, Drops and Particles*, Academic Press, London,1978, pp. 16

[13].   J.P. Foley and J.G. Dorsey, *Anal. Chem.* 55 (1983) 730

[14]   D.C. Shelly and T.J. Edkins, *J. Chromatogr.* 411 (1987) 185

[15]   H. Wang, R.A. Hartwick, N.T. Miller and D.C. Shelly, *J. Chromatogr.* 523 (1990) 23

[16]   C.R. Wilke and P. Chang, *AIChE. J.* 1 (1955) 261

[17]   P.A. Bristow and J.H. Knox, *Chromatographia* 1 (1977) 279

[18]   J.C. Gluckman, A. Hirose, V.L. McGuffin and M. Novotny, *Chromatographia* 17 (1983) 6

CHAPTER 5

HYDRODYNAMIC ASPECTS OF SLURRY PACKING PROCESSES IN MICROCOLUMN LIQUID CHROMA-TOGRAPHY

ABSTRACT

A Stokesian dynamics computer simulation based method is presented for the estimation of the bed porosity of capillary liquid chromatography (LC) columns. A colloidally well-described reversed phase stationary phase – slurry liquid suspension was used as a model system. The applied simulation method takes into account the velocity of the slurry, colloidal interaction forces as well as inter-particle hydrodynamic interactions. The obtained bed porosities suggest that a lower slurry velocity leads to a denser packing structure due to the increased effect of colloidal repulsion effects. The results of the simulations were compared with the external porosity and chromatographic performance of capillary LC columns that were packed at different filtration and compaction pressures. The trends that were observed in the experimental results suggest that hydrodynamic packing parameters have no or little effect on the chromatographic performance of capillary LC columns. No correlations were observed between the filtration and compaction pressure and the chromatographic performance of the capillary LC columns, nor any between the duration of the compaction process and the column porosity and performance.

INTRODUCTION

The packing of microcolumns is – according to Verzele – a matter of technique [1]. In line with this view, many different packing techniques have been suggested in literature to efficiently fill microcolumns. The most commonly applied packing technique involves the use of stationary phase slurries for the transport of the particles to the capillary column, which is often referred to as the slurry technique. Early studies on this technique [2-8] primarily examined the effect of the selection of the slurry solvent. Other ways to transport stationary phase particle into a capillary LC column are the use of gases [9-11] or supercritical fluids [12-17]. The majority of these techniques have in common that they are based on trial-and-error methods and assumptions. Despite this, all these methods seem to provide more or less equal, acceptable column performance with reduced plate heights only slightly higher or equal to 2 for columns with an internal diameter (i.d.) of 150–500 µm.

Several studies have been published that report on the preparation of microcolumns in more detail. The coagulating properties of stationary phase materials in slurry and packing liquids – and their effect on the chromatographic performance of the obtained capillary LC columns – was studied by Shelly and Edkins [18] and Vissers et al. [19,20]. The two latter papers demonstrated a particle-settling-velocity based method to quantitatively describe the extend of particle coagulation, whereas the former one was more qualitatively based. The studies of both research groups indicated that the use of a packing liquid in which the stationary phase particles coagulated was favorable. Other papers focussed more on the effect of the packing pressure and packing velocity. One of the first papers that described the effect of the packing time on the performance of a capillary LC column was published by Gluckman et al. [21]. At about the same time Meyer and Hartwick [22] presented a systematic evaluation on the packing of 1.0 mm i.d. columns with irregularly shaped particles at constant velocity or constant pressure. Also Shelly et al. [23] reported on the performance of microcolumns packed at constant velocity and constant pressure. However, their study involved the packing of capillary sized columns of 250 µm i.d. with spherical particles. Others have reported on the effect of the packing pressure on the LC column properties as well, but those studies involved conventional, large i.d. high performance liquid chromatography columns [24,25]. Zimina and coworkers [26,27] related the kinematic viscosity of the slurry liquid and the column performance of 500 µm i.d. packed polyetheretherketone columns. It was shown that detergent-containing slurry liquids lowered the kinematic viscosity of the slurry suspension, which had a favorable effect on the column performance. A lower slurry viscosity increases however the packing velocity, but this was not included in their studies.

This chapter reports on the bed porosity and chromatographic performance of simulated bed structures as obtained by a Stokesian-dynamics computation method. The investigated parameters included packing velocity and packing pressure. The applied calculation method also takes into account colloidal attraction and repulsion forces. The results of the simulation experiments were compared with practically obtained chromatographic results from a series

of experiments where the packing pressure, compaction pressure and slurry solvent were varied. In addition, the columns were characterized with respect to their bed porosity. Explanations for the discrepancies between theory and practice are suggested. This work is an extension of previous studies [19,20], where the effect of particle coagulation in packing and slurry liquids was investigated and related to the performance of capillary LC columns. However, in these previous studies the effect of the packing pressure – i.e. particle filtration rate – was not examined; this forms the basis of this chapter.

THEORY

The dynamics of the particles are determined by several forces associated with colloidal interaction, hydrodynamics and Brownian motion. Taking into account all these forces would lead to highly complex calculations that require very long computing times. In many situations the complexity of the problem can fortunately be reduced drastically by neglecting specific contributions. Generally speaking, dealing with the inter-particle hydrodynamic interactions remains the most difficult part in suspension flow simulations. The complex nature of the hydrodynamic interactions arises from the fact that the actual hydrodynamic forces experienced by any of the particles is the result of a local fluid velocity field which induced infinite series of interparticle interactions. This can be seen as follows: the movement of a sphere implies the movement of the fluid around it. Other spheres that are in the vicinity will experience the velocity field induced by the first sphere and will respond by moving. The movements of the other spheres affect the velocity field too, which again influences the movement of the first sphere. The motion of the spheres and the fluid are thus an infinite cascade of responses. This implies that a group of spheres in a fluid cannot be treated as if each individual particle of the group was the only one present. Fortunately, there are however some basic conditions that still hold. Firstly, the Langevin-equation applies for each single sphere:

$$m\frac{dv}{dt} = F_H + F_B + F_P \tag{5.1}$$

where m is the mass of the sphere, F_H is the hydrodynamic force, F_B the Brownian force and F_P the colloidal interaction force plus the gravity. If the accelerations of the particles are sufficiently small, the term mdv/dt can be neglected. Hence, a pseudo-equilibrium situation exists – i.e. at every moment the sum of forces on each particle equals zero. In case the Brownian force F_B can be neglected as well – which is realistic in case the particle diameter is typically 5 μm or more – equation (5.1) reduces to:

$$F_H = -F_P \tag{5.2}$$

which states that the total hydrodynamic drag on a particle is the opposite of the colloidal

interaction force at any moment in time. F_p can be calculated by means of the Dejarduin, Landau, Verwey and Overbeek (DLVO) theory for the electrostatic repulsion between colloidal particles. According to this theory, F_p on a spherical particle j, with radius a, surface potential Ψ_0 and Hamaker constant A_{12} is equal to:

$$F_{DLVO,j} = \sum_{i \neq j} -\frac{A_{12}a}{12h_{ij}^2} + 2\pi\varepsilon_r\varepsilon_0 a\psi_0^2 \frac{e^{-\kappa h_{ij}}}{1+e^{-\kappa h_{ij}}} \tag{5.3}$$

where h_{ij} is the distance between the surfaces of particles i and j, ε_r is the relative dielectric constant of the fluid and ε_0 is the permittivity of vacuum. The summation has to be performed over all particles in the suspension apart from particle j itself. With equation (5.3), F_p can be calculated and subsequently from equation (5.2), the hydrodynamic force F_H on each particle. This is very important since F_H is directly related to the velocity of the particle. Relating F_H and the velocity of a particle – with the help of formulas known from hydrodynamics – enables the calculation of the velocity of the particles and hence their displacements after a short time interval Dt throughout which the velocity can be assumed to be constant. In this way, a new configuration of the suspension can be calculated and the process – starting with the calculation of F_p – can be repeated. As mentioned before, the most difficult step in this procedure is the calculation of the velocities from F_H. In the following section it will be shortly explained how this problem is approached in the Stokesian dynamics method. Stokesian dynamics is a simulation method which can be used to model the dynamics of suspensions of which the flow of the dispersing fluid is governed by the Stokes – or creeping flow – equations:

$$\nabla \cdot v = 0 \tag{5.4}$$

and:

$$-\nabla p + \rho\nabla^2 v + f = 0 \tag{5.5}$$

where ∇ is the differential vector operator, p is the hydrodynamic pressure, ρ is the fluid density, v is the particle velocity and f is the force per unit mass. The creeping flow equations are basically a simplified form of the Navier-Stokes equations and are only valid in case the flow around the particles in the suspension is laminar, i.e. Re $\ll$ 1, where Re = $2\rho V a/\eta$ with V equalling the velocity difference between the fluid and the particle. Re $\ll$ 1 is often valid for colloidal systems because a is small. Solving the set of equations (5.4) and (5.5) together with the boundary conditions for a given system – e.g. the definition of the fluid velocity at the borders of the fluid – results in functions describing the fluid velocity field v and dynamic pressure field p as a function of the position x. An important feature of the creeping flow equations is the fact that they are both linear differential equations.

Once two different solutions to a problem which both satisfy the creeping flow equations, their sum is a valid solution too. In case the creeping flow equations apply the relation between the velocities and angular velocities of the spheres and the forces and torques applied to them is a linear relation as well. Mathematically this can be expressed as:

$$
\begin{pmatrix}
V_{1,x} \\
V_{1,y} \\
V_{1,z} \\
\Omega_{1,x} \\
\Omega_{1,y} \\
\Omega_{1,z} \\
V_{2,x} \\
\cdot \\
\cdot \\
\cdot \\
\cdot \\
\cdot \\
\Omega_{N+1,y} \\
\Omega_{N+1,z}
\end{pmatrix}
=
\begin{pmatrix}
\mu_{11} & \mu_{12} & \mu_{13} & \cdot & \cdot & \cdot & \mu_{1\,6(N+1)} \\
\cdot & & & & & & \cdot \\
\cdot & & & & & & \cdot \\
\cdot & & & & & & \cdot \\
\cdot & & & & & & \cdot \\
\cdot & & & & & & \cdot \\
\cdot & & & & & & \cdot \\
\cdot & & & & & & \cdot \\
\cdot & & & & & & \cdot \\
\cdot & & & & & & \cdot \\
\cdot & & & & & & \cdot \\
\cdot & & & & & & \cdot \\
\cdot & & & & & & \\
\mu_{6(N+1)1} & & & & & & \mu_{6(N+1)6(N+1)}
\end{pmatrix}
\begin{pmatrix}
F_{1,x} \\
F_{1,y} \\
F_{1,z} \\
T_{2,x} \\
T_{2,y} \\
T_{2,z} \\
F_{2,x} \\
\cdot \\
\cdot \\
\cdot \\
\cdot \\
\cdot \\
T_{N+1,y} \\
T_{N+1,z}
\end{pmatrix}
\qquad (5.6)
$$

where μ is the 6N x 6N-dimensional mobility matrix. Relation (5.6) is referred to as the mobility equation. The calculation of the exact value of the elements of μ starting from the creeping flow equations (5.4) and (5.5) and the no-slip boundary conditions on the spheres' surfaces is only possible in case N = 2. For systems containing more than two spheres, solutions have to be obtained using numerical techniques. An efficient method to calculate the elements of μ was first proposed by Durlofsky *et al.* [28]. Their approach is based on describing local fluid velocities as linear functions of the forces, torques and so-called higher order multipole moments of the spheres by means of Taylor expansions. Higher order multipoles are quantities with no obvious physical meaning which are in some way related to the force distribution on the particles.

In order to avoid impractically long calculation times, the number of multipoles included in the calculation is restricted. However, in order to account for an adequate calculation of short-range interactions, a substantial number of multipoles have to be included. Durlofsky *et al.* dealt with this problem by adding the exact, known two-body mobility matrices to the 6N body mobility matrix μ – which is only suitable for describing the long range interactions satisfactory. In contrast to μ, these two-body mobility matrices do not show a many body character. This is however not a problem since the elements of the two-body mobility matrices only dominate in case particles are very close to each other which corresponds to a situation where particles only experience their near-drawn neighbour and are barely influenced by the

presence of the other particles. Simulations performed with this method showed that for clusters consisting of 5–15 particles, the precision is acceptable in case only multipoles to the zeroth and first order are included in the calculation.

Recently, Hinsen and coworkers [29] have developed a computer program called "Hydrolib", which allows the efficient calculation of many body mobility matrices for spheres in creeping flow. The method used is outlined in an article by Chichocki et al. [30] and is in fact in many aspects analogous to the method proposed by Durlofsky et al. An important difference is however that "Hydrolib" is capable of performing relatively fast calculations when a higher number of multipole moments are to be included. It was argued by Chichocki et al. that for clusters larger than about 10 spheres, truncation after the first multipole moment is unacceptable.

EXPERIMENTAL SECTION

Simulation experiments

All calculations were performed on a Silicon Graphics Power Challenge XL super computer (Mountain View, CA, USA).

Magnetic Resonance Imaging

Magnetic Resonance Imaging (MRI) experiments were conducted at room temperature on a 0.47 T imager consisting of a Bruker electromagnet (Rheinstetten/FO., Karlsruhe, Germany), a SMIS console and a DOTY probe head with actively shielded gradients and a 4.5 cm diameter cylindrical sample space. The capillary LC columns were placed – together with a test tube that contained neat, stagnant mobile phase doped with a small amount of $MnCl_2$ for reference measurements – in the sample space. Magnetic field gradients were applied by means of a home-made transmitter/receiver coil with a diameter of 1 cm and a length of 3 cm. The spacial resolution of the applied MRI equipment was 80 x 80 x 3000 µm in the x, y and z-direction respectively, where the z-direction was directed along the column axis. Hence, at each axial position z a maximum of about 12 displacement profiles could be probed in each 300 µm i.d. capillary – in practice about 8 profiles could be analyzed. Details on the MRI equipment and the applied pulse sequences are published by the group of Van As [32,33].

In this study, three capillary LC columns were subjected to MRI measurements to study the feasibility of this technique to study the local porosity of the chromatographic bed in capillary LC columns. To this extent, two columns that were packed at different filtration pressures were studied and a reference column that was expected to have a distinctly different bed structure. The latter column had in fact a very poor chromatographic performance – reduced plate height h 32 – and a column resistance factor that is about two to three times as high as normally would be expected. The packing conditions for preparing such an exceptionally

performing column can be found elsewhere [19]. Each column was measured at five different axial positions over the whole capillary length.

Column construction and packing equipment

Columns were constructed from 0.40 m x 320-μm i.d. uncoated fused silica tubing (Chrompack, Middelburg, The Netherlands). An EPM2000 glass filter frit (Whatman, Maidstone, UK) was cut out by the column. To hold the frit in position a 0.080 m x 75-μm i.d./280-μm outer diameter (o.d.) fused silica capillary (Polymicron Technologies, Phoenix, AZ, USA) was fixed into the larger capillary using an two-component epoxy resin.

The packing equipment consisted of a DSTV-122 air driven fluid pump (Haskel Eng., Burbank, CA) for constant pressure packing and a 0.19 x 0.0020 m i.d. stainless-steel slurry reservoir. The column was connected to the slurry vessel by means of a home made double cone.

Stationary phase slurries were prepared at a concentration of 100 kg m^{-3} in acetone or carbontetrachloride by sonication for 10 minutes. Afterwards, the slurry was transferred to the slurry reservoir with a syringe and pneumatically pumped in the capillary. This typically took less then 2 min. Thereafter, the packing pressure was maintained for 30 min unless stated otherwise.

Chromatographic instrumentation

The capillary LC system consisted of a model 100 DM syringe pump (ISCO Inc., Lincoln, NE), a 785A Programmable Absorbance detector (Applied Biosystems, San Jose, CA) equipped with a capillary flow cell (LC Packings, Amsterdam, The Netherlands), and a 200 nl Cl4W injection valve (VICI-AG Valco Europe, Schenkon, Switzerland). A 0.2-μm nylon membrane (Alltech Associates Inc., Deerfield, IL, USA) was positioned into the valve outlet to the column to circumvent stationary phase particles entering the injection valve. UV detection was performed at 254 nm. A 900 Series Interface and Nelson 5.0 software (Perkin Elmer Nelson, Cupertine, CA, USA) were used for data acquisition.

Column evaluation

The reversed phase capillary LC columns were evaluated with a test-mixture containing four components: uracil (dead volume marker), naphthalene, phenanthrene and anthracene. The concentration of all components was approximately 0.1 mol m^{-3}. An acetonitrile/water (70:30, v/v) mixture was used as the mobile phase. The individual solvents of the mobile phase were filtered through a 0.45-μm filter. Prior to use, the mobile phase was degassed with helium. The peak of anthracene was used to calculate the column efficiencies. Plate heights were calculated using an algorithm developed by Foley and Dorsey [31]. In addition, extra column bandbroadening effects were accounted for.

115

Chemicals

Acetone and carbontetrachloride were purchased from Merck (Darmstadt, Germany). Uracil, anthracene, naphthalene and phenanthrene were from Fluka AG (Buchs, Switzerland). All chemicals were of p.a. grade. Water was purified and demineralized with a Milli-Q water purification system (Waters-Millipore Milford, MA) prior to use.

The reversed phase stationary phase BioSil C18 HL 90-5 S was from BioRad RSL nv. (Nazareth, Belgium).

RESULTS AND DISCUSSION

Simulation experiments

All calculations were performed for BioSil C18 HL 90-5 S in acetone – which will also be one of the stationary phase-solvent systems studied in the chromatographic section of this chapter. The relevant physical constants for this system are listed in Table 5.1. The perception of such a set of parameters is described in a previous chapter 3, where the physical constants of other stationary phase-solvent systems can be found too [20].

Simulation of one particle while being filtrated on a packed bed

In this section results will be shown of the packing of a particle bed under practical conditions for chromatographic beds. In practice, packing of a bed is carried out with a fairly concentrated slurry – volume fraction $\phi = 0.10$. When the particles approach the bed, they will interact with each other and with the bed. The interaction of individual particles with the bed may prevail close to the bed. Thus the approach of a single particle towards the bed was investigated as it is expected to give insight in phenomena like coagulation and whether the packing is ballistic rather than colloidal in nature.

A photographic representation of this experiment is given in Fig. 5.1. A virtual bed was composed of 72 particles that were organized in two layers that were two particle radii apart from each other at the centre-to-centre distance. In fact, the bed consisted of two infinite layers, in view of the imposed periodic boundary conditions. The centre-to-centre distance between to particles in the same layers was 2.5 times the particle radius a. The freely moving particle was positioned right above one of the particles in the upper layer of the bed. A liquid flow was imposed normal to the bed, which forced the particle to move towards the bed. If the distance between the surface of the freely moving particle and the surface of the closest particle in the bed is fairly great, the particle's velocity is hardly influenced by the presence of the bed and it will move with the fluid velocity v . At close range however, its velocity will be changed appreciable due to hydrodynamic and colloidal interaction forces. At a distance of about one particle radius – i.e. 2.5 μm – the effect already amounts to a velocity alteration of approximately 10%. At this distance the colloidal interaction forces are still very small and the effect is entirely hydrodynamic. As the particle is approaching further, the hydrodynamic resis-

Table 5.1. Physical constants for the system BioSil C18 HL 90-5 S – acetone

physical constant	symbol	value
Hamaker attraction constant	A	$8.8 \cdot 10^{-21}$ J
surface potential	ψ_0	$-84.5 \cdot 10^{-3}$ V
double layer thickness	κ^{-1}	$3.13 \cdot 10^{-7}$ m^{-1}
particle radius	a	$2.65 \cdot 10^{-6}$ m
di-electric constant	ε_r	21.0 .
solvent viscosity	η	$0.32 \quad 0^{-3}$ Pa s
solvent density	ρ	$0.79 \cdot 10^3$ kg m^{-3}

tance will steadily grow and eventually become so high that a true collision between the freely moving particle and the one in the bed cannot occur in the absence of some attractive force. At such small distances, however, the colloidal repulsive and attractive forces become significant. The effect of these colloidal interaction forces is shown in Fig. 5.2. The velocity of a dragged particle was calculated in case colloidal interaction forces were present (v) and absent v_0. The difference between these two velocities, divided by the latter one is plotted versus the distance to the bed h_{ij}.

It can be seen that in case $h_{ij} > 7$ nm, the ordinate is negative, which means that the colloidal interaction forces will slow down the particle even more due to electrostatic repulsion. If h_{ij} becomes less than 1 nm, the attractive Van der Waals force starts to dominate which will eventually lead to a collision resulting in coagulation.

Simulation of the evolution of a packed bed structure

This section discusses the results of simulations of the filtration of a stationary phase suspension at different fluid velocities. A set of 600 particles randomly placed in a cubic unit cell was used as the start configuration for all simulations. The foot print of the unit cell was taken as 15 times the particle radius a in both the x and y direction. The height of the unit cell equalled 112 times a implying a particle volume fraction of 0.1. A virtual frit – composed of 4 layers of 36 fixed particles – was placed at the bottom of the unit cell. The centre-to-centre distance between particles in the same layer was equal to 2.5 times a. The distance between the layers was 2 times a. A representation of the starting conditions is given in Fig. 5.3.

117

Only those moving particles that were in the proximity of the stationary bed were taken into account in the mobility calculation. To this extend a cubic cell with 15 times a edges was defined of which the top coincides with the plane through the freely moving particles that are at a distance of 4 times a of the stationary bed. The total number of particles in this box was
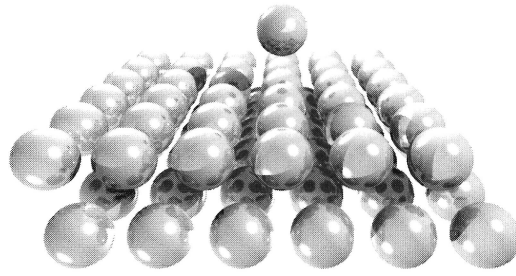
Fig. 5.1. Photographic representation of the effect of colloidal interaction forces on the movement of a single particle approaching a bed. The freely moving particle is positioned exactly above one of the particles of the top layer of an entirely flat bed.

kept constant for numerical reasons. This implies however that an appropriate number of particles at the bottom of the box had to be removed during the simulations. Particles that were not included in the mobility calculation were moving with the fluid velocity. Throughout the simulations it was checked if the mobility calculation included particles formed a bed of at least one layer thick.

Colloidal interactions with particles up to a distance of 15 times a – including periodic images – were taken into account. The time step size was set to $2.7 \cdot 10^{-7}$ m/v_{fluid}. If the particle-to-bed distance was smaller than 0.7 nm the particles were considered to be coagulated. In case of particle overlap the interparticle distance was set at 0.7 nm. The existence of aggregates in the slurry was not taken into account since (i) the suspension is colloidally stable and (ii) the near absence of shear flow – implying very few collisions in the suspension. The possibility of rolling after coagulation was not included in the simulations. In total three of such simulations were conducted. In the first two simulations the total number of particles included in the mobility calculation equalled 98 and in the third one the total number of particles was 150. The fluid velocities were respectively $1.15 \cdot 10^{-2}$, $5 \cdot 10^{-3}$ and $3 \cdot 10^{-4}$ m s^{-1}. A representation of the obtained bed structures using the simulation method described above is given in Fig. 5.4.

The simulated packing structures were characterized based on their external porosity ε_u. A limitation of this characterization method is however that no information is obtained about the presence of irregularities in the simulated bed. The dimension and the total volume of the voids was accessed by positioning randomly a number of points in the bed structure. The number of points that hit a particle reflect the volume fraction of particles within the simulated bed structure. For the points that did not hit a particle, the radius of the largest sphere was determined that could be centered at these points without touching a particle in the
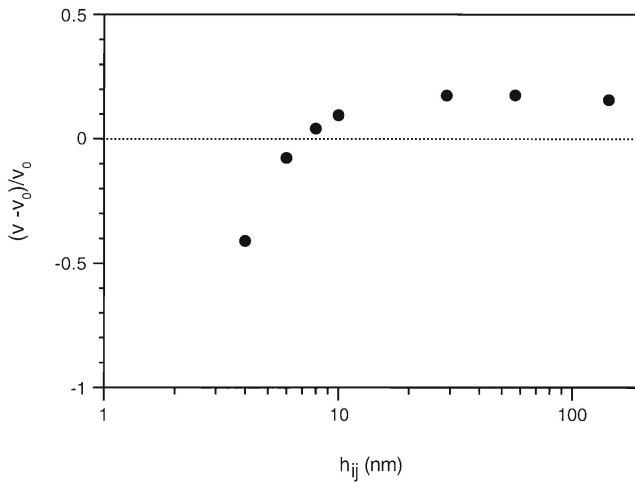
Fig. 5.2. The relative velocity of a freely moving particle – i.e. $(v - v_0)/v_0$ – as a function of the particle-to-particle distance h_{ij} for the the hypothetical situation considered in Fig. 5.1. See the text for details.

formed bed. The number of hits as a function of the radius of the largest fitting sphere – i.e. the area under the resulting curves – provides information about ε_u. All curves were computed by randomly scanning 36000 points in a volume of 15a x 15a x 20a. The external porosity ε_u was found to be 0.55 for fluid velocities of $1.15 \cdot 10^{-2}$ and $5 \cdot 10^{-3}$ m s^{-1}. For a fluid velocity of $3 \cdot 10^{-4}$ m s^{-1}, ε_u was 0.45. For a purely ballistic situation – i.e. settlement of the particles in a straight line – ε_u was found to be equal to 0.76.

A more illustrative method for assessing the anisotropy of the pores is by placing horizontally and vertically orientated lines – i.e. x and z-direction respectively – through points randomly positioned outside the particles. The lines were given lengths so as they just touched the particles. The lengths of the horizontally and vertically placed lines – h_x and h_z respectively – provide information about the volume and the shape of the voids. The results of this method are shown in Fig. 5.5 for the three bed structures that were obtained by simulation and for the ballistic simulated bed structure. The number of points that was scanned in this way was 288 000 in a volume of 15a x 15a x 20a.

The difference between the porosity values and the void sizes obtained at $1.15 \cdot 10^{-2}$ and $5 \cdot 10^{-3}$ m s^{-1} on one hand and at $3 \cdot 10^{-4}$ m s^{-1} at the other hand is remarkable. The bed structure obtained at the lowest fluid velocity is much denser then that at the two higher velocities, implying that the effect of colloidal interaction forces is significantly larger at a fluid velocity of $3 \cdot 10^{-4}$ m s^{-1} than at $5 \cdot 10^{-3}$ and $1.15 \cdot 10^{-2}$ m s^{-1}. Colloidal repulsion forces make particles avoiding each other as much as possible, resulting in a denser packed bed at lower
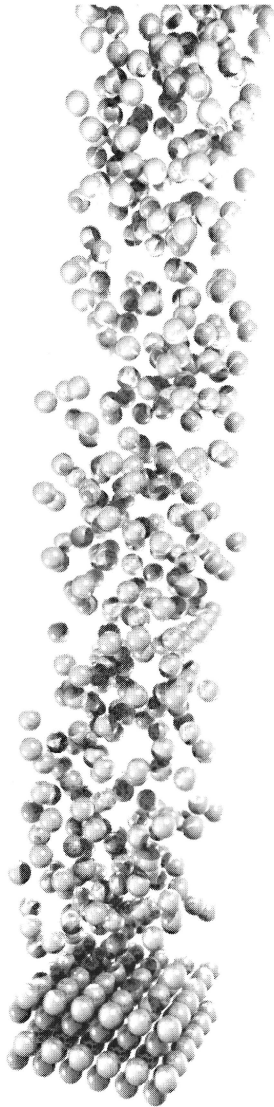
Fig. 5.3. Start configuration for the simulations of the packing process. The virtual frit consisted consists of 144 particles which are ordered in four equidistant layers at a distance of 2 times the particle radius a of each other. The total number of spheres was equal to 600. The unit cell has a length of 15 times a in the x and y-direction and 122 times a in the z-direction.

fluid velocities. The fact that the bed porosities and the void sizes are comparable at fluid velocities of $5 \cdot 10^{-3}$ and $1.15 \cdot 10^{-2}$ m s^{-1} suggests that the colloidal forces at these fluid velocities are completely determined by hydrodynamic forces. Based on the results shown in
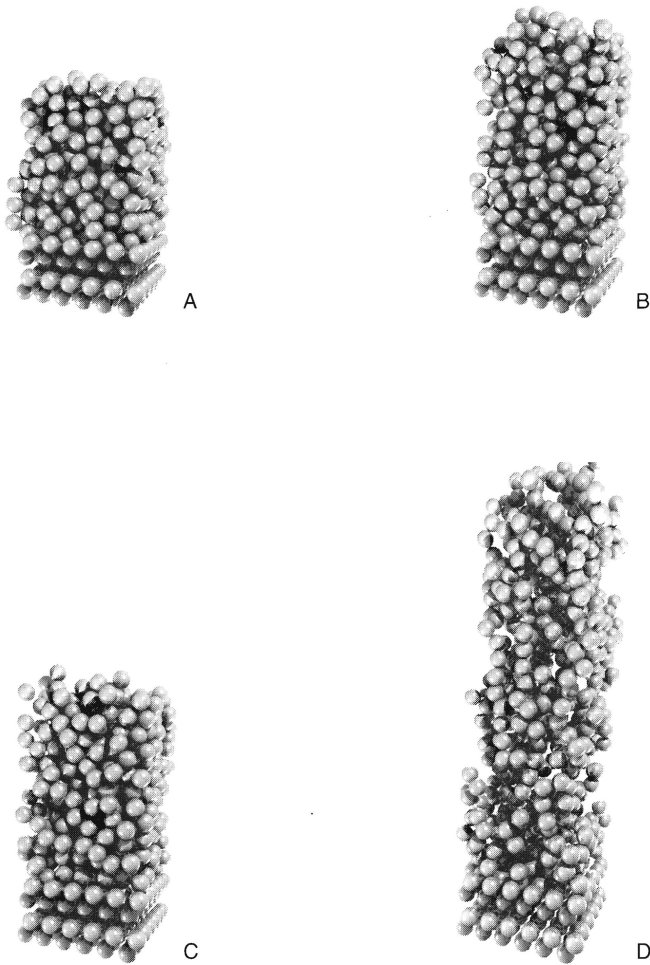
Fig. 5.4. Photographic representation of the bed structures obtained after simulation with a fluid velocity of $3 \cdot 10^{-4}$ m s^{-1} (A), $5 \cdot 10^{-3}$ m s^{-1} (B) and $1.25 \cdot 10^{-2}$ m s^{-1} (C). Structure (D) represents the particle bed in case of a purely ballistic situation, i.e. settlement of the particles in a straight line.

Fig. 5.5 it is concluded that in all cases the void dimensions are smaller than the particle radius of $2.85 \cdot 10^{-6}$ m, which seems to be reasonable since voids of these sizes must be present in any packed bed.

121

Interpretation of the simulation experiments

In the simulations a flat fluid velocity profile was assumed. However, in practice a parabolic fluid profile $v_z(r)$ will exist within the capillary, described by Poiseuille's law:
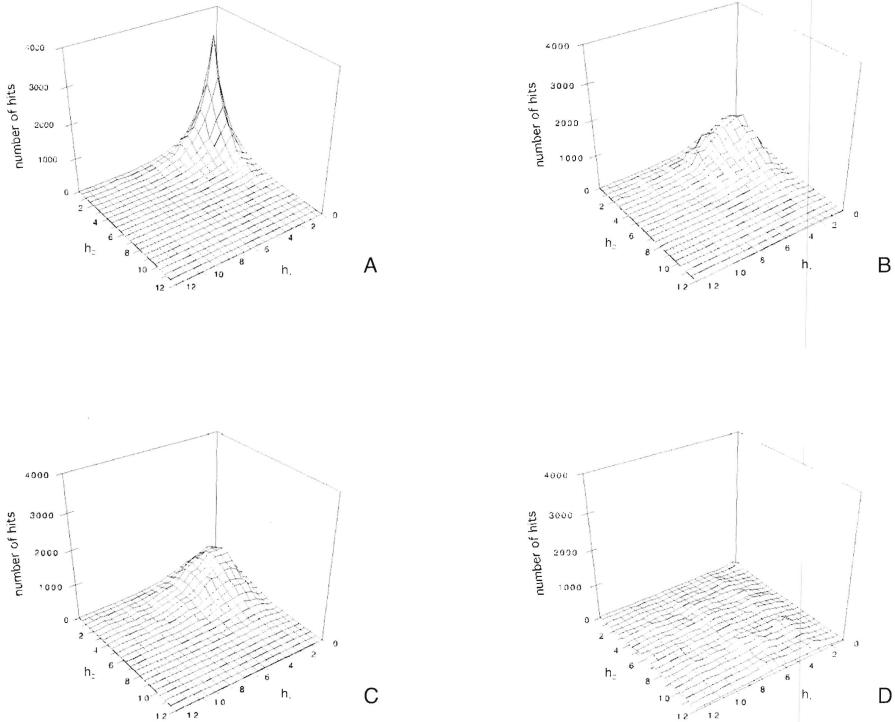
Fig. 5.5. Void size characterization of the bed structures obtained after simulation with a fluid velocity of $3 \cdot 10^{-4}$ m s^{-1} (A), $5 \cdot 10^{-3}$ m s^{-1} (B) and $1.25 \cdot 10^{-2}$ m s^{-1} (C). Graph (D) represents the characterization of the void sizes in case of a purely ballistic situation, i.e. settlement of the particles in a straight line. h_x and h_z represent the lengths of the lines that can be placed in the simulated bed structures in terms of the particle radius a in the x and z direction respectively.

$$v_z(r) = \frac{\Delta p d_c^2}{16\eta(1+k_1\phi)}\left\{1-\left(\frac{2r}{d_c}\right)^2\right\}$$

(5.7)

where Δp is the applied pressure drop over the part L that is filled with slurry, d_c the capillary diameter, ϕ the particle volume fraction in the slurry and r the distance to the capillary axis. k_1 equals 2.5 for dilute particle suspensions, i.e. in the so-called Einstein region. At higher particle fractions, i.e. $\phi \sim 0.1$, the term $(1 + k_1\phi)$ turns into $(1 + k_1\phi + k^2\phi^2 + ...)$. As soon as a sediment is formed, most of the pressure drop will be over the sediment and the maximum value of $v_r(z)$ will be mainly determined by the flow through the sediment, which can be

described by the Carman-Kozeny equation:

$$v_0 \cong \frac{\Delta p}{h_s} \frac{d_p^2}{180\eta} \frac{\varepsilon_u^3}{(1-\varepsilon_u)^2}$$

(5.8)

where v_0 is the superficial velocity, h_s the height of the sediment and and d_p the particle diameter. Thus, the maximum velocity is proportional to h_s^{-1}. Assuming that the presence of the sediment does not change the velocity profile within the slurry near the bed, the velocity profile of the slurry v_z^s as a function of h_s and r during the column filling is given by:

$$v_z^s(r,h_s) = \frac{\Delta p}{h_s} \frac{d_p^2}{180\eta} \frac{\varepsilon_u^3}{(1-\varepsilon_u)^2} \left\{1-\left(\frac{2r}{d_c}\right)^2\right\}$$

(5.9)

Obviously this is only a crude approximation of v_z^s, since equation (5.9) is not valid very close to the formed particle bed. However, it will provide information to the interpretation of the simulation experiments with respect to the filtration pressure and speed. Because of the parabolic profile within the slurry, the rate of particle deposition will be a function of of r too, i.e. the deposition plane is not flat.

Rearrangement of equation (5.9) gives a relationship that describes the deposition plane as a function of the filtration pressure Δp, radius r and particle velocity V:

$$h_s = c \cdot \frac{\Delta p}{V} \left\{1-\left(\frac{2r}{d_c}\right)^2\right\}$$

(5.10)

where c is equal to $(d_p^2 \cdot \varepsilon_u^3)/(180\eta \cdot (1-\varepsilon_u)^2)$ and assumed to be constant. Application of equation (5.10) results in the figures that are depicted in Fig. 5.6, where the impact velocity profile is given as a function of V at differently applied pressure drops. The particle velocity V was varied from $3 . 10^{-4}$ to $8 \cdot 10^{-2}$ to m s^{-1} and Δp from 100 to 500 bar.

Inspection of the results depicted in Fig. 5.6 learns that a particle velocity V of $3 \cdot 10^{-4}$ m s^{-1} in all cases is obtained in the proximity of the capillary wall. Hence, the influence of shear flow and the wall itself are not negligible. The simulation experiments showed however that at this particle velocity the most dense packed bed should be obtainable. The packing structure near the capillary wall will therefore be only partially determined by colloidal forces, e.g. a more loosely packed bed.

123

The results in Fig. 5.6 also show that in the $3 \cdot 10^{-4} - 5 \cdot 10^{-3}$ m s^{-1} particle velocity range – a range where colloidal forces are still expected to be predominant – the column volume taken up by this velocity range are largest at a filtration pressure of 100 bar and lowest at 500
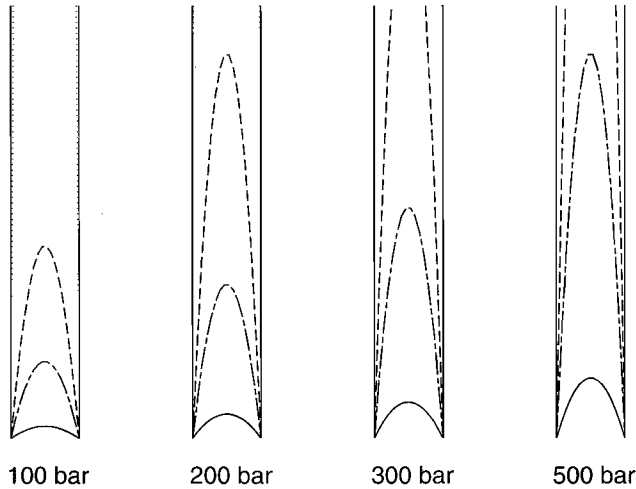
Fig. 5.6. Planes of constant impact velocity during the growth of the bed as a function of constant filtration pressure. V was respectively $8 \cdot 10^{-2}$ m s^{-1} (———), $1.25 \cdot 10^{-2}$ m s^{-1}, (– $\cdot$ –), $5 \cdot 10^{-3}$ m s^{-1} (- - - -) and $3 \cdot 10^{-4}$ m s^{-1} (········). c was calculated with a particle diameter $d_p = 5.3 \cdot 10^{-6}$ m, fluid viscosity $\eta = 0.32 \cdot 10^{-3}$ Pa s and external porosity $\varepsilon_u = 0.4$. The length of the capillary equals 0.40 m.

bar. This suggests that the initial filling pressure during the packing process is of importance with respect to the initial packing structure. According to the results of Fig 5.4, the densest regions are most likely to be expected near the inlet side of the column.

In the $5 \cdot 10^{-3} - 1.25 \cdot 10^{-2}$ m s^{-1} particle velocity range there are no no extreme differences to be expected at a filtration pressure of 100 bar. Going up to a pressure of 200 or 300 bar the parabolic surfaces occupy however a much larger column volume. The simulation experiments indicated that the packing structures for this kind of velocities are almost identical. Comparison of these profiles with the simulations is too speculative a matter. Firstly, the simulations correspond to situations where no shear is present, where the results in Fig. 5.6. show that in regions far from the capillary axis shear may not be neglected. Secondly, the fluid velocity profile will be different from the Poiseuille profile. Especially when the sediment is not flat the deposition of the particles will be very different. Finally, inertial forces in this region are not completely negligible.

The solid lines in Fig. 5.6 correspond to a particle velocity of $8 \cdot 10^{-2}$ m s^{-1}. At this velocity the particle based Re-number is equal to 1. Inertial forces are no longer negligible when Re O(1). The solid line in Fig. 5.6 therefore corresponds to the results where beyond Stokesian dynamics simulation are not valid anymore.

Based on these results it can be concluded that increasing the filtration pressure from 100 to 500 bar will result in reducing the influence of colloidal repulsion forces. The region with

the least repulsive packing is located close to the frit and near the axis of the column. There is however no reason to expect that large irregularities will be found anywhere in the initial packing.

Porosity measurements and chromatographic experiments

Since the particle approaching velocity decreases during the packing of the column at constant pressure, a bed height dependent porosity is to be expected. Chromatographic techniques allow to study the total inter and intraparticle bed porosity, but do not provide information about the local porosity. Packed capillary fused silica columns can be cut in pieces so that the porosity of the individual column pieces can be estimated. However, cutting a column will easily disturb the bed, thus affecting the porosity and was therefore not considered. Magnetic resonance imaging (MRI) is a non-destructive and non-invasive technique which can be used to measure fluidic flow inside an object – either by direct measurement of the displacement of a proton-containing fluid in a well know time interval – or by mapping the effect of a contrast agent or labeled molecules [34]. Both techniques have been applied successfully to study transport phenomena in conventional and preparative high-performance liquid chromatography columns [35-37].

With MRI, proton displacements over a given time interval can be assessed. In this study the displacement of protons in the axial direction of the capillary LC columns was investigated. In case of a flow through a packed bed, such a displacement is a superposition of convective and diffusive contributions [34]. The diffusive contribution would result in a Gaussian displacement distribution, which is – depending on the conditions – possibly disturbed by the presence of particles.

No differences in packed-bed structures could be traced from the MRI measurements – even not for columns that varied considerably in chromatographic performance, i.e. reduced plate height and column resistance factor. The Gaussian-like distributed axial displacements were found to be only slightly increased by the flow. This indicates that diffusive exchange between areas of high and low liquid velocities is fast enough to suppress any bandbroadening due to spacial variations in liquid flow through a bed. No variations were found that are induced by the axial or radial position within the capillary LC column. This means that (i) no significant differences in local porosities were found on the scale of the probed volume or (ii) any inhomogeneities that may exist on smaller scales – e.g. smaller holes – level off at the scale of the probe volume. The former argument might imply that the bed structures of the measured columns are comparable and not critical with respect to the chromatographic performance of the column. If this is indeed the case, it implies – in case of the very poorly packed column – that only well packed regions were probed and defective areas were missed. This would be in agreement with earlier findings [19], where it was suggested that the poor performance and high column resistance factor of these type of columns were due to voids in the bed structure and to tightly packed regions respectively. Argument (ii) implies that the resolution of the applied MRI equipment is too limited to correlate the measured bed porosities with

Table 5.2. Column performance of 320-μm-i.d. capillary LC columns packed at different filtration pressures[a]; n = 2

filtration pressure (bar)	h	ϕ'	E	$K_0 (10^{14} m^2)$	ε_t	ε_u
400 bar compaction pressure						
70	2.5	550	3500	5.94	0.57	0.46
100	2.7	510	3600	5.84	0.56	0.48
150	2.7	520	3700	6.06	0.56	0.48
200	2.4	590	3500	5.94	0.55	0.47
250	2.7	580	4300	5.45	0.59	0.51
300	2.8	510	4100	6.06	0.55	0.48
600 bar compaction pressure						
300	2.6	600	4000	6.32	0.53	0.47
400	2.6	630	4300	5.68	0.53	0.46
500	2.7	560	3200	5.72	0.56	0.47

[a] acetone was the slurry liquid and acetonitrile/water (70:30, v/v) was the packing liquid. The columns were tested with an eluent composition acetonitrile/water (70:30, v/v) at 3 μl min⁻¹; the test component was anthracene (retention factor k ~ 4).

chromatographically obtained parameters. To conform this, the capillaries should be scanned over the whole column length. Especially the areas near the frits should be analyzed.

The results of the packing experiments are given in Table 5.2, where the reduced plate height h, column resistance factor ϕ', separation impedance E, total porosity ε_t and external porosity ε_u are given for different filtration and compaction pressures. Each experiment was at least duplicated. The experimental conditions are identical to those used for the simulation experiments and are summarized in the experimental section of this chapter. The slurry liquid was acetone. ε_t and ε_u were assessed using equation (5.12) and (5.13) respectively [38,39].

$$\varepsilon_t = \frac{4Ft_0}{\pi d_c^2 L} \tag{5.12}$$

and:

$$u = \frac{\Delta p d_p^2}{180\psi^2 \eta L} \cdot \frac{\varepsilon_u^3}{\left(1-\varepsilon_u\right)^2} \tag{5.13}$$

where F is the volumetric flow, t_0 the void time of the column and ψ^2 is the particle shape factor – which is equal to 1 for spherically shaped particles and equal to 1.7 for irregularly shaped particles.

The results given in Table 5.2 suggest that there is neither a relationship between the filtration pressure and the chromatographic performance nor the filtration pressure and the bed porosity. Remarkable is however that the external porosities ε_u appear to be smaller that what was to be expected based on the simulation experiments. The observed filtration speeds were approximately $1 \cdot 10^{-3}$ m s^{-1}. There are a number of thinkable explanations:

(i) ε_u was calculated assuming that ψ^2 equals 1, which is only true for smooth non-porous spheres. In practice this value might be somewhat higher; using a higher value for ψ^2 would have lead to higher calculated ε_u values. The assumption that ψ^2 equals 1 seems however to be valid since the mobile phase flow through the pores is generally negligible and the particles are completely spherical.

(ii) Limitations in the Stokesian-dynamics simulation to describe the filtration process properly, i.e. the simulation process does not exactly reflect what takes place in practice when a column is being filled. The simulation are based on a number of simplifications, especially with respect to the boundary between the slurry and the bed. However, it is expected that this will have only a minor effect.

(iii) The particle size distribution of BioSil C18 HL 90-5 S is not homogeneous. The span – i.e. $(d_{90}-d_{10})/d_{50}$ equals 0.4 for the investigated batch – which possibly can lead lower values for ε_u than 0.37 (lowest possible value for a random packing of equally sized spheres).

(iv) Compaction of the chromatographic bed after filtration. The pressure during the column packing experiments was maintained on the column for 30 min. It is not unlikely that the initial bed structures of the prepared columns are in fact different, but that they ceased to

Table 5.3. Column performance of 320-µm-i.d. capillary LC columns packed at different compaction pressures[a]; n = 2

compaction pressure (bar)	h	ϕ'	E	$K_0 (10^{14} m^2)$	ε_t	ε_u
100 bar filtration pressure						
100	2.1	670	3100	4.27	0.56	0.43
230	2.0	630	2500	5.51	0.54	0.43
360	2.0	550	2200	6.29	0.50	0.45
500	2.1	660	2900	5.26	0.54	0.43

[a] CCl_4 was the slurry liquid and acetonitrile/water (70:30, v/v) as the packing liquid. The columns were tested with an eluent composition acetonitrile/water (70:30, v/v) at 3 µl min⁻¹; the test component was anthracene (retention factor k ~ 4)

occur during the compaction process. In that case, the bed structure would be a function of the compaction pressure, which was more or less the same for all experiments. It is known from the science of soil mechanics that packed beds can be compacted by the application of a compaction pressure. This may in fact be a large effect. When a particle from the slurry starts to become a part of the bed – i.e. at the slurry bed interface – no effective stress (except from the particle drag force) is applied to that part of the bed. Afterwards, the whole, or a substantial part of the packing pressure acts as an effective compaction pressure on the bed.

A second set of columns was packed to study the compaction process in more detail. CCl_4 was used as the slurry liquid instead of acetone for this particular experiment. This will obviously lead to a lower particle impact velocity due to the higher viscosity of CCl_4 compared to acetone – $0.969 \cdot 10^{-3}$ Pa s $vs.$ $0.322 \cdot 10^{-3}$ Pa s respectively. Using equation (5.7) it can be estimated that the particle impact velocity will be O(2) smaller in CCl_4 at the lowest applied filtration pressures in both situations. The compaction pressure in this case was maintained for 1 h. It must be noted however that the results cannot be compared directly to the simulation experiments due to the different double layer thickness' of BioSil C18 HL 90-5 S in CCl_4 and acetone, i.e. different colloidal repulsion and attraction forces. Furthermore, BioSil C18 HL 90-5 S is flocculated in CCl_4 [20]. However, previous experiments have shown that this does not affect the chromatographic performance of a capillary LC column [19]. The agglomerates probably break down during the filtration process since they are believed to be very weak [20]. The results of the packing experiments are given in Table 5.3. Also here hardly any differences are noticeable in chromatographic performance or bed porosity ε_u, suggesting that the compaction pressure and duration are less dominant as was believed. Compared to the results given in Table 5.2 some differences are noticeable. The ε_u and ϕ' values tend to be somewhat higher for the acetone packed columns. This suggests that the columns that were packed with CCl_4 as the slurry liquid are packed more densely, which at first sight would be in accordance with the simulations experiments where lower filtration pressures resulted in denser particle beds. However, some particular details have to be considered:

(i) Displacing an acetone slurry from the slurry vessel takes about 15 min at a filtration pressure of 200–250 bar. Hence, displacing a CCl_4 slurry will roughly take twice as long, i.e. 30 min. Thus, not before the slurry liquid is completely displaced from the vessel and column, comparable conditions will exist in both situations. Filling of the column is typically done in 1–5 min – depending on the filtration pressure, slurry concentration and slurry liquid – which means that during the first 25 min of the compaction process the conditions are different. The rearrangement of the particles during compaction in the radial direction in the case of a CCl_4 slurry suspension is however also three times as slow compared to an acetone slurry due the difference in viscosity of both liquids. This means there is more or less the same overall colloidal effect in rearrangement of the stationary phase particles in the axial and radial direction and consequently no differences are to be expected in the bed porosity at the same compaction pressure in case of different slurry liquids.

(ii) The compaction pressure in the case of columns that were packed with CCl_4 as the slurry liquid was maintained for a 1 h period, whereas the compaction time for an acetone

129

slurries was 30 min. However, the results given in Table 5.2 and 5.3 show that the magnitude of the filtration and the compaction pressure have no effect on the bed porosity and chromatographic performance of the packed columns. Hence, a substantial part of the packing pressure must act as an effective compaction force throughout the complete chromatographic bed. If the duration of the compaction would have been the determining factor, differences should have been noticeable in the results given in Table 5.3.

Based on these observations it can be concluded that the filtration and compaction force are not the predominant packing parameters, i.e. the hydrodynamic packing parameters are less critical than initially was assumed. The initial bed structures of the prepared columns may have been different but cannot be observed in practice due to compaction. It is however very well feasible that the colloidal differences start to become noticeable at filtration pressures that are lower than 100 bar, at which the force on the particles is already more than sufficient to overcome the repulsive colloidal forces between two particles. For the studied materials – i.e. the stationary phase and the slurry and packing liquids – the packing and filtration pressure are not critical parameters in obtaining efficiently packed capillary LC columns. The small differences in performance that were observed for acetone and CCl_4 slurries are apparently due to the chemical differences of both slurry liquids.

CONCLUSIONS

The influence of the particle impact velocity on the chromatographic performance in slurry packing processes can be determined by means of a Stokesian dynamics based simulation method. The simulations indicate that a lower fluid velocity leads to a denser bed structure. This is because the velocity of freely suspended particles that are subjected to colloidal forces in the proximity of the stationary bed is mainly determined by the influence of the repulsion effects, i.e. slowing down the settling process. The external porosities of the simulated structures are below that of the densest structure if a random packing. Hence, compaction due to rolling of the settled particles is still possible. The void sizes in the simulated structures are fairly small and similar in the horizontal and vertical direction. Furthermore, the radial velocity distribution in the column during filling indicated that significant differences in bed structure were to be expected. These velocity variations also showed that the density of the bed is expected to be higher at the frit-side of the capillary LC column.

The chromatographic experiments showed no relationships between the applied filtration pressure, the packing pressure, the bed porosity and the performance of the capillary LC columns. The simulation experiments indicate to bed structures that are dependent of the settling velocities. However, these differences probably vanish in a later stage, due to action of the packing pressure. Columns that were packed with CCl_4 instead of acetone as the slurry liquid were found to be having a somewhat lower external porosity, a higher flow resistance parameter and an improved chromatographic performance. Although the physical constants of the applied slurry liquids result in different hydrodynamic processing conditions, these were

not found to be critical in achieving efficiently packed columns. The origin of the small chromatographic differences is believed to be chemical rather than colloidal or hydrodynamic.

REFERENCES

[1]   M. Verzele, *J. Chromatogr.* 295 (1984) 81

[2]   F. Francolini, C. Borra and M. Novotny, *Anal. Chem.* 59 (1987) 2428

[3]   K.E. Karlsson and M. Novotny, *Anal. Chem.* 60 (1988) 1662

[4]   R.T. Kennedy and J.W. Jorgenson, *Anal. Chem.* 61 (1989) 1128

[5]   H. Menet, P. Gareil, M. Caude and R. Rosset, *Chromatographia* 18 (1984) 73

[6]   A. Capiello, P. Palma and F. Mangani, *Chromatographia* 32 (1991) 389

[7]   S.M. Han and D.W. Armstrong, *Anal. Chem.* 59 (1987) 1583

[8]   K. Masaharu, Y. Mori and T. Amano, *Anal. Chem.* 57 (1985) 2235

[9]   Y. Guan, L. Zhou and Z. Shang, *J. High Resolut. Chromatogr.* 15 (1992) 434

[10]   G. Crescentini and A.R. Mastrogiacomo, *J. Microcol. Sep.* 3 (1991) 539

[11]   G. Crescentini, F. Bruner, F. Mangani and Y. Guan, *Anal. Chem.* 60 (1988) 1659

[12]   A. Malik, W. Li and M.L. Lee, *J. Microcol. Sep.* 5 (1993) 361

[13]   W. Li, A. Malik and M.L. Lee, *J. Microcol. Sep.* 6 (1994) 557

[14]   D. Tong, K.D. Bartle and A.A. Clifford, *J. Microcol. Sep.* 6 (1994) 249

[15]   D. Tong, K.D. Bartle, A.A. Clifford and A. M. Edge, *J. Microcol. Sep.* 7 (1995) 265

[16]   R. Trones, A. Iveland and T. Greibrokk, *J. Microcol. Sep.* 7 (1995) 505

[17]   P. Koivisto, R. Danielsson and K.E. Markides, *J. Microcol. Sep.* 9 (1997) 87

[18]   D.C. Shelly and T.J. Edkins, *J. Chromatogr.* 411 (1987) 185

[19]   J.P.C. Vissers, H.A. Claessens, J. Laven, C.A. Cramers, *Anal. Chem.* 67 (1995) 2103

[20]   J.P.C. Vissers, J. Laven, H.A. Claessens, C.A. Cramers and W. Agterhof, *Colloids Surf A: Physicochem. Eng. Aspects* 126 (1997) 33

[21]   J.C. Gluckman, A. Hirose, V.L. McGuffin and M. Novotny, *Chromatographia* 17 (1983) 303

[22]   R.F. Meyer and R.A. Hartwick, *Anal. Chem.* 56 (1984) 2211

[23]   D.C. Shelly, V.L. Antonucci, T.J. Edkins and T.J. Dalton, *J. Chromatogr.* 458 (1989) 267

[24]   S.A. Karapetyan, L.M. Yakashina, G.G. Vasijarov and V.V. Brazhnikov, *J. HRC&CC* 8 (1985) 148

[25]   H. Guan-Sajonz and G. Guiochon, *J. Chromatogr. A* 743 (1996) 247

[26]   T. Zimina, R.M. Smith, P. Meyers and B.W. King, *Chromatographia* (1995) 662

[27]   T. Zimina. R.M. Smith, J.C. Highfield, P. Meyers and B.W. King, *J. Chromatogr. A* 728 (1996) 33

[28]   L. Durlofsky, J.F. Brady and G. Bossis, *J. Fluid. Mech.* 180 (1987) 21

[29]   K. Hinsen, *Computer Phys. Commun.* 88 (1995) 327

[30]   B. Cichiocki, B.U. Felderhof, K. Hinsen, E. Wajnryb and J. Blawzdziewicz, *J. Chem. Phys.* 100 (1994) 3780

[31]   J.P. Foley and J.G. Dorsey, *Anal. Chem.* 55 (1983) 730

[32]   H.C.W. Donker, H. Van As, H.J. Snijder and H.T. Edzes, *Magn. Reson. Imaging* 15 (1997) 113

[33]   D. van Dusschoten, P.A. de Jager and H. Van As, *J. Magn. Reson., series A* 116 (1995) 22

[34]   H. Van As and D.van Dusschoten, *Geoderma* 80 (1997) 389

[35]   U. Tallarek, E. Baumeister, K. Albert and G. Guiochon, *J. Chromatogr. A* 696 (1995) 1

[36]   E. Bayer, E. Baumeister, U. Tallarek, K. Albert and G. Guiochon, *J. Chromatogr. A* 704 (1995) 37

[37]   U. Tallerek, K. Albert. E. Bayer and G. Guiochon, *AIChE J.* 42 (1996) 3041

[38]   P.A. Bristow and J. Knox, *Chromatographia* 10 (1977) 279

[39]   C.A. Cramers, J.A. Rijks and C.P.M. Schutjes, *Chromatographia* 14 (1981) 439

CHAPTER 6.1

CALCULATION OF RETENTION IN CAPILLARY ELECTROCHROMATOGRAPHY BASED ON CHRO- MATOGRAPHIC AND ELECTROPHORETIC DATA

ABSTRACT

Retention factors in capillary electrochromatography (CEC) were predicted by means of theoretically derived equations and experimentally determined parameters in capillary liquid chromatography and capillary zone electrophoresis. It was found that the retention factor of uncharged components in CEC was about 20% higher than was calculated. The derived equations do not take into account alteration of the nature of the stationary phase or distribution constant by the applied electric field. However, the influence of the electric field on the retention in CEC can be estimated. Individual field contributions could not be determined.

133

INTRODUCTION

Capillary electrochromatography (CEC) is a relatively new technique that still is in development. CEC is performed in packed microcolumns, i.e. packed fused silica capillaries with an internal diameter (i.d.) of 50–100-µm, and the eluent is driven through the column by electro-osmosis. The electro-osmotic flow is induced by applying an electric field of ~ 20–100 kVm^{-1} over the column. The i.d. of the column is limited in order to prevent unwanted temperature gradients along the column radius, i.e. Joule heating. Neutral analytes are separated by normal partition between the mobile phase and the stationary phase, similar as in liquid chromatography (LC). In the case of dissociated or ionized analytes also electrophoresis contributes to the separation.

Only a limited number of scientific publications deal with the theoretical aspects of CEC. Knox and Grant [1] studied the effect of the particle diameter on the electro-osmotic velocity, the effect of the particle diameter on the plate height in pressure driven and electrically driven chromatography, and the effect of the electrolyte concentration on the mobile phase velocity and the plate height. The theory of band-broadening in CEC was investigated by Tsuda [2,3] and of extracolumn band-broadening by Rebscher and Pyell [4]. Other studies mostly involved comparative studies between CEC and microcolumn LC [5-7]. This chapter discusses the prediction of retention of neutral compounds in CEC by means of retention data obtained by LC and capillary zone electrophoresis (CZE). Retention prediction of charged compounds will not be discussed in this paper.

THEORY

CEC involves both partition and electrophoretic mobility [2,3]. Therefore, the mean linear velocity of a chromatographically unretained compound u_0 in CEC can be expressed as the sum of the electro-osmotic flow of the mobile phase u_{eof}, the effective electrophoretic mobility the unretained compound u_{eff} and the the linear flow velocity corresponding to pressurized flow u_{press}:

$$u_0 = u_{eof} + u_{eff} + u_{press} \tag{6.1}$$

The velocity of a retained compound in chromatography is given by:

$$u_r = \frac{u_0}{(1+k)} \tag{6.2}$$

where u_r is the linear velocity of the retained compound and k the retention factor. Substitution of equation (6.2) in equation (6.1) gives:

$$u_r = \frac{u_{eof} + u_{eff} + u_{press}}{(1+k)} \tag{6.3}$$

The electro-osmotic flow of the mobile phase u_{eof} and the effective electrophoretic mobility of a unretained compound u_{eff} can be expressed as the electro-osmotic mobility μ_{eof} and electrophoretic mobilities μ_{eff} using the potential drop V over the total length of the column L_{tot}:

$$u_{eof} + u_{eff} = (\mu_{eof} + \mu_{eff}) \cdot \frac{V}{L_{tot}} \tag{6.4}$$

Combination of equations (6.3) and (6.4) gives:

$$u_r = \left\{ (\mu_{eof} + \mu_{eff}) \cdot \frac{V}{L_{tot}} + u_{press} \right\} \frac{1}{(1+k)} \tag{6.5}$$

The retention time t_r of a compound can be calculated introducing the injector-to-detector length of the column L_{id}. Subsequent substation of equation (6.5) yields:

$$t_r = \frac{L_{id}}{u_r} = \frac{L_{id}(1+k)}{\frac{\mu_{eof} + \mu_{eff}}{L_{tot}} \cdot V + u_{press}} \tag{6.6}$$

As the electro-osmotic mobility is related to the time of the electro-osmotic flow marker t_{eof} by:

$$t_{eof} = \frac{L_{id}L_{tot}}{V\mu_{eof}} \tag{6.7}$$

and u_{press} by:

$$u_{press} = \frac{d_p^2}{\phi' \eta} \cdot \frac{\Delta p}{L_{col}} \tag{6.8}$$

where d_p is the diameter of the stationary phase particles, ϕ' the flow resistance parameter, Δp the pressure drop over the column and L_{col} the column length packed with stationary phase particles, an expression for the retention time of a compound can be derived:

$$t_r = \frac{(1+k)L_{id}}{\dfrac{L_{id}}{t_{eof}} + \dfrac{\mu_{eff}V}{L_{tot}} + \dfrac{d_p^2\Delta p}{\phi'\eta L_{col}}}$$ (6.9)

In the case that no pressurized flow is used – i.e. Δp equals zero. Rearrangement of equation (6.9) gives:

$$t_r = \frac{1+k}{\dfrac{1}{t_{eof}} + \dfrac{\mu_{eff}V}{L_{id}L_{tot}}}$$ (6.10)

Retention time can thus be predicted by means of LC experiments – i.e. retention factor – and CZE experiments, i.e. t_{eof} and m_{eff} respectively.

EXPERIMENTAL

Instrumentation

Capillary LC separations were carried out with a Phoenix 20 CU syringe pump (Carlo Erba Instruments, Milan, Italy) or a model 100 DM syringe pump (ISCO Inc., Lincoln, NE, USA). Injections were made manually with a 60 nl CI4W injection valve (VICI-AG Valco Europe, Schenkon, Switzerland). Detection was performed with a 785 A Programmable Absorbance detector (Applied Biosystems, San Jose, CA, USA) – equipped with a z-shaped detection cell (LC Packings, Amsterdam, The Netherlands) – at a wavelength of 260 nm. The column was thermostated with an Ultra-thermostat NB-33369 (Calora Messtechnik GmbH, Lorch, Germany) and a home made water jacket.

The CEC equipment consisted of a Prince Version 1 Programmable Injector (Lauerlabs, Emmen, The Netherlands) for electrokinetic or pressure driven injections of the samples, a dc HCN 140-35000 power supply (FUG Electronic GmbH, Germany) to generate an electric field across the packed capillary columns and an on-column UV absorbance detector (Unicam Analytical Systems, Cambridge, UK). Platinum wires were used to connect the injection unit to the positive electrode and the buffer reservoir. A home made interface and Caesar software (B*Wise, Geleen, The Nethelands) were employed for data acquisition. All CZE experiments were done on the same equipment as the CEC experiments. A 50-µm i.d. fused silica capillary (Scientific Glass Engineering, Melbourne, Australia) was used during the CZE analysis.

136

Chemicals

As the mobile phase modifier acetonitril was used, which was, like acetone, purchased from E.Merck (Darmstadt, Germany). The applied buffers were sodiumacetate and 3-[morpholine-propanesulfonic acid] (MOPS), both from E. Merck, and 2-[N-morpholine]-

ethanesulfonic acid (MES) from Sigma Chemical Company (St. Louis, MO, USA). 4-amino-acetophenone, o-nitrophenol, 2,6-dimethylphenol and thiourea were from E.Merck and naph-thalene from Fluka AG (Buchs, Switzerland). All chemicals were of analytical reagent grade. Water was purified with a Milli-Q water Purification system of Water-Millipore (Milford, MA, USA) prior to use. The individual solvents of the mobile phase were filtered through a 0.45-µm filter. The mobile phase was degassed with helium before it was used.

Column preparation

The packing procedure to pack the fused silica capillaries and the packing equipment are discussed in detail in previous papers [8,9]. Nucleosil 100-5 C18 (Machery-Nagel GmbH & Co KG, Düren, Germany) was used as the packing material and was suspended in acetone by ultra sonication for a 10 minute period before it transferred into the slurry vessel by means of a syringe. Packing was carried out at 500 bar and acetonitrile/H_2O (70:30, v/v) was used as the packing liquid. The pressure was maintained for a one hour period.

RESULTS AND DISCUSSION

Capillary LC experiments.

The retention of a compound in LC is among others dependent on the distribution of the compound over the mobile and the stationary phase. Therefore, the influence of the pH, ionic strength and modifier concentration on the retention factor of several neutral compounds, i.e. uncharged components under the applied conditions, was investigated by means of a central composite design. The experimental settings of the design are given in Table 6.1. All levels of the central composite design were measured twice. The influences of the investi-gated parameters on the retention factor were calculated for 4-aminoacetophenone, o-nitrophenol, 2,6-dimethylphenol and naphthalene. A backward elimination procedure was applied to determine the significance of the parameters at the 95% confidence level. Single and quadratic interactions terms were also allowed in the experimental central composite design. The equations describing the dependance of the retention factor of the neutral com-pounds on the parameters is given in Table 6.2.

The retention factor is – as expected – not influenced by the pH or the ionic strength of the buffer, since all compounds are uncharged in the applied mobile phases. The pK_a-values of 4-amino-acetophenone, o-nitrophenol and 2,6-methylphenol are 2.29, 7.17 and 10.59 re-spectively [10,11]. Furthermore, the chance to exceed the 95% confidence level is very small because all calculated F-numbers are much larger than the theoretical value of 2.56 [12].

Because of Joule heating – the temperature during an CEC experiment will be higher than the ambient temperature – and has therefore to be corrected for. A large number of chro-matographic systems show linear relationships between the logarithm of the retention factor and the reciprocal of the column temperature – i.e. van 't Hoff plots. The temperature effect can be described by:

Table 6.1. Experimental settings applied to determine the influence of the pH, ionic strength and modifier concentration on the retention factor of neutral compounds

exp. no.	pH	ionic strength (mM)	fraction modifier
1	5.00	2.00	0.40
2	5.00	2.00	0.70
3	5.00	8.00	0.40
4	5.00	8.00	0.70
5	7.00	2.00	0.40
6	7.00	2.00	0.70
7	7.00	8.00	0.40
8	7.00	8.00	0.70
9	6.00	5.00	0.55
10	4.78	5.00	0.55
11	7.22	5.00	0.55
12	6.00	1.36	0.55
13	6.00	8.65	0.55
14	6.00	5.00	0.57
15	6.00	5.00	0.73

$$\ln k = \frac{\Delta S^0}{R} + \frac{-\Delta H^0}{RT} \qquad (6.11)$$

where ΔH^0 is the standard enthalpy, ΔS^0 the standard entropy, T the absolute temperature and R the gas constant. As an example, the results of four of the investigated mobile phases are given in Table 6.3. As can been seen from the results of Table 6.3, all investigated components show a linear relationship between ln k and 1/T.

Capillary zone electrophoretic experiments

The electrophoretic mobility μ_{eff} of the compounds in the different mobile phases was determined with capillary zone electrophoresis and was for almost all the components equal to zero in the investigated mobile phases. Only o-nitrophenol had a μ_{eff} of - 1.01 · 10^{-4} cmV^{-1}s^{-1}. o-Nitrophenol has a relative low pK$_a$-value of 7.17 and shows therefore at high pH-values or high ionic strengths some electrophoretic mobility.

138

Capillary electrochromatographic experiments

The CEC experiments were carried out with the same column as in the capillary LC separations. The total length of the capillary column L$_{tot}$ was 0.544 m, the length from inlet-to-

Table 6.2. Results of the experimental design for neutral compounds

compound	intercept	modifier	modifier²	r	F
4-aminoacetophenone	1.93	-4.3	2.6	0.997	1000
o-nitrophenol	10.9	-28.	19	0.984	180
2,6-dimethylphenol	15.2	-42	29	0.995	630
naphthalene	82	-240	180	0.992	330

detector L_{id} equalled 0.399 m and the packed part L_{col} had a length of 0.274 m. The specific conductivity G, current I, estimated temperature excess ΔT_{excess} and the temperature within the core of the tube ΔT_{core} are – for the previous mentioned example – given in Table 6.4. The applied voltage was 30 kV. ΔT_{excess} and ΔT_{core} were calculated from equation (6.12) and (6.13) respectively [1]. ΔT_{core} represents the temperature excess within the core of a capillary column and arises from the heating of the mobile phase due to ohmic loss. ΔT_{core} is given by:

$$\Delta T_{core} = \frac{E \cdot I}{4\pi K} \tag{6.12}$$

where E is the field strenght, I is the current and K is the thermal conductivity of the mobile phase. The units of E and I are V m^{-1} and A, respectively. With an aqueous eluent K = 0.6 W m^{-1}K^{-1}.

The temperature excess between the capillary column and the surrounding air ΔT_{excess} was approximated by [1,13]:

$$\Delta T_{excess} \cong \frac{1.3 E \cdot I}{d_0^{0.3}} \tag{6.13}$$

where d_0 [m] is the outer diameter of the packed capillary column.

ΔT_{core} is – as can been seen from the data in Table 6.4 – negligible; ΔT_{excess} is about 100 times as large as ΔT_{core} and must be taken into account when retention factors are estimated in CEC. The experimentally obtained retention factors and the temperature corrected factors are given in Table 6.5. The retention factors were corrected for by using the data in Table 6.3. The corrected retention factors are somewhat higher than the uncorrected values.

Since in this study no pressurized flow was applied – i.e. $\Delta p = 0$ – and the electrophoretic mobility μ_{eff} of the uncharged compounds also equals zero, equation (6.9) reduces to:

139

$$t_r = t_{eof}(1+k) \tag{6.14}$$

which is a well known relationship in chromatography. Therefore, retention factors obtained

Table 6.3. Temperature dependance of the retention factor with correlation coefficients (n = 5). The experiment numbers correspond with Table 6.1

compound	$\Delta S^0/R$	$-\Delta H^0/R$	r (n =5)
exp. no. 2.			
4-aminoacetophenone	-3.3	570	1.000
o-nitrophenol	-2.7	720	0.998
2,6-dimethylphenol	-2.3	610	0.999
naphthalene	-1.8	750	0.998
exp. no. 6.			
4-aminoacetophenone	-3.37	570	0.996
o-nitrophenol	-2.4	630	0.999
2,6-dimethylphenol	-2.2	590	0.999
naphthalene	-1.8	760	0.997
exp. no. 8.			
4-aminoacetophenone	-3.3	530	0.999
o-nitrophenol	-2.4	570	1.000
2,6-dimethylphenol	-2.4	600	0.997
naphthalene	-1.8	710	0.999
exp. no. 9.			
4-aminoacetophenone	-3.3	710	1.000
o-nitrophenol	-2.3	850	0.996
2,6-dimethylphenol	-2.0	760	0.998
naphthalene	-1.6	1000	0.998

in capillary LC an CEC can, in the case of uncharged compounds, directly be compared. The ratio of the uncorrected and temperature corrected retention factors k_{CEC}/k_{LC} are given in Table 6.6.

As can been seen from the results in Table 6.6, the retention factors in CEC are about 1–1.4 times as high as in capillary LC. The temperature corrected retention factors are ~ 5% higher than the uncorrected values. Several factors may increase the retention factor in CEC. Namely, alteration of the nature of the stationary phase due to the application of an electric field, changes in the distribution constants of the compounds of interest over the mobile and stationary phase and electric field inhomogeneities in the packed part of the column. To what extent the different factors contribute to the overall effect is not clear. However, the average

Table 6.4. The specific conductivity G, the current I, the temperature excess ΔT_{excess} and the temperature excess within the core of the tube ΔT_{core} of the investigated mobile phases in EC. The experiment numbers correspond with Table 6.1

exp. no.	G (mAV^{-1}m^{-1})	I (mA)	ΔT_{excess} (K)	ΔT_{core} (K)
2	15	5.5	4.1	0.040
6	9.4	2.5	1.9	0.018
8	3.7	10	7.5	0.073
9	19	7.5	5.6	0.054

overall effect can be determined and equals 1.2 for the investigated mobile phases, i.e. retention in CEC for neutral compounds is ~ 20% slower than in capillary LC using the same stationary phase and mobile phases. Similar observations have been made by Eimer *et al.* [14]. The same kind of effects are observed for charged compounds but differ in magnitude. This will – however – be discussed elsewhere.

CONCLUSIONS

Electrochromatography was successfully applied in packed fused silica capillary columns of 320-μm i.d. to theoretically predict the retention of neutral compounds in CEC. The derived equation to predict retention in CEC does not foresee in alterations of the nature of the stationary phase of distribution constants by the applied electric field, or field inhomogeneities, and therefore fails in the exact prediction of the retention times. However, based on the obtained results the overall contribution by the electric field could be estimated for uncharged

Table 6.5. Retention factors and temperature corrected retention factors (in parentheses) in CEC. The numbers of the experiments correspond with Table 6.1

	k							
experiment number	2		6		8		9	
4-aminoacetophenone	0.18	(0.18)	0.24	(0.24)	0.20	(0.21)	0.44	(0.46)
o-nitrophenol	0.58	(0.60)	—	(—)	0.60	(0.63)	1.79	(1.89)
2,6-dimethylphenol	0.60	(0.62)	0.76	(0.77)	0.60	(0.63)	1.72	(1.80)
naphthalene	1.62	(1.68)	2.07	(2.10)	1.60	(1.70)	5.70	(6.07)

Table 6.6. Ratio of the retention factors k_{EC}/k_{LC}, uncorrected and temperature corrected (in parentheses) of neutral compounds. The experiment numbers correspond with Table 6.1

	k_{EC}/k_{LC}							
experiment number	2		6		8		9	
4-aminoacetophenone	0.92	(0.92)	1.22	(1.22)	1.17	(1.23)	1.30	(1.35)
o-nitrophenol	0.99	(1.03)	—	(—)	1.30	(1.37)	1.34	(1.38)
2,6-dimethylphenol	0.97	(1.00)	1.19	(1.20)	1.22	(1.29)	1.37	(1.42)
naphthalene	0.96	(0.99)	1.21	(1.22)	1.26	(1.33)	1.43	(1.52)
mean	0.96	(0.99)	1.21	(1.22)	1.24	(1.31)	1.36	(1.42)
RSD (%)	3.1	(4.8)	1.3	(1.3)	4.5	(4.6)	4.0	(4.8)

compounds. Retention in CEC is ~ 20% slower than in LC. No distinction could be made between the individual contributions to the effect of the electrical field on the retention in CEC.

REFERENCES

[1]   J.H. Knox and I.H. Grant, *Chromatographia* 32 (1991) 317

[2]   T. Tsuda, *Anal. Chem.* 60 (1988) 1677

[3]   T. Tsuda, *LC•GC Int.* 5 (1992) 26

[4]   H. Rebsher and U. Pyell, *Chromatographia* 38 (1994) 737

[5]   C. Yan, D. Schaufelberger and F. Erni, *J. Chromatogr.* 670 (1994) 15

[6]   H. Yamamoto, J. Baumann and F. Erni, *J. Chromatogr.* 593 (1992) 313

[7]   D.B. Gordon, G.A. Lord and D.S. Jones, *Rapid Commun. Mass Spectrom.* 8 (1994) 544

[8]   J.P.C. Vissers, H.A. Claessens, J. Laven and C.A. Cramers, *Anal. Chem.* 67 (1995) 2103

[9]   J.P.C. Vissers, E.C.J van den Hoef, H.A. Claessens, J. Laven and C.A. Cramers, *J. Microcolumn Sep.* 7 (1995) 239

[10]   G. Körtum, W. Vogel and K. Andrussov, *Dissociation Constants of Organic Acids in Aqueous Solutions*, Butterwoods, London, 1961

[11]   D.D. Perin, *Dissociation Constants of Organic Bases in Aqueous Solutions*, Butterwoods, London, 1965

[12]   R.H. Meyers, *Classical and Modern Regression with Applications*, Duxburry Press, Belmont, 1990

[13]   J.H. Knox, *Chromatographia* 26 (1988) 329

[14]   T. Eimer, T. Adam and K.K. Unger, poster 233, 19th International Symposium on Column Liquid Chromatography and Related Techniques

CHAPTER 6.2

AUTOMATED ON-LINE IONIC DETERGENT REMOVAL FROM MINUTE PROTEIN/PEPTIDE SAMPLES PRIOR TO CAPILLARY LC-ESI MS

ABSTRACT

An automated on-line ionic detergent removal pre-column system coupled to capillary liquid chromatography-electrospray mass spectrometry is described. The system involves two micro precolumns – composed of a specific ionic detergent trapping column and a preconcentration column respectively – and a packed 300-µm i.d. analytical column. Sample loading to the micro precolumns – and regeneration of the detergent trapping column – was performed at a flow-rate of 50 µl min^{-1} while the flow-rate through the analytical column was set at 5.0 µl min^{-1}. Ionic detergent containing tryptic digested protein samples were directly applied to the micro precolumns without sample pretreatment and were analysed by UV absorption detection and electrospray-mass spectrometry. The presented system allows for the automated removal of SDS with virtually no loss in protein/peptides. Maximum SDS load and breakthrough have been determined. Excellent protein recovery and complete removal of SDS is found. The chromatographic separation after SDS removal was completely restored and equalled the reference chromatograms. Mass spectral data confirm these findings. Finally, this technique allows for SDS removal from minute protein samples without the need of any sample handling.

143

INTRODUCTION

Reversed-phase liquid chromatography-electrospray mass spectrometry (RPLC/ESI-MS) is currently the method of choice for the separation and identification of complex protein and peptide mixtures. However, protein/peptide samples are often at low concentration and contain buffers and/or detergents, which hamper LC-ESI-MS analysis [1,2]. Commonly used purification and concentration techniques like liquid-liquid extraction [2,3], gel filtration [4-6], and precipitation [7-9] often fail in quantitatively recovering the compounds of interest and are not accessible for minute sample volumes. Furthermore, these techniques are very time consuming and cannot be coupled easily with identification methods such as MS.

Different types of solid-phase extraction cartridges have been introduced recently for conventional and microbore LC to trap ionic and non-ionic surfactants. However, these cartridges are not compatible with capillary LC. The system employed in this study uses miniaturized precolumns to which the samples are applied. By using subsequent wash steps – utilizing different wash solvents – interfering compounds can be selectively removed.

With the presented method it is possible to automatically preconcentrate the sample on cartridge type microcolumns with virtually no dead-volume. Typical loading and clean-up flow-rates are up to 50 µl min^{-1} which results in very fast sample clean-up of less than 1 min. Both steps are performed on-line. The use of micro-precolumns in combination column switching techniques allows for optimal clean-up of small and large sample volumes. The developed technique minimises the risk of sample loss since no additional sample preparation steps are required. Results will be shown on the removal of the ionic detergent sodiumdodecylsulphate (SDS) from minute proteinaceous samples using microcolumn switching in combination with capillary LC. Also demonstrated is the enhancement in selectivity and sensitivity – as will be shown by capillary liquid chromatography and mass spectral analysis.

EXPERIMENTAL

Chemicals and reagents

Acetonitrile and water – both HPLC grade – were purchased from LabScan (Dublin, Ireland). Trifluoroaceticacid (TFA), cytochrome C (from bovine heart), α-lactalbumin B (from bovine milk), and an HPLC peptide standard mixture were obtained from Sigma (St. Louis, MO, USA). Trypsin (from bovine pancreas), tris(hydroxymethyl)-aminomethane, hydrochloric acid sodiumacetate and calciumchloride were from Fluka (Buchs, Switzerland).

Digest preparation

Typical amounts of 1–2 mg/ml of protein were dissolved in digest buffer (100 mM sodium acetate, 100 mM tris(hydroxymethyl)aminomethane and 1 mM calcium chloride, pH 8.3). Protein samples were digested by the addition of trypsin dissolved in 1 mM HCl (trysin/protein, 1:50 w/w) and incubated at 37°C for 4 h – followed by a second enzyme addition to give a
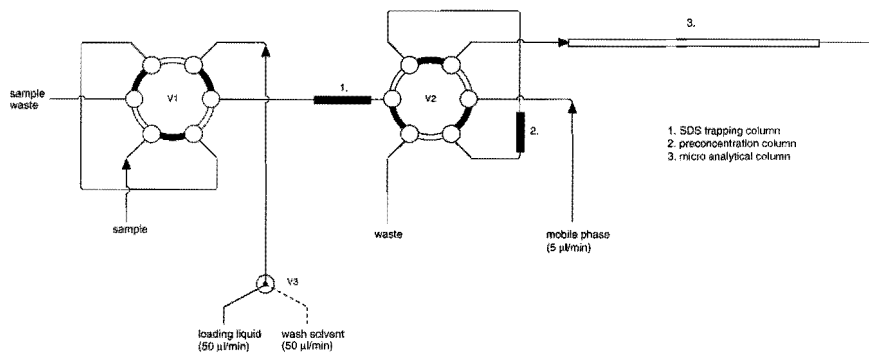
Fig. 6.1. Scheme of the instrumental set up for on-line SDS removal consisting of three six-port valves; injection valve (V1), switching valve (V2), and a third six-port valve that was used as a solvent selection valve (V3). For details see experimental section.

final trypsin/protein concentration ratio of 1:25 (w/w). After 16 h of incubation the samples were diluted five times in the mobile phase and stored at -20°C.

Capillary LC instrumentation

A FAMOS microsampling workstation (LC Packings, Amsterdam, The Netherlands) with two additional built-in six-port valves was used for sample injection, sample clean-up and preconcentration. A schematic overview of the instrumental set-up is given in Fig. 6.1. Sample preconcentration and sample clean-up was performed with a LC-10S pump (Shimadzu, Tokyo, Japan) which was operated at 50 μl min^{-1}. Cartridge type precolumns (LC Packings) with a length of 5 mm and different inner diameters were used to trap SDS or to preconcentrate the peptides originating from the tryptic digest. The packing material in the SDS trapping column consists of an anion-exchange type of stationary phase with a nominal particle diameter of 5-μm. The preconcentration column was filled with a 5-μm standard reversed phase stationary phase packing material. Both micro precolumns were typically replaced after fifty injections. The loading solvent for sample preconcentration and sample clean-up were acetonitrile/H$_2$O mixtures containing 0.1% TFA. Different loading solvent compositions have been studied. For details see section results and discussion. Regeneration of the SDS trapping column was done with 0.1% TFA in acetonitrile.

LC experiments were performed with an LC-10-AD high pressure gradient system (Shimadzu). Micro flows were generated by an AC-400-VAR variable microflow processor (LC Packings) that was connected to the gradient system [10,11]. The micro outlet flow was transferred directly to the workstation. Peptide samples were separated on a 0.15 m x 300-μm i.d. capillary LC column (LC Packings) packed with 3-μm C$_{18}$ base deactivated stationary phase at

a flowrate of 5 µl min^{-1}. The gradient was developed over 20 min from 5% to 80% B for the HPLC peptide mixture, from 5% to 35% B for the cytochrome C tryptic digest, and from 5% to 40% B for the α-lactalbumin B tryptic digest. Mobile phase A consisted of 0.1% TFA in acetonitrile/H$_2$O (5:95, v/v) and mobile phase B of 0.08% TFA in acetonitrile/H$_2$O (80:20, v/v).

Detection was performed at 214 nm using an SPD-10A UV-VIS absorbance detector (Shimadzu) equipped with a 35 nl, 8 mm longitudinal u-shaped capillary flow cell (LC Packings) [12,13]. Data acquisition was performed with MT-2 chromatography software (Kontron Instruments, Milan, Italy).

Mass spectrometry

Pneumatically assisted electrospray (ion spray) ionisation mass spectrometry was conducted with an API 300 triple quadrupole mass spectrometer (Perkin-Elmer Sciex Instruments, Thornhill, ON, Canada) in the positive ion, single scan mode. Scans were taken from m/z 300 to 1500 with a scan duration of 2 s, using a step size of 1 amu and a 2.5 ms dwell time per step. The mass spectrometer was set to the following parameters: ion spray voltage 5.5 kV, orifice voltage 35 V. The nebulizer gas (air) and curtain gas (nitrogen) were adjusted to 1.5 l/min and 0.8 l/min respectively.

RESULTS AND DISCUSSION

SDS presence

The results in Fig. 6.2 demonstrate the effect of the presence of SDS in a sample on the chromatographic separation of a tryptic digest of α-lactalbumin B. The left trace represents the chromatogram of the digested α-lactalbumin B sample in the presence of 0.1% SDS and the right trace represents the same sample without SDS. Peak broadening, increased retention and loss of resolution are usually observed in the presence of SDS. SDS is know to bind to proteins and peptides resulting in more hydrophobic species with overall similar polarity which causes the majority of the individual compounds of the tryptic digest to co-elute. Besides proteins and peptides, SDS also binds to the surface of the applied stationary phase packing material resulting in insufficient protein/peptide separations on reversed phase surfaces. No useful mass spectra could be obtained – as shown later – in the presence of SDS.

Sample preconcentration

The maximum tolerable amount of acetonitrile present in the loading liquid was determined in order to investigate whether partial SDS removal could be achieved during sample preconcentration [14]. Digest and peptide samples were directly loaded onto the preconcentration column. The SDS trapping column – as shown in Fig. 6.1 – was not used in these experiments.
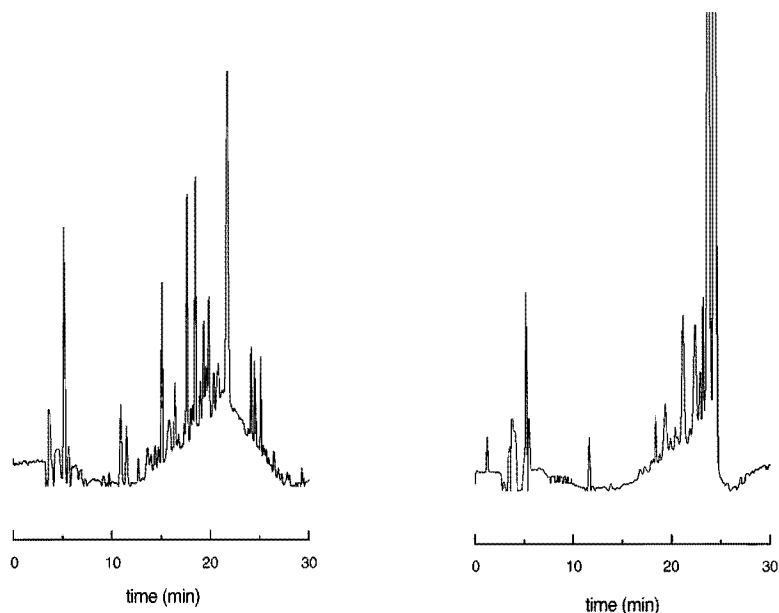
Fig. 6.2. Comparison of peptide separations from tryptic digested α-lactalbumin B on a 0.15 m x 300 μm i.d. packed capillary LC column. The left trace shows the chromatographic separation of an SDS free sample. The right trace shows the separation of the same sample in the presence of 0.1% SDS. For chromatographic conditions see experimental section.

Sample breakthrough was already observed for the more hydrophilic tryptic peptide with as little as 5% acetonitrile in acidified water (0.1% TFA) as the loading solvent. This is in contrast to work published earlier [14], where up to acetonitrile/H_2O (20:80, v/v) could be used for sample loading and complete SDS removal. In the present study, sample loading with acetonitrile/H_2O (20:80, v/v) resulted in almost complete sample breakthrough and only partial SDS removal. No sample breakthrough was observed with 0.1% TFA in H_2O as the carrier liquid. Therefore, all further experiments were performed with 0.1% TFA in H_2O as the loading solvent for sample preconcentration.

Sample recovery

The recovery of the sample preconcentration was determined by comparing peak heights and peak areas of direct 1 and 5 μl sample injections to those using preconcentration. The i.d. of the 5 mm long micro preconcentration column were 0.3 or 0.5 mm.

Complete sample recovery was obtained for the tryptic digest of α-lactalbumin and cytochrome C mixtures for the 0.3 and 0.5 mm i.d. micro preconcentration columns and was independent of the injected sample volumes between 1 to 5 μl. For the HPLC peptide stan-
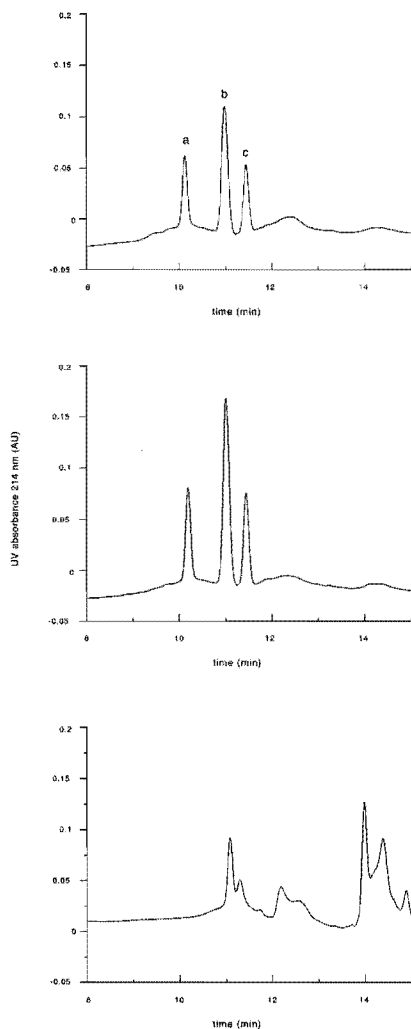
Fig. 6.3. SDS loadability and breakthrough. Chromatographic separation of a 5 μl sample injection containing three pentapeptides (a. methionine enkaphalin; b. leucine enkaphalin and c. anginotensin II) on a 0.15 m x 300 μm i.d. LC column in the absence of SDS (upper trace); 0.5% SDS present in the sample (middle trace); 1.0% SDS present in the sample (bottom trace). For chromatographic conditions see experimental section.

dard mixture – consisting of glycine-tyrosine, valine-tyrosine-valine, methionine enkaphalin, leucine enkaphalin and anginotensin II – the sample recovery was nearly equal to 100% for the tripeptide and the three pentapeptides. Partial sample breakthrough was observed for the dipeptide and was equal to about 50%. However, since the tryptic digest mix-

tures do have much higher retention factors than the di-peptide it was experimentally determined that the tryptic digest samples could be applied to the micro precolumns using 0.1% TFA in H$_2$O at flow-rates up to 50 µl min^{-1} without sample loss.

SDS loadability and breakthrough

Besides sample breakthrough and sample recovery it is also important to determine how much SDS can be loaded onto the SDS-trapping micro precolumn without breakthrough of SDS. For these particular experiments the HPLC standard peptide mixture was used for evaluation. The three pentapeptides elute in a very narrow time space and are very sensitive towards the presence of SDS. The amount of SDS that could be loaded onto the SDS trapping columns was determined for 0.3 and 0.5 mm i.d. micro precolumns. The injection volume was equal to 5 µl.

An example of SDS breakthrough is given in Fig. 6.3. The upper chromatogram shows the separation of the three pentapeptides when there is no SDS present in the sample. The middle chromatogram corresponds to an injection with 0.1% SDS present in the sample. As can been seen chromatographic resolution is preserved. The bottom chromatogram shows the effect of partial breakthrough of SDS on the separation of the HPLC standard peptide mixture. Only the hydrophobic pentapeptides are separated well, meanwhile the more hydrophilic pentapeptides start to co-elute, as can been seen from the bottom trace in Fig. 6.3. It was found that by injecting 5 µl samples containing different amounts of SDS, 0.025 mg of SDS could be loaded on the 0.3 mm i.d. micro precolumn and 0.050 mg SDS on the 0.5 mm i.d. micro precolumn – both of 5 mm length.

On-line SDS removal

The analytical system utilized to remove SDS prior to LC/ESI-MS analysis is already described in detail in the experimental section. The second additional six-port valve of the microsampling workstation was used as a solvent selection device. A 1 ml loop was mounted on the valve and filled with 0.1% TFA in acetonitrile which was used to regenerate the SDS trapping column. The loop was switched into the carrier liquid stream for 1 min. This means that theoretically the micro precolumn can be regenerated twenty times before the 1 ml loop has to be refilled with 0.1% TFA in acetonitrile. In practice however this was done every tenth injection. By simply increasing the loop volume size larger numbers of unattended sample analysis are feasible.

Cytochrome C tryptic digested samples were applied to the SDS-removal system and analyzed with a standard gradient. The results of these experiments are shown in Fig. 6.4. The upper trace of Fig. 6.4 shows the separation of the peptides without any presence of SDS in the sample. The middle trace of Fig. 6.4 shows the same type of sample, however now in the presence of SDS with a final concentration of 0.1%. The bottom trace of Fig. 6.4 corresponds to the sample as in the middle trace, however now after removal of SDS using the trapping

149
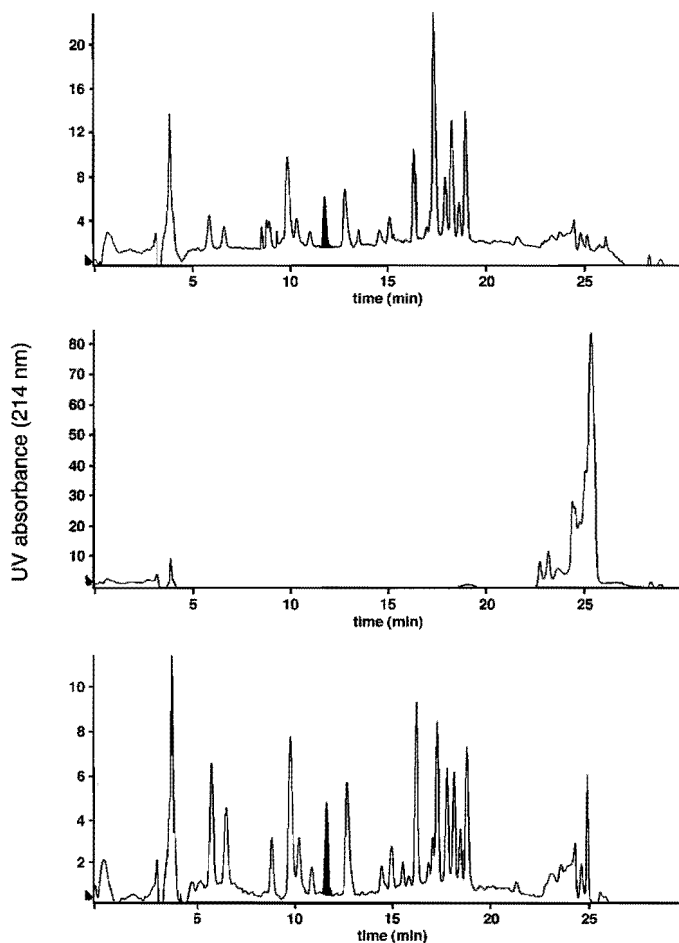
Fig. 6.4. Automated on-line SDS removal from a cytochrome C tryptic digest prior to capillary LC. The sample is run on a 15 m x 300 μm i.d. LC column. The upper UV absorption chromatogram shows the separation of an SDS free cytochrome C digest (reference chromatogram). The middle trace corresponds to the separation of the same sample in the presence of 0.1% SDS. The bottom trace shows the separation of the cytochrome C digest after removal of SDS with the use of the trapping column. For chromatographic conditions see the experimental section.

150

column. The retention times of the peptides are almost identical in comparison to the digest separation without any SDS. The recovery of the peptides is component dependent, and found to be in between 85 and 95% for most peptides. For only one particular peptide fragment recoveries of approximately 50% were obtained. Apparently a part of the peptides binds irreversibly to the SDS that is trapped on the SDS-trapping column. Identification of all the
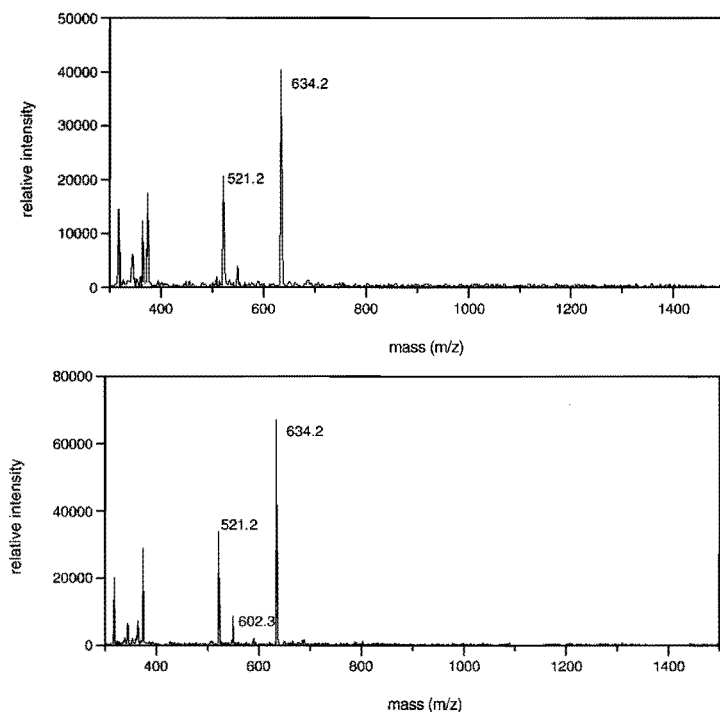
Fig. 6.5. Electrospray mass spectra of a typical digest peptide fragment in the absence of SDS (upper trace; reference electrospray mass spectrum) and after SDS removal (lower trace). The mass spectra correspond to the labelled peaks in Fig. 6.4.

peptides is however only possible after removal of SDS. It must be noted that for peptide mapping solely based on peak area patterns and the number and the number of peaks – to determine for instance the consistency of protein production - can be strongly hampered by incomplete peptide recovery. However, with the use of the presented method the majority of the peptides can unambiguously be identified based on retention time and peak area.

The developed method can be extended to the automated on-line removal of non-ionic detergents, sample concentration or for the desalting of samples. By using micro precolumns with different chemistries – and appropriate sample loading and clean-up solvents – the removal of a wide range of interfering compounds can be addressed. The proposed system can be used for two-dimensional LC separations too. For these type of applications however a second gradient system would be required to fully accommodate such a system. Typical two-dimensional LC column set-ups are ion-exchange/reversed phase and reversed phase/reversed phase.

151
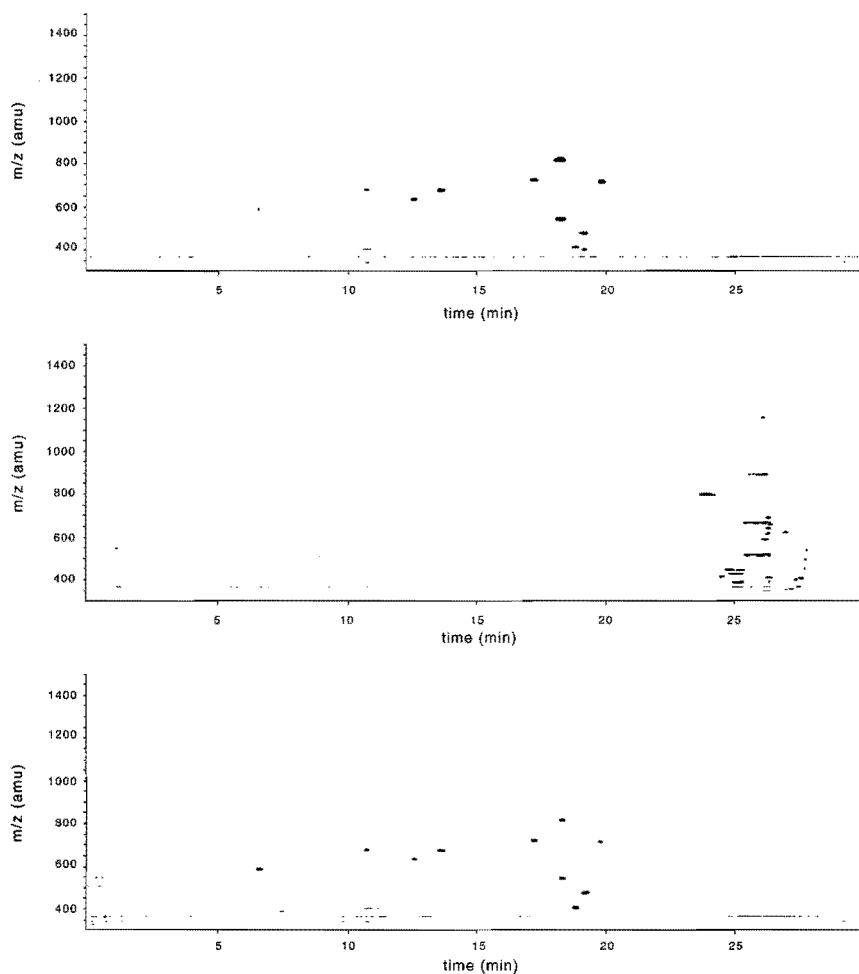
Fig. 6.6. Contour plot of m/z *vs.* retention time of tryptic digested cytochrome C. The upper graph shows the separation of an SDS-free cytochrome C digest (reference chromatogram). The middle graph corresponds to the separation of the same sample in presence of 0.1% SDS. The bottom trace shows the separation of the cytochrome C after removal of SDS. Conditions as in Fig. 6.4.

152 *Mass spectrometry*

To confirm that SDS was completely removed from the tryptic digest samples capillary LC-ESI-MS was performed. The collected ESI-MS spectra correspond to the marked peaks in Fig. 6.4. The ESI-MS spectra in the presence and absence of SDS are given in Fig. 6.5. All peak spectra were averaged and background subtracted. The upper trace shows the spectrum ac-

quired in the absence of SDS and the lower trace the spectrum after SDS has been removed from the sample. Very pure mass spectra were obtained and spectral integrity was preserved. Furthermore, no complex or adduct formation was observed, nor a reduction in the signal intensity of the mass spectrometer.

A complete overview of the efficiency of the developed SDS-removal technique is given by the two-dimensional plot in Fig. 6.6 where m/z is depicted as a function of the retention time t_r. The upper graph shows m/z *vs.* t_r for tryptic digested cytochrome C that is free of SDS. The middle graph shows the same sample type, however now in the presence of 0.1% SDS. The bottom graph of Fig. 6.6 corresponds to the sample as in the middle trace of Fig. 6.6, however now after removal of SDS using the trapping column. The middle trace shows the pronounced effect of SDS on retention time and mass assignment of the individual peptide fragments of the cytochrome C digest. Due to the complexation of SDS to the peptides increased retention times and excessive broadened peaks are obtained. Furthermore, the formation of adducts can be observed by MS. The retention times and assigned masses of the peptides after the removal of SDS are almost identical in comparison to the SDS free reference sample.

The gain in sensitivity is shown by the mass chromatograms which are depicted in Fig. 6.7. The selected ion m/z 634.2 corresponds to the base peak of the mass spectra of Fig. 6.5. This ion is typical for the black labelled peaks in Fig. 6.4. The left trace of Fig. 6.7 is the mass chromatogram of the cytochrome C tryptic digest in the absence of SDS and the middle trace is the mass chromatogram of the same sample in the presence of SDS. The right trace of Fig. 6.7 corresponds to the mass chromatogram after SDS has been removed from the sample. The calculated gain in sensitivity – using the SDS removal precolumn – approximates a factor of 3–4. The results given in Fig. 6.7 also show the enormous shift in retention as a result of the binding of SDS to the peptides and/or stationary phase.

CONCLUSIONS

The presented method allows for the automated and unattended on-line ionic detergent removal from protein digest samples in reversed phase LC/ESI-MS. The data show that the separation capacity of the capillary analytical column can be completely preserved by using micro column switching techniques, i.e. a SDS trapping column, followed by a preconcentration column. Ionic detergents are selectively removed before the sample is applied to the capillary analytical system, thereby identification of the peptides is feasible solely based on retention. The removal of SDS is conducted on-line. Sample preparation, handling and transfer are therefore eliminated. The overall recovery was found to be component dependent and ranged from 50 to 100%.

Mass spectral analysis confirmed the selective removal of SDS. Furthermore, no adduct formation was observed, indicating that the SDS was completely removed. Pure mass spectra were obtained allowing unambiguous identification of the peptide fragments. Finally due to
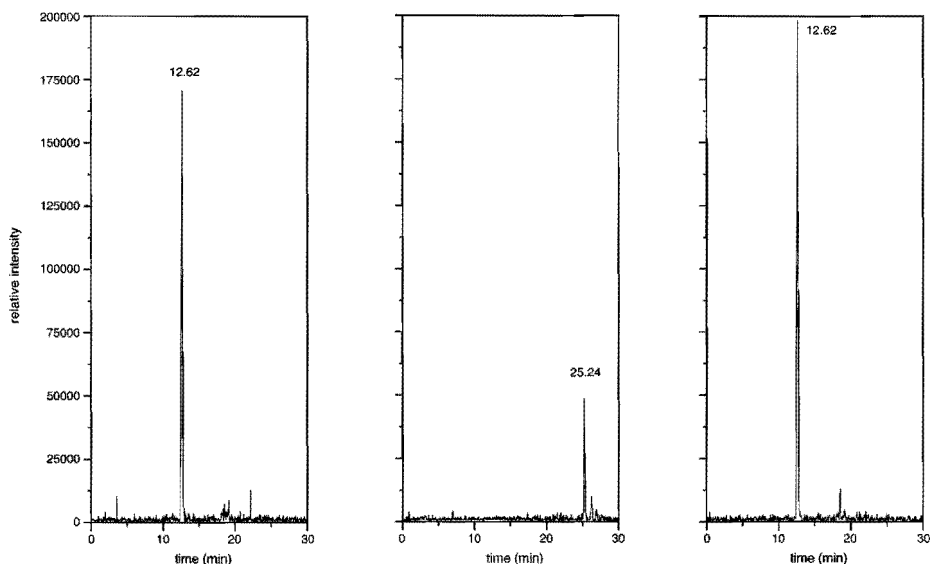
153

Fig. 6.7. Mass chromatograms of the selected m/z 634.2 ion for the cytochrome C tryptic digest that is free in SDS (left trace; reference mass chromatogram), in the presence of SDS (middle trace) and after SDS removal (right trace).

the selective removal of SDS the gain in sensitivity – based on reconstructed selective ion monitoring mass spectra – was a factor 10 to 30.

REFERENCES

[1]   K.M. Swidereck, M.L. Klein, S.A. Hefta and J.E. Shiveley, in J.W. Crabb (ed.), *Techniques in Protein Chemistry VI*, Academic Press, San Diego, 1995, pp. 267

[2]   A. Bosserhoff, J. Wallach and R.W. Frank, *J. Chromatogr.* 473 (1989) 71

[3]   W.H. Konigsberg and L. Henderson, *Methods in Enzymol.* 91 (1983) 254

[4]   B. Kaplan and M. Pras, *Biomedical Chromatogr.* 4 (1990) 89

[5]   B. Kaplan and M. Pras, *J. Chromatogr.* 423 (1987) 376

[6]   R. Amons and P.I. Schrier, *Anal. Biochem.* 116 (1981) 439

[7]   M. Sandri, C. Rizzi, C. Catani and U. Carraro, *Anal. Biochem.* 213 (1993) 34

[8]   K. Takeda, A. Wada, Y. Sato and S. Hamada, *J. Colloid Interface Sci.* 147 (1991) 51

[9]   H. Suzuki and T. Terada, *Anal. Biochem.* 172 (1988) 259

[10]   J.P. Chervet, C.J. Meijvogel, M. Ursem and J.P. Salzmann, *LC•GC Int.* 10 (1992) 140

[11]   D.A. Lewis, A.W. Guzetta, W.S. Hancock and M. Costello, *Anal. Chem.* 66 (1994) 585

[12]   J.P. Chervet, R.E.J. van Soest and M. Ursem, *J. Chromatogr.* 543 (1991) 439

[13]   J.P. Chervet, M. Ursem, J.P. Salzmann and R.W. Vannoort, *J. High Resolut. Chromatogr.* 12 (1989) 278

[14]   W. Burkhart, in R.H. Angeletti (ed.), *Techniques in Protein Chemistry IV*, Academic Press, San Diego, 1993, pp. 399

CHAPTER 6.3

TWO-DIMENSIONAL CAPILLARY LIQUID CHROMA-TOGRAPHY BASED ON μ-FRACTIONATION

ABSTRACT

A two-dimensional capillary LC method is described – which is based on μ-fractionation, auto-mated reinjection and rechromatography using an automated microcolumn switching setup – to separate complex peptide mixtures of different origin. Different type of separations modes, i.e. hydrophobic and charge separation mechanisms, have been applied to increase the selec-tivity and peak capacity, and to approach orthogonal separation mechanisms. The first dimen-sion separations were carried out by either reversed phase chromatography or strong anion exchange chromatography. The second dimension separation was in all cases reversed phase capillary LC. In case of two-dimensional reversed/reversed phase separations, some degree of orthogonality was achieved by using either two different sets of mobile phase solvents and one reversed phase capillary LC column, or by using a single set of mobile phases and two capillary LC columns packed with different reversed phase materials. Electrospray ionization mass spectrometry was conducted to confirm the orthogonality of the developed two-dimen-sional capillary LC technique. The analysis of tryptic digests of cytochrome C and fetuin, and a synthetic peptide mixture are described.

157

INTRODUCTION

The peak capacity and sample dimensionality – i.e. ordered or disordered distribution of component peaks [1,2] – often limit the maximal information that can be obtained with a one-dimensional chromatographic system. It is estimated that merely a fifth of the total peak capacity of a one-dimensional separation method can be used to generate sufficient peak resolution. Because of these limitations, and the demand to separate and identify increasingly complex samples, two-dimensional chromatographic systems have been developed. The maximal theoretical peak capacity of a two-dimensional chromatographic system is the product of the peak capacities of the individual separation dimensions. In practice however this is seldom achievable.

Several papers have appeared in literature that describe different theoretical aspects of multidimensional separation techniques. Expressions for the peak capacity [3,4] and system orthogonality [3] have been discussed, as well as sample orthogonality [1]. More recently, a qualitative method has been described to predict the informational orthogonality, i.e. a maximal multidimensional information state – of a two dimensional separation from its underlying one-dimensional separations [5]. Furthermore, optimization methods have been proposed to optimize a two-dimensional separation using experimental design techniques [6].

Capillary sized liquid chromatography (LC) columns have been applied in different two-dimensional chromatographic modes. Pioneering work in the coupling of capillary LC and capillary size exclusion chromatography (SEC) to gas chromatography has been carried out by Cortes and coworkers [7,8]. This technique has been mainly applied for the analysis of polymers, polymer additives and oil samples [7-11]. Heart-cutting is commonly performed for the coupling of capillary LC columns with GC, resulting in peak capacities that are typical for a single dimension. Basically, the first dimension capillary LC separation can be regarded as a very selective clean-up step prior to the second dimension GC separation. The coupling of capillary LC to other capillary LC columns has attracted some fair attention recently, and has been typically applied for the separation of peptides and proteins. True comprehensive two-dimensional capillary LC separations have been presented by the group of Jorgenson, who coupled ion-exchange to reversed phase capillary LC [12,13]. Other papers focussed more on the heart-cutting of a first-dimension LC separation [14,15]. The latter method obviously allows a higher sample throughput since only the compounds of interest are transferred to the second dimension. In both cases loop-valve interfaces are typically applied. The hyphenation of capillary LC to capillary zone electrophoresis (CZE) has been applied for the separation of proteins and peptides too. For this technique either loop interfaces or a so-called flow gating interfaces – consisting of a PFTE gasket having a 1 mm channel sandwiched in between two stainless steel plates – can be used [16]. A more detailed description of the described two-dimensional techniques described above can be found elsewhere, as well as the coupling of capillary LC to more rarely applied separation techniques such as thin layer chromatography and supercritical chromatography [17].

Capillary LC is typically applied with low-concentration samples and in case of sample limited applications . This due to the reduced chromatographic dilution of small i.d. columns and hence lower achievable limits of detection. Especially for samples of biological and pharmaceutical origin, sensitive and selective techniques are required for the identification or discovery of unknown compounds. Furthermore, coupling to a mass spectrometer seems to be essential. The two latter requirements will be demonstrated by some typical (two-dimensional) capillary LC/electrospray ionization-mass spectrometry applications.

EXPERIMENTAL

Chemicals and reagents

Acetonitrile and water – both HPLC grade – were purchased from LabScan (Dublin, Ireland). Trifluoroacetic acid (TFA), cytochrome C (from bovine heart) and fetuin (from fetal calf serum) were obtained from Sigma (St. Louis, MO, USA). Trypsin was from Promega (Madison, WI, USA) and tris(hydroxymethyl)aminomethane (Tris), ammoniumacetate, hydrochloric acid and sodium chloride were from Fluka AG (Buchs, Switzerland). A synthetic peptide mixture – representing major histocompatibility complex (MHC) class I peptides – was donated by Dr. Peter van Veelen (Department of Immunohematology and Blood Bank, Leiden University Hospital).

Nucleosil 100-3-C_{18} was otained from Machery-Nagel GmbH &Co. (Büren, Germany), Hypersil BDS C_{18} 3 µm from Shandon-Hypersil (Cheshire, UK) and PL-SAX 1000 Å 8 µm from Polymer Laboratories (Shropshire, UK)

Digest preparation

Typical amounts of 1 mg/ml of protein were dissolved in digest buffer (50 mM Tris-HCl, pH 8.0). Protein samples were digested by the addition of trypsin dissolved in digest buffer (trypsin/protein, 1:50 w/w) and incubated at 37°C for 4 h – followed by a second enzyme addition to give a final trypsin/protein concentration ratio of 1:25 (w/w). After 16 h of incubation the samples were diluted five times in the mobile phase and stored at -20°C.

Capillary LC Instrumentation

A FAMOS microsampling workstation (LC Packings, Amsterdam, The Netherlands) with two additional built-in six-port valves was used for sample injection, µ-fractionation and reinjection. A schematic overview of the instrumental setup is given in Fig. 6.8. The system setup is based on three 6-port injection valves with 0.25 mm bores. The A valve is used for sample injection. The injection/fractionation needle is via a 75 µm i.d. fused silica transfer line coupled in between the A and the B 6-port valve. In the injection mode, the needle is placed in-line with the transfer line that connects the A and B valve. In this case, the column effluent is diverted to waste. To start fractionation, the B valve is switched and the column effluent is
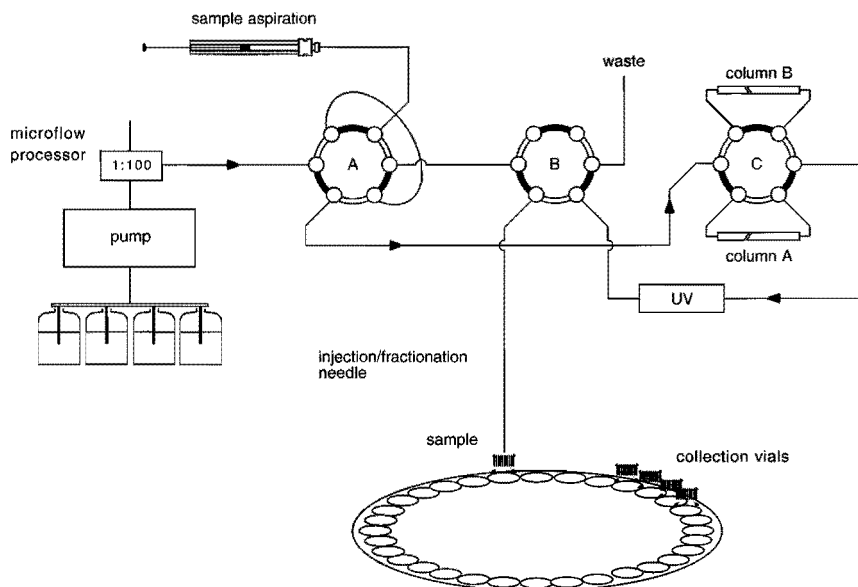
Fig. 6.8. Instrumental setup for automated two-dimensional capillary LC based on µ-fractionation, reinjection and rechromatography. Details are given in the section experimental of the text.

led back into a series of collection vials. The collection vials are prefilled with 5 to 10 µl 0.1% trifluoroacetic acid (TFA) in water. This is to ensure complete collection of the µl-sized fractions and to dilute the fractions into a weaker sample solvent. The latter assures optimal preconcentration and prevents sample breakthrough in case of reinjection on a second re-versed phase column. After time-based collection into a series of vials, the fractions are rein-jected on the second dimension column, which is selected by switching the C valve. All valves are mounted on the µ-sampling workstation and can be controlled from the keyboard of the instrument. Hence, fully automated two-dimensional separations can be performed unattended.

LC experiments were performed with an 1050 series quaternary low pressure gradient system (Hewlett-Packard, Palo Alto, USA). The A and B solvent were typically used for the first dimension separation and the C and D solvent for the second dimension separation. Micro flows were generated by an IC-400-VAR variable microflow processor (LC Packings) that was connected to the gradient system. The micro flow of 2–4 µl/min generated by the flow split of 1:100 was transferred directly to the injection valve of the workstation. Reversed phase sepa-ration were conducted on either a 15 cm x 300-µm i.d. capillary LC column packed with Hypersil BDS C18 3 µm or a 5 cm x 300-µm i.d. column packed with Nucleosil C18 3 µm. The flow rate was 4 µl min^{-1} for both columns. Reversed phase peptide separations were per-formed with either TFA or ammoniumacetate (NH$_4$AC) as the mobile phase additive. Mobile

phase A consisted of 0.1% TFA in acetonitrile/H_2O (5:95, v/v) and mobile phase B of 0.08% TFA in acetonitrile/H_2O (80:20, v/v) in case TFA was used as the mobile phase additive. For ammoniumacetate based separations mobile phase A and B consisted of acetonitrile/15 mM NH_4AC (5:95, v/v) and acetonitrile/15 mM NH_4AC (80:20, v/v) respectively. Detailed gradient conditions are given in the text. Strong anion exchange separations were performed on a 25 cm x 300-μm i.d. column packed with 8 μm, 1000 Å PL-SAX material. The flow rate was kept at 2 μl min^{-1} to keep the chromatographic dilution to a minimum. Mobile phase A consisted in this case of 50 mM Tris, pH 8.0 and mobile phase B of 50 mM Tris, pH 8.0/0.5 M NaCl. All columns were packed in-house.

Detection was performed at 214 nm using an SPD-10A UV-VIS detector (Shimadzu, Tokyo, Japan) equipped with a z-shaped capillary flow cell (LC Packings). Data acquisition was performed with MT-2 chromatography software (Kontron Instruments, Milan, Italy).

Mass spectrometry

Pneumatically assisted electrospray (ion spray) ionization mass spectrometry was conducted with an API 300 triple quadrupole mass spectrometer (Perkin-Elmer Sciex Instruments, Thornhill, ON, Canada) in the positive ion, single scan mode. Scans were taken from m/z 200 to 2000 with a scan duration of 4.5 s, using a step size of 0.2 amu and a 0.5 ms dwell time per step. The mass spectrometer was set to the following parameters: ion spray voltage 5.0 kV, orifice voltage 25 V. The nebulizer gas (air) and curtain gas (nitrogen) were adjusted to 1.5 l/min and 0.8 l/min respectively.

RESULTS AND DISCUSSION

To achieve the highest degree of orthogonality, both dimensions should preferably be based on different separation mechanisms. In the following sections it will be shown however that some degree of orthogonality can be achieved by performing reversed phase separations in both the first and second chromatographic dimension for the analysis of different complex peptide mixtures.

Reversed phase/reversed phase capillary LC (single mobile phase)

The first example involves a peptide separation of tryptic digested cytochrome C. In this particular case, two different C_{18} packed capillary LC columns were used and a single set of gradient solvents. The first dimension separation was carried out on a 15 cm x 300-μm i.d. column packed with Hypersil BDS C_{18} 3 μm. The injected amount of digested protein equalled 8 pmol. The resulting peptide map is given in the upper trace of Fig. 6.9. As can been seen, some coelution occurred in the last part of the chromatogram. 2 min sized fractions were collected and the fractions of interest reinjected on the second dimension column, which consisted of a 5 cm x 300-μm i.d. column packed with Nucleosil C_{18} 3 μm. The lower trace in
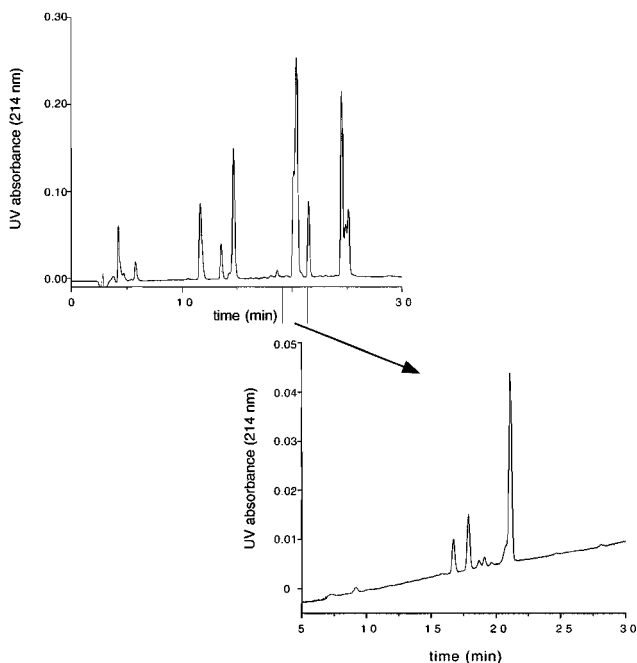
161

Fig. 6.9. Two-dimensional capillary LC reversed phase/reversed phase separation of a tryptic digest of cytochrome C. The first dimension column consisted of a 15 cm x 300-μm packed with Hypersil BDS C_{18} 3 μm. The gradient was run from 5 to 50% B in 30 min. The second dimension column consisted of a 5 cm x 300-μm i.d. column packed with Nucleosil C_{18} 3 μm and the gradient was run from 5 to 35% B in 30 min. The flow rate was 4 μl min^{-1} for both columns. The composition of the gradient solvents is given in the experimental section.

Fig 6.9. depicts the chromatogram of one of the collected fractions. The coeluting peaks from the first dimension are completely resolved in the second dimension.

The investigated tryptic digest is not too complicated in nature and could probably have been completely separated by using a more suitable stationary phase and solvent gradient. However, the results show that it is feasible to perform two-dimensional capillary LC separations with two different C18 columns and a single set of gradient solvents. This implies that "pseudo" two-dimensional capillary LC separations can be conducted with a simple binary LC system after appropriate flow reduction – i.e. flow splitting – and the selection of C_{18} stationary phases that are sufficiently different in selectivity.

Reversed phase/reversed phase capillary LC (single stationary phase)
    The second example involves the separation of a synthetic mixture of major histocompati-
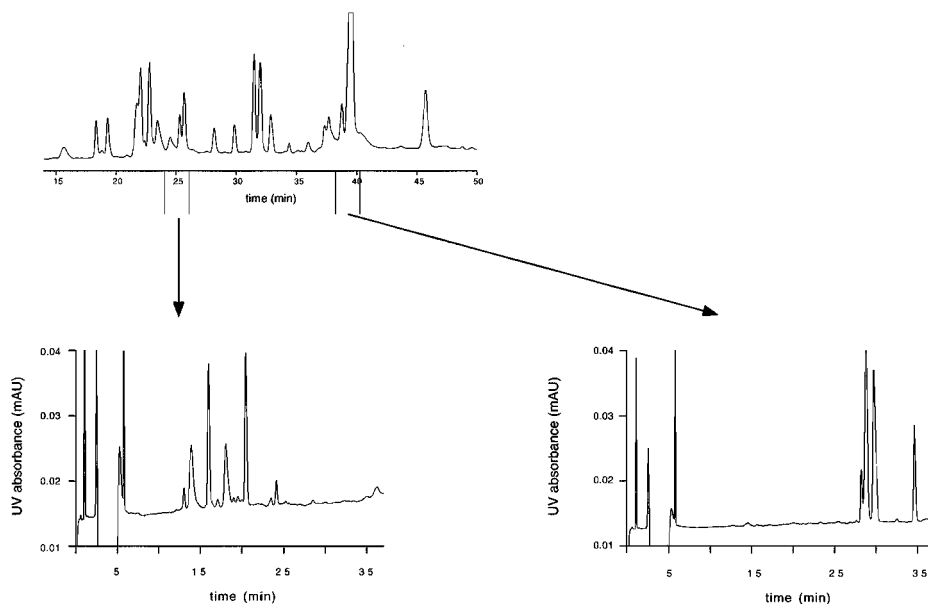
Fig. 6.10. Two-dimensional capillary LC reversed phase/reversed phase separation of MHC class I peptides. The column consisted of a 15 cm x 300-µm capillary LC column packed with Hypersil BDS C_{18} 3 µm. The first dimension gradient was run from 5 to 50% B in 30 min. Solvent A and B consisted of acetonitrile/15 mM NH_4Ac (5:95, v/v) and acetonitrile/15 mM NH_4Ac (5:95, v/v) respectively. The second dimension gradient was run from 10 to 35% B in 30 min. Mobile phase A consisted of 0.1% TFA in acetonitrile/H_2O (5:95, v/v) and mobile phase B of 0.08% TFA in acetonitrile/H_2O (80:20, v/v). The flow rate was 4 µl min^{-1} for both gradients.

bility complex (MHC) class I peptides. MHC peptides are recognized by T-cells, which play a key role in the human immune system. The peptides are presented to the T-cells by MHC molecules and are pathogen, tumor, autoantigen or transplant-specific. Thus, identification of these kind of peptides may lead to the development of immunotherapetic protocols for the treatment and/or prevention of virus infections, tumors, autoimmune diseases and transplant rejection.

The synthetic peptide mixture consists of 30 peptides of which a number are very similar in hydrophobicity and molecular mass. Applying a classical TFA reversed phase gradient to resolve this sample often leads to multiple coelution of a number of the peptides present in the sample. Also in this experiment a reversed phase/reversed phase separation was applied to completely resolve the peptide mixture. However, in this case the same C_{18} column was used for the first dimension separation, as well as the second dimension separation. The column consisted of a 15 cm x 300-µm i.d. capillary LC column packed with Hypersil BDS C_{18} 3 µm.

The mobile phase additive in the first dimension was 15 mM ammonium acetate and in the second dimension it was 0.1% TFA. The difference in selectivity achieved by this type of modifiers is most probably due to the pH difference of the mobile phases. A 15 mM ammonium acetate solution has a pH of 6.8, whereas a 0.1% TFA solution has a pH of 1.9.

The results of this two-dimensional experiment is shown in Fig. 6.10. The upper trace of Fig. 6.10 shows the first dimension separation of the MHC class I peptides applying the ammoniumacetate gradient. The amount of injected peptides was 17 pmol each. Coelution of the peptides occurred at several places in the chromatogram. A total number of 15 fractions was collected. The fraction length was 5 min and fractionation was started 5 min after injection. For clarity only two of the reinjected fractions are shown. The lower traces of Fig. 6.10 represent the chromatograms of the seventh and the twelfth fraction. The second dimension chromatograms reveal 6 and 4 major peaks for the seventh and twelfth fraction respectively. This example demonstrates that it is possible to obtain "pseudo" two-dimensional chromatographic data using a single C_{18} capillary LC column. The difference in mobile phase selectivity was found to be adequate enough to separate most MHC peptides using this single column two-dimensional capillary LC approach.

Strong anion exchange/reversed phase capillary LC

To obtain the highest possible resolution – i.e. highest peak capacity – both dimensions should be based on different separation mechanisms. For this, a complex digested glycoprotein was subjected to a two-dimensional separation, where the first dimension separation was conducted on a strong anion exchange stationary phase, and the second dimension separation on a C_{18} reversed phase stationary phase. Glycoproteins have been investigated very intensively since the introduction of electrospray ionization and matrix assisted laser desorption mass spectrometry. Till then only a few rather time consuming methods were available for structure elucidation of complex glycoproteins, hampering the ability to obtain a better understanding of the biological function of glycoproteins. These type of molecules are know to have a profound effect on the shape, growth and differentiation of adherent cells. Furthermore, they are known to play a key role in cell adhesion. Fetuin was used as a model compound in this study. No reduction or alkylation was carried out prior to the digestion of the protein. The number of peptides will therefore be somewhat smaller than theoretically was to be expected.

A first dimension separation was performed on an strong anion exchange capillary LC column. A salt gradient was applied to obtain a charge based separation of the peptides. The chromatographic conditions are given in the experimental section. The chromatogram that was obtained for a 2 pmol sample is given in Fig. 6.11. The fractions were collected in 5 µl of 0.1% TFA in water and the flow rate through the column was maintained at 2 µl min⁻¹ to keep dilution of the fractions to a minimum. The advantage of applying a salt gradient in the first dimension is that the fractions do not have to be diluted in relatively large quantities of water to prevent sample breakthrough when the collected fractions are reinjected on the second
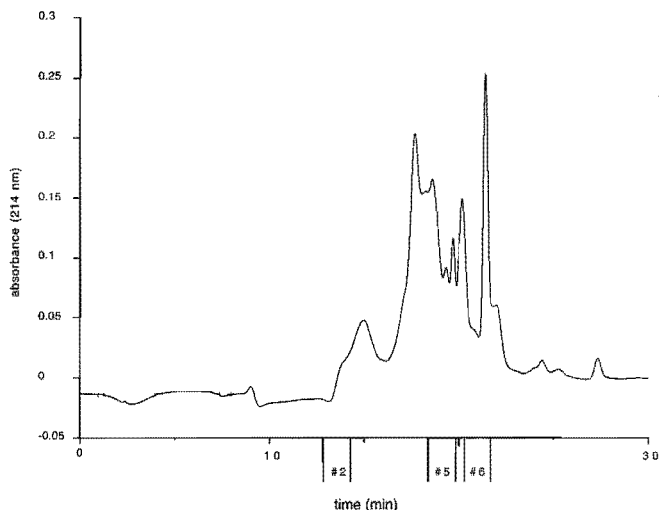
Fig. 6.11. Strong ion exchange first-dimension capillary LC separation of tryptic digested fetuin. The column consisted of a 25 cm x 300-μm capillary LC column packed with PL-SAX 1000 Å 8 μm. The gradient was run from 0 to 100% B in 30 min. Solvent A consisted of 50 mM Tris, pH 8.0 and solvent B of 50 mM Tris, pH 8.0/0.5 M NaCl respectively. The flow rate was 2 μl min^{-1}.

dimension column. A total of 10 fractions was collected with a fraction length of 2 min each. Fractionation was not started until ten minutes of the first dimension separation were elapsed. The SAX separation of the fetuin digest is not that efficient. However, the analysis time of the first dimension was deliberately kept as short as possible to achieve the highest possible sample throughput. The peak capacity of the second dimension was sufficient to separate the complete sample. The fractions that were subjected to the second dimension are identified on the times axis in Fig. 6.11. The corresponding chromatograms are given in Fig. 6.12. The peptide maps shown in Fig. 6.12 are clearly different indicating that the peptides in the first dimension are separated with a different mechanism. The chromatograms show however also some overlap, which indicates that there would have been multiple coelution of the peptides if only a single reversed phase separation would have been conducted.

The two-dimensional capillary LC setup was connected to a mass spectrometer to identify the peptides in the collected fractions. The fractions were analyzed on-line by electrospray ionization mass spectrometry (ESI-MS). The usefulness of 2-dimensional capillary LC is demonstrated in Fig. 6.13 and 6.14. The mass spectra show in Fig. 6.13 were taken from two peaks that were eluting at 15.7 and 16.6 min respectively when the tryptic digested fetuin sample was subjected to a one-dimensional reversed phase capillary LC separation. Coelution was observed of the T19 and T16 coded peptides at 15.7 min and of the T4 and T16 coded peptides at 16.6 min. In case of "de novo sequencing", coelution of peptides would have
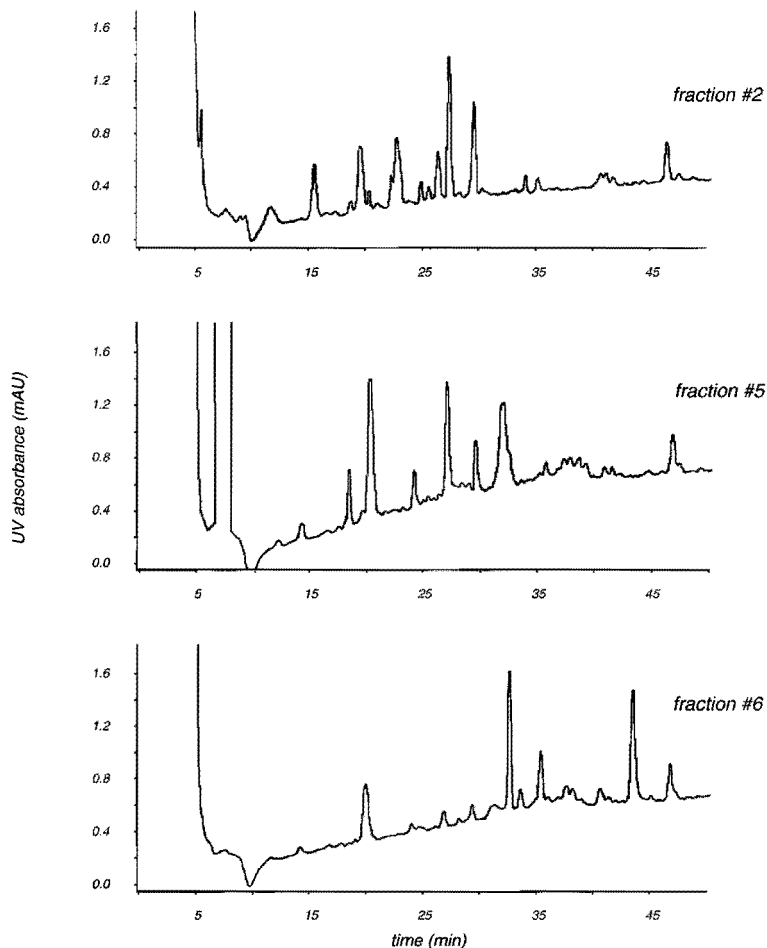
165

Fig. 6.12. Second dimension reversed phase chromatograms of the collected fractions from the SAX capillary LC first dimension separation of tryptic digested fetuin. The column consisted of a 15 cm x 300-μm capillary LC column packed with Hypersil BDS C_{18} 3 μm. Mobile phase A consisted of 0.1% TFA in acetonitrile/H_2O (5:95, v/v) and mobile phase B of 0.08% TFA in acetonitrile/H_2O (80:20, v/v). The gradient was run 5–50% B in 30 min. The flow rate was 4 μl min^{-1}.

hampered the conformation of the molecular mass of the protein. However, in case of fetuin, the peptides could easily be identified since its sequence is well known. The same peptides were traced in the collected fractions after the two-dimensional separation by SAX/reversed phase capillary LC. The mass spectra of the peptides are shown in Fig. 6.14. The T19 coded peptide was found to be only present in the first collected fraction, the T4 coded peptide in
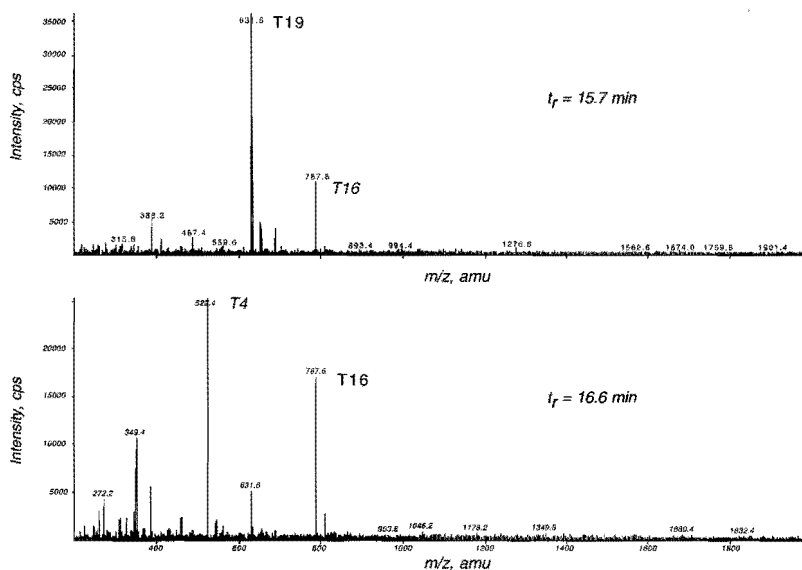
Fig. 6.13. Capillary LC/ESI-mass spectra taken from a one-dimensional reversed phase separation of digest fragments of fetuin eluting at 15.7 min (upper trace) and 16.6 min respectively (bottom trace). The chromatographic conditions are as in Fig. 6.12.

the second fraction and the T16 coded peptide in the fourth fraction. Compared to the mass spectra given in Fig. 6.13, the peptides can be identified unambiguously since coelution was strongly reduced in the chromatograms taken from the collected fractions.

CONCLUSIONS

Different two-dimensional modes have been presented, including reversed phase/reversed phase separations. Two-dimensional reversed phase/reversed phase separation were carried out with either (i) a two C_{18} columns and one set of gradient solvents gradients or (ii) a single C_{18} column and two different sets of gradient solvents. The main advantage of the former method is the need for merely one binary gradient system, which reduces the complexity of the system. The difference in selectivity of the applied C18 phases was found to be sufficient to perform "pseudo" two-dimensional capillary LC separations. Preferably C_4 or C_8 phases should be applied in one of the dimensions to achieve a more selective two-dimensional separation mechanism. C_4 and C_8 phase have generally a lower carbon contact making them less hydrophobic, hence different in selectivity. Alternatively, aqueous capillary size exclusion chromatography can be applied for the first dimension [18]. The latter method allows a higher

167
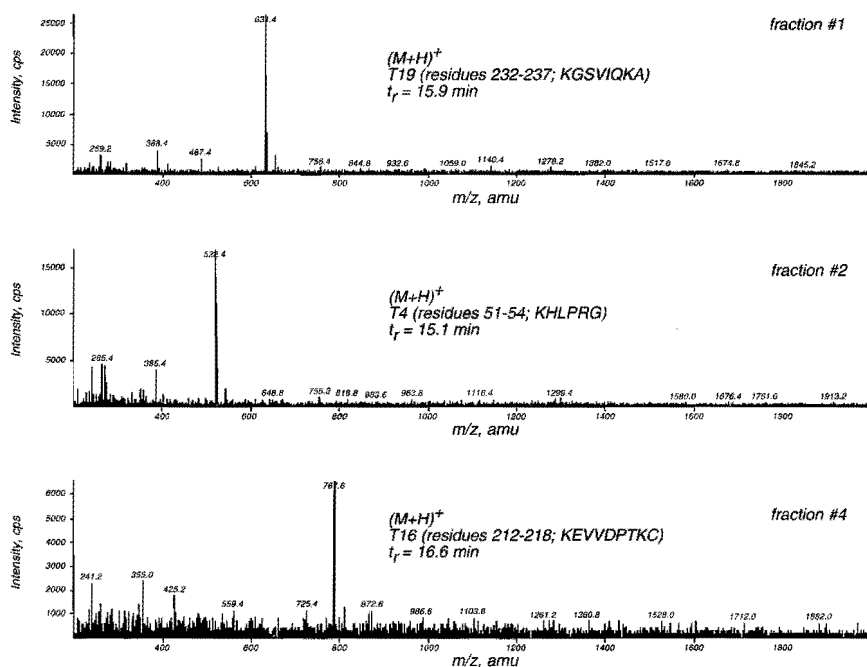
Fig. 6.14. Capillary LC/ESI-mass spectra taken from a two-dimensional capillary LC separation of a digest fragments of tryptic digested fetuin. The mass spectra of the digest fragments shown in the upper, middle and lower trace correspond with the mass spectra of the coeluting peptides shown in Fig. 6.13. The middle, upper and lower mass spectrum were taken from the second dimension reversed phase separation of the first, second and fourth collected fraction respectively. The chromatographic conditions are as in Fig. 6.12.

degree of selectivity compared to the former one due to the flexibility in composing gradient solvents. In this study, the pH-value of the mobile phase was used as the selectivity variable. This type of two-dimensional separation requires a more sophisticated pumping system that allows programming of two independent solvent gradients or two binary gradient systems. Relatively selective two-dimensional separations can be achieved with this approach using a single C_{18} column. More orthogonal multidimensional separations were achieved by combining strong anion exchange chromatography and reversed phase chromatography, which was confirmed by electrospray mass spectrometry analysis to identify the peptides in one-dimensional and two-dimensional separations. Compared to the other two-dimensional modes, this one is by far the most complex. However, the full potential of two-dimensional separations can only be accomplished with a setup of this type. The selectivity and resolution increase that was achieved with this two-dimensional mode was much greater compared to two-dimensional reversed phase/reversed phases capillary LC separations.

Furthermore it was demonstrated that two-dimensional capillary LC can be conducted using an automated column switching setup that allows for injection, μ-fractionation and reinjection of the collected fractions. The system can be run both in the heart-cut and continuous fractionation mode. The only limitation of the system in its current setup is the delay time between the fractions. Depending on the physical distance that has to be covered by the fractionation needle to move from vial to vial – this delay time can be up to 20 s – which can lead to sample loss. This drawback can be overcome by controlling the system from its service mode by a remote computer, thereby reducing the maximum delay time to 5–6 s. This is certainly acceptable in strong anion exchange first dimension separation, where peak widths of 30–40 s are not uncommon.

The fact that the column effluent of the first dimension separation is collected in prefilled vials does not reduce the sensitivity of the system. The complete collection vial content can be transferred to the sample loop without loss of sample due to a special injection routine of the μ-sampling workstation. Next, oncolumn focussing is applied to concentrate the sample on the top of the second dimension column, after which the gradient is started to separate the components. The main advantage of μ-fraction collection over automated loop based two-dimensional systems is the fact that the first dimension can be stored. Hence, the mobile phases do not have to be miscible, the second dimension separation does not have to be performed within a time period that is determined by the first dimension, injection volume overload in the second dimension is not an issue and two-dimensional reversed phase/reversed phase separations can be conducted.

REFERENCES

[1]   J.C. Giddings, *J. Chromatogr. A* 703 (1995) 3

[2]   J.M. Davis and J.C. Giddings, *Anal. Chem.* 55 (1983) 418

[3]   Z. Liu, D. G. Patterson and M.L. Lee, *Anal. Chem.* 67 (1995) 3840

[4]   P.J. Slonecker, X. Li, T.H. Ridgway and J. G. Dorsey, *Anal. Chem.* 67 (1996) 682

[5]   J.C. Giddings, in H.J. Cortes (ed.), *Multidimensional Chromatography*, Marcel Dekker Inc., New York, 1990, pp. 1

[6]   N. Lundell and K. Markides, *Chromatographia* 34 (1992) 369

[7]   H.J. Cortes, L. Green. C. Shayne and M. Robert, *Anal. Chem.* 62 (1991) 2719

[8]   H.J. Cortes, B.E. Richter, C.D. Pfeiffer and D.E. Jenssen, *J. Chromatogr.* 349 (1985) 55

[9]   K. Grob and J.-M. Stoll, *J. High Resolut. Chromatogr. Chromatogr. Commun.* 9 (1986) 518

[10]   I.L. Davis, K.D. Bartle, G.E. Andrews and P.T. Williams, *J. Chromatogr. Sci.* 26 (1988) 125

[11]   K. Welch and N.E. Hoffman, *J. High Resolut. Chromatogr.* 15 (1992) 171

[12]   LA. Holland and J.W. Jorgenson, *Anal. Chem.* 67 (1995) 3275

[13]   G.J. Opiteck, K.C. Lewis, J.W. Jorgenson and R.J. Anderegg, *Anal. Chem.* 69 (1997) 1518

[14]   D.B. Kassel, T.G. Cousler, M. Shalaby, P. Selchri, N. Gorden and T. Nadler, in R.J.W. Crabb (ed.), *Tech. Protein. Chem. VI*, Academic Press, San Diego, 1995, pp. 39

[15]   T.E. Mulligan, R.W. Blain, N.F. Oldfied, B.A. Mico, *J. Liq. Chromatogr.* 17 (1994) 133

[16]   A.V. Lemmo and J.W. Jorgenson, *Anal. Chem.* 65 (1993) 1576

[17]   J.P.C. Vissers, H.A. Claessens and C.A. Cramers, *J. Chromatogr. A* 779 (1997) 1

[18]   G.J. Opiteck, J.W. Jorgenson and R.J. Anderegg, *Anal. Chem.* 69 (1997) 2283

APPENDIX A

VAN DER WAALS INTERACTION OF COMPOSITE PARTICLES

ABSTRACT

On the basis of the superpositional principle of the classical Hamaker-De Boer approach to the Van der Waals interaction, an equation for the interaction energy between two identical composite particles in a medium has been developed. The particles are supposed to be composed of an arbitrary number of components that are intimately mixed so as to avoid appreciable scattering of interacting electromagnetic waves. As an example the result is applied to porous polystyrene particles in water while the pores are not filled with water ("non-wetting surface"). Numerical results are evaluated, using interaction parameters as obtained by various methods that are based either on the Hamaker-de Boer or the Lifshitz approach.

INTRODUCTION

In a number of cases colloidal particles are built of composite materials. Examples are particles with small-sized porous structures like the stationary phases in High Performance Liquid Chromatography columns and catalyst carriers. With such composite materials the Van der Waals attraction between macro bodies (colloidal particles) cannot been derived straightforwardly on the basis of either the Hamaker [1] or the Lifshitz [2] approach, as is the case with single component particles (see e.g. the useful recent study of Bowen and Jenner [3]). This is due to the fact that generally neither Hamaker constants nor spectral data of composite materials are available. If such data would be available the Lifshitz approach is favorable because (i) it automatically takes care of the retardation, an important effect on micrometer scale; (ii) with simple materials the calculations are not too complicated as these can usually be carried out on the basis of only one or a few absorption values from the ultraviolet spectrum; (iii) it in principle also admits taking into account the screening of permanent dipoles due to electrical double layers [4].

With composite materials the situation is more complicated. In view of lack of suitable data, the Van der Waals approach seems to be more suitable for such materials as it allows to describe multi-body interactions on the basis of binary interactions, i.e. on the basis of pair interactions between the different components of composite bodies. However, especially with interactions in a medium the linear superposition method may lead to inaccuracies due to the fact that the net interaction may be a small value as a result of the subtraction of almost equal, large numbers. Another drawback is the retardation, which will have to be included in an approximated way. In this paper we will derive the formalism for the evaluation of the Hamaker constant of a composite material which is internally dispersed to a degree such as to prevent the influence of granularity in the material on the interaction between macro-bodies. This result resembles a result for molecular mixtures as given by Hamaker [1] without a clear derivation. Our approach will be applied to the interaction of porous colloidal particles of micrometer size that contain gas as well as organic coating and liquid in their pores. Using an example we will indicate where in the binary interaction methodology the major inaccuracies are introduced.

THEORY

The Hamaker approach for the assessment of Van der Waals interaction forces is based on the assumption that the force between two macro bodies P and Q (with molecules p_i and q_j) is the sum of the interactions between all pairs of molecules $\{p_i, q_j\}$. In order to apply this approach to composite particles in a dispersion medium, these particles are supposed to contain a number of different materials mixed uniformly and finely enough to eliminate the effects of granularity in the interactions of the particles. The nature of the interactions, i.e. by electromagnetic waves, also implies that scattering may occur which might invalidate existing theoretical re-

sults as these are usually developed under the assumption of negligible scattering. On the other hand, in order to be able to numerically evaluate composite particle properties from single component properties, the components should be admixed on a scale coarse enough to allow use of 'Hamaker' or spectral data of pure components. Examples of particles that may obey this supposition are porous particles that have uniformly distributed pores (homogeneous porosity).

We focus on two composite particles in a medium and study the change in the free energy F of the system when one particle is transported from a large ("infinite") distance with respect to the other particle to a centre-to-centre distance r. A basic supposition is that a composite particle (with n components i = 1...n) in a medium (indicated by index 0) can be considered as a superposition of a number of particles all of the same size and shape as the composite particle itself. In other words, it consists of one hole and n different particles i. It is evident that the porous particles i have lower densities than nonporous particles of material i would have, differing by a factor ϕ, where ϕ is the volume fraction of component i in the composite particle. In case composite particles contain some liquid medium, i.e. we are dealing with porous particles, for convenience that component is considered as being a porous particle of material k with k $\in$ {1,2,3 ... n}. Note that in practice we will have in mind spherical particles, although in principle non-spherical particles can be treated along a similar reasoning.

First the changes of free energy of three basic transport processes that are useful are defined:

(i) The quantity U_i denotes the change in free energy of transporting a (porous) particle i from vacuum and at infinite distance to any other particle, to a cavity in the medium while the cavity is at infinite distance to any other particle. The cavity is supposed to have the same size as the outside of the particle.

(ii) $U_{ij} = U_{ij}(r)$ is the change of free energy in bringing two particles i and j from infinite distance to a distance r between their centres, while being in vacuum.

(iii) $S_{ij} = U_{ij}(0)$ is the change of free energy when the particles i and j (which are in fact components of the composite particle and exactly fit into each other) are transported from infinite distance to a zero centre-to-centre distance, while being in vacuum.

The different steps involved in bringing two particles in a medium from infinite to finite distance are depicted as 8 steps in Fig. A.1. Three distinct locations A, B and C (from left to right) exist in the medium. A is at a large distance from both B and C (that are at a centre-to-centre distance r). All the positions in vacuum are supposed to be at large distances to each other and to the medium.

The first step is to transport an amount of the medium (with size and shape identical to a composite particle) from B to vacuum, while leaving a cavity at B. In order to derive the correct expression we start with considering the transport of that amount of medium (a "nonporous particle of material o") from vacuum to a cavity at B, while C contains material o. The free energy involved is U_o. In case of a cavity at C the free energy involved would be $U_o - U_{oo}$. As position C actually contains a composite particle the free energy also contains a summation
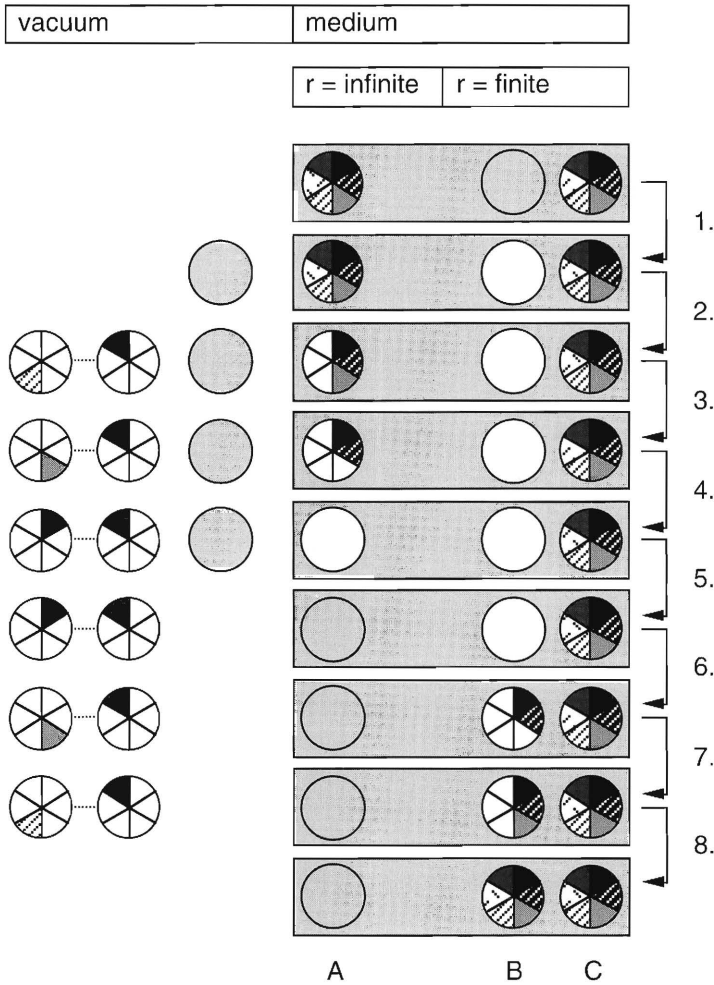
Fig. A.1. Consecutive basic steps in transporting a composite particle of arbitrary shape in a medium from an infinite to a finite distance to nother indentical particle. The different parts within a particle indicate the different components, not there spatial location. A white area represents the absence of any material.

174

over interactions U_{oi}, and finally we arrive at:

$$\Delta F_1 = -U_o + U_{oo} - \sum_{i=1}^{n} U_{oi} \tag{A.1}$$

The second process (steps 2, 3 and 4) involves the transport of a composite particle from position A to vacuum while the composite particle is at the same time being split into separate particles. The different components will be removed sequentially ($i = 1...n$). The removal of a particle of material i, while leaving its part of the volume in A empty, is discussed now. It involves the elimination of the interaction of particle i both with its surroundings ($= -U_i$) and with the particles $j = i + 1 .... n$ with which it exactly fitted in position A ($= \Sigma_j S_{ij}$). Thus the change in free energy of step 3 amounts to:

$$\Delta F_3 = -U_i - \sum_{j=i+1}^{n} S_{ij}$$

(A.2)

leading to a change of the free energy involved in steps 2–4 amounting to:

$$\Delta F_{2-4} = -\sum_{i=1}^{n} U_i - \sum_{i=1}^{n}\sum_{j=i+1}^{n} S_{ij}$$

(A.3)

Step 5 involves the transport of a nonporous particle of material o from vacuum to A. This simply is given by:

$$\Delta F_5 = U_o$$

(A.4)

Steps 6–8 complete the whole process by sequentially putting the parts of the composite particle back into the medium, at position B. In step 7 a particle i is placed at position B. If position C contained medium and position B was empty, this would have led to $\Delta F_7 = U_i$. If position C was empty, this would have led to $\Delta F = U_i - U_{oi}$. Actually position C is filled with a composite particle; this contributes extra terms U_{ij}. Because of the fact that in reality particle i is being superimposed on particles 1 .... i - 1, ΔF_7 has to be corrected with terms S_{ij}. This leads to:

$$\Delta F_7 = U_i - U_{oi} + \sum_{j=1}^{n} U_{ij} - \sum_{j=1}^{i-1} S_{ij}$$

(A.5)

This results for the free energy change of the steps 6–8 in:

175

$$\Delta F_{6-8} = \sum_{i=1}^{n} U_i - \sum_{i=1}^{n} U_{oi} - \sum_{i=1}^{n}\sum_{j=1}^{n} U_{ij} + \sum_{i=1}^{n}\sum_{j=1}^{i-1} S_{ij}$$

(A.6)

The free energy ΔF_t of the whole process of approaching of two composite particles in a medium is the summation of $\Delta F_1 \ldots \Delta F_8$, leading to:

$$\Delta F_t = U_\infty - 2\sum_{i=1}^{n} U_{oi} - \sum_{i=1}^{n}\sum_{j=1}^{n} U_{ij} \qquad (A.7)$$

The interactions indicated by the terms U_{oi} and U_{ij} involve particles that are not necessarily solid – i.e. with porosity $[1 - \phi_i]$ 0. Because Van der Waals attractions are additive the terms U_{ij} can be rewritten as $\phi_i\phi_j V_{ij}$ where V_{ij} is the interaction between solid particles of the materials i and j, and where $\phi_o = 1$. Substituting this into the last equation leads to:

$$\Delta F_t = V_{oo} - 2\sum_{i=1}^{n} \phi_i V_{oi} - \sum_{i=1}^{n}\sum_{j=1}^{n} \phi_i\phi_j V_{ij} \qquad (A.8)$$

In the case of non-retarded interaction the Van der Waals energies of interaction can be written as: $\Delta F(r) = -A\, f(r)$, where A is called the Hamaker constant, being positive in the case of attraction. Thus the Hamaker constant for the interaction between two identical composite particles in a medium is:

$$A_{coc} = A_{ovo} - 2\sum_{i=1}^{n} \phi_i A_{ovi} - \sum_{i=1}^{n}\sum_{j=1}^{n} \phi_i\phi_j A_{ivj} \qquad (A.9)$$

where A_{ijk} is the Hamaker constant for the interaction between materials i and k across a medium j. The indices c and v denote a composite particle and vacuum respectively. Equation 9 indicates that on the basis of the Hamaker approach the interaction between composite particles across a medium can be interpreted as a summation of interactions across vacuum between all materials involved.

DISCUSSION

General

The main purpose of this discussion is to analyze the inaccuracies involved in using the formula derived, and is focussed on two aspects. First, we will discuss how the equations derived can actually be applied and see what problems arise for a specific example. In doing so effects from retardation and electrostatic double layer screening will be neglected [5]. The example is a system consisting of porous polystyrene particles in water; the porosity of the polystyrene particles can be varied; part of the pores may be filled with air. The second aspect

is whether scattering of radiation by the granules may affect the level of the Van der Waals interaction. For that purpose a dispersion of air bubbles in water ('foam') is considered.

The evaluation of Hamaker constants of composite materials

In this section the final result of our theory, Eqn. (A.9), will be evaluated numerically, and "Hamaker" results of A_{coc} will be compared with results as obtained from the Lifshitz theory. The indices w, v, c and p will be used to indicate water, vacuum, composite and polystyrene. The pores in the particles are supposed to be very small and not filled with water ("non-wetting"). This means that the composite particle defined here is rather special: it contains polystyrene and/or vacuum. We think this system is illustrative for several reasons.

(i) The components used are well studied; reliable spectroscopic data, both an extensive set (Parsegian; ref. [5]) and a single line (Israelachvili; ref. [6]) are available.

(ii) Specific theories neglect any difference in absorption frequencies of the components. As the components in our system have considerably different absorption frequencies the effect of such approximations can be assessed well.

(iii) Dispersion media often screen the Van der Waals interaction between particles to a large extent. Numerically this is the result of taking the difference between two almost equal, large numbers. This screening especially occurs when the particles and the medium have matching refractive indices. By variation of the porosity of the particles this phenomenon can be investigated; any non-negligible approximations will easily manifest as significant deviations.

In order to evaluate A_{cwc} as predicted by Eqn. (A.9) we need values of A_{ivj}. They can be obtained by using the Hamaker methodology (deriving A_{ivj} from A_{ivi}) or just by using the most accurate data available, as derived within the Lifshitz approach. We will follow both lines. Within the Hamaker approach the classical method is to employ what is called the Berthelot' approximation $A_{ivj}^2 = A_{ivi}A_{jvj}$ [7]; an alternative method is by using the more accurate relationship [8]:

$$A_{ivj}^2 = A_{ivi}A_{jvj}\frac{4v_1v_2}{\left(v_1+v_2\right)^2} \tag{A.10}$$

where v_i is the frequency of an individual molecular oscillator. Note that $A_{ivi} = v_i\alpha_{oi}^2\rho^2M^{-2}$ and $v_i^2 \propto \alpha_{oi}$ in which ρ is the density, α_{oi} is the reference polarizability of component i – (i.e. the part of α_i that is independent of the presence of any permanent dipole – and M is the molar mass [8]. Thus the value of n_i depends only weakly on A_{ivi}, according to $v_i^2 \propto A_{ivj}^{-1/3}\rho^{2/3}M^{-2/3}$. Even with $A_{ivi}/A_{jvj} = 10$ the last factor on the right hand sight of Eqn. (A.10) differs from unity only by 13% provided ρ and M are constant. However, differences in ρ are more serious sources of deviations. As an example, the molar masses of a system of polystyrene spheres in water differ by a factor 6. This has the same effect as an A_{ivi}/A_{jvj} ratio of 36 has. Although the error introduced in evaluating A_{ivj} generally speaking is not large, the
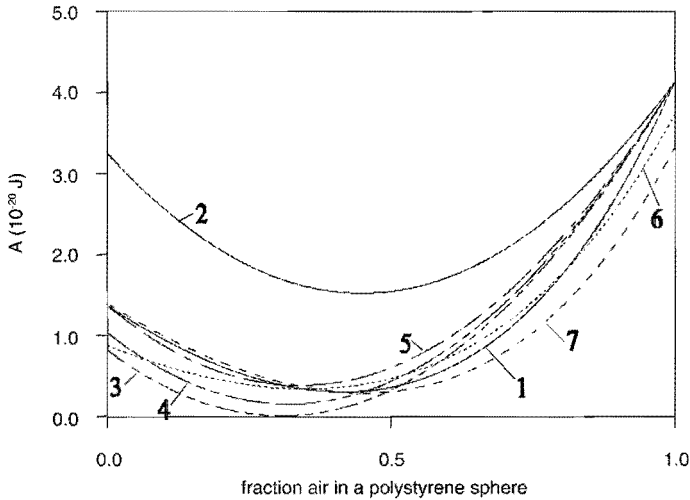
Fig. A.2. The Hamakar constant for the interaction of two porous polystyrene particles in water. The pores are void; their volume fraction in the spheres is the independent variable Data from Parsegian (P) or from Israelachvili (I). 1. Lifshitz theory, data from (P); 2. Hamakar theory, A_{ivi} from (P); 3. as 2, but with Berthelot' approximation; 4. as but with A_{ivi} from (P); 5. as 2 but with A_{iji} from (P); 6. Lifshitz, data from (I); 7. as 6, but with averaging of the absorption frequencies.

relative error may become very significant when evaluating the Hamaker constant A_{ijk} between particles of type i and k in a medium j. This is because relatively large numbers are subtracted from each others, leaving a small net number.

In order to avoid effects from using different data sources, in all cases the values of A_{ivi} are obtained by using the data set of Parsegian [5,9] within the Lifshitz theory, using the formula for non-retarded interaction between particles 1 and 2 across a medium 3 [6]:

$$A_{132} = \frac{3kT}{2} \sum_{n=0}^{\infty} \cdot \frac{\varepsilon_1(iv_n) - \varepsilon_3(iv_n)}{\varepsilon_1(iv_n) + \varepsilon_3(iv_n)} \cdot \frac{\varepsilon_2(iv_n) - \varepsilon_3(iv_n)}{\varepsilon_2(iv_n) + \varepsilon_3(iv_n)}$$

(A.11)

where $v_n = 2\pi kTn/h$ with n = 0,1 ..., k and h are Boltzmann's and Planck's constants, T is the absolute temperature. $\varepsilon_i(iv)$ is the dielectric response function for imaginary arguments. The results found are: $A_{pvp} = 8.60 \cdot 10^{-20}$ J and $A_{www} = 4.11 \cdot 10^{-20}$ J. On the basis of the Lifshitz theory, using Parsegians' data, we also evaluated A_{cwc} and used this as a reference (curve 1 in Fig. A.2). For that purpose, values of ε_c had to be evaluated. In accordance with Beer's law it

178

was assumed that the absorption spectra of the components may be summed when calculating that of the composite, in other words, additivity of the $\phi_i[\varepsilon_i - 1]$ of the components was assumed. This is justified if scattering due to granularity in the composite is negligible.

The non-retarded Hamaker constants are evaluated in Fig. A.2 using Eqn. (A.9), without (curve 2) and with the Berthelot' approximation (curve 3). Without the Berthelot approximation this calculation along the classical approach leads to a large overestimation (factor ~ 2–3) of A_{cwc}. On the other hand, the Berthelot approximation leads to an underestimation, smaller in absolute sense but relatively of the same order. Additionally the latter predicts a condition at which the Van der Waals interaction completely vanishes. In reality this phenomenon will only occur when the absorption spectra of the materials involved have exactly the same characteristics, which is not the case here. Note that although the Van der Waals force will almost never vanish, dispersions may well be transparent optically. Thus the practical rule that Van der Waals forces vanish in transparent dispersions is based on the Berthelot' approximation. Without such approximation one can only state that in an optically matching medium the Van der Waals forces between particles are at a low value.

In order to avoid possible inaccuracy in the data on A_{ivj} as evaluated on the basis of the classical Hamaker theory, curve 4 was constructed using again Eqn. (A.9) but with values of A_{ivj} as derived with Parsegian's data and Lifshitz formula ($A_{pvw} = 5.8 \cdot 10^{-20}$ J). It is clear that this significantly improves the agreement with the reference curve 1.

Here the question arises whether the remaining disagreement, i.e. between curves 1 and 4, is due either to (i) any inaccuracy of the Hamaker theory in assessing the effect of screening of the attraction forces by the medium, or to (ii) the inadequacy of Eqn. (A.9) in describing a composite particle as a volume-fraction-weighed superposition of its components. The effect of (i) can be eliminated to a large extent by retaining the A_{ivi} values mentioned but by adjusting the A_{ivj} values in such a way that perfect agreement exists for the conditions with ϕ_p is 0 and 1 respectively. The result for A_{cwc} calculated in this way are shown in curve 5. This curve shows only minor deviations from the reference curve. Thus the conclusion is that the finally derived equation (Eqn. (A.9) fairly well describes the Van der Waals interaction of composed spheres, provided the calculation is not hampered by inadequate values of A_{ivj} and A_{iji}).

For comparison, also the often employed data of Israelachvili (Table 11.2 from ref. [6]) have been used in combination of Eqn. (A.11) to produce curve 6. This curve indicates a fairly good agreement with curve 1 although A_{pwp} is underestimated by ~ 40%. Usually the data of Israelachvili are applied in such a way that differences in the single absorption line frequencies are ignored. Only if each individual frequency is substituted by the geometrical average of all of them, fairly good agreement is found (curve 7). This result is very sensitive to small variations in the value used for the averaged frequency.

The use of the Berthelot' approximation also leads to another interesting result. On that basis, equation (A.9) can be rewritten as:

$$\sqrt{A_{ioi}} = \left| \sum_i^n \phi_i \sqrt{A_{ivi}} - \sqrt{A_{ovo}} \right|$$ (A.12)

which shows that Hamaker constants of components in a mixture would be additive on the basis of their volume fractions provided the square roots of the Hamaker constants are used. This was also noted by Vincent [10] for a two-component molecular mixture; however for such a case it is questionable if pure component data can be employed, as spectral properties of a molecule are influenced by neighboring molecules. Eqn. (A.12) clearly demonstrates how the medium weakens the inter particle interaction. According to the Berthelot approximation the Van der Waals interaction would vanish if the volume average value of $A^{1/2}$ of the particles equals that of the medium. Note that in case of a one-component particle we retain an expression previously derived (see e.g. ref. [7]):

$$\sqrt{A_{iji}} = \left| \sqrt{A_{ivi}} - \sqrt{A_{jvj}} \right|$$ (A.13)

For one-component particles in a medium with matching Hamaker constant it is easy to demonstrate that not making the Berthelot approximation generally will lead to nonzero values of the Hamaker constant. This is evident after substituting Eqn. (A.10) into Eqn. (A.9) with n = 1, leading to:

$$A_{1o1} = \left(\sqrt{A_{ovo}} - \sqrt{A_{1v1}} \right)^2 + \frac{(v_o - v_1)^2}{(v_o + v_1)^2} \sqrt{A_{ovo}} \sqrt{A_{ivi}}$$ (A.14)

Equation (A.14) shows that, except when both $A_{ovo} = A_{1v1}$ and $v_o = v_1$, the value of A_{1o1} is always positive.

SUMMARY

On the basis of the superpositional principle of the classical Hamaker theory a description has been developed for the non-retarded Van der Waals attraction between composite particles in a medium, while the components in the particles are finely divided. It has been shown that the interaction is attractive even when the net Hamaker constant of the composite particle matches that of the medium. Only when the resonance frequencies match as well, the Van der Waals interaction will vanish. The description derived is fairly accurate. Any inaccuracies originate from the way A_{ivj} and A_{iji} values are evaluated in the classical Hamaker approach rather than from the superposition of the components in the composite material. Additionally a method is forwarded by which the interaction between composite particles in a medium can be described using Lifshitz theory. Accurate data – either A_{ivj} or spectra – are required in order

to make even rough estimations of Hamaker constants in media, both with the Hamaker and with the Lifshitz approach. It is shown that scattering of electromagnetic waves due to the granular character of the particles can be neglected. Improved parameters are forwarded for the absorption band characteristics of water as employed in literature.

REFERENCES

[1]   H.C. Hamaker, *Physics* 4 (1937) 1054
[2]   E.M. Lifshitz, *Sov. Phys. JETP* 2 (1956) 73
[3]   W.R. Bowen and F. Jenner, *Adv. Colloid Interface Sci.* 56 (1995) 201
[4]   J. Mahanty and B.W. Ninham, *Dispersion Forces*, Academic Press, 1976
[5]   V.A. Parsegian, in H. van Olphen and K.J. Mysels (eds.), *Physical Chemistry: Enriching Topics in Colloid and Surface Chemistry*, Theorex, 1975, pp. 27
[6]   J. Israelachvili, *Intermolecular & Surface Forces*, Academic Press, London, 2nd edition, 1992
[7]   J. Lyklema, *Fundamentals of Interface and Colloid Science*, Vol. 1, Academic Press, London, 1991
[8]   P.C. Hiemenz, *Principles of Colloid and Surface Chemistry,* Dekker, New York, 2nd edition, 1986
[9]   W.B. Russel, D.W. Saville and W.R. Schowalter, *Colloidal Dispersions*, Oxford University Press, 1st paperback ed., 1991
[10]   B. Vincent, *J. Colloid Interface Science* 42 (1973) 270

SUMMARY

Analytical separation techniques play a dominant role in the identification and quantitation of unknown compounds. Gas and liquid chromatography (LC) are by far the most important ones and their application can be found in many research and routine laboratories. There is – however – a continuous need for analyzing increasingly smaller sample quantities and lower concentrations – especially in the bioanalytical and environmental field. Capillary LC – applying packed columns with an inner diameter of 100–500 µm – has proven to be a suitable technique for such a demanding task for the analysis of polar, non-volatile, thermally label and ionic compounds. In particular, the limits of detection that are obtainable with capillary LC for such compounds are favorable compared to conventional LC columns with inner diameters of 4.6 mm. For several reasons, capillary LC columns are not widely applied in the analytical community. One of the reasons was the limited availability of dedicated equipment. Another was the often relative limited column stability and lifetime. The lack of fundamental knowledge of the parameters involved in packing LC columns on the column performance is believed to be the main contributor for this drawback. The goal of this thesis is to study the correlation between the packing parameters – involving colloidal and hydrodynamic aspects – and the chromatographic quality of the obtained capillary LC columns.

A general introduction to column liquid chromatography is presented in chapter 1, as well as an overview of currently available stationary phase packings and applied filling techniques. The emphasis is on recently developed packing methods for miniaturized LC columns and the use of monolithic column supports. In addition, the chromatography efficiency of different type of stationary phases and monolithic supports is compared. The current status of microcolumn LC – in particular capillary LC – is reviewed in chapter 2. A brief theoretical discussion on a number of major issues, like column characterization, chromatographic dilution effects and extracolumn bandbroadening in microcolumn LC is given. Recent progress in column technology and the demands and developments of instrumentation and accessories for capillary LC are also reviewed. Besides that, the developments in a large number of established and also more recent detection techniques for capillary LC are discussed. The potential of hyphenation of microcolumn LC with other techniques, more particularly of multidimensional chromatography and microcolumn LC coupled to mass spectrometry (MS) are reviewed. Finally, the perspectives of microcolumn LC separation methods are stressed by a number of examples.

In chapter 3 the colloidal properties and sedimentation behaviour of porous, chemically modified silicas – i.e. reversed phase stationary phase packings – in non-aqueous solvents are described. The free settling behaviour of non-aggregated silica suspensions can effectively be

183

described with a modified Stokes' equation that takes into account the possible inclusion of gas in the pores of the particles. The effects of hindered settling are investigated too. The colloidal properties of the silica particles are compared with predictions by the DLVO theory. The Hamaker and Lifshitz theories are utilized to describe the attraction forces between the chemically-modified silica particles. The electrophoretic mobilities of the particles in the non-aqueous liquids are determined in order to quantify the electrostatic repulsion forces. The electrostatic repulsion appears to generate a large barrier against coagulation with all investigated porous silicas. However, the way in which the particle suspensions are prepared determines whether the particles remain in the primary minimum or are colloidally stable.

The relationship between the particle coagulation and the chromatographic performance of capillary LC columns is studied in chapters 4. The outcome of the results of chapter 3 form the basis of the column packing experiments in chapter 4.1, where the relationship between the coagulating properties of slurry suspensions, type of packing liquids, and final performance of capillary LC columns is investigated. The colloidal stability of spherical particles with completely and incompletely filled pores, and irregularly shaped particles with incompletely filled pores in the applied slurry and packing liquids is examined by means of sedimentation. The performance of the slurry-packed capillary LC column was predominantly determined by the selection of the packing liquid. It is also shown that the packing liquid preferably has to be coagulating to obtain efficient and stable capillary LC columns. The selection of the slurry liquid on the column performance is of minor importance.

In chapter 4.2 a more qualitative method is presented to determine particle coagulation in slurry and packing liquids. This method provides only relative information about the degree of coagulation of the particles. However, the method is relatively easy and provides a good first impression about the suitability of certain liquids for the slurry packing of capillary LC columns. The chromatographic performance of the columns was measured with conventional parameters from plate and rate theories, and the column resistance parameter and separation impedance. Also studied was the time of analysis. The performance of spherical and irregular packings was comparable with a light preference for spherically shaped materials when time of analysis is concerned.

The results of a fundamental study on the effect of particle velocity and packing pressure on the porosity and chromatographic performance of a capillary LC column are presented in chapter 5. A Stokesian dynamics computer simulation based method is presented for the estimation of the bed porosity of capillary LC columns. A colloidally well-described reversed phase stationary phase – slurry liquid suspension is used as a model system. The applied simulation method takes into account the velocity of the slurry, colloidal interaction forces as well as inter-particle hydrodynamic interactions. The obtained bed porosities suggest that a lower slurry velocity leads to a denser packing structure due to the increased effect of colloidal repulsion effects. The results of the simulations are compared with the external porosity and chromatographic performance of capillary LC columns that are packed at different filtration and compaction pressures. The trends that are observed in the experimental results suggest

that hydrodynamic packing parameters have no or little effect on the chromatographic performance of capillary LC columns. No correlations are observed between the filtration and compaction pressure and the chromatographic performance of the capillary LC columns, nor any between the duration of the compaction process and the column porosity and performance.

A number of applications are presented to illustrate the potential of capillary LC columns in certain research areas and chemical fields. The first example involves the calculation of retention in capillary electrochromatography (CEC). Retention factors in CEC are predicted by means of theoretically derived equations and experimentally determined parameters in capillary LC and capillary zone electrophoresis. It was found that the retention factor of uncharged components in CEC was about 20% higher than was calculated. The derived equation does not take into account alteration of the nature of the stationary phase or distribution constant by the applied electric field. However, the influence of the electric field on the retention in CEC can be estimated. Individual field contributions could not be determined.

The identification of tryptic peptides by capillary LC/MS in the presence of ionic detergents is presented in chapter 6.2. A microcolumn switching setup is demonstrated to remove the ionic detergent from the peptide sample. The system comprises two micro precolumns – composed of a specific ionic detergent trapping column and a preconcentration column respectively – and an analytical capillary LC column. Sodium dodecyl sulphate (SDS) containing tryptic digested protein samples are directly applied to the micro precolumns without sample pretreatment and were analysed by UV absorption detection and electrospray-ionization MS. The presented system allows for the automated removal of SDS with virtually no loss in peptides. Maximum SDS loadability and breakthrough on the detergent trapping precolumn are determined as well. Overall good protein recovery and complete removal of SDS are found.

The last application involves the use of capillary LC columns in two-dimensional liquid chromatography to separate complex peptide mixtures from different origins. This two-dimensional method is based on μ-fractionation, automated reinjection and rechromatography using an automated microcolumn switching setup. Different types of separations modes – i.e. hydrophobic and charge separation mechanisms – are applied to increase the selectivity and peak capacity, and to approach orthogonal separation mechanisms. The first dimension separations are carried out by either reversed phase chromatography or by strong anion exchange chromatography. The second dimension separation is in all cases reversed phase capillary LC. In the case of two-dimensional reversed/reversed phase separations, some degree of orthogonality is achieved by using either two different sets of mobile phase solvents and one reversed phase capillary LC column, or by using a single set of mobile phases and two capillary LC columns packed with different reversed phase materials. Electrospray-ionization MS was conducted to confirm the orthogonality of the developed two-dimensional capillary LC technique. The analysis of tryptic digests of cytochrome C and fetuin, and a synthetic peptide mixture are described.

In appendix A an equation is presented – on the basis of the superpositional principle of the classical Hamaker-De Boer approach to the Van der Waals interaction – for the interaction

energy between two identical composite particles in a medium. The particles are supposed to be composed of an arbitrary number of components that are intimately mixed so as to avoid appreciable scattering of interacting electromagnetic waves. As an example, the result is applied to porous polystyrene particles in water, while the pores are not filled with water. Numerical results are evaluated, using interaction parameters as obtained by various methods that are based either on the Hamaker-de Boer or the Lifshitz approach.

SAMENVATTING

Analytische scheidingstechnieken spelen een belangrijke rol bij de identificatie en vervolgens kwantificering van onbekende verbindingen. Gas- en vloeistofchromatografie (LC) zijn veruit de twee belangrijkste scheidingstechnieken en hun toepassing kan gevonden worden in vele research- en routinelaboratoria. Echter, er is een continue behoefte aan technieken waarmee steeds kleinere hoeveelheden en lagere concentraties geanalyseerd kunnen worden – met name in het geval van bioanalytische en milieutechnische stellingen. Capillaire LC – waarbij gepakte kolommen worden toegepast met een inwendige diameter van 100–500 μm – heeft aangetoond een geschikte techniek te zijn voor een dergelijke taak voor de analyse van polaire, niet-vluchtige, thermisch labiele en ionogene verbindingen. Met name de detectielimieten die bereikt kunnen worden met behulp van capillaire LC zijn veel lager dan met conventionele LC, waarbij kolommen met een inwendige diameter van ~ 4.6 mm worden toegepast. Om een aantal redenen wordt capillaire LC nog niet breed toegepast in analytische laboratoria. Eén van de redenen is de beperkte beschikbaarheid van speciaal ontwikkelde apparatuur. Een andere reden is de vaak geringe kolomstabiliteit en -levensduur. Het gebrek aan fundamentele kennis van de invloed van de parameters die betrokken zijn bij het vulproces op de kolomkwaliteit wordt in het algemeen beschouwd als de belangrijkste bijdrage aan de laatst genoemde tekortkoming. Het doel van dit proefschrift is om de relatie tussen de vulparameters – waarbij bovendien colloïdale en hydrodynamische aspecten worden onderzocht – en de chromatografische kwaliteit van de verkregen capillaire LC kolommen te bestuderen.

In hoofdstuk 1 wordt een algemene inleiding over LC gegeven, alsmede een overzicht van stationaire fasen en vultechnieken. De nadruk ligt echter op recent ontwikkelde vultechnieken voor geminiaturiseerde LC kolommen en het gebruik van monolytische dragermaterialen. Daarnaast wordt de chromatografische efficiëntie van verschillende soorten stationaire fasen en monolitische dragermaterialen vergeleken. Een overzicht van de huidige status van geminiaturiseerde LC – in het bijzonder van capillaire LC – wordt gegeven in hoofdstuk 2. Allereerst wordt een korte theoretische behandeling over kolomkarakterisering, chromatografische verdunningseffecten en buitenkoloms-bandverbreding gepresenteerd. Verder worden de recente ontwikkelingen in de kolomtechnologie en van de apparatuur en accessoires voor capillaire LC beschreven. Daarnaast wordt de toepassing van een groot aantal detectietechnieken – zowel traditionele als meer recente – besproken. De koppeling van geminiaturiseerde LC met andere technieken – in het bijzonder multidimensionele chromatografie en de koppeling van geminiaturiseerde LC met massaspectrometrie – wordt toegelicht. Tenslotte wordt het potentieel van geminiaturiseerde LC aangetoond aan de hand van een aantal voorbeelden.

In hoofdstuk 3 wordt het colloïdale gedrag en de sedimentatie van poreuze, chemisch gemodificeerde silica's – dat will zeggen *reversed phase* stationaire fase pakkingsmaterialen – in niet-waterige oplosmiddelen beschreven. De sedimentatie van niet-geaggregeerde silica-suspensies kan effectief worden beschreven met een aangepaste vergelijking van Stokes, waarbij met de mogelijke insluiting van lucht in de deeltjesporiën rekening wordt gehouden. De colloïdale eigenschappen van de silicadeeltjes worden vergeleken met de voorspelling van de slurriestabiliteit aan de hand van de DLVO theorie. De Hamaker en Lifschitz benaderingen van deze theorie worden toegepast om de attractiekrachten tussen chemisch gemodificeerde silica's te beschrijven. De electroforetische mobiliteit van de deeltjes in niet-waterige vloeistoffen is bepaald om de repulsiekrachten tussen de deeltjes te kunnen kwantificeren. De electrostatische repulsie blijkt een grote barrière tegen coagulatie van de onderzochte poreuze silica's te genereren. Echter, de bereidingswijze van de deeltjessuspensies bepaalt voornamelijk of de deeltjes in het primaire minimum verblijven of colloïdaal stabiel zijn.

De relatie tussen de coagulatie van de stationaire fase deeltjes en de chromatografische kwaliteit van capillaire LC kolommen wordt bestudeerd in hoofdstuk 4. De resultaten van het onderzoek in hoofdstuk 3 vormen de basis voor de kolompakkings-experimenten in hoofdstuk 4.1, waar de correlatie tussen de colloïdale eigenschappen van stationaire fase suspensies, het soort pakvloeistof, en de uiteindelijke chromatografische kwaliteit van de capillaire LC kolom is onderzocht. De colloïdale stabiliteit van bolvormige deeltjes met deels en volledig gevulde poriën, en onregelmatig gevormde deeltjes met deels gevulde poriën in de toegepaste slurrie- en pakvloeistoffen wordt onderzocht met behulp van sedimentatie-experimenten. De kwaliteit van de slurrie-gepakte capillaire LC kolommen blijkt voornamelijk te worden bepaald door de keuze van de pakvloeistof. Daarnaast wordt aangetoond dat de deeltjes bij voorkeur moeten coaguleren in de pakvloeistof om efficiënte en stabiele capillaire LC kolommen te verkrijgen. De keuze van de slurrievloeistof is minder belangrijk.

In hoofdstuk 4.2 wordt een kwalitatieve methode gepresenteerd om de coagulatie van deeltjes in slurrie- en pakvloeistoffen te bepalen. De methode biedt slechts relatieve informatie over de mate waarin de deeltjes gecoaguleerd zijn. Echter, de methode is eenvoudig en biedt een goede eerste indruk over de geschiktheid van bepaalde vloeistoffen voor het slurrie-pakken van capillaire LC kolommen. De kwaliteit van de kolommen is gemeten aan de hand van conventionele parameters uit schotel- en stromingstheoriën. De kwaliteit van de kolommen die gepakt zijn met bolvormige en onregelmatig gevormde deeltjes is vergelijkbaar, met een lichte voorkeur voor de onregelmatig gevormde deeltjes wanneer de analysetijd wordt vergeleken.

De resultaten van een fundamentele studie naar het effect van de deeltjessnelheid en de pakdruk op de porositeit en de chromatografische kwaliteit van gepakte kolommen wordt gepresenteerd in hoofdstuk 5. Een methode – gebaseerd op computer-gesimuleerde *Stokese* dynamica – wordt gepresenteerd voor de bepaling van de bedporositeit van capillaire LC kolommen. Een colloïdaal goed-beschreven *reversed phase* stationare fase-slurrievloeistof combinatie is gebruikt als een modelsysteem. De toegepaste simulatiemethode houdt rekening

met de snelheid van de slurrie, colloïdale interactiekrachten en hydrodynamische interacties tijdens het vulproces. De berekende bedporositeiten geven aan dat een lagere slurriesnelheid leidt tot een dichtere pakking, hetgeen toe te schrijven is aan de relatief sterke invloed van de repulsiekrachten bij lage deeltjessnelheden. De resultaten van de simulatie-experimenten zijn vergeleken met de externe porositeit en de kwaliteit van capillaire LC kolommen die gevuld zijn bij verschillende filtratie- en compacteringsdrukken. De trends die zijn waargenomen in de experimenten suggereren dat de hydrodynamische vulparameters nauwelijks of geen effect hebben op de kwaliteit van de capillaire LC kolommen. Tussen zowel de filtratie- en compacteringsdruk en de kwaliteit van de capillaire LC kolommen, als tussen de duur van het compacteringsproces en de kolomporositeit en -kwaliteit zijn geen correlaties waarneembaar.

Een aantal toepassingen wordt gepresenteerd om het potentieel van capillaire LC in bepaalde onderzoeksgebieden te illustreren. Het eerste voorbeeld toont de berekening van de retentie van verbindingen in capillaire electrochromatografie, hetgeen wordt behandeld in hoofdstuk 6.1. De retentiefactoren in capillaire electrochromatografie worden voorspeld door middel van een theoretisch afgeleide vergelijking en experimenteel bepaalde parameters in capillaire LC en capillaire zone electroforese. De retentiefactor van niet-geladen verbindingen is in capillaire electrochromatografie ongeveer 20% hoger dan berekend. De afgeleide vergelijking houdt geen rekening met verandering van de eigenschappen van de stationaire fase en de verdelingsconstanten onder invloed van het electrische veld. Echter, de orde grootte van de invloed van het electrische veld kan worden bepaald. Individuele bijdragen kunnen niet worden onderscheiden.

De identificatie van tryptische-peptiden in de aanwezigheid van ionogene detergentia met behulp van capillaire LC–massaspectrometrie wordt beschreven in hoofdstuk 6.2. Een microkolom schakelingsschema wordt gedemonstreerd om de ionogene detergentia van de peptiden te isoleren. Het systeem bestaat uit twee micro-voorkolommen – bestaande uit respectievelijk een specifieke detergent-val en een voorkolom gepakt met C_{18} stationaire fase – en een analytische capillaire LC kolom. Trypsine-enzymatisch afgebroken eiwitten – waaraan natriumdodecylsulfaat is toegevoegd – worden zonder enige monstervoorbewerking beladen op de voorkolommen en geanalyseerd met behulp van UV absorptiedetectie en electrospray-ionisatie massaspectrometrie. Met behulp van het systeem kan natriumdodecylsulfaat volledig geautomatiseerd worden verwijderd zonder enig verlies van de peptiden. Daarnaast is de maximale natriumdodecylsulfaat belaadbaarheid en doorbraak op de detergent val bepaald. In het algemeen wordt een goede eiwit opbrengst waargenomen en wordt het natriumdodecylsulfaat volledig verwijderd.

De laatste toepassing heeft betrekking op het gebruik van capillaire LC kolommen in tweedimensionale LC voor de bepaling van complexe peptide-monsters. De twee-dimensionale methode is gebaseerd op µ-fractionering, en de automatische her-injectie en -chromatografie met behulp van een automatische micro-kolom schakelings-opstelling. Verschillende soorten scheidingsmechanismen – dat wil zeggen hydrofobe en lading-scheidingsmechanismen – worden toegepast om de selectiviteit en piekcapaciteit te verhogen en om meer orthogonale

scheidingsmechanismen te benaderen. De eerste dimensie-scheiding wordt met behulp van *reversed phase* chromatografie of ionenwisselingschromatografie uitgevoerd. De tweede dimensie-scheiding is in alle gevallen *reversed phase* capillaire LC. In het geval van *reversed phase/reversed phase* scheidingen kan enige mate van orthogonalitiet worden bereikt door gebruik te maken van twee verschillende mobiele fase gradiënten en één *reversed phase* capillaire LC kolom, of met één mobiele fase gradiënt en twee capillaire LC kolommen die gevuld zijn met verschillende *reversed phase* materialen. Electrospray-ionisatie massa-spectrometrie wordt uitgevoerd om de orthogonaliteit van de ontwikkelde twee-dimensionale capillaire LC techniek te bevestigen. De analyse van tryptisch-afgebroken cytochroom C en fetuïne, en een synthetisch peptide-mengsel wordt beschreven.

In appendix A wordt een vergelijking gepresenteerd – die gebaseerd is op het superpositie-principe van de Hamaker-De-Boer benadering voor de Van der Waals interactie – voor de interactie-energie tussen twee gelijke deeltjes die samengesteld zijn uit meerdere componenten in een medium. Aangenomen wordt dat de deeltjes zijn samengesteld uit een arbitraire hoeveelheid componenten die zeer fijn verdeeld zijn over het bolvolume, zodat verstrooiïng van de electromagnetische energie wordt voorkomen. Als een voorbeeld wordt het resultaat van de afgeleide vergelijking toegepast op poreuze polystyreen deeltjes in water, waarvan de poriën niet gevuld zijn met water. Numerieke resultaten worden geëvalueerd, daarbij gebruik makend van de interactieparameters die worden verkregen met behulp van verschillende methoden, die gebaseerd zijn op de Hamaker-De Boer of de Lifschitz benadering.

DANKWOORD

Een groot aantal personen heeft een bijdrage geleverd aan de totstandkoming van dit proefschrift. Op deze plaats wil ik hen graag bij name noemen en bedanken voor hun medewerking.

Op de eerste plaats wil ik mijn promotor Carel Cramers bedanken dat ik op deze toch unieke wijze een promotie-onderzoek heb kunnen uitvoeren. De overstap van Amsterdam naar Eindhoven was in het begin even wennen, maar na verloop van tijd ben ik zijn manier van begeleiding en inbreng zeer gaan waarderen. De samenwerking met mijn copromotor Jos Lavèn is van onschatbare waarde gebleken voor het onderzoek. De colloïd chemische en hydro-dynamische inbreng in dit proefschrift is voornamelijk van zijn hand. Bedankt voor de kritische blik op hoe je nu eigenlijk een kolom zou moeten vullen. Henk Claessens wil ik graag bedanken voor de dagelijkse begeleiding, het leggen van nuttige contacten met het bedrijfsleven en zijn bijdrage aan het overzichtsartikel over geminiaturiseerde vloeistofchromatografie.

De leden van de vakgroep instrumentele analyse voor hun bijdrage aan het genoten werkplezier. In het bijzonder wil ik Denise Tjallema bedanken voor haar secretariële steun tijdens het totstandkomen van het overzichtsartikel en het lange-afstands coördineren van het navolgen van het promotiereglement, Huub van Leuken voor het vervaardigen van vele fijnmechanische onderdelen en Henri Snijders voor zijn hulp tijdens een middagje meten aan peptiden met behulp van een massaspectrometer. Special thanks to Pavel Coufal, Charles University, Prague, for initiating the work on capillary electrochromatography and his ethousiasm during performing our mutual work.

Aan de praktische uitvoering van het onderzoek hebben ook een aantal mensen een bijdrage geleverd. De stagiaires van het hoger laboratorium onderwijs in Sittard – Mieke van den Broeck en Edgar van den Hoef – voerden met veel enthousiasme een groot deel van de preliminaire experimenten uit en hebben hiermee de basis gelegd voor de rest van het onderzoek. Martin Waals heeft – om in een paar weken kennis over geminiaturiseerde LC op te doen – ondersteunend werk uitgevoerd voor de beschrijving van het retentiegedrag van neutrale verbindingen in capillaire electrochromatografie. Martijn Hoeben heeft geheel zelfstandig een belangrijk deel van het onderzoek ingevuld. Zijn onderscheidend- en doorzettingsvermogen hebben geleid tot een betere begripsvorming van het effect van de vulsnelheid op de chromatografische kwaliteit van een capillaire LC kolom. De deadline van zijn verslag werd gelukkig toch nog gehaald door de fax en een geduldige medewerkster van een Belgisch hotel.

CURRICULUM VITAE

Hans Vissers werd geboren op 16 november 1965 te Zevenbergen. Na het behalen van het diploma aan het Hoger Laboratorium Onderwijs te Etten-Leur startte hij zijn doctoraalstudie aan de Vrije Universiteit, Amsterdam. Tijdens deze studie werd een zomerstage gevolgd aan Bates College, Maine, USA, onder leiding van prof.dr. T.J. Wenzel en betrof de synthese van chromoforen voor postcolumn reactiedetectie in vloeistofchromatografie. Het afstudeer-onderzoek aan de Vrije Universiteit werd verricht binnen de vakgroep Algemene en Analytische Chemie onder leiding van prof.dr. N.H. Velthorst en betrof de ontwikkeling van toepassingen voor lanthanide (III) luminescentie-detectie in vloeistofchromatografie.

Vanaf maart 1993 tot en met februari 1995 is hij in het kader van een twee-jarige tweede fase opleiding werkzaam geweest binnen de vakgroep Instrumentele Analyse aan de Technische Universiteit Eindhoven. Onder leiding van prof.dr.ir. C.A. Cramers is onderzoek verricht naar de colloïd chemische en hydrodynamische aspecten van het vullen van geminiaturiseerde vloeistofchromatografie kolommen, waarvan de resultaten zijn beschreven in dit proefschrift. Sinds maart 1995 is hij werkzaam bij de firma LC Packings.

BIBLIOGRAPHY

A part of the contents of this thesis has been or will be published as regular contributions in scientific journals:

- J.P.C. Vissers, H.A. Claessens, J. Lavèn and C.A. Cramers, Colloid Chemical Aspects of Slurry Packings Techniques in Microcolumn Liquid Chromatography, *Anal. Chem.* 67 (1995) 2103 - 2109

- J.P.C. Vissers, E.C.J. van den Hoef, H.A. Claessens, J. Lavèn and C.A. Cramers, Comparison of Spherically and Irregularly Shaped Stationary Phase Packings in Microcolumn Liquid Chromatography, *J. Microcol. Sep.* 7 (1995) 239 - 245

- J.P.C. Vissers , H.A. Claessens and P. Coufal, Calculation of Retention Factors in Capillary Electrochromatography from Chromatographic and Electrophoretic Data, *J. High Resol. Chromatogr.* 18 (1995) 540 - 544

- J.P.C. Vissers, W.P. Hulst, J.-P. Chervet, H.M.J. Snijders and C.A. Cramers, Automated On-line Ionic Detergent Removal from Minute Protein/Peptide Samples Prior to Liquid Chromatography–Electrospray Mass Spectrometry, *J. Chromatogr. B.* 686 (1996) 119 - 128

- J.P.C. Vissers, J. Lavèn, H.A. Claessens, C.A. Cramers and W.G.M. Agterhof, Sedimentation Behaviour and Colloidal Properties of Porous, Chemically Modified Silicas in Non-Aqueous Solvents, *Colloids Surf. A: Physicochem. Eng. Aspects* 126 (1997) 33 - 44

- J.P.C. Vissers, H.A. Claessens and C.A. Cramers, Microcolumn Liquid Chromatography: instrumentation, detection and applications (review), *J. Chromatogr.* A 777 (1997) 1 - 28

- J.P.C. Vissers, M.A. Hoeben, J. Lavèn, H.A. Claessens and C.A. Cramers, Hydrodynamic Aspects of Slurry Packing Processes in Microcolumn Liquid Chromatography, *submitted for publication*

- J.P.C. Vissers, R.E.J. van Soest, J.-P. Chervet and C.A. Cramers, 2-Dimensional Capillary Liquid Chromatography Based on µ-Fractionation, *submitted for publication*

-   J. Lavèn and J.P.C. Vissers, Van der Waals Interaction of Composite Particles, *submitted for publication*

Additional papers on other subjects:

-   M. Schreurs, J.P.C. Vissers, C. Gooijer and N.H. Velthorst, Determination of Orotate by Liquid Chromatography with Sensitized Lanthanide Ion Luminescence Detection, *Anal. Chim. Acta* 262 (1992) 201 - 208

-   J.P.C. Vissers, A.H. de Ru, M. Ursem and J.-P. Chervet, Optimized Injection Techniques for Micro and Capillary Liquid Chromatography, *J. Chromatogr. A* 746 (1996) 1 - 7

STELLINGEN

1. Naast de chromatografische eigenschappen van een kolom, zou ook het slagingspercentage om een geminiaturiseerde vloeistofchromatografie kolom te maken in wetenschappelijke publicaties moeten worden vermeld.

    S. Hsieh en J.W. Jorgenson, Anal. Chem. 68 (1996) 1212

2   Het gebruik van magnetic resonance imaging om de dispersie in een chromatografisch bed te bepalen is af te raden.

    U. Tallarek, K. Albert, E. Bayer en G. Guiochon, AIChE. J. 42 (1996) 3041

3. De combinatie van de beperkingen van capillaire zone electroforese en geminiaturiseerde vloeistofchromatografie vormt momenteel nog een belangrijk obstakel voor de brede toepasbaarheid van capillaire electrochromatografie.

    M.M. Ditmann, K. Wienand, F. Bek and G.P. Rozing, LC•GC Int. 13 (1995) 800

4. Lanthanide luminescentie detectie vormt geen uitzondering op de regel dat een hoge mate van selectiviteit ten koste gaat van de algemene toepasbaarheid van een detectietechniek.

    M. Schreurs, J.P.C. Vissers, C. Gooijer en N.H. Velthorst, Anal. Chim. Acta 262 (1992) 201

5. Het gebruik van gereduceerde parameters in vloeistofchromatografie – met name waar het vergelijkend onderzoek van vulmaterialen betreft – is alleen zinvol, indien de stationaire fasen toereikend gekarakteriseerd zijn.

    F. Andreolini, C. Borra en M. Novotny, Anal. Chem. 59 (1987) 2428

6. Ondanks de sterke opkomst van tandem-massaspectrometrische technieken – en het gegeven dat massaspectrometristen chromatografische technieken vaak als een noodzakelijk kwaad beschouwen – bedienen zij zich regelmatig van on-line scheidings/identificatietechnieken.

    Voorjaarsbijeenkomst Nederlandse Vereniging voor Massaspectrometrie, Amsterdam, 1998

7. Superkritisch water zal – in tegenstelling tot superkritisch koolstofdioxide – weinig of geen toepassing vinden als mobiele fase.

    R.M. Smith en R.J. Burgess, J. Chromatogr. A 785 (1998) 49

8. Het exotische karakter van sommige vulopstellingen doet soms vermoeden dat het vervaardigen van geminiatuuriseerde vloeistofchromatografie kolommen inderdaad meer een kunst dan een wetenschap is.

    A.M. Fernier en L.A. Colón, 20th International Symposium on High Performance Liquid Phase Separations and Related Techniques, San Francisco, June 1996
    K. Bächmann, I. Haag en T. Prokop, Fresenius' J. Anal. Chem. 345 (1993) 545

9. Het originele idee om de stuctuur van een bed aan de hand van successievelijke gekleurde lagen stationaire fasen te visualiseren lijkt alleen toepasbaar voor kolommen die door middel van compressietechnieken gemaakt worden.

    T. Yun en G. Guiochon, J. Chromatogr. 760 (1997) 17

10. De tijdstermijn tussen het indienen van een manuscript en de goedkeuring tot publicatie wordt vaak ten onrechte beschouwd als een maat voor de kwaliteit van een wetenschappelijk artikel.

11. De reductie van het aantal analytisch chemische vakgroepen aan de Nederlandse universiteiten, zal de (bio-) chemische industrie dwingen om zelf onderwijs te gaan verzorgen of dit financieel elders mogelijk te maken.

Eindhoven, 18 december 1998   Hans Vissers